2006

Development of novel fluorinated high performance polymers and new biomaterials from renewable resources

Dejan Dragoslava Andjelković
Iowa State University

Development of novel fluorinated high performance polymers and new biomaterials from renewable resources

by

Dejan Dragoslava Andjelković

A dissertation submitted to the graduate faculty

in partial fulfillment of the requirements for the degree of

DOCTOR OF PHILOSOPHY

Major: Organic Chemistry

Program of Study Committee:
Richard C. Larock, Major Professor
William S. Jenks
Malika Jeffries-EL
Marc D. Porter
Surya K. Mallapragada

Iowa State University

Ames, Iowa

2006

Graduate College
Iowa State University

This is to certify that the doctoral dissertation of

Dejan Dragoslava Andjelković

has met the dissertation requirements of Iowa State University

Signature was redacted for privacy.

Major Professor

Signature was redacted for privacy.

For the Major Program

TABLE OF CONTENTS

PART I. UTILIZATION OF NICKEL(0)-COUPLING POLYMERIZATION FOR THE DEVELOPMENT OF NOVEL FLUORINATED HIGH PERFORMANCE POLYMERS

CHAPTER 1. GENERAL INTRODUCTION

Introduction

The discovery of high performance polymers represents one of the most important engineering achievements of the 20th century. Since then, these materials have found widespread utility in a range of industrial and everyday life applications. Their existence and further developments have transformed our way of life and revolutionized the way modern industries view and do business. The main reason for their importance lies in the combination of their useful chemical, physical and thermo-mechanical properties.[1-3] Due to the fact that they possess higher strength-to-weight ratio than their metallic counterparts, they have replaced metals in a range of applications causing drastic weight reduction and energy conservation.[1,4]

There exists an ever increasing demand in industry for new high performance materials. One of the most important steps in the development of new polymers relies on the design of new monomers and synthetic techniques needed for their polymerization. This further requires an extensive knowledge in organic and polymer chemistry, and significant knowledge in polymer engineering. Coupled with an understanding of the structure-property relationships in polymeric materials,[5] this knowledge allows a polymer scientist to tailor materials for specific applications.

After the initial boom in the polymer industry at the beginning of the 20th century, it was this approach that allowed further advancements in this area in the second half of the century.[1] During that time, a range of high performance materials, such as semi-conducting polymers, high-modulus engineering plastics, nonlinear optical (NLO) polymers and new membrane materials for gas separations and fuel cell applications have been developed.

Some of the most important polymers in this group are shown in **Figure 1**. They include: perfluoropolymers, like Teflon®,[6,7] known for its low surface energy, low coefficient of friction and excellent solvent resistance; polyparaphenylenes, like poly(1,4-phenylene) or Parmax®,[8-11] materials for use as thermoengineering plastics and nonlinear optical (NLO) materials; aromatic polyamides, like the high modulus fibers Kevlar® and Nomex®;[12,13] polyimides, like heat-resistant Kapton® or the injection-moldable polyamide imide Torlon®;[14] polycarbonates, like high impact resistant Lexan®;[15] polysulfides, like flame resistant PPS or Ryton®;[16] etc.

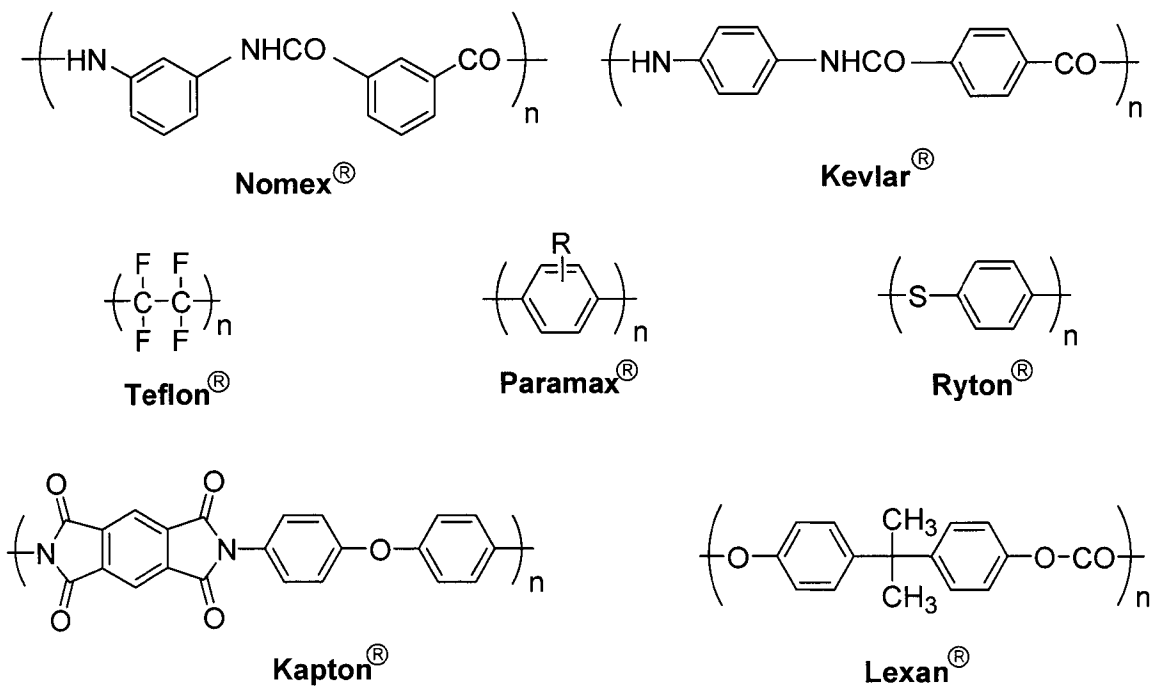

Figure 1. Structures of several important high performance polymers.

These and many other examples prove that a polymer's properties are a direct consequence of their structural features. Furthermore, they demonstrate the usefulness and importance of a macromolecular design approach toward new high performance polymers.

Synthetic Approaches to the Development of High Performance Polymers

High performance polymers are materials used in applications that demand service at elevated temperatures, while maintaining their structural integrity and excellent combinations of chemical, physical, and mechanical properties. Polyparaphenylenes and hexafluoroisopropylidene (HFIP)-containing polymers are two important classes of high performance polymers and are the major focus of the first part of this thesis. The general structures of these polymers are shown in Figure 2. Due to their structural features, these polymers have outstanding physical and thermal properties, and have current and potential utility in automotive, aerospace, electrical and separation membrane applications.

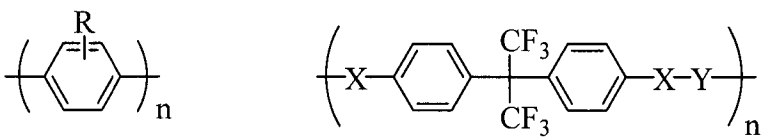

Polyparaphenylenes (PPPs) **HFIP-containing polymers**

Figure 2. General structures of polyparaphenylenes (PPPs) and HFIP-containing high performance polymers.

Polyparaphenylenes. PPPs are unique polymers with conjugated and conformationally rigid backbones. These structural features make them attractive candidates for numerous high-performance, liquid crystalline and optoelectronic applications, while at the same time, rendering their synthesis difficult. For instance, the main obstacle for production of high molecular weight PPPs was the low solubility of their growing rigid-rod chains during polymerization.[17] Several early polymerization processes, which focused on oxidative polymerization (**Method A**, **Scheme 1**),[18] transition metal-catalyzed Grignard-type

condensation (Yamamoto method, **Method B**, **Scheme 1**),[19] Ni(0)-mediated coupling polymerization of 4,4'''-dichloroquaterphenyls (**Method C**, **Scheme 1**)[20] and thermal aromatization process (**Method D**, **Scheme 1**),[21-23] failed to furnish processable, structurally defined high molecular weight PPP materials.

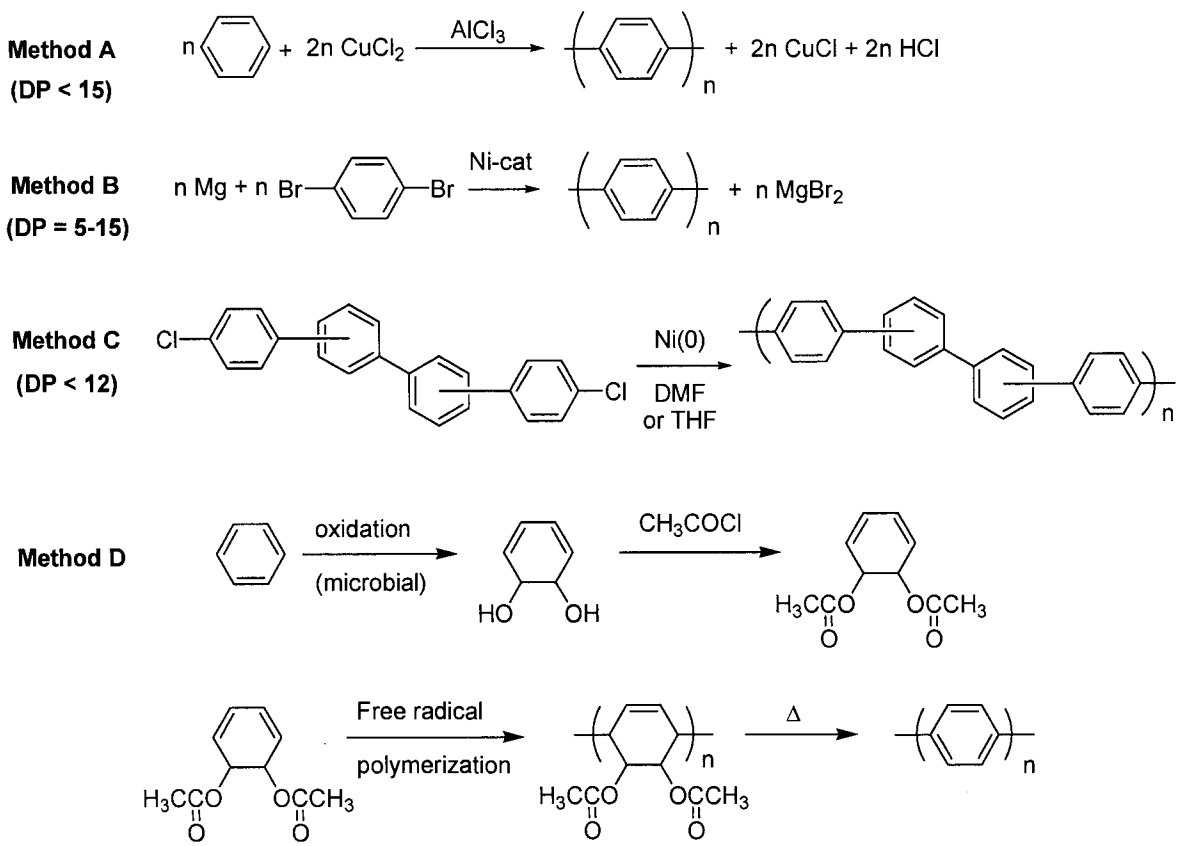

Scheme 1. Early synthetic approaches toward PPPs.

More recent transition metal-catalyzed polymerization methods, such as Suzuki polycondensation (SPC)[24] (**A**, **Scheme 2**) and the Ni(0)-catalyzed polymerization methods (**B**, **Scheme 2**)[25] in particular, were more effective in producing soluble high molecular weight PPPs. In these processes, the low solubility issues were circumvented by attachment

of various lateral substituents, which resulted in an increase of configurational entropy and, consequently, the solubility and processability of the resulting PPP polymers. Furthermore, the improved solubility of the growing polymer chains during polymerization allowed for the production of high molecular weight PPPs with degrees of polymerization (DP) in the range 80-600.[26-30] The best results were achieved with benzoyl pendant groups, which allowed for the formation of high molecular weight PPPs (polybenzophenones or PBPs) with retention of their useful properties.[9-11,26-31] Contrary to other solubilizing lateral groups,[32-34] the aromatic character of the benzophenone repeat units gives PBPs with high thermal stability and 5% weight loss temperatures of 496 and 495 °C in N_2 and air respectively, as well as exceptional strength and stiffness.[9] The tensile modulus of these materials reaches 7-17 GPa (1-2.5 MPSI), which is 2-4 times higher than that of other high performance thermoplastics, such as poly(phenylenesulfide)s, poly(ether sulfone)s, and poly(ether imides)s.[35]

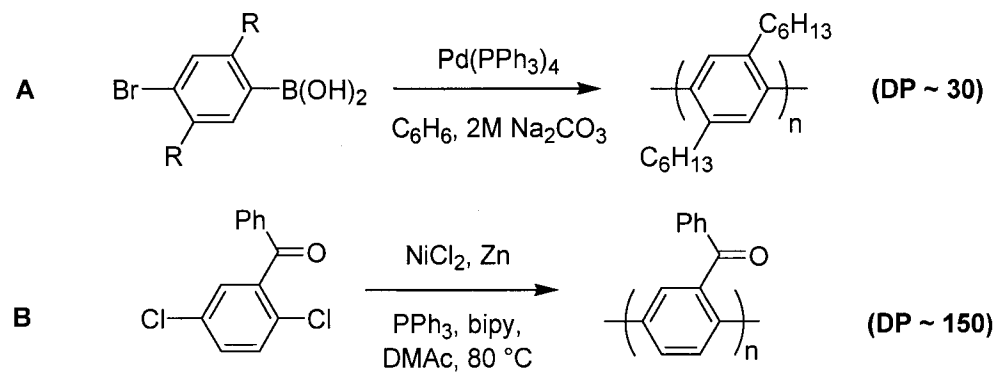

Scheme 2. Synthesis of PPPs via the SPC method (**A**) and Colon method (**B**).

The industrial importance of PPPs has recently been recognized by Maxdem, Inc. (San Dimas, CA), who has developed and commercialized PPP technology, which consists of

a family of extremely strong and scratch resistant amorphous thermoplastics.[9-11,36] These materials represent a range of polymers and copolymers, which are structurally similar to PBPs. Also, this technology has recently been transferred to Maxdem's subsidiary, Mississippi Polymer Technologies, Inc., which is manufacturing and selling these materials for use as engineering thermoplastics under the trade name Parmax® Self-Reinforced Polymers (SRPs).[37] Parmax® derivatives can be processed using conventional solution and melt processing techniques and are used for the manufacture of automotive and aircraft parts, medical tubing and devices, semiconductor components, nonlinear optical (NLO) devices, bushings, bearings, gears, light-weight vehicle suspension systems, and as an alternative to structural materials, such as aluminum, steel, fiber reinforced composites and sheet molding compounds, in a range of construction, automotive, aerospace and defense applications.

Unfortunately, one of the major drawbacks of PBPs, and PPPs in general, includes the formation of brittle films. Film forming ability is crucial for certain applications, such as coatings, membranes for separation, and electronics. The novel structure of poly(2,5-benzophenone) and its derivatives offers great potential for use as separation membranes. Therefore, materials that form flexible and creasable films are required. To address this particular issue, chapter 2 of this dissertation focuses on the synthesis of novel PBP materials, isomeric HFIP-linked PBP polymers. The research described in this chapter presents a new methodology for their synthesis, which allows for the production of PBP materials with better film forming properties.

Hexafluoroisopropylidene-Containing Polymers. HFIP-containing polymers have also received considerable attention over the past four decades.[38-41] Incorporation of the HFIP unit into the polymer backbone has proven to be highly beneficial and resulted in the

preparation of a variety of solution or melt-processable materials from previously intractable polymers. Increased thermal stability, improved solubility, decreased water absorption, low dielectric constant, decolorization and decreased crystallinity are only a few of many benefits of the inclusion of an HFIP moiety in the polymer backbone. For example, the improved thermal stability is mainly attributed to the strong C-F bond (132 kcal/mol or 485 kJ/mol), while decolorization is the result of disrupted conjugation by the HFIP group. Furthermore, the bulkiness of the HFIP unit results in an increased free volume for the polymer, thus improving the polymer's insulating properties and affecting its permeability. A majority of the changes in the polymer's physical properties, on the other hand, are manifestations of a change in the electronic properties due to the strong electron-withdrawing character of the HFIP group. Because of their properties, HFIP materials have found wide application in the automotive, aerospace, construction and electronic industries. They are excellent candidates for gas separation membranes, seals, coatings and a range of high temperature applications.[41]

The structures of some of the most important classes of HFIP-containing polymers are shown in Figure 3. These include polyamides (**A**), polyimides (**B**), polyesters (**C**), polycarbonates (**D**), and polyethers (**E**). Many classes of HFIP polymers have been developed due to the availability of a wide range of bis-arylhexafluoroisopropylidene monomers. These monomers are usually prepared by high pressure condensation reaction of aromatic nuclei with hexafluoroacetone[42,43] in the presence of HF at high temperatures to give 2,2-bis-arylhexafluoroisopropylidene (**Scheme 3**).[44,45] Furthermore, this class of HFIP monomers can further be synthetically modified, which drastically expands the range of available monomers.[46,47]

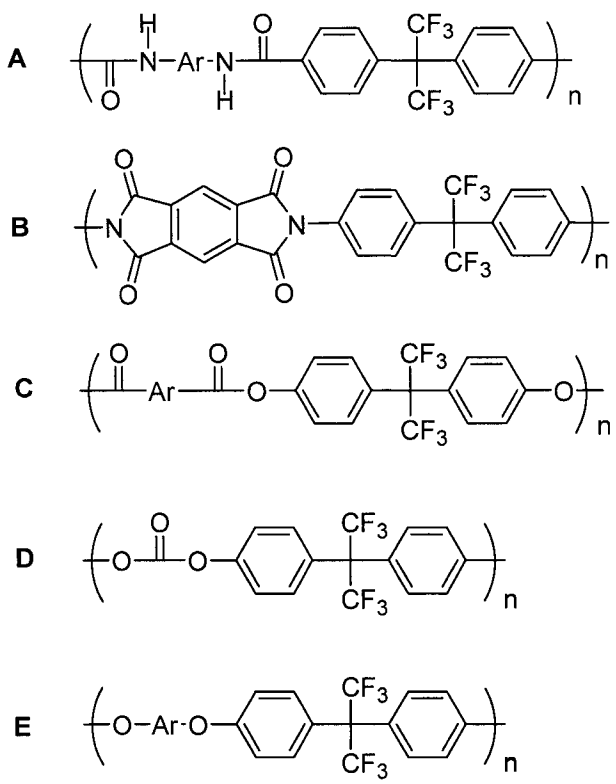

Figure 3. Structures of several important types of HFIP-containing polymers.

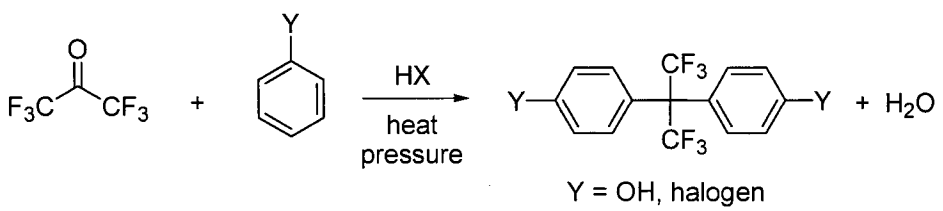

Scheme 3. Condensation of hexafluoroacetone with aromatic nuclei.

The majority of HFIP-containing high performance polymers are synthesized via polycondensation methods based on nucleophilic acyl or nucleophilic aromatic substitution reactions.[39-41] These methods account for the formation of carbon-heteroatom bonds and are used for the synthesis of polyamides, polyimides, polyesters, polycarbonates, poly(ether ketone)s, poly(ether sulfones)s, etc. Polymerization techniques which involve the formation

of aromatic carbon-carbon bonds are also important, since they provide excess to a range of valuable high-performance materials, such as polyparaphenylenes, polyfluorenes and polythiophenes, which cannot be synthesized by previously mentioned nucleophilic-based polycondensation methods. These polymerization methods, on the other hand, are chiefly based on transition metal catalyzed reactions, which include palladium-[3,24,48,49] and nickel-catalyzed or mediated polymerization methods.[20,25-33,50-52]

Ni(0)-Catalyzed Polymerization Route Toward HFIP Materials. The discovery of an efficient synthesis of various functionalized biaryls by Colon and Kelsey[25] represents the focal point in the development and utilization of Ni(0)-mediated coupling polymerization methods for the preparation of a variety of useful high performance polymers. The first efficient syntheses of poly(arylether sulfone)s,[53,54] poly(ether ketone)s,[55] and substituted poly(2,5-thiophene)s[56] proved that the polymerization of carefully designed difunctional monomers under mild conditions can easily provide an array of polymeric materials for targeted applications. Furthermore, considerable interest in the mechanism of this reaction has resulted in a better understanding of the role of monomer structure, ligands, temperature and reducing metal on the polymerization.[25,27] In the following years, this technique was extensively employed for the preparation of poly(paraphenylene)s (PPP),[8-11,26-31] poly(thiophene)s,[57] poly(arylene phosphine oxide)s (PAPO),[58,59] aromatic polyketones,[60] polyamides,[61] polyimides[62] and fluorinated polymers.[63-65]

Among the aryldihalide monomers, aryl dichlorides have been the most frequently employed in polymerization reactions. This is mainly due to their high reactivity and low cost when compared to their dibromo and diiodo analogues (**B, Scheme 2**). The introduction of bistriflate and bismesylate monomers by Percec and coworkers[32,33,66] took the synthesis of

high performance polymers a major step forward. The use of these monomers significantly widened the applicability of this Ni(0)-catalyzed polycondensation and provided a simple route toward functionalized high performance materials.[67,68]

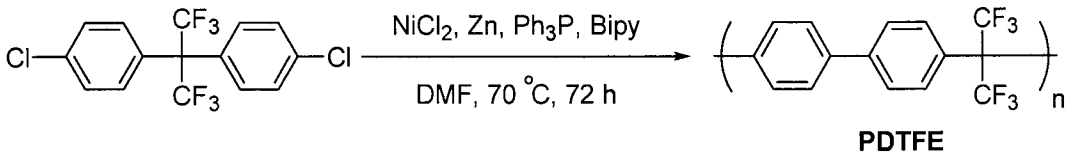

Scheme 4. Ni(0)-catalyzed approach toward a PDTFE polymer.

Prior to our work[63,64] (**Scheme 4**), there were no reports on the utilization of Ni(0)-catalyzed polymerization methodology for the synthesis of HFIP-containing polymers. One of the more recent attempts by Carter and co-workers described a synthesis of a number of soluble and processable poly(biphenylmethylene) homo- and thermally crosslinkable polymers, including HFIP-containing ones, by the Ni(0)-mediated polymerization of bistriflate monomers derived from different bisphenols (**Scheme 5**).[52] The ease of aryl carbon-carbon bond formation during the Ni(0)-catalyzed polymerization, along with the ability to incorporate a variety of useful functional groups into the polymer backbone, has allowed us to extend this methodology further and synthesize novel fluorinated materials.[65]

The second chapter of this thesis describes the synthesis of novel HFIP-linked isomeric benzophenone polymers by the Ni(0)-catalyzed coupling polymerization of newly developed bis(aryl chloride) and bis(aryl triflate) monomers. The unique structural characteristics of these novel HFIP-interrupted poly(paraphenylene)s make them potentially

interesting candidates for gas separation applications, as well as for electrical applications, such as nonvolatile organic memory.

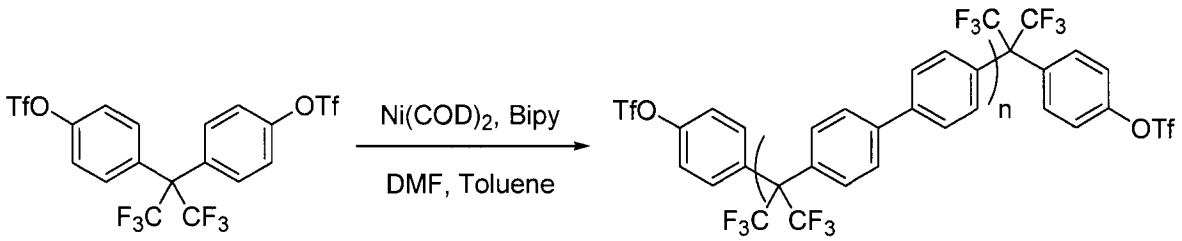

Scheme 5. Yamamoto approach toward a PDTFE polymer.

Dissertation Organization

This dissertation is organized into two parts and seven chapters. The first part consists of two chapters and focuses entirely on high performance polymers. The first chapter is a general introduction to the development of high-performance polymeric materials. The synthesis, properties and general utility of the most important high performance polymers are addressed. An overview of two polymers of interest, poly(paraphenylene)s and HFIP-containing polymers, is included. Chapter two is a paper ready for submittion to the journal Macromolecules. It describes the synthesis of novel HFIP-linked benzophenones and a novel Ni(0)-catalyzed copolymerization approach for optimization of the polymer properties.

The second part of the dissertation focuses on biobased materials prepared from commercially available vegetable oils, as an annually renewable resource. Chapter 3 presents a general introduction to the area of vegetable oil-based bioplastics. It gives a broad review of bioplastics prepared by the cationic copolymerization of soybean oil and aromatic alkene comonomers. Chapters 4 through 6 are papers that have been published or submitted

for publication to scientific journals. The first two research chapters in part two, chapters 4 and 5, address the synthesis and characterization of a series of novel bioplastics by the cationic copolymerization of a range of commercially available vegetable oils and alkene comonomers, such as styrene, divinylbenzene and dicyclopentadiene, catalyzed by modified boron trifluoride diethyl etherate. The main focus of these chapters is on the structure-property relationships in these materials. Chapter 6 describes the elucidation of the structural isomers formed by the homogeneous rhodium-catalyzed isomerization of model compounds and vegetable oils. It also describes the overall utility of the method for the production of conjugated linoleic acids. Chapter 7 states some general conclusions and gives suggestions for future research. The appendices contain supplemental data to that presented in the indicated chapters.

References

1. *High Performance Polymers: Their Origin and Development*; Seymour, R. B.; Kirshenbaum, G. S., Eds.; Proceedings of the Symposium on the History of High Performance Polymers at the ACS Meeting held in New York, April 15-18, 1986; Elsevier, New York, 1986.
2. *High Performance Polymers*; Baer, E.; Moet, A., Eds.; Hansen Publishers: Munich, Germany, 1991.
3. Percec, V.; Hill, D. H. In *Step-Growth Polymers for High-Performance Materials - New Synthetic Methods*; Hedrick, J. L.; Labadie, J. W., Eds.; ACS Symposium Series 624; American Chemical Society: Washington DC, 1996, p 2-56.
4. Rosato, D. V.; Di Mattia, D. P.; Rosato, D. V. *Designing with Plastics and Composites, a Handbook.* Van Nostrand Reinhold: New York, 1991, p 1-9.

5. *Structure-Property Relationships in Polymers*; Seymour, R. B.; Carraher, C. E., Eds.; Plenum Press: New York, 1984.

6. Scheirs, J. *Fluoropolymers - Technology, Markets and Trends*, A Rapra Industry Analysis Report; Rapra Technology Ltd.: Shorpshire, UK, 2001.

7. Odian, G. *Principles of Polymerization*, 3rd edition; Wiley-Interscience: New York, 1991, p 313-314.

8. Taylor, D. K.; Samulski, E. T. *Macromolecules* **2000**, *33*, 2355-2358.

9. Marrocco, M. L.; Gange, R. R.; Trimmer, M. S. (Maxdem Inc.). U. S. Patent 5,227,457, 1993.

10. Marrocco, M. L.; Trimmer, M. S.; Hsu, L.-C.; Gange, R. R. *SAMPE Proceedings* **1994**, *39*, 1063-1072.

11. Marrocco, M. L.; Gange, R. R.; Trimmer, M. S. (Maxdem Inc.). U. S. Patent 6,087,467, 2000.

12. Strong, B. A. *Plastics: Materials and Processing*, Prentice Hall: Englewood Cliffs, New Jersey, 1996; p 192.

13. Odian, G. *Principles of Polymerization*, 3rd edition; Wiley-Interscience: New York, 1991, p 102-105.

14. Odian, G. *Principles of Polymerization*, 3rd edition; Wiley-Interscience: New York, 1991, p 158-162.

15. Odian, G. *Principles of Polymerization*, 3rd edition; Wiley-Interscience: New York, 1991, p 100-102.

16. Hill, H. W. History of Polyphenylene Sulfide. In *High Performance Polymers: Their Origin and Development*; Seymour, R. B.; Kirshenbaum, G. S., Eds.; Proceedings of

the Symposium on the History of High Performance Polymers at the ACS Meeting held in New York, April 15-18, 1986; Elsevier, New Your, 1986, p 135-148.

17. Lacaze, P. C.; Aeiyach, S.; Lacroix, J. C. In *Handbook of Organic Conductive Molecules and Polymers*, Nalwa, H. S., Ed., John Wiley & Sons, Inc.: New York, 1997, p 205-270.

18. Kovacic, P.; Kyriakis, A. *J. Org. Chem.* **1964**, *29*, 100-104.

19. Yamamoto, T.; Hayashi, Y.; Yamamoto, A. *Bull. Chem. Soc. Jpn.* **1978**, *51*, 2091-2097.

20. Percec, V.; Okita, S. *J. Polym. Sci. Part A: Polym. Chem.* **1993**, *31*, 877-884.

21. Billard, D. G. H.; Courtis, A.; Shirley, I. M.; Taylor, S. C. *J. Chem. Soc., Chem. Commun.* **1983**, *17*, 954-960.

22. Marvel, C. S.; Hartzell, G. E. *J. Am. Chem. Soc.* **1959**, *81*, 448-452.

23. Cassidy, P. E.; Marvel, C. S.; Ray, S. *J. Polym. Sci. Part A: Polym. Chem.* **1965**, *3*, 1553-1565.

24. Schluter, A. D. *J. Polym. Sci. Pt. A: Polym. Chem.* **2001**, *39*, 1533-1556 and references cited therein.

25. Colon, I.; Kelsey, D. R. *J. Org. Chem.* **1986**, *51*, 2627-2637.

26. Phillips, R. W.; Sheares, V. V.; Samulski, E. T.; DeSimone, J. M. *Macromolecules* **1994**, *27*, 2354-2356.

27. Hagberg, E. C.; Olson, D. A.; Sheares, V. V. *Macromolecules* **2004**, *37*, 4748-4754.

28. Wang, Y.; Quirk, R. P. *Macromolecules* **1995**, *28*, 3495-3501.

29. Pasquale, A. J.; Sheares, V. V. *J. Polym. Sci. Pt. A: Polym. Chem.* **1998**, *36*, 2611-2618.

30. Wang, Z. Y.; Franklin, J.; Venkatesan, D. *Macromolecules* **1999**, *32*, 1691-1693.

31. Bloom, P. D.; Jones III, C. A.; Sheares, V. V. *Macromolecules* **2005**, *38*, 2159-2166.

32. Percec, V.; Okita, S.; Weiss, R. *Macromolecules* **1992**, *25*, 1816-1823.

33. Percec, V.; Bae, J.-Y.; Zhao, M.; Hill, D. H. *Macromolecules* **1995**, *28*, 6726-6734.

34. Rehahn, M.; Schluter, A. D.; Wegner, G.; Feast, W. J. *Polymer* **1989**, *30*, 1060-1062.

35. Mohanty, D. K.; Lowery, R. C.; Lyle, G. D.; McGrath, J. E. *Int. SAMPE Symp. Exp.* **1987**, *32*, 408-419.

36. www.maxdem.com/polyphenylenes.html

37. www.mptpolymers.com/srp_about.html

38. Rodgers, F. E. (E. I. du Pont de Nemours and Co.). U. S. Patent 3,356,648, 1967.

39. Cassidy, P. E.; Aminabhavi, T. M.; Farley, J. M. *J. Macromol. Sci. – Rev. Macromol. Chem. Phys.*, **1989**, *C29(2&3)*, 365-429 and references cited therein.

40. Cassidy, P. E. *J. Macromol. Sci. – Rev. Macromol. Chem. Phys.*, **1994**, *C34(1)*, 1-24 and references cited therein.

41. Bruma, M.; Fitch, J. W.; Cassidy, P. E. *J. Macromol. Sci. – Rev. Macromol. Chem. Phys.*, **1996**, *C36(1)*, 119-159 and references cited therein.

42. Sprague, L. G. (Halocarbon Products Co.). U. S. Patent 6,274,005, 2001.

43. Ohtsuka, T.; Yamamoto, Y. (Daikin Industries, Ltd.). U. S. Patent 6,933,413, 2005.

44. Otto, S. (Isovolta Osterreichische Isolierstoffwerke Aktiengesellschaft). U. S. Patents 4,467,122, 1984 and 4,503,266, 1985.

45. Carvill, B.; Glasgow, K.; Roland, M. (Cantor Colburn, LLP). U. S. Pat. Appl. 20050004406 A1, 2005.

46. Kelleghan, W. J. (Hughes Aircraft Co.). U. S. Patent 4,503,254, 1985.

47. Lau, K. S. Y.; Kelleghan, W. J. (Hughes Aircraft Co.). U. S. Patent 4,695,655, 1987.

48. Marsitsky, D.; Vestberg, R.; Blainey, T. T.; Hawker, C. J.; Karter, K. R. *J. Am. Chem. Soc.* **2001**, *123*, 6965-6972.

49. Bunz, U. H. F. *Chem. Rev.* **2000**, *100*, 1605-1644.

50. Yamamoto, T.; Morita, A.; Miyazaki, Y.; Maruyama, T.; Wakayama, H.; Zhou, Z.-H.; Nakamura, Y.; Kanbara, T.; Sasaki, S.; Kubota, K. *Macromolecules* **1992**, *25*, 1214-1223.

51. Yamamoto, T. *Prog. Polym. Sci.* **1992**, *17*, 1153-1205.

52. Beinhoff, M.; Bozano, L. D.; Scott, J. C.; Carter, K. R. *Macromolecules* **2005**, *38*, 4147-4156.

53. Colon, I.; Kwiatkowski, G. T. *J. Polym. Sci. Pt. A Polym. Chem.* **1990**, *28*, 367-383.

54. Ueda, M.; Ito, T. *Polymer Journal* **1990**, *23*, 297-303.

55. Ueda, M.; Ichikawa, F. *Macromolecules* **1990**, *23*, 926-930.

56. Ueda, M.; Miyaji, Y.; Ito, T.; Obu, Y.; Sone, T. *Macromolecules* **1991**, *24*, 2694-2697.

57. Wang, J.; Sheares, V. V. *Macromolecules* **1998**, *31*, 6769-6775.

58. Ghassemi, H.; McGrath, J. E. *Polymer* **1997**, *38*, 3139-3143.

59. Rusch-Salazar, L. A.; Sheares, V. V. *J. Polym. Sci. Pt. A: Polym. Chem.* **2003**, *41*, 2277-2287.

60. Yonezawa, N.; Ikezaki, T.; Nakamura, H.; Maeyama, K. *Macromolecules* **2000**, *33*, 8125-8129.

61. Ueda, M.; Ito, T.; Seino, Y. *J. Polym. Sci. Pt. A: Polym. Chem.* **1992**, *30*, 1567-1573.

62. Gao, C.; Zhang, S.; Gao, L.; Ding, M. *Macromolecules* **2003**, *36*, 5559-5565.

63. Havelka, P. A.; Kazukiyo, N.; Freeman, B. D.; Sheares, V. V. *PMSE Preprints* **1999**, *81*, 533-534.

64. Havelka, P. A.; Kazukiyo N.; Freeman, B. D.; Sheares, V. V. *Macromolecules* **1999**, *32*, 6418-6424.

65. Sheares, V. V. (Iowa State University Research Foundation, Inc.). U.S. Patent 6,515,101, February 4, 2003.

66. Percec, V.; Bae, J.-Y.; Zhao, M.; Hill, D. *J. Org. Chem.* **1995**, *60*, 176-185.

67. Percec, V.; Zhao, M.; Bae, J.; Hill, D. *Macromolecules* **1996**, *29*, 3727-3735.

68. Grob, M. C.; Feiring, A. E.; Auman, B. C.; Percec, V.; Zhao, M.; Bae, J.; Hill, D. *Macromolecules* **1996**, *29*, 7284-7293.

CHAPTER 2. ISOMERIC HEXAFLUOROISOPROPYLIDENE-LINKED BENZOPHENONE POLYMERS VIA NICKEL CATALYSIS

A paper to be submitted to *Macromolecules*.

Dejan D. Andjelkovic and Valerie V. Sheares

Abstract

High performance hexafluoroisopropylidene (HFIP)-linked benzophenone polymers were synthesized by means of Ni(0)-catalyzed polymerization of newly developed bis(aryl triflate) and bis(aryl chloride) monomers. All polymers were amorphous and soluble in most common organic solvents, thus allowing molecular weight determination and spectroscopic analysis. Number average molecular weights were in the range of 14-29 x 10^3 g/mol (GPC/RI) and 24-43 x 10^3 g/mol (GPC/MALLS). Polymers exhibited high thermal stabilities with 10% weight loss temperatures ranging from 509-573 °C and 497-559 °C in nitrogen and air, respectively. Glass transition temperatures ranged from 161 to 190 °C. All polymers were pale yellow to yellow powders with UV absorption in the range of 246 to 304 nm. As with most previously synthesized 2,5-benzophenone polymers, these new materials exhibited poor film-forming properties and produced brittle films when cast from $CHCl_3$. Consequently, a new strategy based on nickel-catalyzed copolymerization was developed to circumvent this problem and to prepare polymers with higher molecular weights, improved film-forming ability and excellent mechanical properties. The unique structural characteristics of these new HFIP-interrupted poly(paraphenylene)s make them potentially

interesting candidates for separations applications, as well as for electronics applications, such as nonvolatile organic memory.

Introduction

Ni(0)-catalyzed polycondensation of bifunctional monomers has been used extensively over the past two decades as a very attractive approach toward high performance polymers.[1-8] The process leads to the formation of aromatic carbon-carbon bonds under mild conditions, while also being quite tolerant of numerous aprotic functional groups.[9] Considerable interest in the mechanism of this reaction has resulted in a better understanding of the role of monomer structure, ligands, temperature and reducing metal on the polymerization.[1,9,10] It has been shown that polymerization of carefully designed difunctional monomers can easily provide an array of polymeric materials for targeted applications from structural to optoelectronic materials.[3-5,11-15]

Our efforts in this area have been focused on the preparation of a number of functionalized poly(benzophenone)s (**PBP**)[3,5,10,16] and hexafluoroisopropylidene (HFIP)-containing materials (Figure 1).[11,12,17] **PBPs** are unique polymers with conjugated and conformationally rigid backbones. They possess superb thermal stability and exceptional strength and stiffness.[4] The tensile modulus of these materials reaches 7-17 GPa (1-2.5 MPSI), which is 2-4 times greater than other high performance thermoplastics.[13,14]

In spite of the excellent thermal and mechanical properties of the poly(2,5-benzophenone)s, it has been a challenge to synthesize materials having good film-forming properties. This is due to the inherent structural rigidity of the 2,5-benzophenone repeat units that increase the modulus and simultaneously decrease flexibility and film-forming ability.[3,10,13,16] Flexible, creasable films are highly desirable as they are a requirement for

potential electronic, coating, and membrane applications.[11,15,18] As such, numerous approaches have been taken to address this issue. Our group has shown that neither a significant increase in the molecular weight (from $<M_n>$ of 25 to 50 x 10^3 g/mol) or the incorporation of various flexible side groups improves the film-forming properties of the homopolymers.[10] In fact, the only flexible films that have been formed have been made from multiblock copolymers with bisphenol-A based polyarylene ether ketone or from crosslinked copolymers that formed thermoset films.[16,19,20]

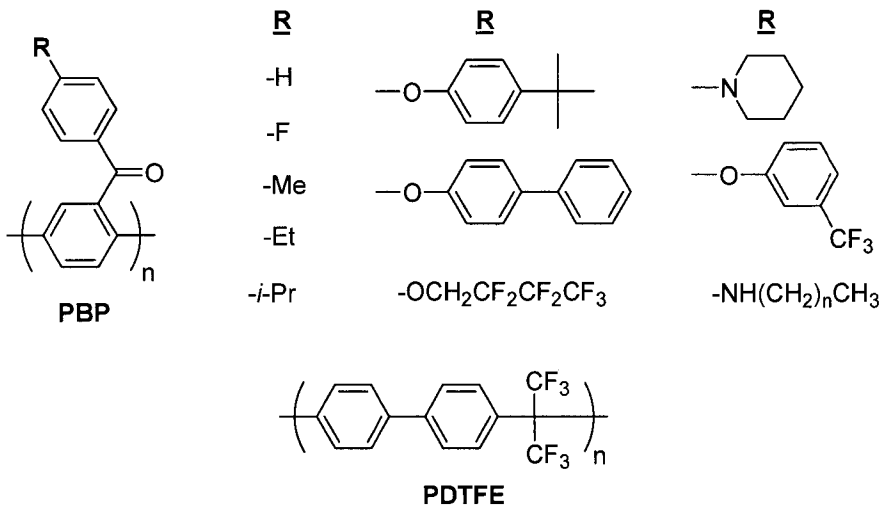

Figure 1. Chemical structures of selected polybenzophenone and HFIP-containing polymers.

As previously mentioned, we have also synthesized a new class of HFIP-containing polymers by Ni(0)-catalyzed polymerization of the corresponding bischloride monomers.[11,12] For example, poly[[1,1'-biphenyl]-4,4'-diyl[2,2,2-trifluoro-1-(trifluoromethyl) ethylidene]] (**PDTFE**), a highly soluble, aromatic glassy polymer with excellent thermal stability, minimal moisture absorption, low dielectric constant and very good gas permeability properties has been produced. In contrast to the polybenzophenones, the HFIP-interrupted

polyparaphenylene backbone has increased flexibility and solubility, allowing the formation of flexible, creasable films when cast from chloroform solution.

The goal of the present work is the development of a new class of HFIP-containing polymers with the combined structural features of the above mentioned **PBPs** and HFIP-polymers. This combination of structural features may extend the utility of these materials to applications that were previously inaccessible. Specifically, the design and synthesis of HFIP-linked isomeric benzophenone polymers via Ni(0)-catalyzed coupling polymerization of newly developed bis(aryl chloride) and bis(aryl triflate) monomers is described. Based on our model studies, a new method for the optimization of polymer properties using Ni(0)-catalyzed copolymerization of newly developed multifunctional monomers is presented.

Experimental Procedure

Materials. All materials were purchased either from Aldrich or Fisher and used without further purification unless otherwise noted. Tetrahydrofuran (THF) was distilled from sodium and benzophenone prior to use. Bipyridine (Bipy) was purified by recrystallization from ethanol while triphenylphosphine (TPP) was recrystallized from cyclohexane. Both reagents were dried under vacuum for 24h at room temperature and stored in the glove box under nitrogen. The catalyst $(Ph_3P)_2NiCl_2$ and powdered (100 mesh) zinc (99.999%) were purchased from Aldrich and stored under nitrogen.

Characterization. ^{1}H, ^{13}C, and ^{19}F NMR spectra were obtained using either a Varian VXR400 (400 MHz) or a VXR300 (300 MHz) spectrometer in deuterated methylene chloride (CD_2Cl_2). FT-IR measurements were conducted on a Schimadzu 8300 instrument in attenuated total reflectance (ATR) mode. Elemental analysis of the synthesized monomers and polymers was performed using a Perkin-Elmer model 2400 series II CHN/S instrument.

Molecular weights, relative to narrow polystyrene standards, were measured using a Waters GPC system consisting of a Waters 510 pump, a Waters 717 autosampler, a Wyatt Optilab DSP refractometer, and a Wyatt Dawn EOS light scattering detector. THF was used as the mobile phase at a flow rate of 1 mL/min with a sample injection volume of 200 μL. The system was equipped with four styragel columns (Polymer labs PLgel 100, 500, $1x10^4$, and $1x10^5$ Å) and heated at 40 °C. The dn/dc measurements were performed in THF at a flow rate of 0.2 mL/min using the above mentioned Wyatt Optilab DSP refractometer connected to the GPC system. Sample solutions were injected manually through the 1 mL loop connected to the switchboard. Glass transition temperatures were determined by differential scanning calorimetry (DSC) at the inflection point of the endotherm using a Perkin Elmer Pyris 1 instrument under a nitrogen purge at a heating rate of 20 °C/min. Monomer melting points were also measured using DSC. Thermogravimetric analysis (TGA) was carried out on a Perkin-Elmer TGA-7 in nitrogen and in air at a heating rate of 20 °C/min. UV-Vis spectra were measured on a HP 8542A Diode Array Spectrophotometer using polymer solutions in THF with 0.05 mmol/L concentrations calculated with respect to the repeating units. Dynamic mechanical analysis (DMA) data were obtained using a Perkin Elmer dynamic mechanical analyzer DMA Pyris-7e in the three-point bending mode. Rectangular specimens of 1 mm thickness and 5 mm depth were used for the analysis. The width to depth ratio was maintained at approximately 3.

Monomer Synthesis. 2,2-Bis(*p*-methoxyphenyl)hexafluoropropane (1). Commercially available 60% sodium hydride in oil (7.2 g, 0.18 mol) was added to a 500 mL three-necked round bottom flask equipped with a condenser. The flask was sealed with a rubber septum and purged with argon. *n*-Pentane (40 mL) was added to the flask via syringe,

stirred for 5 minutes, and then allowed to settle for 1 minute. Pentane solution above the solid sodium hydride was removed using a syringe and the process repeated twice with pentane and once with dry THF. After all of the oil was removed from the suspension, the flask was charged with 100 mL of dry THF and stirred for 10 minutes. Commercially available 2,2-bis(hydroxyphenyl)hexafluoropropane (BisAF) (20.0 g, 0.06 mol) was dissolved in 150 mL of THF into a 250 mL round bottom flask and sealed with a septum. The BisAF solution was added dropwise to the NaH solution via cannula under an Argon purge and the reaction mixture left to reflux for 12 hours. The solution was cooled in an ice bath and slowly charged with a mixture of dimethylsulfate (17 mL, 0.18 mol) in 200 mL of THF. After addition, the ice bath was removed and the reaction mixture was refluxed for 4 hours. The mixture was allowed to cool to room temperature and filtered. The filtrate was concentrated under reduced pressure, dissolved in 500 mL of *n*-pentane and purified by flash chromatography on basic alumina. Pentane was removed under reduced pressure to give 21.0 g (96%) of colorless dense liquid. Anal.: Calcd. for $C_{17}H_{14}O_2F_6$: C, 56.04; H, 3.85. Found: C, 56.35; H, 4.14. FT-IR: 3009 cm^{-1} (weak), 2964 cm^{-1}, 1609 cm^{-1}, 1516 cm^{-1}, 1250 cm^{-1}, 1166 cm^{-1}, 1037 cm^{-1}, 966 cm^{-1}, 925 cm^{-1}, 823 cm^{-1}, 740 cm^{-1}. ^1H NMR (300 MHz, CD_2Cl_2) δ = 7.35 (d, J_{ortho} = 8.79 Hz, 2H); 6.90 (dt, J_{ortho} = 9.18 Hz, J_{meta} = 2.10 Hz, 2H); 3.84 (s, 3H); ^{13}C NMR: δ = 64.41 (septet, $^2J_{C-F}$ = 100.08 Hz, $C(CF_3)_2$), 125.34 (quartet, $^1J_{C-F}$ = 1131.24 Hz, CF_3), 55.85 (s, $2CH_3$) , 114.23, 126.03, 132.14, 160.70. ^{19}F NMR: δ = -64.88 (s, 6F, $2CF_3$).

2,2-Bis((3-benzoyl)-4-hydroxyphenyl)hexafluoropropane (2). 2,2-Bis(*p*-methoxyphenyl)hexafluoropropane (115.23 g, 0.317 mol), 300 mL of nitromethane, and 114 mL (1.266 mol) of benzoyl chloride were mixed in a 1L round bottom flask equipped with a

$CaCl_2$ drying tube and stirred in an ice bath. The $AlCl_3$ (169.05 g, 1.27 mol) was added in small portions. Upon the addition of $AlCl_3$, the reaction mixture was left to stir overnight at room temperature. HCl that evolved during the reaction was collected in a $NaHCO_3$ trap. The reaction mixture was then poured into 500 mL of 10% HCl in ice water. The precipitate was extracted with CH_2Cl_2, washed twice with saturated $NaHCO_3$ and brine, dried over anhydrous sodium sulfate and decolorized three times with activated charcoal. The solvent was removed under reduced pressure and the product recrystallized from *n*-heptane/ethyl acetate (4:1) to yield 120.5 g (70%) of yellow crystals. Mp = 149.4 °C (DSC). Anal.: Calcd. for $C_{29}H_{18}O_4F_6$: C, 63.97; H, 3.31. Found: C, 63.98; H, 3.70. FT-IR: 3063 cm^{-1} (broad, weak, OH), 1627 cm^{-1} (C=O), 1490 cm^{-1}, 1334 cm^{-1}, 1205 cm^{-1}, 1179 cm^{-1}, 1135 cm^{-1}, 1005 cm^{-1}, 704 cm^{-1}. ^1H NMR: δ = 7.12 (d, J = 9.0 Hz), 7.47 (t, J = 7.4 Hz), 7.54 (d, J = 8.96 Hz), 7.57-7.64 (m), 7.70 (d, J = 1.92 Hz), 12.05 (s, OH). ^{13}C NMR: δ = 63.53 (septet, $^2J_{C\text{-}F}$ = 103.12 Hz, $C(CF_3)_2$), 124.30 (quartet, $^1J_{C\text{-}F}$ = 1144 Hz, CF_3), 115.55, 118.86, 123.01, 128.56, 129.55, 132.87, 135.49, 137.05, 137.45, 163.54, 201.02 (CO). ^{19}F NMR: δ = -65.10 (s, 6F, $2CF_3$).

2,2-Bis(3-(4-fluorobenzoyl)-4-hydroxyphenyl)hexafluoropropane (3). Following the same procedure for the synthesis of **2**, 24.8 g (0.068 mol) of **1** was acylated using 32 mL (0.273 mol) of 4-fluorobenzoyl chloride in the presence of 36.3 g (0.273 mol) of $AlCl_3$. Recrystallization yielded 30.19 g (74.5%) of yellow crystals. Mp = 146.6 °C (DSC). Anal.: Calcd. for $C_{29}H_{16}O_4F_8$: C, 60.0; H, 2.76. Found: C, 60.02; H, 3.43. FT-IR: 3080 cm^{-1} (broad, weak, OH), 1627 cm^{-1} (C=O), 1601 cm^{-1}, 1485 cm^{-1}, 1334 cm^{-1}, 1227 cm^{-1}, 1205 cm^{-1}, 1152 cm^{-1}, 1006 cm^{-1}, 850 cm^{-1}, 793 cm^{-1}. ^1H NMR: δ = 7.10-7.20 (m, 6H), 7.51 (dd, J_{ortho} = 8.96 Hz, J_{meta} = 1.76 Hz, 2H), 7.60-7.63 (m, 4H), 7.64 (d, J_{meta} = 1.48 Hz, 2H), 11.89 (s, 2H, OH). ^{13}C NMR: δ = 63.88 (septet, $^2J_{C\text{-}F}$ = 101.6 Hz, $C(CF_3)_2$), 116.17, (d, $^2J_{C\text{-}F(ortho)}$ = 87.96 Hz,

C_{aryl}), 119.13, 119.30, 123.37, 124.61 (quartet, $^{1}J_{C\text{-}F}$ = 1141.84 Hz, CF_3), 132.62 (d, $^{3}J_{C\text{-}F(meta)}$ = 36.4 Hz, C_{aryl}), 133.67 (d, $^{4}J_{C\text{-}F(para)}$ = 12.12 Hz, C_{aryl}), 135.41, 137.83, 163.77, 165.92 (d, $^{1}J_{C\text{-}F}$ = 1011.44 Hz, C_{aryl}-F), 199.72 (CO). ^{19}F NMR: δ = -65.11 (s, 6F, $2CF_3$), -106.23 (m, 1F, $C_{ring}F$).

2,2-Bis(3-(4-chlorobenzoyl)-4-hydroxyphenyl)hexafluoropropane (4). Following the same procedure for the synthesis of **2**, 20.7 g (0.057 mol) of **1** was acylated using 28.9 mL (0.228 mol) of 4-chlorobenzoyl chloride in the presence of 45.4 g (0.341 mol) of $AlCl_3$. Recrystallization gave 17.1 g (49%) of yellow crystals. Mp = 138.8 °C (DSC). Anal.: Calcd. for $C_{29}H_{16}O_4F_6Cl_2$: C, 56.78; H, 2.61. Found: C, 56.91; H, 3.11. FT-IR: 3063 cm^{-1} (broad, weak, OH), 1631 cm^{-1} (C=O), 1592 cm^{-1}, 1490 cm^{-1}, 1330 cm^{-1}, 1254 cm^{-1}, 1210 cm^{-1}, 1179 cm^{-1}, 1121 cm^{-1}, 921 cm^{-1}, 779 cm^{-1}. ^{1}H NMR: δ = 7.11-7.13 (d, J_{ortho} = 9.0, 2H), 7.46 (dt, J_{ortho} = 8.48 Hz, J_{meta} = 1.92 Hz, 4H), 7.51 (dd, J_{ortho} = 9.16, J_{meta} = 1.76 Hz, 2H), 7.56 (dt, J_{ortho} = 8.6 Hz, J_{meta} = 1.92 Hz, 4H), 7.67 (d, J_{ortho} = 2.12, 2H), 11.89 (s, 2H, OH). ^{13}C NMR: δ = 63.88 (septet, $^{2}J_{C\text{-}F}$ = 101.56 Hz, $C(CF_3)_2$), 124.60 (quartet, $^{1}J_{C\text{-}F}$ = 1141.84 Hz, CF_3), 119.04, 119.38, 123.40, 129.30, 131.39, 135.32, 135.77, 137.97, 139.64, 163.83, 199.95 (CO). ^{19}F NMR: δ = -65.06 (s, 6F, $2CF_3$).

2,2-Bis(3-benzoyl-4-(trifluoromethanesulfonyl)-oxyphenyl) hexafluoropropane (5). To an ice cooled biphasic mixture of toluene (20 mL), 30% (w/v) aqueous K_3PO_4 (40.5 mL), and **2** (5.515 g, 10.14 mmol) was added dropwise 4.1 mL of trifluoromethanesulfonic anhydride (24.3 mmol) at a rate to keep the reaction temperature below 10 °C. The reaction was allowed to warm to ambient temperature and stirred for one hour. The layers were separated and the toluene layer was washed twice with 50 mL of distilled water, dried over anhydrous sodium sulfate, and concentrated. The resulting dense pale yellow liquid was

dissolved in a small amount of ether and precipitated into *n*-pentane. The white precipitate was collected by filtration and was recrystalized twice from ethanol to give 4.46g (55%) of white crystals. Mp = 118 °C (DSC). Anal.: Calcd. for $C_{31}H_{16}O_8F_{12}S_2$: C, 46.04; H, 1.98; S, 7.92. Found: C, 45.78; H, 2.18; S, 7.95. FT-IR: 3110 cm^{-1} (weak), 1670 cm^{-1} (C=O), 1430 cm^{-1}, 1250 cm^{-1}, 1209 cm^{-1}, 1135 cm^{-1}, 1088 cm^{-1}, 1004 cm^{-1}, 886 cm^{-1}. ^1H NMR: δ = 7.46-7.59 (m, 3H), 7.62-7.68 (m, 1H), 7.70-7.78 (m, 3H). ^{13}C NMR: δ = 64.33 (septet, $^2J_{C-F}$ = 104.64 Hz, $C(CF_3)_2$), 119.08 (quartet, $^1J_{C-F}$ = 1273.76 Hz, F_3C-SO_3-), 124.12 (quartet, $^1J_{C-F}$ = 1143.36 Hz, F_3C-C), 123.72, 129.44, 130.62, 133.07, 133.38, 133.56, 134.76, 134.94, 136.37, 148.08, 191.73 (CO). ^{19}F NMR: δ = -65.00 (s, 3F, F_3C-C), -74.68 (s, 3F, F_3C-SO_3-).

2,2-Bis(3-(4-fluorobenzoyl)-4-(trifluoromethanesulfonyl)-oxyphenyl) hexafluoropropane (6). Following the same procedure for the synthesis of **5**, 15.39 g (26.53 mmol) of **3** was acylated using 11.2 mL (66.3 mmol) of trifluoromethanesulfonic anhydride. Recrystallization from ethanol gave 13.21 g (59%) of white crystals. Mp: 127.4 °C (DSC). Anal.: Calcd. for $C_{31}H_{14}O_8F_{14}S_2$: C, 44.07; H, 1.66; S, 7.59. Found: C, 43.71; H, 1.835; S, 7.215. FT-IR: 3110 cm^{-1} (weak), 1670 cm^{-1} (C=O), 1433 cm^{-1}, 1252 cm^{-1}, 1209 cm^{-1}, 1188 cm^{-1}, 1135 cm^{-1}, 1089 cm^{-1}, 1007 cm^{-1}, 886 cm^{-1}, 706 cm^{-1}. ^1H NMR: δ = 7.17-7.24 (m, 4H), 7.53-7.58 (m, 4H), 7.75-7.82 (m, 6H). ^{13}C NMR: δ = 64.67 (septet, $^2J_{C-F}$ = 104.64 Hz, $C(CF_3)_2$), 118.98 (quartet, $^1J_{C-F}$ = 1275.28 Hz, F_3C-SO_3-), 124.01 (quartet, $^1J_{C-F}$ = 1137.28 Hz, F_3C-C), 116.70 (d, $^2J_{C-F(ortho)}$ = 87.96 Hz, C_{aryl}), 123.72, 132.78 (d, $^4J_{C-F(para)}$ = 12.16 Hz, C_{aryl}), 133.11, 133.18, 133.33, 133.38 (d, $^3J_{C-F(meta)}$ = 40.0 Hz, C_{aryl}), 134.75, 147.84, 167.04 (d, $^1J_{C-F}$ = 1020.52 Hz, C_{aryl}-F), 190.17 (CO). ^{19}F NMR: δ = -64.49 (s, 3F, F_3C-C), -74.09 (s, 3F, F_3C-SO_3-), -103.66 (m, 1F, F-C_{ring}).

2,2-Bis(3-(4-chlorobenzoyl)-4-methoxyphenyl) hexafluoropropane (7). A mixture of 5.38 g (8.6 mmol) of **4**, 16.2 mL (172 mmol) of dimethyl sulfate, 23.7 g (172 mmol) of K_2CO_3, 250 mL of acetone, and 5 mL of DMF was heated to reflux for 24 hours. The reaction mixture was cooled to room temperature and the potassium salts were removed by suction filtration. The solvent was removed in a rotary evaporator to give a pale yellow solid. Double recrystalization from ethanol provided 3.88 g (70.6% yield) of colorless crystals. Mp: 194 °C (DSC). Anal.: Calcd. for $C_{31}H_{20}O_4F_6Cl_2$: C, 58.04; H, 3.12. Found: C, 57.955; H, 3.505. FT-IR: 3060 cm^{-1} (weak), 2964 cm^{-1} (weak), 1671 cm^{-1}(C=O), 1587 cm^{-1}, 1503 cm^{-1}, 1419 cm^{-1}, 1246 cm^{-1}, 1183 cm^{-1}, 1166 cm^{-1}, 1121 cm^{-1}, 828 cm^{-1}. ^1H NMR: δ = 3.75 (s, 6H, $2CH_3$), 7.06 (d, 2H, J = 9.0 Hz), 7.33 (d, J = 2.0 Hz, 2H), 7.40 (dt, 4H, J_{ortho} = 8.52 Hz, J_{meta} = 2.20 Hz), 7.61 (d, broad, 2H, J = 8.88 Hz), 7.69 (dt, 4H, J_{ortho} = 8.52 Hz, J_{meta} = 2.20 Hz). ^{13}C NMR: δ = 56.34 (s, CH_3), 64.07 (septet, J = 103.12 Hz, $C(CF_3)_2$), 124.75 (quartet, J = 1106.4 Hz, CF_3), 111.99, 125.56, 128.8, 129.23, 131.52, 131.8, 134.2, 136.31, 140.05, 158.22, 194.16 (CO). ^{19}F NMR: δ = -64.86 (s, 3F, F_3C-C).

General Polymerization Procedure. Poly[(2,2'-dibenzoylbiphenyl-4,4'-diyl)[bis(trifluoromethyl)methylene]] (P1). A previously flame-dried two-necked 50 mL pear-shaped flask equipped with an overhead stirrer was charged with 0.63 g (9.6 mmol, 3.1 eq) of zinc, 0.4 g (0.62 mmol, 0.2 eq) of catalyst $(Ph_3P)_2NiCl_2$, 0.162 g (0.62 mmol, 0.2 eq) of Ph_3P, 0.048 g (0.31 mmol, 0.1 eq) of Bipy, and 0.23 g (0.62 mmol, 0.2 eq) of tetrabutylammonium iodide. The reagents were combined in the glove-box under a nitrogen atmosphere. The flask was sealed with the septum, evacuated and refilled with argon three times, and charged with 6 mL of anhydrous THF via syringe. The catalyst mixture was stirred and heated in an oil bath at 25 °C under the argon purge. Once the color of the

catalyst mixture changed from deep green to dark red, 2.5 g (3.1 mmol) of monomer **5** dissolved in 3 mL THF was added via syringe. The reaction continued at 65 °C for 24 hours. The reaction mixture was then precipitated into 40% HCl/methanol to remove excess zinc and stirred overnight. The precipitate was collected by suction filtration, washed with saturated sodium bicarbonate and methanol, redissolved in chloroform, and reprecipitated into neutral methanol. The mixture was stirred for additional 24 hours and filtered. The recovered solid was dried in a vacuum oven to give 1.45 g (83% yield) of pale yellow powder. Anal.: Calcd. for $(C_{29}H_{16}O_2F_6)_n$: C, 68.24; H, 3.14. Found: C, 68.10; H, 3.46. FT-IR: 3060 cm^{-1} (weak), 1670 cm^{-1}(C=O), 1251 cm^{-1}, 1213 cm^{-1}, 1184 cm^{-1}, 1137 cm^{-1}, 1014 cm^{-1}, 698 cm^{-1}. ^{1}H NMR: δ = 7.10-7.45 (m, 12H), 7.56 (d, J = 7.48 Hz, 4H). ^{13}C NMR: δ = 64.67 (septet, J = 104.6 Hz, $C(CF_3)_2$), 124.35 (quartet, J = 1137.3 Hz, CF_3), 128.68, 130.51, 131.39, 131.84, 132.15, 132.53, 133.64, 137.28, 138.99, 140.52, 196.27 (CO). ^{19}F NMR: δ = -64.45 (s, 6F, F_3C-C).

Poly[(2,2'-di(4-fluorobenzoyl)biphenyl-4,4'-diyl)[bis(trifluoromethyl)methylene]] (P2). (72% yield). Anal.: Calcd. for $(C_{29}H_{14}O_2F_8)_n$: C, 63.74; H, 2.56. Found: C, 63.62; H, 2.86. FT-IR: 3074 cm^{-1} (weak), 1670 cm^{-1}(C=O), 1596 cm^{-1}, 1503 cm^{-1}, 1237 cm^{-1}, 1209 cm^{-1}, 1184 cm^{-1}, 1156 cm^{-1}, 851 cm^{-1}. ^{1}H NMR: δ = 6.93 (t, J = 8.52 Hz, 4H), 7.30-7.50 (m, 6H), 7.58 (m, 4H). ^{13}C NMR: δ = 64.73 (septet, J = 104.6 Hz, $C(CF_3)_2$), 115.8 (d, $^2J_{C\text{-}F(ortho)}$ = 87.96 Hz, C_{aryl}), 124.33 (quartet, $^1J_{C\text{-}F}$ = 1147.88 Hz, F_3C-C), 131.44, 132.01, 132.37, 132.63, 133.32 (d, $^3J_{C\text{-}F(meta)}$ = 37.92 Hz, C_{aryl}), 133.56 (d, $^4J_{C\text{-}F(para)}$ = 10.6 Hz, C_{aryl}), 138.66, 140.65, 164.99, 166.27 (d, $^1J_{C\text{-}F}$ = 1014.2 Hz, C_{aryl}-F), 194.69 (CO). ^{19}F NMR: δ = -64.47 (s, 3F, F_3C-C), -105.52 (m, 1F, F-C_{ring}).

Poly[biphenyl-4,4'-diylcarbonyl(6-methoxy-1,3-phenylene)[bis(trifluoromethyl)methylene](4-methoxy-1,3-phenylene)carbonyl] (P3). (87% yield). Anal.: Calcd. for $(C_{31}H_{20}O_4F_6)_n$: C, 65.26; H, 3.51. Found: C, 64.59; H, 4.06. FT-IR: 3053 cm^{-1} (weak), 2947 cm^{-1} (weak), 2840 cm^{-1} (weak), 1670 cm^{-1} (C=O), 1606 cm^{-1}, 1251 cm^{-1} (ArC-O-C), 1173 cm^{-1}, 1120 cm^{-1}, 1028 cm^{-1}, 1003 cm^{-1}, 815 cm^{-1}. ^1H NMR: δ = 3.75 (s, 6H, CH_3), 7.06 (d, 2H, J = 9.08 Hz), 7.30-7.38 (m, broad low intensity), 7.39 (d, 2H, J = 1.28 Hz), 7.42-7.54 (m, broad low intensity), 7.59 (d, 2H, J = 8.32), 7.69 (d, 4H, 8.44 Hz), 7.82 (d, 4H, 8.32 Hz). ^{13}C NMR: δ = 56.37 (s, CH_3), 64.10 (septet, J = 100.08 Hz, $C(CF_3)_2$), 111.98, 124.79 (quartet, J = 1137.32 Hz, CF_3), 125.49, 127.76, 129.17, 130.79, 131.72, 134.05, 137.30, 144.79, 158.23, 194.79 (CO). ^{19}F NMR: δ = -64.84 (s, $(F_3C)_2C$).

Results and Discussion

Monomer Design and Synthesis. The first step towards the synthesis of HFIP-linked benzophenone polymers was the selection of the monomers shown in Figure 2. Structures **A** and **B** were designed to resemble 2,2-bis(*p*-chlorophenyl)hexafluoropropane and 2,5-dichlorobenzophenone, whose Ni(0)-mediated polymerizations yield the above mentioned **PDTFE** and poly(2,5-benzophenone) materials. Type **A** monomers were structured such that the direction of polymerization coincided with the Bis-AF axis and produced the desired HFIP-linked benzophenone polymers. Due to the ease of synthesis, bistriflates rather than bischlorides were chosen for the type **A** monomers.

Type **B** monomers incorporated chlorobenzoyl groups as lateral substituents, allowing the chlorine atoms to serve as reactive sites, while protected hydroxyl groups of the corresponding bisphenol were left available for further chemistry. In this case, the polymerization direction did not coincide with the BisAF axis, but with the lateral substituent

axis, leading to a polymer backbone consisting of aromatic rings, carbonyl groups and HFIP units. Both types of newly developed monomers are symmetrical, rendering triflate and chloro groups of equal reactivity and evading problems related to regioselectivity and regularity present in Ni(0)-catalyzed polymerization of unsymmetrical *p*-ditriflates or *p*-dihaloarenes.[1,21]

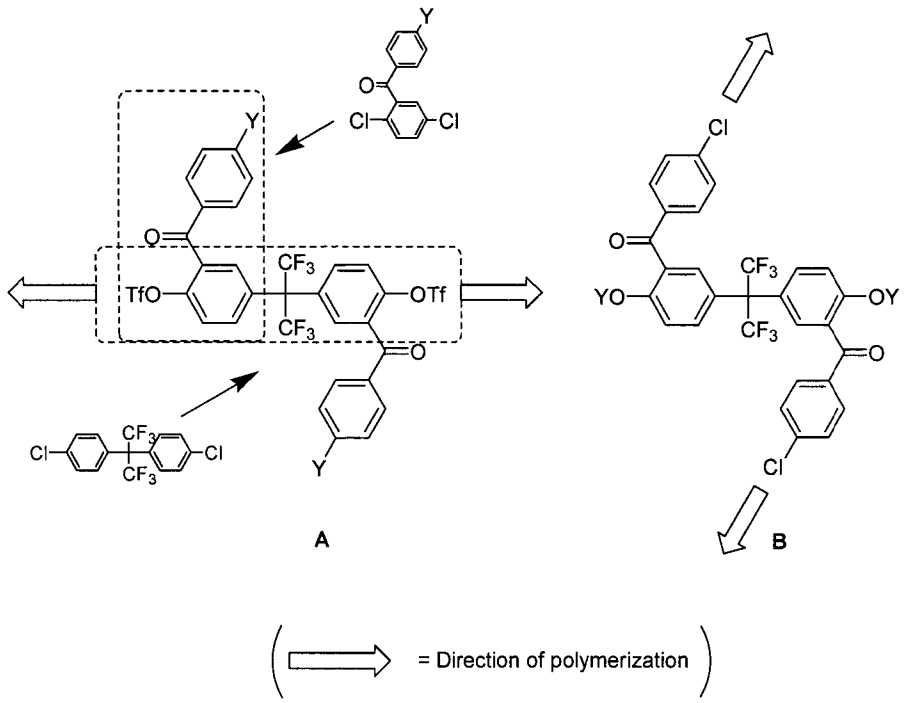

Figure 2. Design of bistriflate (type **A**) and dichloro (type **B**) monomers.

All monomers were derived from commercially available Bis-AF following the synthesis outlined in Scheme 1. Methylation of Bis-AF yielded 2,2-bis(*p*-methoxyphenyl)hexafluoropropane **1**, which was subjected to Friedel-Crafts reaction with substituted benzoyl chlorides as acylating agents. Excess $AlCl_3$ catalyzed the demethylation reaction of the acylation products,[20] resulting in symmetrical bisphenols **2-4** in 50-75% yield.

To the best of our knowledge, this is the first reported synthesis of these bisphenols. The chemical structures of **2-4** were verified by NMR, FT-IR and high resolution mass spectrometry.

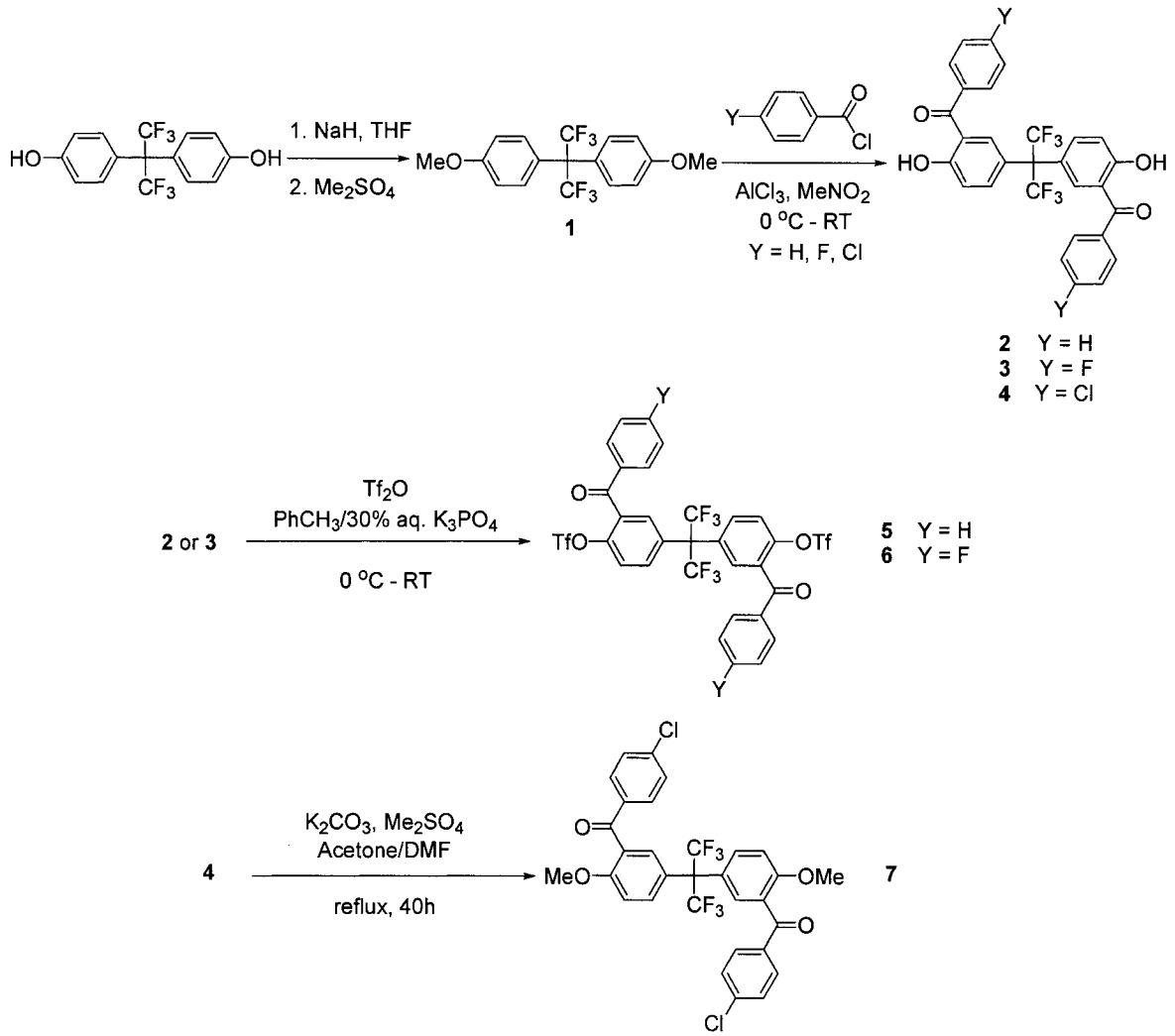

Scheme 1. Synthesis of new bistriflate and dichloro monomers **5-7**.

Bisphenols **2** and **3** were converted to bistriflates **5** and **6**, respectively, according to the procedure described by Frantz *et al.*[22] This method is a straightforward and efficient synthesis of pure aryl triflates under biphasic basic aqueous conditions, avoiding the use of

amine bases and time consuming chromatographic separation. Using this procedure, bistriflate monomers were produced in 55-60% yield. Chemical structures of these new monomers were confirmed by NMR, FT-IR, and high resolution mass spectrometry. Representative ^{13}C and ^{19}F NMR spectra of **6** are shown in Figure 3. ^{13}C NMR revealed a quintet at 64.6 ppm (**a**) for the quaternary carbon in HFIP. This peak actually represents a septet due to the coupling with six equivalent fluorine atoms with the outer most peaks hidden in the baseline. ^{13}C also shows two quartets at 119 and 124 ppm (**b** and **c**), which correspond to the carbons of the CF_3 groups in trifluoromethanesulfonate (OTf) and HFIP moieties, respectively. The aromatic carbon bound directly to the fluorine atom in the 4-fluorobenzoyl group appeared at 167 ppm (**d**) as a doublet ($^1J_{C\text{-}F}$ = 1020.52 Hz) due to the very strong C-F coupling. In addition, the carbonyl carbon is prominent at 190 ppm. The ^{19}F NMR spectrum, as expected, showed three different peaks corresponding to the different types of fluorine atoms present in the monomer.

Type **B** monomer **7** was prepared by methylation of **4** in 55-70% yield. It has been shown earlier that methoxy groups are compatible with Ni(0)-catalyzed coupling chemistry.[9,23] However, their presence on the benzene ring bearing active (chlorine or triflate) centers has also been shown to promote side reactions, such as phenyl transfer from TPP ligand, which causes premature cease of polymerization and reduction of molecular weights.[9] One of the advantages of monomer **7** is that the methoxy groups are located on the benzene ring which does not bear reactive chlorine atoms (Scheme 1). As a result, the likelihood of side reactions and retardation of reaction rates during polymerization are drastically lowered. Furthermore, if desired, the methoxy groups could be removed during the postpolymerization to yield hydroxyl groups available for further substitution.[24,25]

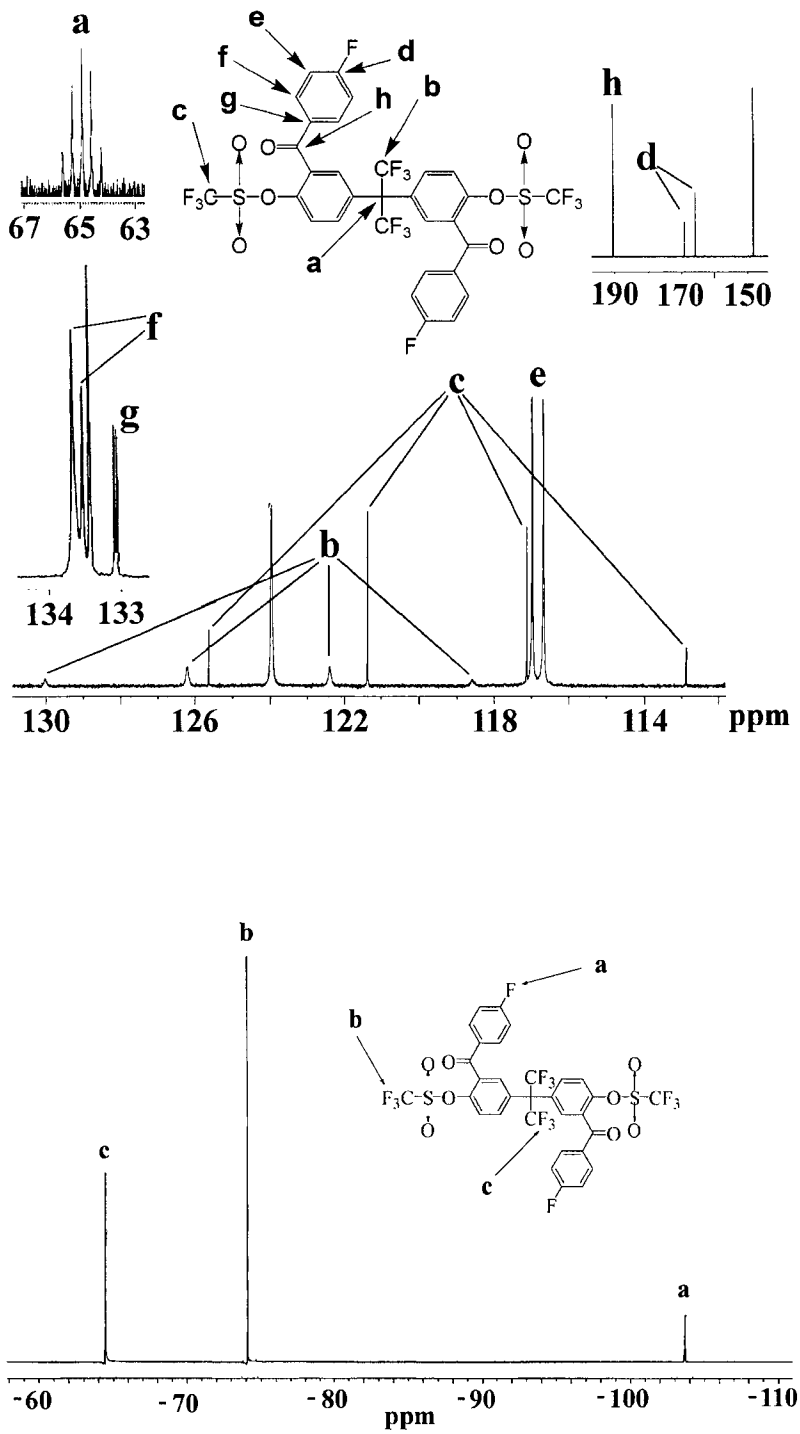

Figure 3. ^{13}C and ^{19}F NMR spectra of monomer **6**.

The monomer structure was confirmed by NMR, FT-IR, and high resolution mass spectrometry. Representative ^{1}H, and ^{19}F NMR spectra of **7** are shown in Figure 4. The ^{1}H NMR showed a singlet at 3.75 ppm corresponding to the hydrogen atoms of the methoxy group and several peaks in the 7.0-7.7 ppm region, corresponding to the aromatic hydrogens. Integration of aliphatic to aromatic peaks gave the correct 3:7 ratio. As expected, the ^{19}F NMR spectrum revealed a single peak corresponding to the fluorine atoms in the HFIP unit.

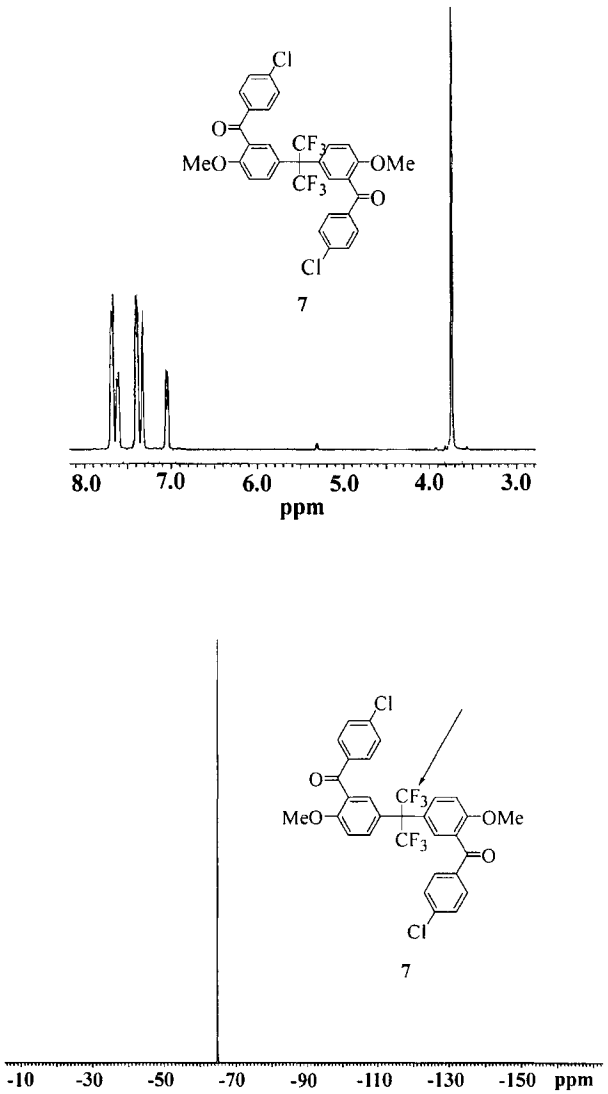

Figure 4. ^{1}H and ^{19}F NMR spectra of monomer **7**.

Polymer Synthesis and Characterization. The syntheses of HFIP-linked benzophenone polymers **P1-P3** are shown in Scheme 2. All polymerization reactions were conducted in THF using $(Ph_3P)_2NiCl_2$ as a catalyst, Zn as a reducing agent, *n*-Bu_4NI as a bridging agent, and TPP and Bipy as ligands. THF was chosen as the solvent as polymerization of bistriflates, bismesylates, and bischlorides in THF has been shown to minimize reduction and polymer degradation side reactions.[3,10,16,26,27]

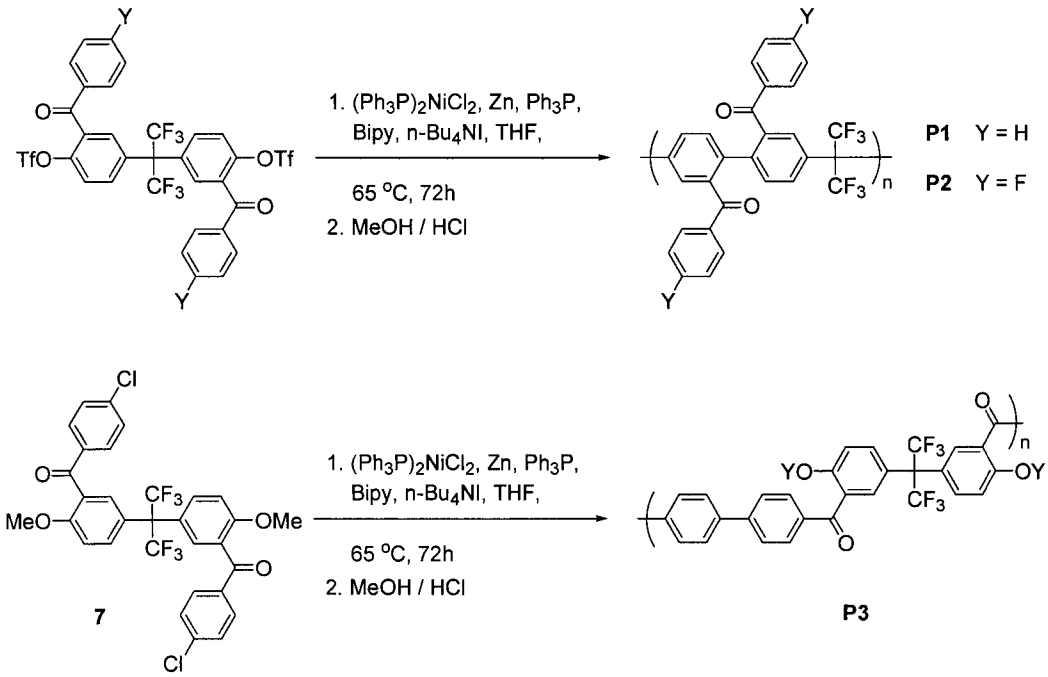

Scheme 2. Synthesis of HFIP-linked benzophenone polymers **P1-P3** via Ni(0)-mediated homocoupling of monomers **5-7**.

Optimization of the reaction conditions (temperature, time, ratio of catalyst components) resulted in the synthesis of moderate to high molecular weight polymers as evidenced by GPC (Table 1). Number average molecular weights were in the range of 14-28

x 10^3 g/mol by GPC/RI and 24-43 x 10^3 g/mol by GPC/MALLS. The $<M_n>$ values determined by GPC/MALLS were higher than those detected by GPC/RI by a factor of 1.5-1.7. These findings were in agreement with our previous observations related to **PDTFE** and were attributed to the differences in the hydrodynamic volumes of polymers **P1-P3** and polystyrene, used as the calibration standard.[11] Similar observations were reported by Carter and coworkers,[15] who also found that GPC/RI underestimated the molecular weight of similar materials by a factor of 1.6-1.8 in comparison with their quasi-elastic light scattering (QELS) data.

Table 1. Molecular weight data for polymers **P1-P3** and comparison with the properties of **PBPs** and **PDTFE.**

Polymer	$<M_n>_{GPC\ /\ MALLS}$ ($x10^{-3}$ g/mol)	$PDI_{GPC\ /\ MALLS}$	$DP_{GPC\ /\ MALLS}$	dn/dc (mL/g)
PBP1[28]	24.5	2.40	135	-
PBP2[16]	21.1	2.77	106	0.221
PDTFE[11]	19.2 / 27.5	1.61 / 1.25	63 / 91	0.075
P1	28.6 / 43.0	1.53 / 1.89	56 / 84	0.066
P2	14.2 / 24.4	1.72 / 1.55	26 / 45	0.050
P3	17.1 / 31.4	1.62 / 1.57	30 / 55	0.083
P1CRS	43.9 / 205.0	4.05 / 6.50	86 / 402	-

Polymerization conditions: $(Ph_3P)_2NiCl_2$ (0.2 eq.), Zn (3.1 eq.), Ph_3P (0.2 eq.), Bipy (0.1 eq.), *n*-Bu_4NI (0.2 eq.), 65 °C, 24h, equivalents given with respect to the monomer.

Polymers **P1-P3** were confirmed to be the desired HFIP-linked benzophenone materials by ^{1}H, ^{13}C, ^{19}F NMR, UV-Vis and IR spectroscopies, as well as by elemental analysis. In addition, ^{19}F NMR spectral analysis of each polymer showed that all trifluoromethanesulfonate groups at the ends of the polymer chains had been reduced during the acidic workup, rendering the polymer chain ends unreactive. This was confirmed by the complete absence of the resonances at -74 ppm, corresponding to fluorine atoms in these functional groups. Interestingly, this observation was the opposite of that reported by Carter and co-workers, regarding their materials prepared via Ni(0)-mediated Yamamoto-type polycondensation of bisphenol-derived bistriflate monomers.[15] The reason for these differing observations is most likely related to the differences between the two Ni(0)-based polycondensation methods. While Yamamoto's polycondensation method[29,30] requires stoichiometric amounts of Ni(0) catalyst, Bipy and 1,5-cyclooctadiene (COD) as ligands for the reductive aryl-aryl coupling reaction, the approach that we utilized requires catalytic amounts of Ni(II)-salt, bridging agent and ligands, along with excess reducing agent needed for *in situ* generation of Ni(0) catalyst.

All polymers were amorphous pale yellow to yellow solids soluble in most common organic solvents such as tetrahydrofuran and chloroform. The materials showed no evidence of crystallinity by wide-angle X-ray diffraction or DSC. A representative X-ray diffraction pattern of polymer **P1** (Figure 5) revealed two peaks at 15 and 24 degrees and closely resembled the X-ray diffraction pattern of the parent **PDTFE** polymer.[11]

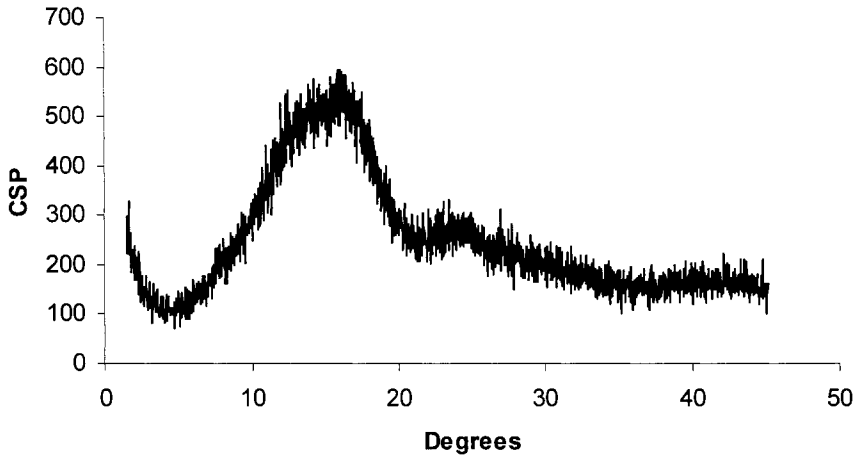

Figure 5. Representative powder X-Ray diffraction pattern of P1.

Thermal Analysis. The glass transition temperatures (T_g) of the new materials were measured by differential scanning calorimetry (DSC). The results are shown in Table 2. When compared to the parent **PDTFE** (T_g = 255 °C), **P1** and **P2** had significantly lower T_g values of 161 and 163 °C, respectively. This can be attributed to the presence of the bulky benzoyl pendant groups, which effectively separate **P1** and **P2** polymer chains, thus increasing segmental mobility and lowering the activation energy needed for the onset of the long-range cooperative motion of polymer chains.[30] In contrast, the effect of the HFIP unit on **PBP** materials is quite small, indicating the dominating effect of the benzophenone moiety on conformational rotation in these hybrid structures. Specifically, the T_g values of **P1** and **P2** of 161 °C and 163 °C, respectively, are similar to their poly(2,5-benzophenone) analogues (**PBP1** = 158 °C, **PBP2** = 167 °C)[16, 28] However, the molecular weight of **P2** is significantly lower than the **PBP2** material used for comparison and serves as an indication that the maximum T_g of the polymer has not been achieved. **P3** was compared to a non-

HFIP-containing analogue, wholly aromatic polyketone (**WAPK**) with a T_g of 218 °C, synthesized by Yonezava *et al.*[31] As expected, **P3** has a much lower T_g due to the presence of the flexible HFIP groups.

Table 2. Thermal and UV-Vis data for polymers **P1-P3** and their comparison with the properties of **PBPs** and **PDTFE**.

Polymer	$<M_n>_{GPC\ /\ MALLS}$ ($x10^{-3}$ g/mol)	T_g (°C)	$T_{5\%}$ (°C)[a] N_2/Air	$T_{10\%}$ (°C)[b] N_2/Air	λ_{max} Abs. (nm)[c]
PBP1[28]	24.5	159	526/530	566/568	-
PBP2[16]	21.1	167	576 / 536	611 / 566	-
PDTFE[11]	19.2 / 27.5	255	515 / 515	533 / 535	266
P1	28.6 / 43.0	161	548 / 520	573 / 553	246
P2	14.2 / 24.4	163	537 / 539	557 / 559	246
P3	17.1 / 31.4	190	484 / 469	509 / 497	304
P1CRS	43.9 / 205.0	165	527 / 538	563 / 558	248

[a] 5% weight loss temperatures determined in nitrogen and air respectively. [b] 10% weight loss temperatures determined in nitrogen and air respectively. [c] THF solutions of polymers were used for the analysis.

Thermal stabilities of the polymers were examined by thermogravimetric analysis (TGA). Polymers **P1** and **P2** showed good thermal stability with 5% weight loss temperatures of 548 and 537 °C in nitrogen, and 520 and 539 °C in air, respectively. These values were higher than those for **PDTFE** polymer. Also, these values were higher than

those for **P3** (440 °C), whose methoxy groups led to decreased thermal stability. The same trend was observed for 10% weight loss temperatures.

UV-Vis Analysis. The UV-Vis spectra of the synthesized polymers were measured in THF solution (Figure 6). Polymers **P1** and **P2** had the same λ_{max} absorbance values of 246 nm, which were blue-shifted when compared to the 266 nm λ_{max} value for **PDTFE** measured in THF. This effect is most likely due to the steric repulsion of the two *ortho* benzoyl groups in the 2,2'-dibenzoylbiphenyl segments of **P1** and **P2**. Namely, bulky groups are known to increase the deviation from coplanarity in biphenyl systems with a consequent loss of conjugation and decrease in λ_{max}.[33] Apparently, this effect is not present in **P3** due to the lack of bulky benzoyl groups on biphenyl segments, which results in a red shift (λ_{max} = 304 nm) when compared to the **PDTFE**. As expected, absorption maxima of the synthesized polymers **P1** and **P2** were much lower than those of analogous **PBP1** and **PBP2** (> 350 nm) due to the disrupted conjugation caused by the presence of non-conjugated HFIP unit.

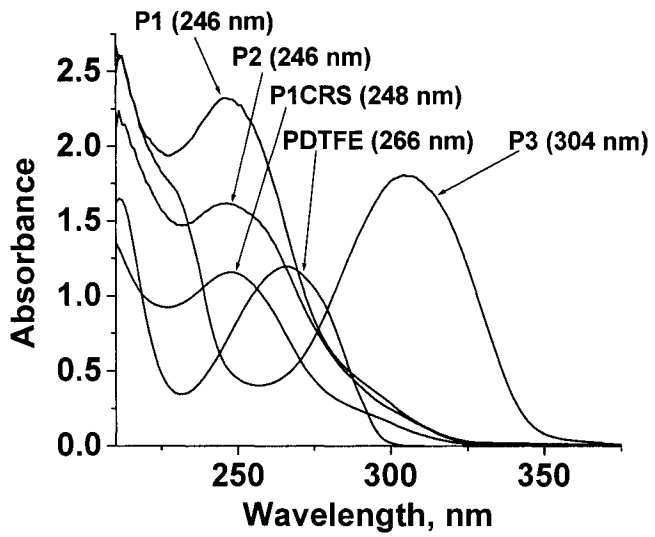

Figure 6. UV-Vis spectra of the HFIP-containing polymers measured in THF solution.

New Crosslinking Methodology. While new high performance polymers have been described, the goal of the work was to address the important problems that remain unsolved for 2,5-benzophenone type polymers. Specifically, the goal was to produce materials with the processable, film-forming properties of our previously synthesized HFIP materials, but with mechanical properties resembling those of the poly(2,5-benzophenone)s. Although the new homopolymers **P1-P3** did have good thermal stability and are soluble in common organic solvents, the materials do not have good film-forming properties and gave brittle, non-creasable films when cast from $CHCl_3$. In our previous work, postpolymerization crosslinking chemistry based on nucleophilic aromatic substitution (S_NAr) was used to produce thermoset films with increased chemical resistance, thermal stability and improved flexibility.[16,20] This method proved to be efficient in the modification of polyparaphenylenes such as poly(4'-fluoro-2,5-diphenylsulfone)s and poly(4'-fluoro-2,5-benzophenone)s, as well as poly(4'-fluorophenyl-bis(4-phenyl)phosphine oxide)s.[8] However, only polymer **P2** meets the structural requirements for this type of modification. Moreover, the resulting materials are thermoset polymers. While useful, the goal here was to gain the desired properties in thermoplastic materials. Therefore, in order to develop a general strategy applicable to any of the polymers made by the nickel coupling chemistry, a different synthetic approach was required. The new method involved Ni(0)-catalyzed copolymerization of the already synthesized monomers **5-7** and a newly developed comonomer that is polyfunctional with respect to the polymerization method. This comonomer was used in very small amounts to branch or slightly crosslink the materials.

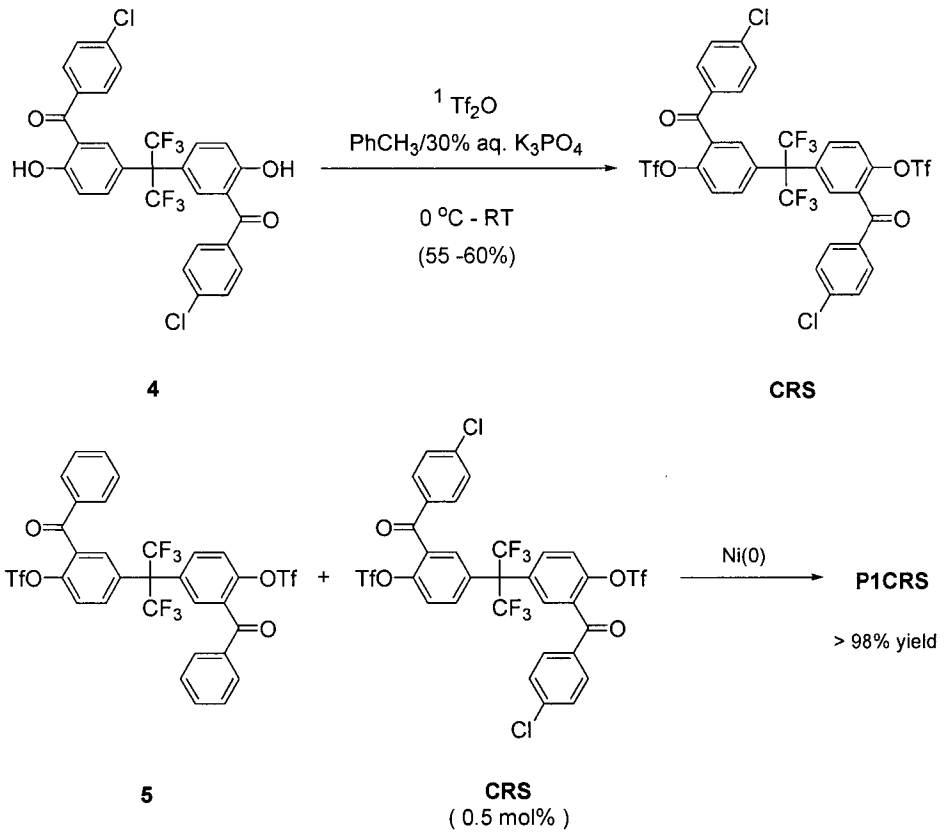

Scheme 3. Synthesis of **CRS** comonomer and copolymerization with monomer **5** to produce copolymer **P1CRS**.

Again, the first step in this process was the design and synthesis of an effective comonomer. We decided to use the already developed synthetic approach for type **A** monomers and convert bisphenol **4** into the corresponding bistriflate comonomer 2,2-bis(3-(4-chlorobenzoyl)-4-(trifluoromethanesulfonyl)oxyphenyl) hexafluoropropane (**CRS**) as shown on Scheme 3. **CRS** is a tetrafunctional crosslinker since both chloro and triflate groups are able to effectively undergo Ni(0)-catalyzed coupling. In a model study, the **CRS** crosslinker was used for Ni(0)-mediated copolymerization with monomer **5**.

The **CRS** load, as low as 0.5 mol% with respect to monomer **5**, gave almost quantitative yield of soluble, pale yellow copolymer **P1CRS**. The synthesized polymer had a number average molecular weight of 43 x 10^3 g/mol with a PDI of 4.05 (by GPC/RI) and 20 x 10^4 g/mol and a PDI of 6.50 (by GPC/MALLS) (Table 1). As previously mentioned, in the case of other polymers, GPC/MALLS data gave much higher M_n value than GPC/RI data. The **P1CRS** molecular weight was underestimated by a factor of 4.7. ^{1}H-NMR spectra of **P1** and **P1CRS** revealed two types of peaks in the aromatic region, the low intensity peaks attributed to the end-groups of corresponding polymers and high intensity peaks attributed to the aromatic hydrogens along the polymer backbone (Figure 7). Their integration provided a good estimate of the average degree of polymerization (DP) for **P1** (DP = 123) and **P1CRS** (DP = 476). Further comparison of ^{1}H-NMR data with the GPC data (Table 1) revealed better correlation with GPC/MALLS data than with GPC/RI data, indicating that the light scattering data were more reliable.

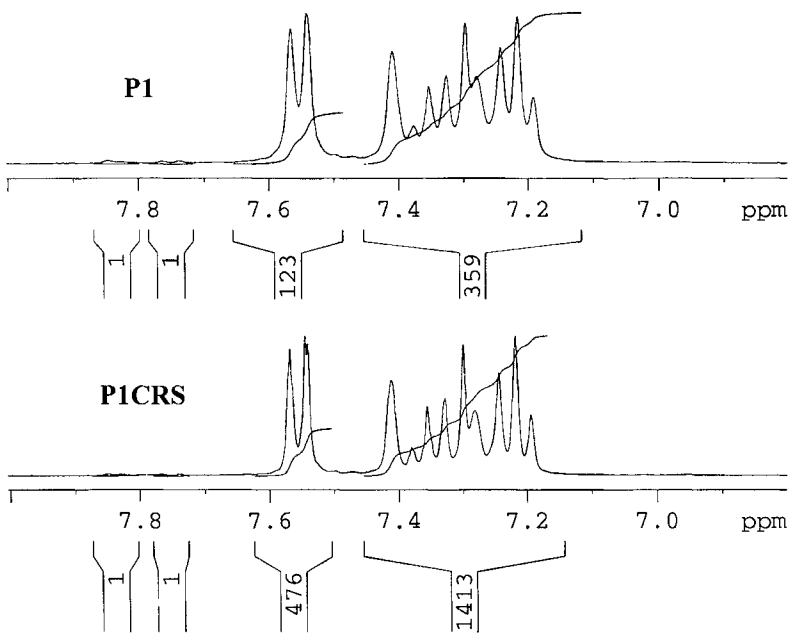

Figure 7. ^{1}H-NMR spectra of polymers **P1** and **P1CRS**.

In contrast to the brittle, yellow, opaque films formed when homopolymers of **P1-P3** were compression molded or cast from chloroform, polymer **P1CRS** showed significantly improved properties and led to the formation of more flexible films, which resisted cracking under the same conditions. In addition, **P1CRS** was easily fabricated into rectangular test samples for dynamic mechanical analysis (DMA). DMA of **P1CRS** (Figure 8) was performed in flexure mode with a three-point bending apparatus. The storage modulus of **P1CRS** was very high (approximately 10 GPa at 50 °C). In fact, this value was much higher than the literature values for storage moduli of Nylon 6/6 (2.5 GPa), poly(ether imide) (3.0 GPa), and poly(ether ether ketone) (3.6 GPa) recorded at 50 °C.[34] Furthermore, this value was even higher than the values of **PBP2** (7.5 GPa) and its 4'-biphenyloxy-substituted derivative (6.4 GPa), the highest modulus benzophenone homopolymer prepared earlier in our group.[16]

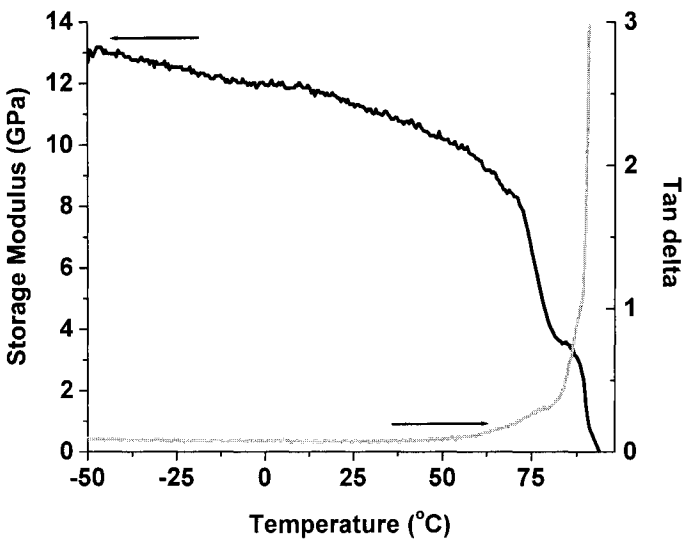

Figure 8. Storage modulus (black) and loss factor (gray) curves obtained form DMA analysis of **P1CRS**.

These initial results confirm that polymer **P1CRS** represents an example of a thermally stable, high modulus, processable high MW HFIP-linked benzophenone polymer. The unique structural features of these materials also make them potentially interesting in electrical applications where wide band gap materials with low current density and good thermoxidative stability are required.[35,36] It has recently been shown that HFIP-containing materials, such as **PDTFE**, demonstrate more stability in terms of a lifetime and thermal stability than poly(9,9-di-*n*-hexylfluorene) and poly-[(4-*n*-hexyltriphenyl)amine]-based diode-type devices.[15] Moreover, this approach represents a new method of improving the mechanical and film-forming properties of a number of new benzophenone type materials made via nickel coupling chemistry.

Conclusions

This paper demonstrates the versatility of Ni(0)-mediated polymerization method for the synthesis of variety of isomeric HFIP-containing polymers. Specifically, the results show the efficiency of synthesizing HFIP-linked benzophenone polymers by means of Ni(0)-catalyzed polymerization of newly developed bis(aryl triflate) and bis(aryl chloride) monomers. As with other 2,5-benzophenone containing homopolymers, it was not possible to form flexible tough films. As such, a new strategy was developed incorporating a tetrafunctional monomer. The results confirm that this is a viable route to new 2,5-benzophenone containing materials that not only are high molecular weight, but that also are thermally stable and mechanically tough with excellent film-forming properties. Based upon these initial studies, a range of polymers incorporating 2,5-benzophenone and various functional groups could be synthesized giving materials with a similar combination of desirable properties for electronic, coating, and separation applications.

Acknowledgements

Financial support provided by the Director, Office of Energy Research, Office of Basic Energy Sciences, Material Sciences Division of the U.S. Department of Energy under contracts No. DE-AC03-765F00098 and W-405-Eng-82 is gratefully acknowledged. We would also like to thank Professor Surya K. Mallapragada and her graduate students, Michael Determan and Sim-Siong Wong (Chemical Engineering Department), for their assistance with the GPC, TGA, and DSC analysis, as well as Brian G. Trewyn and Hung-Ting Chen from Professor Victor Lin's group for their assistance with the UV-Vis analysis.

References

(1) Percec, V.; Okita, S.; Weiss, R. *Macromolecules* **1992**, *25*, 1816-1823.

(2) Phillips, R. W.; Sheares, V. V.; Samulski, E. T.; DeSimone, J. M. *Macromolecules* **1994**, *27*, 2354-2356.

(3) Pasquale, A.J.; Sheares, V.V. *J. Polym. Sci. Pt. A: Polym. Chem.* **1998**, *36*, 2611-2618.

(4) Marrocco, M. L.; Gange, R. R.; Trimmer, M. S. (Maxdem Inc.). U.S. Patent 6,087,467, July 11, 2000.

(5) Hagberg, E. C.; Goodridge, B.; Ugurly, O.; Chumbley, S.; Sheares, V. V. *Macromolecules* **2004**, *37*, 3642-3650.

(6) Wang, J.; Sheares, V. V. *Macromolecules* **1998**, *31*, 6769-6775.

(7) Ghassemi, H.; McGrath, J. E. *Polymer* **1997**, *38*, 3139-3143.

(8) Rusch-Salazar, L. A.; Sheares, V. V. *J. Polym. Sci. Pt. A: Polym. Chem.* **2003**, *41*, 2277-2287.

(9) Colon, I.; Kelsey, D. R. *J. Org. Chem.* **1986**, *51*, 2627-2637.

(10) Hagberg, E. C.; Olson, D. A.; Sheares, V. V. *Macromolecules* **2004**, *37*, 4748-4754.

(11) Havelka, P. A., Kazukiyo N., Freeman, B. D., Sheares, V.V. *Macromolecules* **1999**, *32*, 6418-6424.

(12) Sheares, V. V. (Iowa State University Research Foundation, Inc.). U.S. Patent 6,515,101, February 4, 2003.

(13) Marrocco, M. L.; Trimmer, M. S.; Hsu, L.-C.; Gange, R. R. *SAMPE Proceedings* **1994**, *39*, 1063-1072.

(14) Mohanty, D. K.; Lowery, R. C.; Lyle, G. D.; McGrath, J. E. *Int. SAMPE Symp. Exp.* **1987**, *32*, 408-419.

(15) Beinhoff, M.; Bozano, L. D.; Scott, J. C.; Carter, K. R. *Macromolecules* **2005**, *38*, 4147-4156.

(16) Bloom, P. D.; Jones III, C. A.; Sheares, V. V. *Macromolecules* **2005**, *38*, 2159-2166.

(17) Andjelkovic, D. D.; Sheares, V. V. *Polymer Preprints* **2003**, *44*, 899-900.

(18) Pixton, M. R.; Paul, D. R. In *Polymeric Gas Separation Membranes*; Paul, D. R., Yampol'skii, Y. P., Eds.; CRC Press, Inc.: Boca Raton, FL, 1994; Chapter 3, p 83-153.

(19) Bloom, P. D.; Sheares, V. V. *J. Polym. Sci. Pt. A: Polym. Chem.* **2001**, *39*, 3505-2512.

(20) Bloom, P. D.; Sheares, V. V. *Polymer Preprints* **2000**, *41*, 109-110.

(21) Wang, Y.; Quirk, R. P. *Macromolecules* **1995**, *28*, 3495-3501.

(22) Frantz, D. E.; Weaver, D. G.; Carey, J. P.; Kress, M. H.; Dolling, U. H. *Org. Lett.* **2002,** *26*, 4717-4718.

(23) Semmelhack, M. F.; Helquist, P.; Jones, L. D.; Keller, L.; Mendelson, L.; Ryono, L. S.; Smith, J. G.; Stauffer, R. D. *J. Am. Chem. Soc.* **1981**, *103*, 6460-6471.

(24) McOmie, J. F. W.; Watts, M. L.; West, D. E. *Tetrahedron* **1968**, *24*, 2289-2292.

(25) McOmie, J. F. W.; West, D. E. *Org. Synth.* **1969**, *49*, 50-51.

(26) Percec, V.; Bae, J.-Y.; Zhao, M.; Hill, D. H. *Macromolecules* **1995**, *28*, 6726-6734.

(27) Percec, V.; Bae, J.-Y.; Zhao, M.; Hill, D. *J. Org. Chem.* **1995**, *60*, 176-185.

(28) Poly(2,5-benzophenone) (PBP1) used for comparisons was synthesized in the following manner:

Materials. All reagents were purchased from Aldrich and used as received except when reported. Bipyridine (Bipy) and triphenylphosphine (TPP) were purified by recrystallization from ethanol and *n*-heptane respectively. Both reagents were dried under vacuum for 24h at room temperature and stored in the glove box under nitrogen. The catalyst $(Ph_3P)_2NiCl_2$ and powdered (100 mesh) zinc (99.999%) were purchased from Aldrich and stored used as received. Tetrahydrofuran (THF) was distilled from sodium and benzophenone prior to use. Monomer 2,5-dichlorobenzophenone was recrystallized from ethanol until its ^1H NMR spectrum corresponded to the expected structure and 99.9% purity was confirmed by DSC melting point and GC/MS.

Polymerization. A previously flame-dried two-necked 50 mL pear-shaped flask was placed in a glove box and charged with 2.23g (3.1 eq) of Zn, 0.726g (0.1 eq) of $NiCl_2(PPh_3)_2$ catalyst, 0.576g (0.2 eq) TPP and 0.172g (0.1 eq) of Bipy. The flask was equipped with an overhead stirrer, sealed, and removed from the glove box. It was then evacuated and refilled with argon three times, charged with 10 mL of

anhydrous THF via syringe, and placed in a 60 °C preheated oil bath. Once the color of the catalyst mixture changed from deep green to dark red, a solution of 2.76 g (1.0 eq) of 2,5-dichlorobenzophenone in 5mL dry THF was added to the catalyst mixture via syringe. The reaction was allowed to stir for 6h at 60 °C. The viscous polymer solution was then precipitated into 500mL of ethanol/HCl (4:1=v:v) mixture to remove excess zinc and stirred overnight. The yellow polymer was collected via filtration and washed with methanol, saturated sodium bicarbonate solution, and again methanol. The collected powder was vacuum dried at 60 °C overnight to give 1.86g of polymer **PBP1** (94% yield).

Characterization of the polymer was performed in a similar manner as described in the text and the corresponding results are given in Tables 1 and 2.

(29) Yamamoto, T.; Morita, A.; Miyazaki, Y.; Maruyama, T.; Wakayama, H.; Zhou, Z.-h.; Nakamura, Y.; Kanbara, T.; Sasaki, S.; Kubota, K. *Macromolecules* **1992**, *25*, 1214-1223.

(30) Yamamoto, T. *Prog. Polym. Sci.* **1992**, *17*, 1153-1205.

(31) Sperling, L. H. *Introduction to Physical Polymer Science*; 3rd Ed., John Wiley and Sons: New York, 2001; Chapter 8, p 295-362.

(32) Yonezawa, N.; Ikezaki, T.; Nakamura, H.; Maeyama, K. *Macromolecules* **2000**, *33*, 8125-8129.

(33) Mohan, J. *Organic Spectroscopy – Principles and Applications*. CRC Press LLC: Boca Raton, FL, 2000, p 159-162.

(34) Sepe, M. *Dynamic mechanical analysis for plastics engineering*. Plastics Design Library: Norwich, NY, 1998; p 62-63, 100-101 and 102-103.

(35) Ma, L.; Pyo, S.; Ouyang, J.; Xu, Q.; Yang, Y. *Appl. Phys. Lett.* **2003**, *82*, 1419-1421.

(36) Ma, L.; Liu, J.; Pyo, S.; Xu, Q.; Yang, Y. *Mol. Cryst. Liq. Cryst. Sci. Technol., Sect. A* **2002**, *378*, 185-189.

PART II. DEVELOPMENT OF NOVEL BIOMATERIALS FROM RENEWABLE RESOURCES

CHAPTER 3. GENERAL INTRODUCTION

A book chapter published in ACS Symposium Series 921. Reproduced with permission from "Novel Polymeric Materials from Soybean Oils – Synthesis, Properties and Potential Applications", in *Feedstocks for the Future: Renewables for the Production of Chemicals and Materials*; Bozell, J. J., Patel, M., Eds.; ACS Symposium Series 921; ACS: Washington DC, 2006; Chapter 6, p 67-81.

Dejan D. Andjelkovic, Fengkui Li and Richard C. Larock

Introduction

The growing worldwide demand for petroleum-based polymeric materials has raised environmental concerns about these non-biorenewable, indestructible materials, and also increased our dependence on crude oil. The rapid growth of the industrial world has placed increased pressures on the finite petroleum reserves and forced us to look for alternative resources. Biorenewable resources represent a promising new alternative, but they require new approaches and developments in order to be successfully utilized.

Biopolymers produced from renewable and inexpensive natural resources have drawn considerable attention over the past decade, due to their low cost, ready availability, environmental compatibility, and their inherent biodegradability (*1*). Application of these biomaterials has a huge potential market, because of the current emphasis on sustainable technologies. Many naturally-occurring biopolymers, such as cellulose, starch, dextran, as well as those derived from proteins, lipids and polyphenols, are widely used for material

applications (*2,3*). The exciting new area of biorenewables, which lies on the border of molecular biology and polymer chemistry, offers many opportunities to expand the range of exciting new bio-based materials. Particularly promising is the development of new biopolymers from functionalized, low molecular weight natural substances, like natural oils, utilizing polymerization methods widely used for petroleum-based polymers.

Natural oils represent one of the most promising renewable resources. These molecules possess a triglyceride structure with fatty acid side chains possessing varying degrees of unsaturation (*4-6*). The presence of carbon-carbon double bonds makes these biological oils ideal monomers of natural origin for the preparation of biopolymers. Soybean oil is the most abundant vegetable oil, accounting for approximately 30% of the world's vegetable oil supply (*7*). The bulk of the soybean oil (~80%) produced annually is used for human food. The remaining 20% is used for animal feed (~6%) and non-food uses, such as soaps, lubricants, coatings and paints (~14%). The most promising new applications for soybean oils are expected to be in non-food uses. So far, these applications have mainly involved the polymerization of soybean oil derivatives, such as fatty acids, epoxidized oils, polyols, etc. (*4,8*). The advantages of soybean oil as a monomer are its ready availability on a huge scale, its low cost (~$0.24/lb) (*9*) and high purity, the possibility of genetically engineering the number of C=C bonds present in the oil (*4*), its significantly higher molecular weight when compared to other conventional alkene monomers (~880 g/mol), and the existence and availability of many structurally related vegetable oils. These advantages make natural oils ideal starting materials for biopolymer synthesis.

Considerable recent effort has been directed towards the conversion of vegetable oils into solid polymeric materials. These vegetable oil-based polymers generally possess viable

mechanical properties and thus show promise as structural materials in a variety of applications. For example, Wool and co-workers have prepared rigid thermosets and composites via free-radical copolymerization of soybean oil monoglyceride maleates and styrene (*10-12*). The new maleate monomers are obtained by glycerol transesterification of soybean oil, followed by esterification with maleic anhydride (*10*). It has been found that the original C=C bonds of the soybean oil side chains participate in this free-radical copolymerization. Petrovic and co-workers, on the other hand, have successfully converted the C=C bonds of soybean oil into polyols by epoxidizing the C=C bonds of the triglyceride oil, and then carrying out oxirane ring-opening of the epoxidized oil. The newly synthesized polyols are then reacted with a variety of isocyanates to produce polyurethanes (*13-17*).

More recently, a variety of exciting new polymeric materials have been prepared in our group by the cationic copolymerization of soybean and other vegetable oils with a variety of alkene comonomers (*18-35*). These biopolymers possess industrially viable thermophysical and mechanical properties and thus may find structural applications. This chemistry takes advantage of the original C=C bonds of the soybean (*18-27*), tung (*28,29*), corn (*30*) and fish oils (*31-35*) to effect crosslinking. In this chapter, we shall focus primarily on the synthesis and characterization of soybean oil-based polymers, which result from the direct copolymerization of the C=C bonds of soybean oils with other comonomers via cationic polymerization (*18-27*).

Soybean Oils as Cationic Monomers

Commercially available soybean oils have a triglyceride structure. Oleic (C18:1), linoleic (C18:2) and linolenic acid (C18:3) are the primary fatty acid components of soybean oils (Table 1). Regular soybean oil (SOY) has approximately 4.5 C=C bonds per triglyceride,

while low saturation soybean oil (LSS) has approximately 5.1 C=C bonds. LSS oil is a commercially available soybean oil with considerably more linoleic acid (*4*). The fatty acid side chains in these two soybean oils are non- conjugated. Conjugated LSS oil (CLS) has been prepared in our laboratories from LSS by Rh-catalyzed isomerization (*36*).

Table 1. Compositions of the Various Soybean Oils

Oils	*C=C*		*Fatty Acids*				
	Number[a]	*Conjugated*	*C16:0*	*C18:0*	*C18:1*	*C18:2*	*C18:3*
SOY	4.5	No	10.5	3.2	22.3	54.4	8.3
LSS	5.1	No	4.5	3.0	20.0	63.6	9.0
CLSS	5.1	Yes	4.5	3.0	20.0	63.6	9.0

[a] The average number of C=C bonds per triglyceride has been calculated by ^{1}H NMR spectral analysis.

The cationic polymerization of soybean oils is possible only when certain basic thermodynamic requirements are met. This means that a negative change in free energy is required ($\Delta H - T\Delta S < 0$). Since the entropic component decreases during cationic polymerizations, because of the loss of translational degrees of freedom caused by connecting triglyceride units together, the thermodynamic feasibility of the polymerization will depend on enthalpic factors. Thus, cationic polymerizations must be sufficiently exothermic to compensate for the loss in entropy. In the case of soybean oil, this is accomplished through conversion of the C=C bonds in the triglyceride to C-C single bonds in the polymer. The C=C bonds in the soybean oil represent sites for electrophilic attack of the reactive species generated by the initiator. Because of that, electronic effects within the triglyceride monomers will have a crucial effect on their reactivity. Soybean oil triglycerides,

like all other alkene monomers, are expected to polymerize cationically by the addition of monomers to the growing carbocation. Thus, triglyceride monomers must be nucleophilic and capable of stabilizing the intermediate carbocation (*37*). Since nucleophilicity increases with increasing substitution on the C=C bond, due to the positive inductive effect of the alkyl substituents, the C=C bonds of the SOY and LSS are considered more nucleophilic than those of ethylene and propylene. They are therefore capable of stabilizing the positive charge to a greater extent and are prone to cationic polymerization. For the same reason, conjugated C=C bonds in the CLS are considered even more reactive toward cationic polymerization, since they will generate very stable allylic carbocations as intermediates. Thus, the SOY, LSS and CLS oils are cationically polymerizable monomers.

Unlike ethylene, propylene, isobutylene or styrene, soybean oils are considered polyfunctional monomers due to the presence of multiple C=C bonds within the triglyceride. Along with their relatively high molecular weights (~ 880 g/mol) and ability to efficiently stabilize intermediate carbocations, it is not surprising that their cationic polymerization easily affords high molecular weight polymers with crosslinked polymer networks.

Polymer Synthesis and Microstructure

Several classes of compounds are capable of initiating the cationic polymerization of vegetable oils, including protonic and Lewis acids (*35*). Among these, boron trifluoride diethyl etherate (BFE) has proven to be the most efficient catalyst. Its initiation and propagation mechanisms are well understood and described (*37,38*). Simple homopolymerization of soybean oils typically results in viscous oils or soft rubbery materials containing approximately 50 weight % of unreacted oil (*27*). These rubbery materials appear to be very weak and possess rather limited utility. In order to overcome this problem,

soybean oils have been copolymerized with either divinylbenzene (DVB) or mixtures of DVB and styrene (ST) (Scheme 1). In general, copolymerization with the more reactive DVB comonomer yields hard, rigid polymers with very high crosslink densities and a nonuniform crosslinking structure (*19*). Because of that, these hard plastics are brittle, which drastically limits their applications. On the other hand, copolymerization with ST-DVB mixtures yields a variety of polymers ranging from elastomers to tough and rigid plastics with much more uniform crosslinking structures (*20*). During the copolymerization, the BFE initiator typically has to be modified by a fatty acid ester, such as soybean oil methyl esters or more commonly Norway fish oil ethyl ester (NFO), to allow homogeneous copolymerization. In the absence of the initiator modifier, the copolymerization becomes heterogeneous (*19*), presumably due to poor miscibility between the oil and the initiator. Since the modifier is completely miscible with both the soybean oil triglyceride and the alkene comonomers, it enhances their mutual

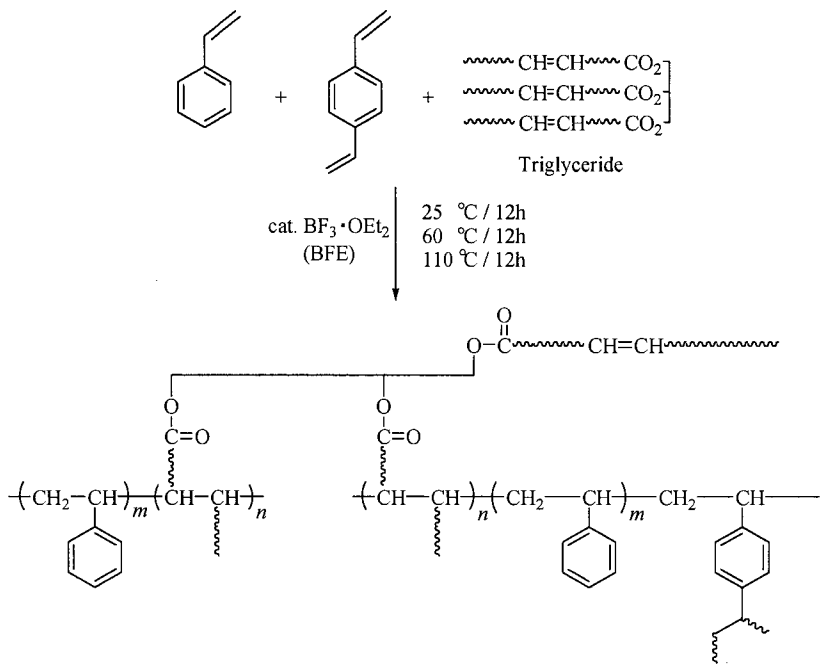

Scheme 1. Copolymerization of soybean oil triglyceride with ST and DVB.

solubility and provides a homogeneous reaction mixture. Upon mixing, reaction mixtures are typically cured for 12 h at room temperature, 12 h at 60 °C and finally 24 h at 110 °C. It has been found that, besides DVB, the soybean oil triglyceride also contributes directly to crosslinking (*27*). Gelation times of the reaction mixtures vary from a few minutes to several hours and depend on the type of soybean oil used in the mixture, the stoichiometry and the curing temperatures. The activation energies for the gelation process are 95-122 kJ/mol, which appear to be slightly higher than those of epoxy resins (70-90 kJ/mol) (*25*). Generally, 20-50 weight % of the soybean oil reactants are converted into crosslinked polymers at gelation and subsequent vitrification. Fully-cured thermosets are obtained after post-curing at elevated temperatures. It has been noted that an increase in the ST and DVB content in the starting mixture increases the percentage of the soybean oil incorporation. However, the soybean oil is not readily incorporated when the alkene content dominates. The most efficient consumption of the soybean oil occurs when 45-55 weight % of the oil is employed.

The resulting bulk polymers appear as opaque materials with a glossy dark brown color and a slight odor. These polymers can be made into various shapes by *in situ* reaction molding or cutting. Their microstructures have been determined by Soxhlet extraction with methylene chloride as a solvent, followed by subsequent ^{1}H NMR spectral analysis. Analyses have shown that bulk polymers are composed primarily of soybean oil-ST-DVB crosslinked polymers (insoluble fraction), a small amount of linear or less crosslinked soluble polymers, minimal amounts of unreacted soybean oil, and residual initiator fragments (soluble fraction). It has been determined that the ST and DVB completely participate in the copolymerization to form crosslinked polymers. The yield of the crosslinked polymer increases with the increase of DVB content in the mixture. Among the three soybean oils employed, CLS gives

the smallest percent of the soluble fraction due to its higher reactivity. The maximum incorporation of the soybean oil into the crosslinked polymer occurs when the soybean oil constitutes approximately 45-50 wt % of the reactants. Careful choice of the reaction conditions results in almost complete conversion of the CLS oil into the crosslinked polymer (*27*). Similarly, the more reactive CLS oil yields polymers with higher crosslink densities than the SOY and LSS oils with the same stoichiometries. The crosslink densities of the soybean oil-based polymers range from 1×10^2 to 4×10^4 mol/m^3 (*21*).

Thermophysical and Mechanical Properties

Soybean oil-based polymers exhibit good thermal stability below 200 °C under both air and nitrogen atmospheres. These thermosetting materials typically show three-stage thermal degradation at 200-400 °C (stage I), 400-500 °C (stage II), and >500 °C (stage III), with the second stage being the fastest (*19,20*). The first stage degradation is attributed to evaporation and decomposition of the unreacted oil and other soluble components in the bulk material. The second step corresponds to degradation and char formation of the crosslinked polymer structure, while the third stage corresponds to gradual oxidation of the char residue. In general, these biomaterials lose 10% of their weight in the temperature range of 310-350 °C, depending on the content of the unreacted oil present in the bulk polymers. For example, Figure 1 shows the thermal degradation behavior of the polymer LSS45-ST32-DVB15-(NFO5-BFE3). The formula refers to a polymer prepared by the copolymerization of 45 weight % LSS, 32 weight % ST and 15 weight % DVB initiated by adding 5 weight % NFO mixed with 3 weight % BFE.

DMA analysis shows that these soybean oil-based polymers are typical thermosetting polymers (*21*). This is evidenced by the rubbery plateau in the DMA curve, which indicates

the existence of a crosslinked network structure. The glass transition regions are fairly broad and are ascribed to the segmental heterogeneities upon crosslinking. Some soybean oil-DVB polymers exhibit two glass transition temperatures (T_g's) during DMA analysis (*19*). The high temperature transition (α_1) at about 80 °C represents the glass transition of the crosslinked polymer, while the low temperature transition (α_2) at 0-10 °C corresponds to the glass transition of the unreacted oil. Conversely, soybean oil-ST-DVB polymers possess a single glass transition, indicating better mixing of the small amounts of unreacted oil with the polymer main chains (*21*). Greater amounts of DVB in the starting mixture result in polymers with higher crosslink densities and consequently higher T_g's. Similarly, more reactive CLS oil affords polymers with higher T_g's and crosslink densities than the corresponding SOY and LSS oils. The glass transition temperatures of these soybean oil polymers vary from 0 °C to 105 °C.

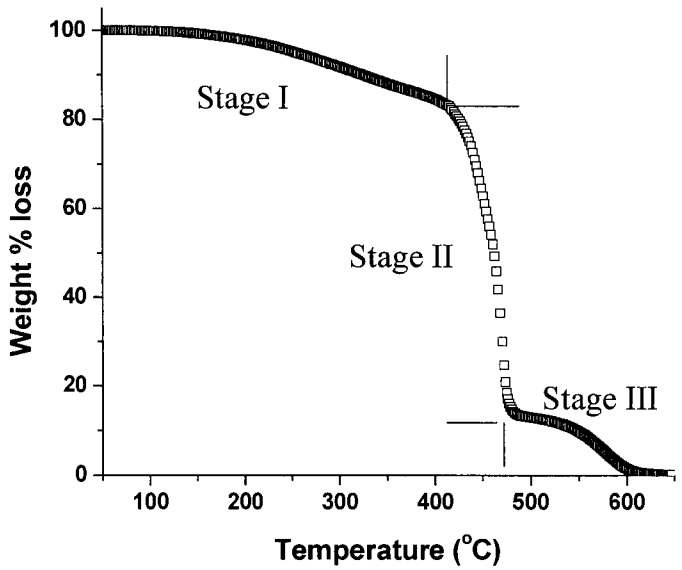

Figure 1. Three stages of the thermal degradation of the polymer LSS45-ST32-DVB15-(NFO5-BFE3) in air at 20 °C/min heating rate.

The bulk polymers have been further characterized through tensile measurements in order to elucidate their tensile mechanical properties. Analyses have proven that these materials exhibit characteristics typical of materials ranging from elastomers to tough and rigid plastics. For example, Figure 2 shows the evolution of the polymeric material from an elastomer, through a ductile plastic with yielding behavior, to a rigid plastic, just by varying the DVB content from 0% to 47%, while keeping the total ST + DVB concentration constant (*22*).

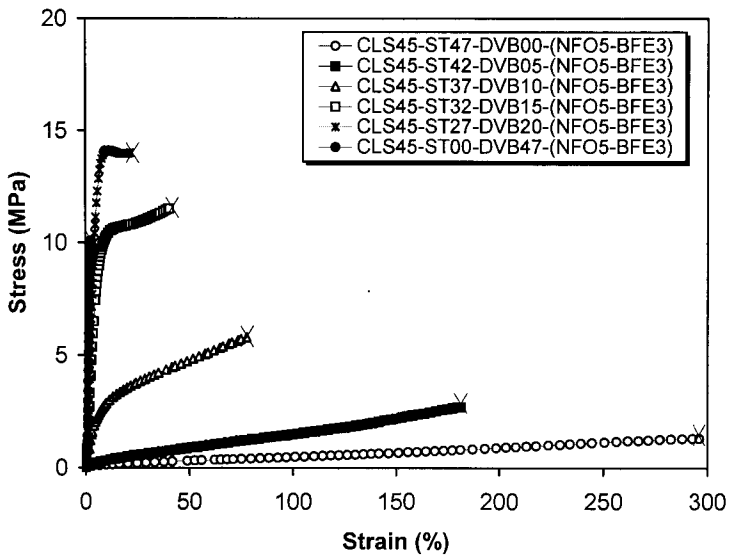

Figure 2. Tensile stress-strain behavior of soybean oil polymers.(Reproduced from reference 22. Copyright 2001 John Wiley & Sons, Inc.)

Table II summarizes some thermal and mechanical properties of several soybean oil polymers and compares them with two of the most useful industrial thermoplastics, low density polyethylene (LDPE) and polystyrene (PS). The results show that the CLS polymers possess higher mechanical properties than the SOY and LSS polymers with the same

stoichiometries. Also, the highest toughness of the resulting polymers is reached when the amount of the soybean oil is equivalent to the amount of alkene comonomers. With a proper choice of the polymer composition and the reaction conditions, soybean oil polymers can be tailored to possess comparable or better properties than those of LDPE and PS.

Table II. Summary of the Properties of Soybean Oil-Based Polymers

Polymer	T_g (°C)	v_e (mol/m^3)	T_{max}[a] (°C)	E[b] (MPa)	σ_b[c] (MPa)	ε_b[d] (%)	*Toughness (MPa)*
Polyethylene (LDPE)[e]	-68	-	355	370	9.6	46	5.2
Polystyrene[e]	90	-	420	1330	30.3	4	0.5
CLS45-ST47-DVB00-I[f,g]	10	1.0×10^2	448	12	1.3	300	2.0
CLS45-ST32-DVB15-I[f,h]	76	2.2×10^3	475	225	11.5	41	4.0
CLS35-ST39-DVB18-I[f,i]	82	3.4×10^3	477	500	21.0	3	0.8
SOY45-ST32-DVB15-I[f]	68	1.8×10^2	468	71	4.1	57	1.7
LSS45-ST32-DVB15-I[f]	61	5.3×10^2	470	90	6.0	64	2.9
CLS45-ST32-DVB15-I[f]	76	2.2×10^3	475	225	11.5	41	4.0

[a] The temperature at the maximum degradation rate. [b] Young's modulus. [c] Break strength. [d] Elongation at break. [e] Analyses were performed on commercially available LDPE and PS samples. [f] I = modified BFE initiator, typically (NFO5-BFE3). [g] A typical elastomer. [h] A ductile plastic. [i] A rigid plastic.

Good Damping and Shape Memory Properties

Many important engineering plastics and composite materials possess damping properties important for their applications in the aircraft, automotive, and construction industries (*39*). This class of polymeric materials is used for the reduction of unwanted noise, as well as for the prevention of vibration fatigue failure (*39*). The damping properties of materials arise from their ability to transform mechanical energy into some other forms of energy, for example, by dissipation of mechanical energy through heat, while undergoing

vibrations (*40*). Most common thermoplastics exhibit efficient damping in the 20-30 °C range. Good damping materials, on the other hand, should exhibit a high loss factor (tan δ > 0.3) over a temperature range of at least 60-80 °C (*41*). Soybean oil-ST-DVB polymers with proper compositions have been shown to have good damping properties (*23*). With increasing DVB content, the damping profiles evolve from a narrow, extremely intense damping peak to less intense, but significantly broadened, damping peaks, as shown on Figure 3. DVB, as an efficient crosslinker, increases the degree of crosslinking with increasing content, thus reducing the damping intensity and considerably broadening the damping region of the bulk polymers. It can be seen that the temperature regions for efficient damping vary from 80-110 °C when DVB constitutes 5-15 weight % of the polymer, which indicates very good damping properties for the resulting materials. The overall damping capacity of the soybean oil polymers (TA) is represented by the area under the loss factor-

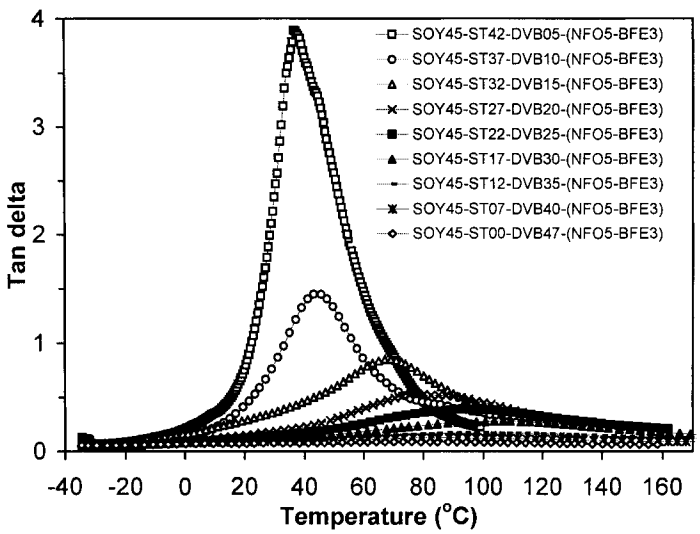

Figure 3. Temperature dependence of the loss factor for SOY45-(ST+DVB)47-(NFO5-BFE3) copolymers prepared by varying the DVB content. (Reproduced from reference 23. Copyright 2002 John Wiley & Sons, Inc.)

temperature curve. In general, an increase in polymer crosslink density decreases its TA value and noticeably broadens the damping temperature region. It has also been shown that greater incorporation of the soybean oil into the crosslinked network results in higher TA values. Therefore, it is not surprising that CLS polymers possess higher TA values than the LSS and SOY polymers with the same crosslink densities (*23*). These findings suggest that one can tailor good damping soy oil-based materials by carefully designing their structures. The greater the number of fatty acid ester groups in the polymer network, the higher the damping intensities. Unfortunately, the triglycerides alone afford strong damping peaks over only a very narrow temperature range. The crosslinking thus appears necessary and beneficial to a certain degree, since it yields segmental inhomogeneities and thus effectively broadens the damping region. Overall, the two opposite effects (crosslinking density and triglyceride incorporation) need to be balanced in order to achieve optimum damping properties for the soybean oil polymers. So far, the most promising damping soy-based materials show loss factor maxima $(\tan \delta)_{max}$ of 0.8-4.3, TA values of 50-124 and temperature ranges for efficient damping of ΔT = 80-110 ^{o}C (*23*).

Along with the good damping properties, the soybean oil-ST-DVB polymers show classical shape memory properties (*24*). Shape memory polymers are a group of "intelligent" materials, which have the ability to recover their permanent shape on demand after intended or accidental deformation (*43*). Generally, some kind of external stimuli is required to trigger the shape memory effect. Thermoresponsive shape memory polymers, such as soybean oil copolymers, require heat to revert from their temporary shape to their permanent shape. Structural requirements play a crucial role, since they determine the thermal and mechanical properties of the material and their shape memory properties. As described earlier, soybean

oil copolymers are polymer networks composed of long polymer chains interconnected by chemical crosslinks. Soybean oil materials with appropriate compositions have high T_g's and appear as hard plastics at room temperature. However, upon heating they become elastomers capable of undergoing rapid deformation by an external force. Once cooled below its T_g (glassy state), the polymer is capable of retaining the deformation for an unlimited time, due to the very limited chain mobility. Raising the temperature above the T_g triggers the shape memory effect and the polymer returns to its original shape.

Several parameters, including the polymer's ability to deform at $T > T_g$, the ratio of fixed deformation to the original deformation at room temperature, and the polymer's final recovery upon being reheated, have been determined using a bending test (*24*). Simple variation in the composition of the soybean oil-ST-DVB polymers reveals that the higher deformability at the elastomeric state is always accompanied by a lower ratio of fixed deformation to the original deformation at room temperature, and vice versa. It has been determined that crosslinking density strongly affects deformability in the elastomeric state and that a relatively low degree of crosslinking is favorable for the deformation. The increased rigidity of the polymer backbone allows better fixation of the mechanical deformation at ambient temperature. Unfortunately, increasing rigidity and decreasing crosslinking density represent two opposite effects and do not allow simultaneous optimization of the polymer's deformability and fixation of its deformation. Substituting DVB with more rigid but less effective crosslinkers, such as dicyclopentadiene (DCP) and norbornadiene (NBD), circumvents this problem and allows the preparation of materials with an appropriate combination of chain rigidity and crosslink density. The resulting polymers are able to fix over 97% of their deformation at room temperature and completely recover

their original shape upon being reheated. Additionally, soybean oil polymers also possess good reusability, with a constant shape memory effect over at least seven processing cycles (*24*).

Potential applications

The current state of the art in the area of biomaterials design and synthesis indicates that there exist a large number of materials with specific thermal and mechanical properties comparable to those of widely used industrial plastics (*1-3*). Soybean oil-based materials possess such qualities as well. These biomaterials can be made into a variety of complex structures currently made from petroleum-based plastics, by either cutting or injection molding techniques. The soybean oil-based resins can also be fabricated into biocomposites having excellent mechanical properties (*11*). These biocomposites may serve as replacements in a range of applications where engineering plastics are currently being used.

Due to their good damping properties, soybean oil polymers may also find applications in places where the reduction of noise and prevention of vibration fatigue failure is required (*39*). Several conventional polymers, such as polyacrylates, polyurethanes, polyvinyl acetate, as well as natural, silicone and SBR rubbers, which are currently used as damping materials, might be replaced by soybean oil polymers. Unlike the above-mentioned thermoplastics, soybean oil polymers are capable of efficient damping over wider temperature and frequency ranges (*23*).

Soybean oil polymers are the first thermoresponsive shape memory materials prepared from renewable natural resources (*24*). Their good shape memory properties extend their application range even further. They have great potential as materials for construction (heat-shrinkable rivets, gaskets and tube joints), electronics (electromagnetic shielded

materials and cable joints), printing and packaging (shrinkable films, laminate covers, trademarks), mechanical devices (automatic valves, lining material, joint devices), medical materials (bandages, splints, orthopedic apparatus), as well as a variety of household, sport and recreational applications (*42*).

Conclusions

A series of new polymeric materials ranging from elastomers to tough and rigid plastics have been prepared by the cationic copolymerization of different soybean oils and alkenes in the presence of a modified BFE initiator. Polymerization reactions have been conducted at relatively low temperatures and pressures, employing at least 50% of natural and renewable starting materials. Manipulations in polymer composition and reaction conditions allow efficient control over the polymer structure and properties. Soybean oil polymers possess good combination of thermal and mechanical properties, including excellent damping and shape memory properties. Because of this unique combination of valuable properties, these novel biomaterials show promise as replacements for conventional plastics.

The commercialization of this new technology greatly depends on the mutual efforts of polymer chemists, material scientists and chemical engineers, since it involves not only technical problems, but also economic and political issues that need to be resolved. The time is coming when we must seriously look into alternative sources of energy and raw materials. It is our belief that the use of natural and renewable materials represents the future of the polymer industry in the years to come.

Acknowledgements

The authors gratefully acknowledge the Iowa Soybean Promotion Board, the Iowa Energy Center, the Consortium for Plant Biotechnology Research, Archer Daniels Midland, and the USDA for funding our own research in this area.

References

1. *Biopolymers from Renewable Resources*; Kaplan, D. L., Ed.; Macromolecular Systems – Materials Approach; Springer: New York, 1998.
2. *Biorelated Polymers – Sustainable Polymer Science and Technology*; Chiellini, E.; Gil, H.; Braunegg, G.; Buchert, J.; Gatenholm, P.; van der Zee, M.; Kluwer Academic-Plenum Publishers: New York, 2001.
3. Kaplan, D. L.; Wiley, B. J.; Mayer, J. M.; Arcidiacono, S.; Keith, J.; Lombardi, S. J.; Ball, D.; Allen, A. L. In *Biomedical Polymers: Designed to Degrade Systems;* Shalaby, W. S., Ed.; Carl Hanser: New York, 1994; Chapter 8.
4. O'Brien, R. D.; *Fats and Oils – Formulating and Processing for Applications*; 2nd Ed., CRC Press LLC: Boca Raton, FL, 2004.
5. Eckey, E. W.; *Vegetable Fats and Oils*; The ACS Monograph Series; New York: Reinhold Publishing Co., 1954; Chapters 1-4.
6. Salunkhe, D. K.; Chavan, J. K.; Adsule, R. N.; Kadam, S. S. *World Oilseeds: Chemistry, Technology and Utilization*; New York: Van Nostrand Reinhold, 1991.
7. Fehr, W. R. In *Oil Crops of the World: Their Breeding and Utilization*; Robbelen, G., Downey, R. K. and Ashri, A., Eds.; McGraw-Hill: 1989, Chapter 13.
8. Gunstone, F. D. *Industrial Uses of Soybean Oil for Tomorrow*, Special Report '96, Iowa State University and the Iowa Soybean Promotion Board, 1995.

9. *Chemical Market Reporter*, October 11, 2004, pp 24-26.

10. Can, E.; Kusefoglu, S.; Wool, R. P. *J. Appl. Polym. Sci.* **2001**, *81*, 69.

11. Khot, S. N.; Lascala, J. J.; Can, E.; Morye, S. S.; Williams, G. I., Palmese, G. R.; Kusefoglu S. H.; Wool, R. P. *J. Appl. Polym. Sci.* **2001**, *82*, 703.

12. Can, E.; Kusefoglu, S.; Wool, R. P. *J. Appl. Polym. Sci.* **2002**, *83*, 972.

13. Petrovic, Z. S.; Guo, A.; Zhang, W. *J. Polym. Sci. Part A Polym. Chem.* **2000**, *38*, 4062.

14. Javni, I.; Petrovic, Z. S.; Guo, A.; Fuller, R. *J. Appl. Polym. Sci.* **2000**, *77*, 1723.

15. Guo, A.; Javni, I.; Petrovic, Z. S. *J. Appl. Polym. Sci.* **2000**, *77*, 467.

16. Guo. A.; Demydov, D.; Zhang, W.; Petrovic, Z. S. *J. Polym. Environ.* **2002**, *10,* 49.

17. Petrovic, Z. S; Zhang, W.; Zlatanic, A.; Lava, C. C.; Ilavsky, M. *J. Polym. Environ.* **2002**, *10*, 5.

18. Larock, R. C.; Hanson, M. W. U.S. Patent 6,211,315, 2001.

19. Li, F.; Hanson, M. W.; Larock, R. C. *Polymer* **2001**, *42*, 1567.

20. Li, F.; Larock, R. C. *J. Appl. Polym. Sci.* **2001**, *80*, 658.

21. Li, F.; Larock, R. C. *J. Polym. Sci. Part B Polym. Phys.* **2000**, *38*, 2721.

22. Li, F.; Larock, R. C. *J. Polym. Sci. Part B Polym. Phys.* **2001**, *39*, 60.

23. Li, F.; Larock, R. C. *Polym. Adv. Tech.* **2002**, *13*, 436.

24. Li, F.; Larock, R. C. *J. Appl. Polym. Sci.* **2002**, *84*, 1533.

25. Li, F.; Larock, R. C. *Polym. Int.* **2002**, *52*, 126.

26. Li, F.; Larock, R. C. *Polym. Mater. Sci. Eng.* **2002**, *86*, 379.

27. Li, F.; Larock, R. C. *J. Polym. Environ.* **2002**, *10*, 59.

28. Li, F.; Larock, R. C. *J. Appl. Polym. Sci.* **2000**, *78*, 1044.

29. Li, F.; Larock, R. C. *Biomacromolecules* **2003**, *4*, 1018.

30. Li, F.; Hasjim, J.; Larock, R. C. *J. Appl. Polym. Sci.* **2003**, *90*, 1830.

31. Li, F.; Marks, D.; Larock, R. C.; Otaigbe, J. U. *SPE ANTEC Technical Papers* **1999**, *3*, 3821.

32. Li, F.; Marks, D.; Larock, R. C.; Otaigbe, J. U. *Polymer* **2000**, *41*, 7925.

33. Li, F.; Larock, R. C.; Otaigbe, J. U. *Polymer* **2000**, *41*, 4849.

34. Li, F.; Perrenoud, A.; Larock, R. C. *Polymer* **2001**, *42*, 10133.

35. Marks, D.; Li, F.; Larock, R. C. *J. Appl. Polym. Sci.* **2001**, *81*, 2001.

36. Dong, X.; Chung, S.; Reddy, C. K.; Ehlers, L. E.; Larock, R. C. *J. Am. Oil Chem. Soc.* **2001**, *78*, 447.

37. *Cationic Polymerizations – Mechanisms, Synthesis, and Applications*; Matyjaszewski, K., Ed.; Marcel Dekker, Inc.: New York, 1996.

38. Odian, G.; *Principles of Polymerization*, 3rd Ed.; John Wiley & Sons, Inc.: New York, 1991, Chapter 5.

39. *Sound and Vibration Damping with Polymers*; Corsaro, R. D., Sperling, L. H., Eds.; ACS Symposium Series No. 424; American Chemical Society: Washington, DC, 1990.

40. Aklonis, J. J.; MacKnight, W. J. *Introduction to Polymer Viscoelasticity*; 2nd Ed.; Wiley-Interscience: New York, 1983.

41. Yao, S. In *Advances in Interpenetrating Polymer Networks*; Klempner, D.; Frisch, K. C., Eds.; Technomic Publishing Co.: Lancaster, PA, 1994, Vol. IV.

42. Lendlein, A.; Kelch, S. *Angew. Chem. Int. Ed. Engl.* **2002**, *41*, 2034.

CHAPTER 4. NOVEL THERMOSETS PREPARED BY CATIONIC COPOLYMERIZATION OF VARIOUS VEGETABLE OILS - SYNTHESIS AND THEIR STRUCTURE-PROPERTY RELATIONSHIPS

A paper published in Polymer. Reproduced with permission from Polymer, 2005, 46, 9674-9685.

Dejan D. Andjelkovic, Marlen Valverde, Phillip Henna, Fengkui Li, and Richard C. Larock

Abstract

A range of thermoset plastics have been prepared by the cationic copolymerization of olive, peanut, sesame, canola, corn, soybean, grapeseed, sunflower, low saturation soy, safflower, walnut, and linseed oils with divinylbenzene or a combination of styrene and divinylbenzene comonomers catalyzed by boron trifluoride diethyl etherate. The chemical, physical, thermal, and mechanical properties of these new polymers have been investigated as a function of the vegetable oil composition. The vegetable oil reactivity has a direct effect on most of the polymers' properties, which can be reasonably predicted by careful choice of the vegetable oil. Coupled with variations in the comonomer and stoichiometry, the choice of vegetable oil allows one to tailor the polymer's properties for specific applications.

Introduction

Recent years have witnessed an increasing interest in biomaterials derived from renewable resources. One major initiative has been the synthesis of a wide range of biopolymers from annually renewable and environmentally benign starting materials

obtained from agricultural, animal and microbial sources [1-3]. These materials often possess thermal and mechanical properties comparable to or better than those of widely used industrial polymers. As such, they might replace petroleum-based polymers resulting in waste reduction and overall petroleum resource preservation.

Vegetable oils are one of the cheapest and most abundant, annually renewable natural resources available in large quantities from various oilseeds [4-6]. In general, the bulk of vegetable oils produced each year is used for human food or animal feed, whereas the remainder finds non-food uses, such as the production of soaps, lubricants, coatings and paints [7]. These oils are generally triglycerides of different fatty acids with varying degrees of unsaturation. The presence of multiple C=C bonds makes biological oils ideal, natural building blocks for the preparation of a range of useful polymeric materials. Their conversion into industrially useful plastics usually proceeds through either fatty acid C=C bond functionalization and subsequent copolymerization or through direct copolymerization of the fatty acid C=C bonds with a variety of alkene comonomers. For instance, Petrovic and coworkers have successfully converted the C=C bonds of soybean oil into polyols by epoxidizing the C=C bonds of the triglyceride oil, followed by oxirane ring-opening of the epoxidized oil [8-12]. The newly synthesized polyols are then reacted with a variety of isocyanates to produce polyurethanes. Wool and coworkers, on the other hand, have prepared rigid thermosets and composites via free-radical copolymerization of soybean oil monoglyceride maleates and styrene [13-15]. The maleate monomers have been obtained by glycerol transesterification of soybean oil, followed by esterification with maleic anhydride [13].

We have successfully prepared a wide range of industrially promising biopolymers by the cationic copolymerization of soybean [16-18], corn [19], tung [20] and fish [21,22] oils without any prior chemical modifications. The copolymerization of soybean oils and divinylbenzene (DVB), for example, results in rigid and relatively brittle plastics with glass transition temperatures (T_g) of approximately 60-80 °C [16]. On the other hand, a variety of viable polymeric materials ranging from elastomers to rigid and tough plastics are produced by the cationic copolymerization of soybean oils, styrene (ST) and DVB [17]. Their glass transition temperatures (T_g) vary from 0-105 °C, Young's moduli vary from 0.03-0.63 GPa, while tensile strengths vary from 0.3-21 MPa [23,24]. The resulting thermosets possess excellent thermal and mechanical properties, including damping [25] and shape memory [26] properties, and show promise as replacements for petroleum-based rubbers and conventional plastics.

In addition to soybean, corn, tung and fish oils, there exist many other commercially available vegetable oils with different triglyceride structures. Their compositions mainly differ in their fatty acid content, leading to variations in their degrees of unsaturation and, consequently, their reactivity. Until now, variations in the polymer properties have been the direct result of variations in the polymer composition resulting from changes in the comonomer (ST and DVB) content. Herein, we wish (1) to determine if cationic polymerization, which has been so effective for soybean, corn, tung, and fish oils, can be extended to the polymerization of other readily available vegetable oils, (2) to convert a number of vegetable oils to bulk polymers by varying only the type of the oil while keeping the composition constant, (3) to characterize the materials, and most importantly, (4) to

determine their structure-property relationships. This kind of structure-property elucidation is necessary for tailoring the properties of these promising new bioplastics.

Experimental Procedure

Materials. The vegetable oils used in this study were Grand olive (OLV), Planters peanut (PNT), Loriva sesame (SES), Wesson canola (CAN), Mazola corn (COR), Wesson soybean (SOY), grapeseed (GRP), Wesson sunflower (SUN), Grand low saturation soy (LSS), Hain safflower (SAF), Loriva walnut (WNT), and Superb linseed (LIN) oils. All of the oils were purchased in the local supermarket, except the Superb linseed oil (supplied by Archer Daniels Midland Co. Decatur, IL), and used without further purification. ST and DVB (80% DVB and 20% ethylvinylbenzene) were purchased from Aldrich Chemical Company and used as received. Norway fish oil ethyl ester (NFO) (EPAX 5500 EE, Pronova Biocare) was used to modify the catalyst, boron trifluoride diethyl etherate (BFE) (distilled grade, Aldrich).

Cationic Copolymerization and Nomenclature. The desired amounts of comonomers (DVB or a mixture of ST and DVB) were measured out and added to the vegetable oil and the mixture stirred vigorously in an ice bath, followed by addition of an appropriate amount of the modified BFE catalyst. The modified catalyst was prepared by mixing the NFO with BFE, which was usually required to produce homogeneous polymers [15,16]. The reaction mixture was then injected into a glass mold, sealed by silicon adhesive and heated for 12 h at room temperature, followed by 12 h at 60 °C and 24 h at 110 °C. The resulting thermosets were obtained in essentially quantitative yield. The nomenclature adopted in this paper for the polymer samples is as follows: a polymer sample prepared from

45 wt % LIN, 32 wt % ST, 15 wt % DVB using 8 wt % NFO-modified BFE catalyst (5 wt % NFO + 3 wt % BFE) is designated as LIN45-ST32-DVB15-(NFO5-BFE3).

Soxhlet Extraction. A 2-3 g sample of the bulk polymer was extracted with 100 mL of refluxing methylene chloride for 24 h using a Soxhlet extractor. Following the extraction, the resulting solutions were concentrated under vacuum and the extracts were dried in a vacuum oven overnight. The soluble substances were characterized by ^{1}H NMR spectroscopy. The recovered insoluble portion was dried under a vacuum prior to weighing.

Characterization. ^{1}H NMR spectroscopic analyses of the extracted soluble substances were recorded in $CDCl_3$ using a Varian Unity spectrometer at 300 MHz. Cross-polarization magic angle spinning (CP MAS) ^{13}C NMR analysis of the insoluble materials remaining after Soxhlet extraction of the bulk polymers was performed using a Bruker MSL 300 spectrometer. Samples were examined at two spinning frequencies (3.2 and 3.7 kHz) in order to differentiate between actual signals and spinning side bands. FTIR spectra were recorded on a Nicolet 740 FT-IR spectrometer (KBr pill). Dynamic mechanical analysis (DMA) data were obtained using a Perkin Elmer dynamic mechanical analyzer DMA Pyris-7e in a three-point bending mode. Rectangular specimens of 2 mm thickness and 5 mm depth were used for the analysis and the width to depth ratio was maintained at approximately 3. The measurements were performed at a heating rate of 3 °C/min and a frequency of 1 Hz in He with a gas flow rate of 20 mL per minute and applied static and dynamic forces of 110 and 100 mN respectively. Thermogravimetric analysis (TGA) was performed on a Perkin Elmer Pyris-7 thermogravimeter. The percent weight loss temperatures of the polymeric materials were measured in air with a gas flow rate of 20 mL/min. The samples were heated from 50-650 °C at a heating rate of 20 °C/min. The

tensile tests were conducted at room temperature according to ASTM-D638M specifications using an Instron universal testing machine (Model-4502) at a cross-head speed of 5 mm/min. The dumbbell-shaped test specimen (type M-I specimen in ASTM D638M) had a gauge section with a length of 50 mm, a width of 10 mm, and a thickness of 3 mm. The gauge section was joined to the wider end sections by two long tapered sections. The dumbbell-shaped specimens were prepared by cutting the material out of a polymer plate, followed by precise machining. At least 5 identical specimens were tested for each polymer sample. The Young's modulus (E), ultimate strength (σ_b) and elongation at break (ε_b) of the polymers were obtained from the tensile tests and reported as average values. The tensile toughness of the polymer, which is the fracture energy per unit volume of the specimen, was obtained from the area under the corresponding tensile stress-strain curve. The gelation time is the time elapsed from initial mixing of the reactants at the given temperature to the time when solidification commences, which was determined by the complete cessation of flow of the liquid reactants. Measurements were performed in reference to the ASTM standard D2471-99. The gelation time was averaged from five individual measurements at a specific temperature. Viscosity measurements on the vegetable oils were performed at 23 °C using a Haake RS-150 Rheo Stress Rheometer (Karlsruhe, Germany). Shear stress was applied using a 60 mm 2° titanium cone over the range of 10-2000 s^{-1}. Each sample was tested at least three times and the results reported as average viscosities at maximum shear rate.

Results and Discussion

Chemical Compositions of the Vegetable Oils. The commercially available vegetable oils employed in this study are listed in Table 1, along with their fatty acid compositions and corresponding viscosities. These oils are primarily composed of saturated

stearic (C16-0) and palmitic (C18-0) acids, as well as unsaturated oleic (C18-1), linoleic (C18-2) and linolenic (C18-3) fatty acids. The content of other saturated and unsaturated fatty acids is negligible. The unsaturated fatty acid content determines the degree of unsaturation of the vegetable oil, and consequently, its reactivity. Figure 1 shows a representative ^{1}H NMR spectra of Superb linseed oil, along with a detailed peak assignment. The signals at 4.1-4.4 ppm (**A**) correspond to the protons on the C-1 and C-3 atoms of the glyceride unit, which indicate that these vegetable oils have a triglyceride structure. The vinylic hydrogens (**I**) of these oils are typically detected at 5.2-5.5 ppm, while the CH_2 protons positioned between two C=C bonds, also know as bis-allylic protons (**J**), are observed at 2.7-2.9 ppm, indicating that the C=C bonds are non-conjugated. Detailed triglyceride peak assignments are well documented in the literature [27-29].

Table 1. Fatty acid compositions of various vegetable oils

	OLV	*PNT*	*SES*	*CAN*	*COR*	*SOY*	*GRP*	*SUN*	*LSS*	*SAF*	*WNT*	*LIN*
η [a]	60.6	59.1	53.7	55.4	49.9	49.3	48.5	48.8	47.8	45.9	42.5	38.8
D [b]	2.86	3.27	3.81	3.97	4.07	4.31	4.49	4.61	5.03	5.04	5.46	6.07
D [c]	2.85	3.37	3.87	3.91	4.45	4.61	4.57	4.69	5.16	5.06	5.24	6.24
14:0	-	0.1	0.1	0.1	0.1	0.1	-	0.1	-	0.1	-	0.2
16:0	9.0	11.1	8.2	4.1	10.9	10.6	7.0	7.0	3.0	6.8	4.6	5.4
18:0	2.7	2.4	3.6	1.8	2.0	4.0	3.0	4.5	1.0	2.3	0.9	3.5
18:1	80.3	46.7	42.1	60.9	25.4	23.3	27.4	18.7	31.0	12.0	17.8	19.0
18:2	6.3	32.0	43.4	21.0	59.6	53.7	62.5	67.5	57.0	77.7	73.4	24.0
18:3	0.7	-	-	8.8	1.2	7.6	-	0.8	9.0	0.4	3.3	47.0
20:0	0.4	1.3	1.1	0.7	0.4	0.3	-	0.4	-	0.3	-	0.6
20:1	-	1.6	-	1.0	-	-	-	0.1	-	0.1	-	-

[a] Viscosities are given in cP units. [b] Degree of unsaturation as calculated by ^{1}H NMR spectral analysis. [c] These values are calculated from the oil compositions found in references 4 and 5. Numbers given in the far left column represent fatty acids found in these vegetable oils; for example, 18:3 represents linolenic acid, which has straight 18-carbon chain with three C=C double bonds.

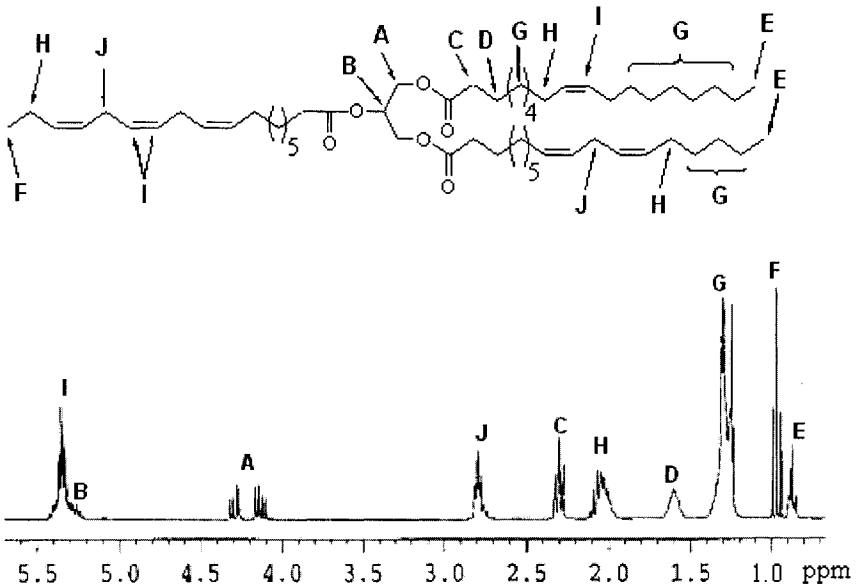

Figure 1. ^{1}H NMR spectra of LIN with peak assignments.

The oils listed in Table 1 are arranged according to their degrees of unsaturation (**d**). Degrees of unsaturation, expressed as numbers of C=C bonds per triglyceride, are calculated using the following equation:

$$d = (4A - B) / 2B \quad (1)$$

where A is the integrated area of the convoluted peaks above 5.20 ppm (including the C-2 hydrogen atom of the glycerol group) and B is the integrated area of the peaks at 4.10-4.40 ppm. Calculated **d** values are shown in Table 1 and compared to the values given in parentheses, which represent the number of C=C bonds per triglyceride calculated from the fatty acid compositions found in the literature [4,5]. It should be noted that the literature values differ slightly from the values obtained by ^{1}H NMR spectral analysis. When comparing the reactivities of the oils in question, one must keep in mind that the composition of the oil may vary significantly and depends on the region where the oil was produced, as

well as the methods used for their isolation and processing [4]. Table 1 shows that the **d** values increase from 2.86 for OLV to 6.07 for LIN, suggesting significant differences in their reactivities. Thus, it is interesting to investigate the effect of the degree of unsaturation on the synthesis, structure, and thermophysical and mechanical properties of the novel bioplastics prepared from these vegetable oils.

Vegetable Oil Copolymerization and Molecular Structure Determination. The presence of multiple C=C bonds in vegetable oils allows their copolymerization into solid polymeric materials via cationic polymerization. BFE has proved to be a very effective catalyst in cationic polymerizations [30,31]. However, the homopolymerization of vegetable oils typically results in viscous fluids of limited use [16]. To produce viable hard plastics, vegetable oils have to be copolymerized with more rigid and reactive aromatic comonomers, such as ST and DVB. As in our soybean oil polymerizations [16,17], an NFO-modified BFE catalyst has to be employed in order to produce homogeneous reactions. Basically, 8 wt % NFO-modified BFE catalyst is able to generate homogeneous reactions with all vegetable oils herein employed. The vegetable oils listed in Table 1 were cationically copolymerized with either DVB or a mixture of ST and DVB to give two series of copolymers, namely OIL62-DVB30-(NFO5-BFE3) and OIL45-ST32-DVB15-(NFO5-BFE3). These two compositions have been chosen because they approximate the compositions of maximum oil incorporation into the resulting copolymers as shown in our previous work on soybean oil plastics [16,18].

The gelation times for both the OIL-DVB and OIL-ST-DVB systems were determined by measuring the time required for liquid reactants to reach a certain viscosity at which cessation of flow was observed. The presence of very reactive ST and DVB

comonomers facilitates the gelation process and drastically reduces the gelation times when compared to vegetable oil homopolymerization. The gelation times have been determined at three different temperatures (room temperature, 40 °C and 50 °C) and the data are summarized in Table 2. Room temperature gelation times range from 130 to 348 minutes for OIL-DVB systems and 80 to 233 minutes for OIL-ST-DVB systems. The gelation times determined at higher temperatures are naturally substantially shorter. Our results indicate that OIL-ST-DVB mixtures gel faster than the corresponding OIL-DVB mixtures. This can be attributed to the higher concentration of the more reactive comonomers (ST + DVB) in the OIL-ST-DVB compositions. Surprisingly, the gelation times determined at all temperatures appear to be completely independent of the degrees of unsaturation of the vegetable oils. This independence strongly suggests the presence of two opposite effects. The fact that the gelation process involves drastic changes in the viscosity of the reaction mixture leads us to believe that differences in the oil viscosities may be partially responsible for such behavior, especially since the vegetable oil in a given composition accounts for approximately 50 weight % of the whole reaction mixture. In order to examine this phenomenon further, we have measured and compared viscosities of the vegetable oils employed in this study (Table 1). As expected, all vegetable oils exhibit typical Newtonian behavior with viscosities ranging from 38.8 to 60.6 cP. In general, the greater the degree of unsaturation of the vegetable oil, the lower the viscosity. Higher degrees of unsaturation result in higher oil reactivity during polymerization and, consequently, shorter gelation times. At the same time, higher degrees of unsaturation result in lower oil and initial reaction mixture viscosities, which lead to longer gelation times.

Table 2. Gelation times for the OIL– ST– DVB and OIL–DVB copolymers [a]

OIL	OIL45 – ST32 – DVB15			OIL62 – DVB32		
	RT	*40 °C*	*50 °C*	*RT*	*40 °C*	*50 °C*
OLV	**185**	**19.3**	**14.0**	**256**	**39.7**	**6.3**
PNT	**113**	**15.9**	**5.1**	**277**	**35.0**	**3.2**
SES	**80**	**19.3**	**3.5**	**130**	**34.9**	**2.4**
CAN	**118**	**18.2**	**4.6**	**189**	**33.3**	**2.7**
COR	**209**	**23.2**	**16**	**292**	**37.5**	**2.7**
SOY	**130**	**18.3**	**12.5**	**214**	**29.5**	**4.1**
GRP	**233**	**35.1**	**14.7**	**348**	**78.7**	**6.7**
SUN	**156**	**23.9**	**9.3**	**216**	**34.7**	**4.1**
LSS	**163**	**29.9**	**9.4**	**213**	**50.7**	**5.4**
SAF	**84**	**20.4**	**7.5**	**144**	**29.1**	**5.4**
WNT	**184**	**19.2**	**7.0**	**249**	**37.5**	**4.2**
LIN	**185**	**28.6**	**19.7**	**255**	**54.5**	**6.6**

[a] All gelation times are given in minutes and represent an average value of at least three individual runs.

In general, the OIL-DVB copolymers range from soft to hard and brittle plastics, while the OIL-ST-DVB terpolymers range from soft to hard ductile plastics. All copolymers have a dark brown glossy color and a slight odor. The presence of multiple C=C bonds in both the vegetable oils and the DVB results in crosslinked structures for the final copolymers. The yields of crosslinked polymers and soluble fractions have been determined by Soxhlet extraction analysis. Extraction results for OIL-DVB and OIL-ST-DVB copolymers are presented in Tables 3 and 4 respectively. Our results show that the amount of crosslinked polymer increases with increasing degree of unsaturation of the vegetable oil employed in the original composition. For example, the yields of crosslinked OIL-DVB and OIL-ST-DVB polymers increase from 64.9 to 87.8% and 67.5 to 85.9% respectively, when the **d** values of the corresponding vegetable oils increase gradually from 2.86 (OLV) to 6.07 (LIN). A more detailed analysis, however, reveals that an increase in **d** value of the

vegetable oils does not result in a linear dependence of the yield of the crosslinked copolymers. The results indicate that there exists a two-stage dependence (Figure 2). The first stage represents a rapid increase in the yield of the crosslinked polymer with an increase in **d** value of the vegetable oil. This stage is representative of vegetable oils with **d** values in the range of 3-5 (Table 1, entries 1-10). As **d** increases further (**d** > 5, Table 1, entries 11 and 12), the dependence levels off (stage two) as shown by the flat plateau above **d** = 5.

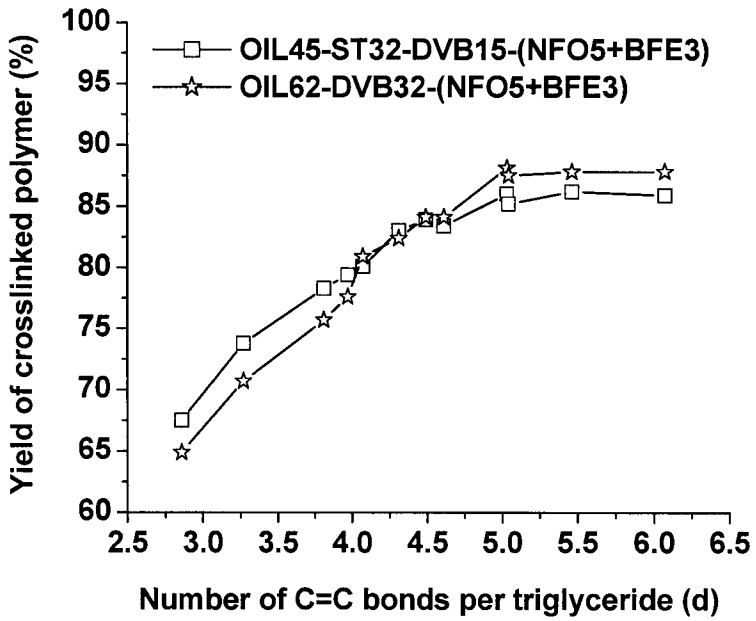

Figure 2. The effect of the degree of unsaturation on the yield of the crosslinked copolymer.

We believe that there exists a certain amount of unreacted fatty acid double bonds left in the crosslinked material after curing. These double bonds are covalently linked to the crosslinked network. Thus, not every double bond in the fatty acid chain of the triglyceride participates actively in crosslinking. Thus, there exists a limit in **d** value of the non-

conjugated oils after which a further increase in the number of double bonds no longer results in an increase in the yield of the crosslinked material.

Table 3. Properties of the OIL-DVB copolymers

Copolymer	T_g (°C)	ν_e[a] (mol/m^3)	T_{10}[b] (°C)	T_{50}[c] (°C)	ΔT[d] (°C)	(T_{max})[e] (°C)
OLV62-DVB30-I8	0 & 49	7.61×10^3	269	462	193	477.8
PNT62-DVB30-I8	-6 & 48	1.21×10^4	282	461	179	474.6
SES62-DVB30-I8	-8 & 45	1.33×10^4	284	469	179	480.6
CAN62-DVB30-I8	-13 & 45	1.27×10^4	284	463	179	476.6
COR62-DVB30-I8	-12 & 50	1.31×10^4	295	465	171	479.5
SOY62-DVB30-I8	-8 & 50	1.34×10^4	296	470	173	483.6
GRP62-DVB30-I8	-3 & 55	1.97×10^4	312	470	158	483.5
SUN62-DVB30-I8	-10 & 50	2.05×10^4	321	468	147	476.7
LSS62-DVB30-I8	-7 & 50	2.23×10^4	324	468	144	474.0
SAF62-DVB30-I8	-10 & 56	2.26×10^4	332	478	146	490.1
WNT62-DVB30-I8	5 & 58	2.25×10^4	331	472	141	484.7
LIN62-DVB30-I8	11 & 55	2.28×10^4	342	473	130	485.6

I8 = (NFO5-BFE3). [a] Crosslink densities. [b] 10 % weight loss temperature. [c] 50 % weight loss temperature. [d] $\Delta T = T_{50} - T_{10}$. [e] Maximum thermal degradation temperature.

Table 3. Continued

Copolymer	% Insol.	% Sol.	E[f] (MPa)	σ_b[g] (MPa)	ε_b[h] (%)	Toughness (MPa)
OLV62-DVB30-I8	64.9	35.1	27.2	1.2	8.4	0.06
PNT62-DVB30-I8	70.7	29.3	35.9	1.7	9.4	0.09
SES62-DVB30-I8	75.7	24.3	37.7	2.2	10.4	0.13
CAN62-DVB30-I8	77.6	22.4	43.9	1.7	7.7	0.07
COR62-DVB30-I8	80.9	19.1	45.1	2.2	8.2	0.13
SOY62-DVB30-I8	82.4	17.6	46.6	2.5	8.1	0.12
GRP62-DVB30-I8	84.1	15.9	50.8	3.0	10.7	0.18
SUN62-DVB30-I8	84.1	15.9	54.0	3.0	11.2	0.20
LSS62-DVB30-I8	88.1	11.9	58.4	3.0	10.7	0.23
SAF62-DVB30-I8	87.5	12.5	62.8	3.1	8.6	0.14
WNT62-DVB30-I8	87.5	12.5	62.4	3.8	11.8	0.26
LIN62-DVB30-I8	87.8	12.2	99.9	5.6	10.5	0.35

I8 = (NFO5-BFE3). [f] Young's Modulus. [g] Ultimate strength. [h] Elongation at break.

Table 4. Properties of the OIL-ST-DVB copolymers

Copolymer	T_g (°C)	ν_e[a] (mol/m^3)	T_{10}[b] (°C)	T_{50}[c] (°C)	ΔT[d] (°C)	(T_{max})[e] (°C)
OLV45-ST32-DVB15-I8	16 & 62	6.03 x 10^2	276	455	179	465.6
PNT45-ST32-DVB15-I8	19 & 62	7.47 x 10^2	281	461	178	468.8
SES45-ST32-DVB15-I8	60	8.03 x 10^2	294	459	167	468.4
CAN45-ST32-DVB15-I8	60	9.38 x 10^2	295	456	162	468.2
COR45-ST32-DVB15-I8	50	1.34 x 10^3	294	459	164	465.4
SOY45-ST32-DVB15-I8	53	1.39 x 10^3	316	463	148	475.2
GRP45-ST32-DVB15-I8	58	1.83 x 10^3	321	462	141	477.1
SUN45-ST32-DVB15-I8	58	1.85 x 10^3	309	457	149	462.6
LSS45-ST32-DVB15-I8	66	2.22 x 10^3	324	462	138	468.8
SAF45-ST32-DVB15-I8	54	2.24 x 10^3	343	462	119	475.6
WNT45-ST32-DVB15-I8	59	2.24 x 10^3	332	461	129	477.2
LIN45-ST32-DVB15-I8	56	2.27 x 10^3	339	465	126	476.6

I8 = (NFO5-BFE3). [a] Crosslink densities. [b] 10 % weight loss temperature. [c] 50 % weight loss temperature. [d] $\Delta T = T_{50} - T_{10}$. [e] Maximum thermal degradation temperature.

Table 4. Continued

Copolymer	% Insol.	% Sol.	E[f] (MPa)	σ_b[g] (MPa)	ε_b[h] (%)	Toughness (MPa)
OLV45-ST32-DVB15-I8	67.5	32.5	13.0	1.9	38.6	0.46
PNT45-ST32-DVB15-I8	73.8	26.2	17.6	3.1	56.3	1.13
SES45-ST32-DVB15-I8	78.3	21.7	36.8	3.7	77.3	2.10
CAN45-ST32-DVB15-I8	79.4	20.6	37.0	4.2	76.7	2.18
COR45-ST32-DVB15-I8	80.1	19.9	38.3	4.7	78.8	2.34
SOY45-ST32-DVB15-I8	83.0	17.0	46.3	5.3	86.0	2.56
GRP45-ST32-DVB15-I8	83.9	16.1	53.8	5.6	62.8	2.59
SUN45-ST32-DVB15-I8	83.4	16.6	54.1	5.7	75.3	3.21
LSS45-ST32-DVB15-I8	86.0	14.0	61.9	7.0	77.2	3.94
SAF45-ST32-DVB15-I8	85.2	14.8	62.2	7.0	78.1	4.02
WNT45-ST32-DVB15-I8	86.2	13.8	63.1	7.5	85.8	4.79
LIN45-ST32-DVB15-I8	85.9	14.1	125.6	10.9	69.4	5.83

I8 = (NFO5-BFE3). [f] Young's Modulus. [g] Ultimate strength. [h] Elongation at break.

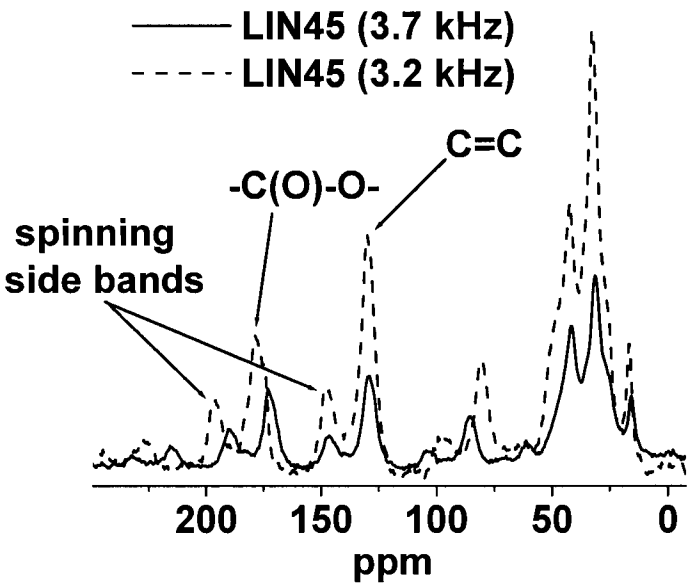

Figure 3. Solid state ^{13}C NMR spectra of the insoluble materials remaining after Soxhlet extraction of the LIN45-ST32-DVB15-(NFO5-BFE3) bulk copolymer.

FT-IR and solid-state ^{13}C NMR spectral analyses have been performed to fully characterize the resulting polymeric materials. A representative solid-state CP MAS ^{13}C NMR spectrum of the LIN45-ST32-DVB15-(NFO5-BFE3) terpolymer after Soxhlet extraction is shown in Figure 3. The spectrum confirms the presence of ester carbonyl groups (δ = 165-175 ppm), due to incorporation of the LIN into the crosslinked matrix, as well as the presence of C=C bonds (δ = 125-135 ppm). Unfortunately, the broad nature of the latter peak prevents us from distinguishing between the sp^2 carbons of unreacted C=C bonds in the fatty acid side chains and those of the benzene rings in the ST and DVB units. Similar to the CP MAS ^{13}C NMR spectra, the FT-IR spectrum of the insoluble materials obtained from Soxhlet extraction of the LIN45-ST32-DVB15-(NFO5-BFE3) terpolymer

(Figure 4) confirms the presence of carbonyl groups (~1750 cm^{-1}) from incorporation of the LIN oil, as well as the presence of C=C bonds, but it does not allow us to clearly distinguish between the C=C bonds of the fatty acids and the benzene rings.

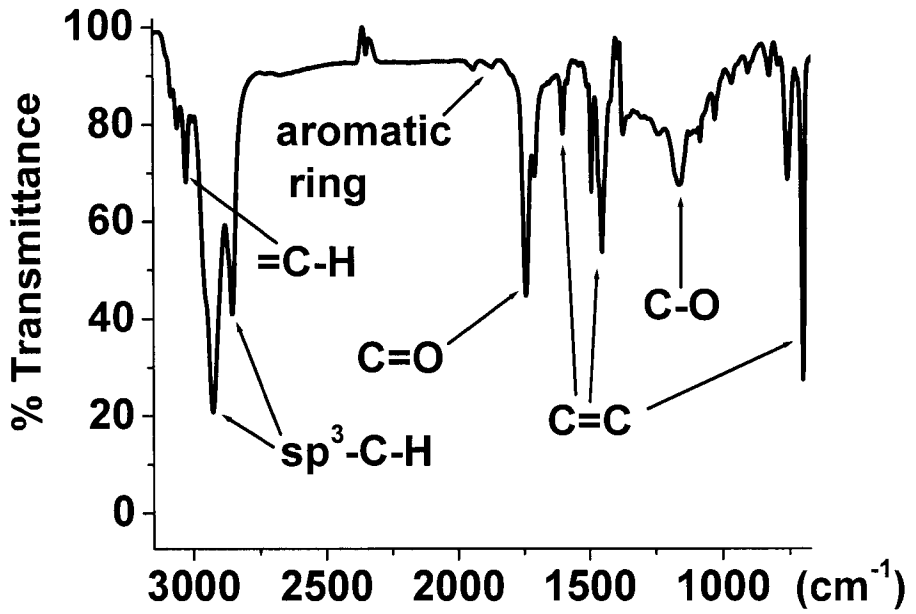

Figure 4. FT-IR spectra of the insoluble materials remaining after Soxhlet extraction of the LIN45-ST32-DVB15-(NFO5-BFE3) bulk copolymer.

To determine the microstructures of the resulting copolymers, the soluble fractions from the Soxhlet extractions have been subjected to ^1H NMR spectral analysis. Representative ^1H NMR spectra of the soluble materials from the PNT45-ST32-DVB15-(NFO5-BFE3) and PNT62-DVB32-(NFO5-BFE3) copolymers are shown in Figure 5. The ^1H NMR spectrum of the pure catalyst BFE is also included for comparison purposes. The spectral data confirm that the extract consists of several soluble components. The signals at 4.1-4.2 ppm confirm the presence of residual initiator fragments, while the signals at 4.1-4.4

ppm and 5.3-5.5 ppm correspond to glycerol and vinylic protons of the unreacted PNT oil respectively. Also, the existence of a broad signal in the aromatic region (6.5-7.5 ppm) of the spectrum of the PNT45-ST32-DVB15-(NFO5-BFE3) extract suggests the presence of low molecular weight ST-PNT copolymers. These oligomers are soluble in CH_2Cl_2 and readily extracted during Soxhlet extraction. In contrast, this type of signal was not observed in the spectrum of the PNT62-DVB32-(NFO5-BFE3) extract, suggesting that DVB is completely incorporated into the crosslinked network. Similar results have been obtained during ^1H NMR spectral analyses of the soluble extracts from other vegetable oil copolymers.

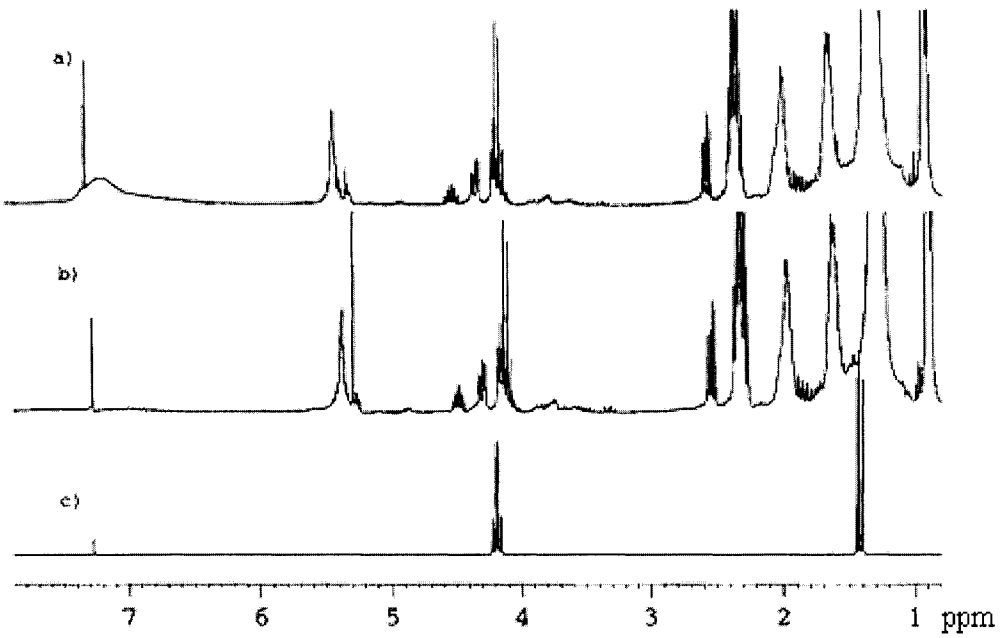

Figure 5. ^1H NMR spectra of a) soluble materials from PNT45-ST32-DVB15-(NFO5-BFE3), b) soluble materials from PNT62-DVB32-(NFO5-BFE3), and c) pure initiator BFE.

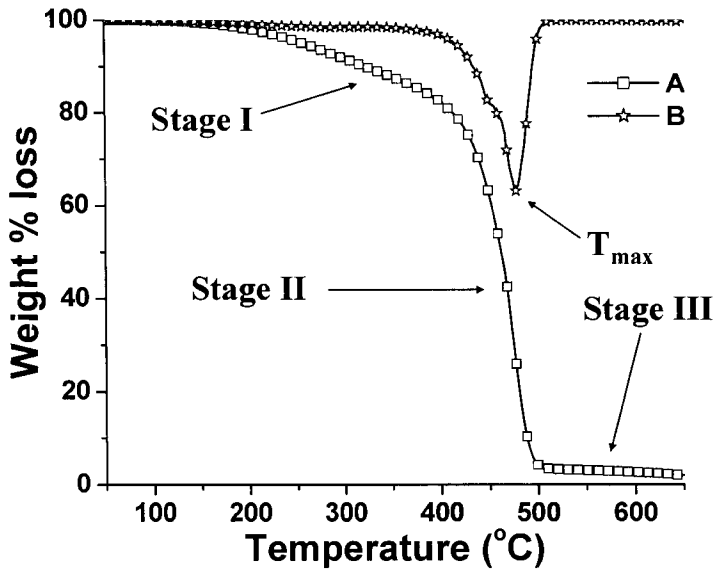

Figure 6. TGA thermogram of the GRP45-ST32-DVB15-(NFO5-BFE3) copolymer in air (A) and its derivative curve (B).

Thermogravimetric Analysis of the Vegetable Oil Copolymers. Tables 3 and 4 summarize the thermal data for the OIL-DVB and OIL-ST-DVB copolymers respectively. These include 10 and 50% weight loss temperatures (T_{10} and T_{50}), their differences (ΔT), as well as the temperatures of maximum thermal degradation (T_{max}). Thermogravimetric analysis indicate that the OIL-DVB and OIL-ST-DVB bulk polymers are thermally stable in air below 200 °C and exhibit a three-stage thermal degradation above this temperature (Figure 6, curve A). The first stage degradation (200-400 °C) is attributed to evaporation and decomposition of unreacted oil and other soluble components in the bulk material. The second stage (400-500 °C) is the fastest and corresponds to degradation and char formation of the crosslinked polymer structure, while the last stage (>500 °C) corresponds to gradual

oxidation of the char residue. The second stage is also characterized by a T_{max} value determined from the minimum of the corresponding derivative % weight loss curve (Figure 6, curve B). The data in Tables 3 and 4 indicate that the bulk of the OIL-DVB and OIL-ST-DVB copolymers lose 10% of their weight at temperatures ranging from 269–342 °C and 276–339 °C respectively. In general, an increase in **d** value of the vegetable oil results in higher T_{10} values for both the OIL-DVB and OIL-ST-DVB copolymers. For example, an increase in **d** value from 2.86 (OLV) to 6.07 (LIN) results in a 73 °C and 63 °C increase in T_{10} value for the OIL-DVB and OIL-ST-DVB copolymers respectively. More unsaturated vegetable oils result in polymers with better thermal properties. In spite of the noticeable differences in the T_{10} values, all of the polymers lose half of their weight within a very narrow temperature region, as indicated by the ΔT values. This value is defined as the difference between the T_{10} and T_{50} temperatures and denotes the rate of thermal decomposition in the first and second stages of the polymers' thermal decomposition. Our results show that copolymers composed of oils with higher **d** values have lower ΔT values. This is in agreement with the fact that copolymers of more unsaturated oils contain less unreacted oil. The smaller amount of unreacted oil in the bulk polymer degrades faster and thus results in smaller ΔT values. The results also indicate that the T_{50} values increase as well with increasing **d** values of the oils. However, unlike the differences for the T_{10} values (73 °C and 63 °C), these differences are much smaller (11 °C and 10 °C). The closer these temperatures get to T_{max}, the smaller the differences are. This indicates that the thermal decompositions in the T_{max} region are almost independent of the **d** values of the vegetable oils. Figure 7 represents the TGA thermograms of several OIL-DVB and OIL-ST-DVB

copolymers. These thermograms indicate that both systems exhibit quite similar thermal behaviors.

a)

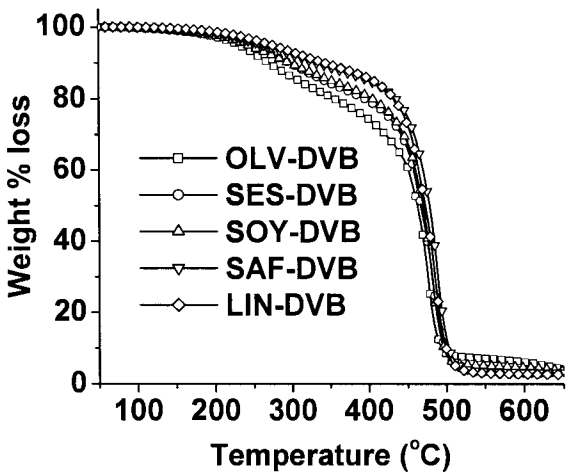

b)

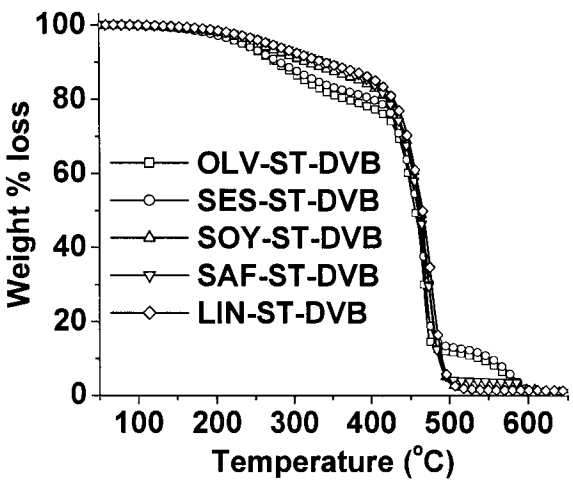

Figure 7. TGA thermograms of several OIL-DVB (a) and OIL-ST-DVB (b) copolymers acquired in air.

Dynamic Mechanical Properties of the Vegetable Oil Copolymers. Figures 8 and 9 illustrate the temperature dependence of the storage moduli of the OIL-DVB and OIL-ST-DVB copolymers respectively. Dynamic mechanical analysis (DMA) reveals that all copolymers behave as typical thermosets as evidenced by the presence of rubbery plateaus in their DMA curves. As expected, the storage moduli decrease gradually with increasing temperature until the rubbery plateau region appears above approximately 80 °C. The room temperature storage moduli appear dependent on the degree of unsaturation of the vegetable oils employed for copolymer synthesis. Figures 8 and 9 show that the storage moduli at room temperature steadily increase from 0.19 (OLV) to 0.87 (LIN) GPa and 0.22 (OLV) to 1.84 (LIN) GPa for the OIL-DVB and OIL-ST-DVB copolymers respectively. The presence of the rubbery plateau in the DMA curves is evidence for the existence of a crosslinked network in the bulk polymers. According to the kinetic theory of rubber elasticity [32-34], the experimental crosslink densities of all copolymers (ν_e) can be determined from the rubbery moduli using the following equation:

$$E' = 3\nu_e RT$$

where E' represents the storage modulus of the crosslinked copolymer in the rubbery plateau region above the glass transition temperature (T_g), R is the universal gas constant and T is the absolute temperature. The values of the storage moduli E' used for the calculations were taken at approximately 50 °C above the T_g. Typical crosslink densities of the OIL-DVB copolymers are in the range of 7.6×10^3 to 2.3×10^4 mol/m^3 and are much higher than those of the OIL-ST-DVB copolymers, which are in the range of 6.0×10^2 to 2.3×10^3 mol/m^3 (Tables 3 and 4). Like regular soybean oil (SOY) [18], all vegetable oils used in this study contribute directly to the crosslink densities of their corresponding copolymers.

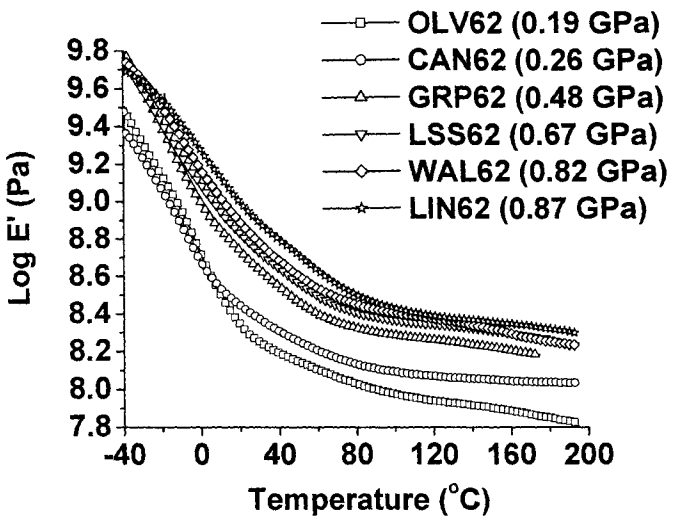

Figure 8. Temperature dependence of the storage modulus E' for several OIL62-DVB30-(BFE3-NFO5) copolymers with their room temperature E' values given in parentheses.

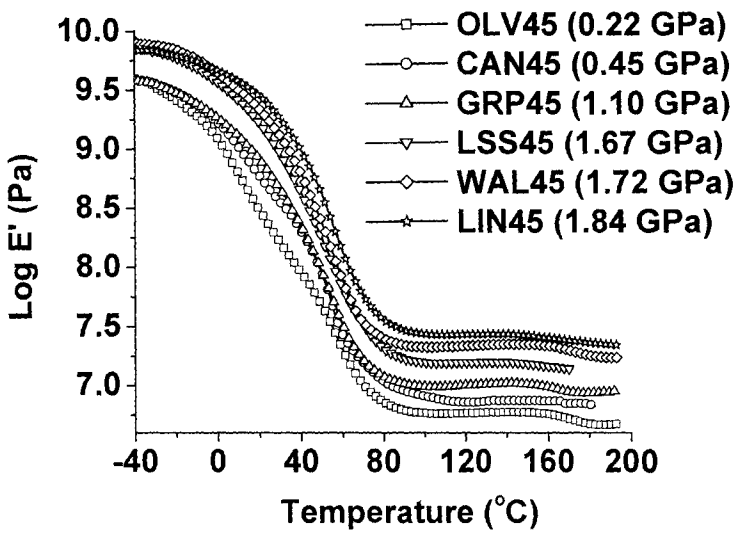

Figure 9. Temperature dependence of the storage modulus E' for several OIL45-ST32-DVB15-(NFO5-BFE3) copolymers with their room temperature E' values given in parentheses.

Keeping in mind that the only variable in both the OIL-DVB and OIL-ST-DVB systems is the vegetable oil employed, it is important to note that copolymers prepared from more unsaturated oils have higher crosslink densities. This means that a careful choice of the vegetable oil employed as the comonomer may also be used as a tool for tuning the polymer properties.

Tables 3 and 4 also summarize the glass transition temperatures (T_g) obtained from DMA analysis of the OIL-DVB and OIL-ST-DVB copolymers respectively. All OIL-DVB copolymers have two glass transition temperatures, which merge into a very broad transition. The OIL-DVB copolymer matrixes appear as complex heterogeneous systems composed of "DVB-rich" phases and "OIL-rich" phases with their own individual glass transitions (Figure 10). At the very beginning of the reaction, DVB, as the much more reactive monomer, starts to homopolymerize and forms the core of the DVB-rich phase (hard domain). This is evidenced by the formation of white flakes, which correspond to polydivinylbenzene. As the DVB concentration drops, the DVB starts to copolymerize with the OIL, which is present in far greater concentration, until the DVB is completely consumed. During that stage of the reaction, a certain amount of the OIL is incorporated into the copolymer structure. The amount of the oil incorporated is directly related to the reactivity of the oil, which is expressed through its **d** value. At the end of the reaction, a certain amount of OIL is left unreacted, as evidenced by our extraction data. This oil acts as a plasticizer in the bulk copolymer. The insoluble crosslinked materials are therefore composed of "DVB-rich" domains (formed in the early stages of the reaction) and "OIL-rich" domains (formed in the later stages of the reaction). The glass transition temperatures we observe from the tan delta curves are considerably lower than expected for the glass transition temperatures of these two

domains minus any plasticizer. The low glass transition temperatures are presumably due to plasticization by the soluble components, which are statistically distributed throughout the bulk polymer. Thus, the high temperature transitions (α_1) (from 45 to 58 °C) represent the glass transitions of the plasticized "DVB-rich" phases, while the low temperature transitions (α_2) (from -13 to 11 °C) correspond to the glass transitions of the plasticized "OIL-rich" phases. In contrast, most of the OIL-ST-DVB terpolymers (with the exception of the OLV and PNT oil terpolymers) possess a single glass transition (Figure 11). The glass transition temperatures of the OIL-ST-DVB terpolymers are in the 50-66 °C range, which is slightly higher than the range of the OIL-DVB copolymers. In general, the glass transition temperatures for both the OIL-DVB and OIL-ST-DVB systems show no dependence on the degree of unsaturation of the oils employed in their synthesis. The existence of the dual thermal transitions in the OLV45-ST32-DVB15-(NFO5-BFE3) and PNT45-ST32-DVB15-(NFO5-BFE3) terpolymers is a consequence of the low degrees of unsaturation of these two oils. Their lower reactivities result in formation of heterogeneous systems as opposed to those of the other OIL-ST-DVB terpolymers. Similar to our explanation regarding the OIL-DVB systems, the high glass transitions correspond to plasticized "ST-DVB-rich" phases, while the low glass transitions correspond to plasticized "OIL-rich" phases (Figure 11). Furthermore, when compared to the α_2 transitions in the corresponding OIL-DVB copolymers, the α_2 transitions of the OLV-ST-DVB (16 °C) and PNT-ST-DVB (19 °C) terpolymers are considerably higher. This is a consequence of the lower amounts of OLV and PNT oils and greater amounts of aromatic comonomers incorporated into the "OIL-rich" phases of the OLV-ST-DVB and PNT-ST-DVB terpolymers respectively. This is not a surprise, since the initial amounts of individual vegetable oils in the OIL-ST-DVB systems

(45 wt %) are lower than those in the corresponding OIL-DVB systems (62 wt %). Of course, the opposite is true for the initial amounts of aromatic comonomers.

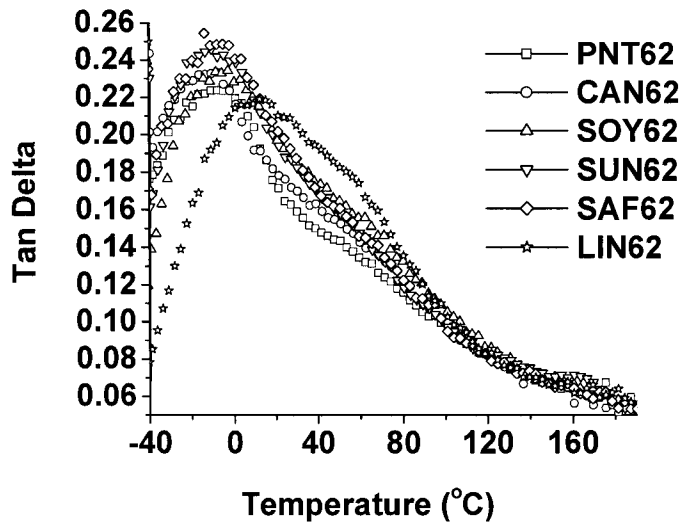

Figure 10. Temperature dependence of the loss factor tan δ for several OIL62-DVB30-(NFO5-BFE3) copolymers.

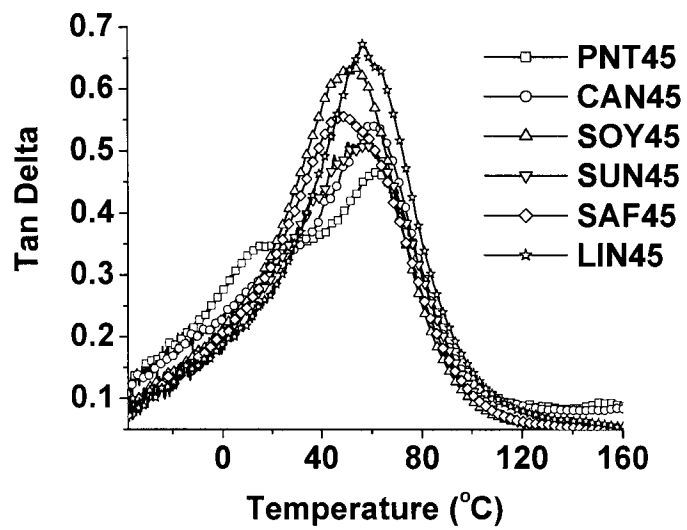

Figure 11. Temperature dependence of the loss factor tan δ for several OIL45-ST32-DVB15-(NFO5-BFE3) copolymers.

Tensile Stress-Strain Performance of the Vegetable Oil Copolymers. Figures 12 and 13 illustrate the tensile stress-strain behavior of several OIL-DVB and OIL-ST-DVB copolymers respectively. The OIL-DVB copolymers exhibit a variety of stress-strain behaviors depending on the oil used in their synthesis. In general, all of these copolymers are brittle in nature. Their Young's moduli are in the range of 27.2-99.9 MPa and show clear dependence on the **d** values of the vegetable oils employed for their synthesis (Table 3). For example, the initial slopes of the LIN, WNT and SAF copolymers are rather steep, indicating the high elastic moduli of these materials. Quite the opposite is observed for the OLV, PNT and SES copolymers, which have significantly lower Young's moduli and are very soft in nature. The stress-strain curves of all OIL-DVB copolymers show a constant increase in stress with strain until rupture occurs. Elongation-at-break values of these materials are fairly small and similar for all copolymers. They are in the range of 7.7-11.8% and show no dependence on the reactivity of the vegetable oil. The brittle nature of the OIL-DVB copolymers is mainly due to the relatively high crosslink densities of these copolymers, which drastically reduce the copolymers' flexibilities and elongations at break (Table 3).

The increase in the crosslink densities of the OIL-DVB copolymers with increasing oil reactivity substantially reduces the mobility of polymer chains between the junctions and, therefore, the number of conformations which they can adopt. On the other hand, the stiffness of these polymers, as well as the energy required for crack propagation during the tensile deformation, progressively increases. Because of that, the ultimate strengths of the OIL-DVB copolymers follow the same trend. These values increase gradually with increasing oil reactivity and are in the range of 1.2-5.6 MPa.

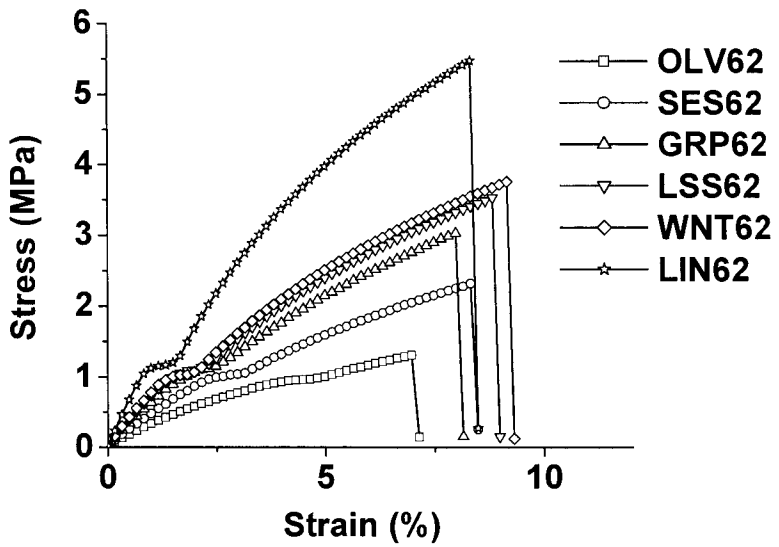

Figure 12. Tensile stress-strain curves for several OIL62-DVB30-(NFO5-BFE3) copolymers.

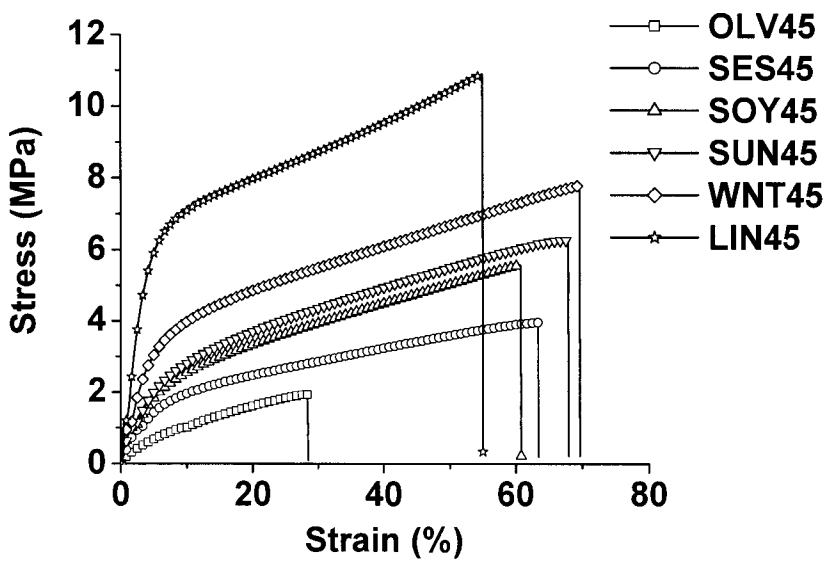

Figure 13. Tensile stress-strain curves for several OIL45-ST32-DVB15-(NFO5-BFE3) copolymers.

In addition to the Young's modulus and ultimate strength data, tensile tests also provide information about the polymers' tensile toughness. Tensile toughness is measured by the area under the stress-strain curve and represents the work expended in deforming the material [35]. Both tensile strength and the elongation-at-break contribute to tensile toughness. In general, brittle materials have low tensile toughness, while ductile materials have high. The tensile toughness of the OIL-DVB copolymers is in the range of 0.06-0.35 MPa. In spite of the independent nature of the elongation-at-break values of the OIL-DVB copolymers and the reactivity of the corresponding oil, Table 3 indicates that the tensile toughness of most of the OIL-DVB copolymers increases gradually with the increasing reactivity of the oil. The only exceptions are the CAN62-DVB30-(NFO5-BFE3), SOY62-DVB30-(NFO5-BFE3) and SAF62-DVB30-(NFO5-BFE3) copolymers, whose values deviate from the expected trend. At this moment we are unable to account for these discrepancies.

The OIL-ST-DVB terpolymers, on the other hand, exhibit stress-strain behavior typical of ductile plastics. They have Young's moduli ranging from 13.0-125.6 MPa and cover a much wider range than those of the OIL-DVB copolymers (Table 4). The deformation of all OIL-ST-DVB terpolymers under the applied load appears closely related to the vegetable oil used in their synthesis. Typically, these materials exhibit tensile yielding behavior with two characteristic regions of deformation in their stress-strain curves (Figure 13). The first region ($\varepsilon<10\%$) is characterized by a rapid increase in stress with strain until the yield point. The initial slopes of the curves for the copolymers prepared from the highly unsaturated oils (LSS, SAF, WNT and LIN) are steep, indicating the high Young's moduli of these materials. Conversely, the slopes for the OIL-ST-DVB terpolymers made from the

least reactive oils (OLV and PNT) have the lowest Young's moduli of all vegetable oil copolymers prepared in this study. After the yield point (ε>10%), the OIL-ST-DVB terpolymers show a slow increase in stress with strain until fracture occurs. Their ultimate strengths are in the range from 1.9-10.9 MPa and exhibit a gradual increase with increasing reactivity of the corresponding vegetable oil. Their elongation-at-break values are substantially higher than those of the OIL-DVB copolymers and are in the range from 38.6 to 86.0%. Similar to the values for the OIL-DVB copolymers, these values show no clear dependence on the reactivity of the vegetable oil. Presumably, an increase in the degree of unsaturation of the oil creates two opposite effects, namely an increase in the crosslink density and an increase in vegetable oil incorporation, which may be responsible for this independence. The latter effect contributes to the materials' overall softness and flexibility by increasing incorporation of the flexible triglyceride monomers, while the former effect increases the polymers' stiffness and brittle nature by increasing the polymers' crosslink density. Conversely, the toughness values for the OIL-ST-DVB copolymers range from 0.46-5.83 MPa and clearly increase with the increasing reactivity of the vegetable oil.

Conclusions

A range of thermosets have been prepared by the cationic copolymerization of olive, peanut, sesame, canola, corn, soybean, grapeseed, sunflower, low saturation soy, safflower, walnut and linseed oils with DVB or a combination of ST and DVB initiated by an NFO-modified BFE catalyst. The physical, thermal and mechanical properties of these new polymers have been investigated as a function of the vegetable oil reactivity.

The gelation times of these copolymers are independent of the degree of unsaturation of the vegetable oil. Thermogravimetric analysis shows that both the OIL-DVB and OIL-ST-

DVB copolymers are thermally stable below 200 °C with 10% weight loss temperatures in air of 276 -339 °C and 269-342 °C respectively. The T_{10} and T_{50} values of both copolymer series gradually increase with the increasing reactivity of the corresponding vegetable oil. According to Soxhlet extraction analysis, higher yields of crosslinked polymers have been obtained by employing more unsaturated oils. Dynamic mechanical analysis (DMA) shows that the resulting products are typical thermosets with densely crosslinked structures. Their crosslink densities vary from 7.6×10^3-2.3×10^4 mol/m^3 and 6.0×10^2-2.3×10^3 mol/m^3 for the OIL-DVB and OIL-ST-DVB copolymers respectively and show a gradual increase with the increasing reactivity of the vegetable oil used in their synthesis. Most of the OIL-ST-DVB terpolymers have single glass transition temperatures ranging from 50-66 °C. Conversely, all of the OIL-DVB copolymers have two glass transition temperatures due to extensive microphase separation caused by thermodynamic immiscibility between the crosslinked matrix and the unreacted oil. The thermal transitions of both the OIL-DVB and OIL-ST-DVB systems show no observable dependence on the reactivity of the vegetable oil.

The tensile-stress strain behavior of these new vegetable oil-based materials demonstrates properties characteristic of polymers ranging from hard and brittle to relatively soft and ductile plastics. Typically, polymers prepared from the more unsaturated vegetable oils possess better mechanical properties. The room temperature Young's moduli, ultimate strengths and toughness of all polymers are ultimately related to the reactivity of the corresponding vegetable oil. All of these parameters show a gradual increase with increasing oil reactivity.

Acknowledgements

The authors gratefully acknowledge the Iowa Soybean Promotion Board and the Iowa Energy Center for financial support. We also thank Dr. Surya K. Mallapragada and her graduate students, Michael Determan and Sim-Siong Wong, of the Department of Chemical Engineering, as well as Dr. Jay-Lin Jane, Dr. Perminus Mungara and Dr. Stephanie Jung of the Department of Food Science and Human Nutrition at Iowa State University for valuable discussions and use of their facilities.

References

1. Kaplan DL. Biopolymers from Renewable Resources, New York: Springer, 1998.
2. Kumar GS. Biodegradable Polymers: Prospects and Progress, New York: Marcel Dekker, 1987.
3. Vert M. Biodegradable Polymers and Plastics, Cambridge, England: Royal Society of Chemistry, 1992.
4. O'Brien RD. Fats and Oils – Formulating and Processing for Applications, 2nd ed. CRC Press, 2004.
5. Eckey EW. Vegetable Fats and Oils, The ACS Monograph Series, New York: Reinhold Publishing Co., 1954.
6. Salunkhe DK, Chavan JK, Adsule RN, Kadam SS. World Oilseeds: Chemistry, Technology and Utilization, New York: Van Nostrand Reinhold, 1991.
7. Wang C, Erhan S. J. Am. Oil Chem. Soc. 1999;76:1211-1216.
8. Petrovic ZS, Guo A, Zhang W. J. Polym. Sci., Part A Polym. Chem. 2000;38:4062-4069.
9. Javni I, Petrovic ZS, Guo A, Fuller R. J. Appl. Polym. Sci. 2000;77:1723-1734.
10. Guo A, Javni I, Petrovic ZS. J. Appl. Polym. Sci. 2000;77:467-473.

11. Guo A, Demydov D, Zhang W, Petrovic ZS. J. Polym. Environ. 2002;10:49-52.

12. Petrovic ZS, Zhang W, Zlatanic A, Lava CC, Ilavskyy M. J. Polym. Environ. 2002;10:5-12.

13. Can E, Kusefoglu S, Wool RP. J. Appl. Polym. Sci. 2001;81:69-77.

14. Khot SN, Lascala JJ, Can E, Morye SS, Williams GI, Palmese GR, Kusefoglu SH, Wool RP. J. Appl. Polym. Sci. 2001;82:703-723.

15. Can E, Kusefoglu S, Wool RP. J. Appl. Polym. Sci. 2002;83:972-980.

16. Li F, Hanson MW, Larock RC. Polymer 2001;42:1567-1579.

17. Li F, Larock RC. J. Appl. Polym. Sci. 2001;80:658-670.

18. Li F, Larock RC. J. Polym. Environ. 2002;10:59-67.

19. Li F, Hasjim J, Larock RC. J. Appl. Polym. Sci. 2003;90:1830-1838.

20. Li F, Larock RC. J. Appl. Polym. Sci. 2000;78:1044-1056.

21. Li F, Marks D, Larock RC, Otaigbe JU. SPE ANTEC Technical Papers 1999;3:3821.

22. Li F, Marks D, Larock RC, Otaigbe JU. Polymer 2000;41:7925-7939.

23. Li F, Larock RC. J. Polym. Sci., Part B: Polym. Phys. 2000;38:2721-2738.

24. Li F, Larock RC. J. Polym. Sci., Part B: Polym. Phys. 2001;39:60-77.

25. Li F, Larock RC. Polym. Adv. Tech. 2002;13:436-449.

26. Li F, Larock RC. J. Appl. Polym. Sci. 2002;84:1533-1543.

27. Miyake Y, Yokomizo K, Matsuzaki N. J. Am. Oil Chem. Soc. 1998;75:1091-1094.

28. Sacchi R, Addeo F, Paolillo F. Magn. Reson. Chem. 1997;35:S133-S145.

29. Guillen MD, Ruiz A. Eur. J. Lipid Sci. Technol. 2003;105:688-696.

30. Kennedy JP, Matechal E. Carbocationic Polymerizations, New York: John Wiley & Sons, 1982.

31. Matyjaszewski K. Cationic Polymerization: Mechanisms, Synthesis, and Applications, New York: Marcel Dekker, Inc., 1996.

32. Flory PJ. Principles of Polymer Chemistry, Cornell University Press: Ithaca, NY, 1953 (chapter 6).

33. Murayama T. Dynamic Mechanical Analysis of Polymeric Materials, Elsevier: Amsterdam, 1978.

34. Ward IM. Mechanical Properties of Solid Polymers, Wiley Interscience: London, 1971 (chapter 5).

35. Sperling LH. Introduction to Physical Polymer Science, 3rd ed. New York: John Wiley & Sons, 2001 (chapter 11).

CHAPTER 5. NOVEL RUBBERS FROM CATIONIC COPOLYMERIZATION OF SOYBEAN OILS AND DICYCLOPENTADIENE. I. SYNTHESIS AND CHARACTERIZATION

A paper published in Biomacromolecules. Reproduced with permission from *Biomacromolecules* **2006**, *7*, 927-936.

Dejan D. Andjelkovic and Richard C. Larock

Abstract

Novel thermosetting copolymers, ranging from tough and ductile to very soft rubbers, have been prepared by the cationic copolymerization of regular (SOY) and 100% conjugated soybean oils (C_{100}SOY) with dicyclopentadiene (DCP) catalyzed by Norway fish oil (NFO)-modified and SOY- and C_{100}SOY-diluted boron trifluoride diethyl etherate (BFE). The gelation time of the reactions varies from 4-991 minutes at 110 °C. The yields of the bulk copolymers are essentially quantitative, while the yields of the crosslinked copolymers remaining after Soxhlet extraction with methylene chloride range from 69-88%, depending on the monomer stoichiometry and the catalyst used. ^{1}H NMR spectroscopy and Soxhlet extraction data indicate that these copolymers consist of a crosslinked soybean oil-DCP network plasticized by certain amounts of methylene chloride-soluble linear or less crosslinked soybean oil-DCP copolymers, unreacted oil, and some low molecular weight hydrolyzed oil. The molecular weights of these soluble fractions are in the range from 400-10,000 g/mol based on polystyrene standards. The bulk copolymers have glass transition

temperatures ranging from -22.6 to 56.6 °C, while their tan delta peak values range from 0.7 to 1.2. Thermogravimetric analysis (TGA) indicates that these soybean oil-DCP copolymers are thermally stable below 200 °C, with 10% and 50% weight loss temperatures ranging from 280–372 °C and 470–554 °C respectively. These properties suggest that these biobased thermosets may prove useful alternatives to current petroleum-based plastics and find widespread utility.

Introduction

Biomaterials, chemicals, and energy from renewable resources have received considerable interest in recent years.[1-3] The growing demand for petroleum-based products and the resulting negative impact on the environment, plus the scarcity of non-renewable resources, are just a few of many factors that have encouraged the scientific community to find more sustainable and environmentally responsible solutions for these problems. Considerable interest has focused on the utilization of annually renewable starting materials, such as starch, cellulose, vegetable oils, and proteins for the synthesis of a wide range of bioplastics.[4-8] Deployment of these biodegradable starting materials protects the environment by reducing or completely substituting petroleum-based materials. Furthermore, polymers based on biorenewable resources have often been shown to possess properties comparable or better than those of widely used industrial polymers. As such, they show promise as replacements for petroleum-based plastics, thus reducing waste and preserving our dwindling petroleum reserves.

Soybean oil represents one of the cheapest and most abundant annually renewable natural resources available in large quantities.[9-11] The food market accounts for more than 90% of soy product demand,[12] whereas the remainder accounts for rapidly increasing

industrial applications, such as the production of soaps, lubricants, varnishes, coatings, paints,[13,14] and more recently, bioplastics and composites.[1-3] The expansion of industrial applications is mainly fuelled by the growing desire by government and business to reduce their dependence on petroleum imports, and the increasing number of price-competitive, soy-based chemicals and materials available. The use of vegetable oils as starting materials offers numerous advantages, such as low toxicity, inherent biodegradability, high purity, and ready availability. For instance, the annual U.S. soybean oil production in 2005/06 is forecast at approximately 20 billion pounds.[15] Like all other vegetable oils, soybean oil is a high molecular weight (MW ~ 880 g/mol), unsaturated monomer, which makes it an ideal building block for high MW polymer synthesis. Furthermore, its structure can be altered through genetic engineering in order to improve its reactivity towards polymerization.[16] One such example is production of the genetically modified soybean oil, known as Select Oil™.[17] This Low Saturation Soybean oil has 0.5-0.7 C=C bonds more per triglyceride than regular soybean oil.

In order to further expand non-food applications of these biorenewable materials, our group has focused on conversion of vegetable oils into industrially useful biopolymers.[18-20] We have recently shown that a variety of promising new polymeric materials, ranging from soft rubbers to hard, tough and rigid plastics, can be prepared by the cationic copolymerization of readily available soybean oils with styrene (ST) and divinylbenzene (DVB), catalyzed by Norway fish oil (NFO)-modified boron trifluoride diethyl etherate (BFE).[21-23] The resulting polymers exhibit good thermal and mechanical properties, including good damping[24] and shape memory[25] properties, and show promise as replacements for petroleum based rubbers and conventional plastics. By varying the

structure and stoichiometry of the alkene comonomers[21] and the vegetable oils,[26] we have been able to achieve excellent control over the polymer properties. However, in order to obtain more rigid polymers, high-priced DVB has been required as a crosslinker, reducing the commercial appeal of these materials. Furthermore, the large difference in reactivity between the aromatic comonomers (ST and DVB) and the soybean oils has required us to modify the catalyst by adding NFO in order to produce homogeneous samples.[27]

Herein, we wish to report the synthesis and initial characterization of a range of novel biobased-rubbers prepared by the cationic copolymerization of regular (SOY) and 100% conjugated (C_{100}SOY) soybean oils with dicyclopentadiene (DCP). The replacement of DVB (~ \$3.00/lb) with inexpensive DCP (~\$0.29/lb)[28] as a crosslinker effectively addresses some of the above-mentioned drawbacks and offers a simple route to a range of new and exciting rubbers.

Experimental Section

Materials. Wesson soybean oil (SOY) was purchased in a local supermarket and used without further purification. Conjugated soybean oil (C_{100}SOY) was prepared according to our previously published procedure.[29] *endo*-DCP (typically 95% pure) was purchased from VWR chemical company and used as received. Norway fish oil ethyl ester (NFO) (EPAX 5500 EE, Pronova Biocare) was used to modify the original catalyst, boron trifluoride diethyl etherate (BFE) (distilled grade, Aldrich).

Cationic Copolymerization and Nomenclature. Pre-weighed amounts of soybean oil and DCP (92 wt % total) were mixed in a beaker and stirred vigorously at ambient temperature until a homogeneous solution was obtained. During this time, 3 wt % of BFE catalyst was diluted with 5 wt % of soybean oil and added slowly to the mixture of soybean

oil and DCP. The reaction mixture was stirred vigorously until it became homogeneous and then poured into a glass mold and cured for 12 h at 60 °C and 24 h at 110 °C. Resulting polymers were obtained in essentially quantitative yields. The nomenclature adopted in this paper for the polymer samples is as follows: a polymer sample prepared from 75 wt % SOY, 17 wt % DCP, 8 wt % SOY-diluted BFE catalyst (5 wt % SOY + 3 wt % BFE) is designated as SOY75-DCP17-(SOY5-BFE3).

Soxhlet Extractions. A 3-4 g sample of the bulk polymer was extracted with 100 mL of refluxing methylene chloride for 24 h using a Soxhlet extractor. Following the extraction, the resulting solution was concentrated under reduced pressure and dried in a vacuum oven at 60 °C overnight. The recovered insoluble portion was also dried under a vacuum prior to weighing.

Polymer Characterization. ^{1}H NMR spectroscopic analyses of the soluble substances extracted by methylene chloride were recorded in $CDCl_3$ using a Varian Unity spectrometer at 300 MHz. Cross-polarization magic angle spinning (CP MAS) ^{13}C NMR analysis of the insoluble materials remaining after Soxhlet extraction of the bulk polymers was performed using a Bruker MSL 300 spectrometer. Samples were examined at two spinning frequencies (3.2 and 3.7 kHz) in order to differentiate between actual signals and spinning side bands. FTIR spectra were recorded on a Nicolet 740 FT-IR spectrometer (KBr pellet). Gelation times were determined as the time elapsed from initial mixing of the reactants at the given temperature to the time when solidification commences, as determined by the complete cessation of flow of the liquid reactants. Measurements were performed in reference to the ASTM standard D2471-99. Gelation times are the average of five individual measurements at a certain temperature. Molecular weights (relative to narrow polystyrene

standards) were measured using a Waters Breeze GPC system equipped with a Waters 1515 pump, Waters 717-plus auto-sampler, and Waters 2414 RI-detector. HPLC-grade THF was used as the mobile phase at a flow rate of 1 mL/min with a sample injection volume of 200 μL. The system was equipped with a set of two columns (PL-Gel Mixed C 5μm, Polymer Lab., Inc.) and heated at 40 °C. Prior to analysis, each polymer sample was dissolved in THF (~ 2.0 mg/mL) and passed through a Teflon 0.2 mm filter into a sample vial. Dynamic mechanical analysis (DMA) data were obtained using a Perkin Elmer dynamic mechanical analyzer DMA Pyris-7e in a three-point bending mode. Rectangular specimens of 2 mm thickness and 5 mm depth were used for the analysis and the width to depth ratio was maintained at approximately 3. The measurements were performed at a heating rate of 3 °C/min and a frequency of 1 Hz in He with a gas flow rate of 20 mL per minute and static and dynamic forces applied of 110 and 100 mN respectively. Thermogravimetric analyses (TGA) were performed on a Perkin Elmer Pyris-7 thermogravimeter. The % weight loss temperatures of the polymeric materials were measured in air with a gas flow rate of 20 mL/min. The samples were heated from 50-650 °C at a heating rate of 20 °C/min.

Results and Discussion

Chemical Compositions of the Soybean Oils. Commercially available soybean oil employed in this study has a triglyceride structure, consisting of saturated stearic (C16-0) and palmitic (C18-0) acids (15%), as well as unsaturated oleic (C18-1, 23.3%), linoleic (C18-2, 53.7%) and linolenic (C18-3, 7.6%) fatty acids.[9,10] The percent of other saturated and unsaturated fatty acids is negligible. The unsaturated fatty acid content determines the degree of unsaturation of the soybean oil and consequently its reactivity. Figure 1 shows representative ^{1}H NMR spectra for the SOY and C_{100}SOY oils. The signals at 4.1-4.4 ppm

correspond to the protons on the C-1 and C-3 carbons of the glyceride unit, which indicate that both SOY and C_{100}SOY have triglyceride structures. The vinylic hydrogens of SOY are typically detected at 5.2-5.5 ppm, while the bis-allylic protons are observed at 2.7-2.9 ppm, indicating that the C=C bonds in SOY are non-conjugated. Conversely, the vinylic hydrogens of C_{100}SOY (Figure 1, b) are detected in the 5.2-6.4 ppm range as a group of four multiplets, which indicates the existence of conjugation in the polyene system. Furthermore, complete disappearance of the bis-allylic signal at 2.7-2.8 ppm confirms that C_{100}SOY is completely conjugated. Detailed triglyceride peak assignments are well documented in the literature.[30-32] Based on our ^{1}H NMR spectral analysis, SOY has 4.3 C=C bonds per triglyceride. C_{100}SOY has the same degree of unsaturation, which indicates that hydrogenation of the SOY did not take place during Rh-catalyzed conjugation.[29]

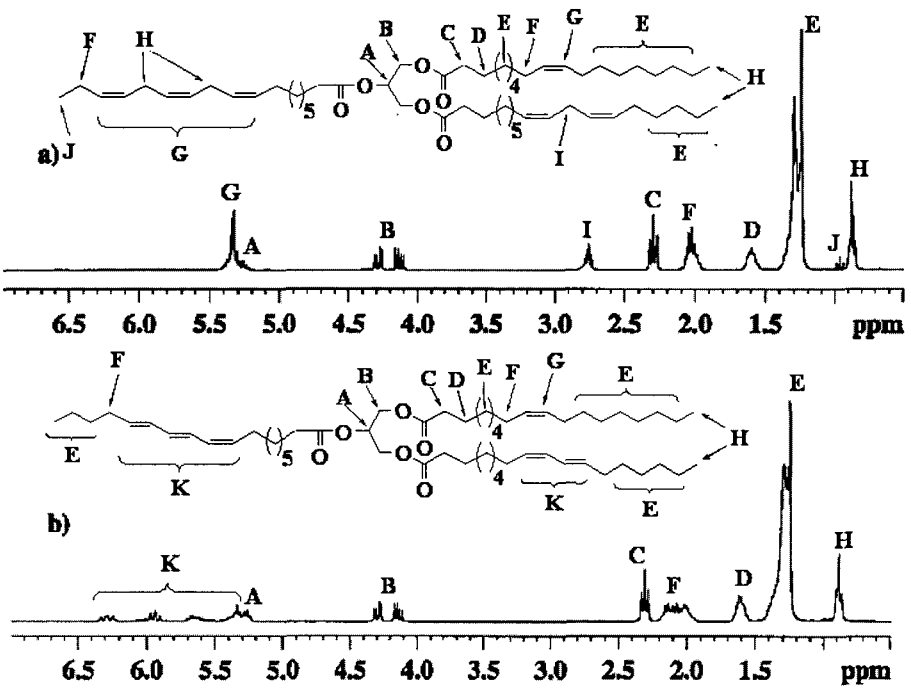

Figure 1. ^{1}H NMR spectra of a) SOY and b) C_{100}SOY.

Soybean Oil and Dicyclopentadiene as Cationic Monomers. According to basic thermodynamics, cationic polymerization of SOY is possible only if a negative change in free energy is achieved ($\Delta H - T\Delta S < 0$). During cationic polymerization, the loss of translational degrees of freedom caused by connecting triglyceride units together causes a decrease in entropy. Therefore, the thermodynamic feasibility of the polymerization will depend solely on enthalpic factors, meaning that cationic polymerization must be sufficiently exothermic to compensate for the loss in entropy. This is accomplished through conversion of the soybean oil C=C bonds to C-C bonds in the polymer. The C=C bonds in the soybean oil represent sites for electrophilic attack of the reactive species generated by the BFE catalyst. Because of that, electronic effects within the triglyceride monomers will have a crucial effect on their reactivity. SOY, like all other alkene monomers, is expected to polymerize cationically by the addition of monomers to the growing carbocation chain. Thus, the triglyceride monomers must be sufficiently nucleophilic and capable of stabilizing the intermediate carbocation.[33] Since nucleophilicity increases with increasing carbon substitution on the C=C bond, due to the positive inductive effect of alkyl substituents, the C=C bonds of the soybean oils are considered more nucleophilic than those of ethylene and propylene.[34,35] They are, therefore, capable of stabilizing the positive charge to a greater extent and are prone to cationic polymerization. For the same reason, the conjugated C=C bonds in C_{100}SOY are considered even more reactive toward cationic polymerization, since they will generate more stable allylic carbocations as intermediates.[33-35] Thus, both SOY and C_{100}SOY should be cationically polymerizable monomers. Furthermore, unlike ethylene, propylene, isobutylene or styrene, both SOY and C_{100}SOY are polyfunctional monomers due to the presence of multiple C=C bonds within the triglyceride. Because of their relatively

high molecular weights and ability to efficiently stabilize intermediate carbocations, these oils readily afford high molecular weight polymers with crosslinked polymer networks.

DCP is a well known Diels-Alder dimer of cyclopentadiene, which forms rapidly at room temperature. DCP has been one of the most widely used diene comonomers for the synthesis of ethylene-propylene terpolymers, also known as EPDM elastomers.[36] It has also been used as a diluent for unsaturated polyesters and alkyd resins.[37] DCP provides olefinic sites in EPDM elastomers and in blends with other olefins and diolefins that are readily polymerized to hydrocarbon resins. Such resins are used in a variety of materials, including adhesives, printing inks, rubbers, paints, varnishes, textiles, and floor coverings.[38,39]

Due to the importance of DCP-based petroleum resins, the cationic polymerization of DCP and other bicyclo[2.2.1]alkenes has been studied in great detail in the past.[40-43] Particular attention has been paid to microstructural elucidation of cationic DCP polymers, because of the fact that DCP contains two polymerizable C=C bonds of different reactivities. It is known that the norbornene-like (NB) C=C bond of DCP is more reactive than the cyclopentene-like (CP) C=C bond.[36-43] This dissimilarity means that different structural units can be incorporated into the poly(dicyclopentadiene) (PDCP) backbone. For example, Corner *et al.* polymerized DCP using $PdCl_2(PhCN)_2$ and BFE as initiators and determined that the resulting polymers incorporated both *endo*-(1) and *exo*-(2) DCP units into their backbones with either 1,2- or 1,3-substitution patterns (Scheme 1).[41] These structural units are generated exclusively by electrophilic attack on the NB C=C bond of the DCP unit, while the CP C=C bond is left intact. Addition of an electrophile (H^+) to the NB C=C bond leads to an *endo*-unit A, which can then rearrange to give an *exo*-unit B. If A acts as a propagating species, then the polymer incorporates unit 1 into its backbone. However, if rearrangement

of A occurs before propagation, then B will be the active propagating species and the polymer will incorporate unit 2 into its backbone. It is also important to mention that conversion of *endo*-DCP to *exo*-DCP units proceeds through a Wagner-Meerwein rearrangement and that the reverse reaction has never been observed. This is supported by the fact that *exo*-DCP is energetically favored by 9 kcal/mol over *endo*-DCP. According to Becker and Roth, the heat of combustion of *endo*-DCP is 1377 kcal/mol, while that of *exo*-DCP is 1368 kcal/mol.[44]

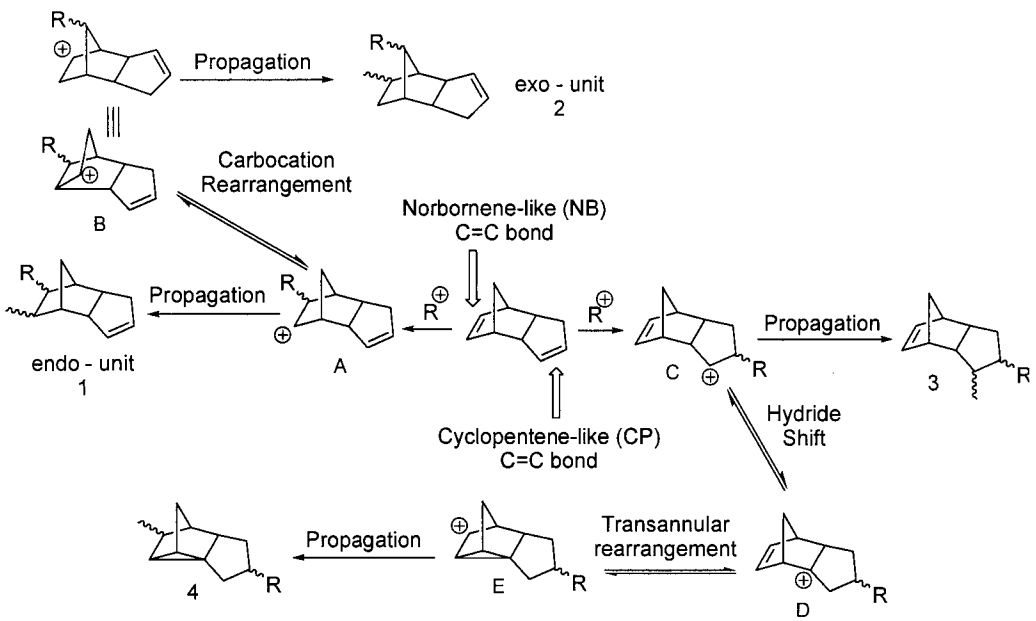

Scheme 1. Formation of different structural units during the cationic polymerization of DCP.

More recently, Peng *et al.* have polymerized DCP using several acid, Al, B, and Ti-based initiators in toluene, CH_2Cl_2, or *n*-hexane as solvents and determined that under specific conditions, besides units 1 and 2, DCP polymers incorporate certain amounts of units 3 and 4 (Scheme 1).[43] In this case, units 3 and 4 are generated by electrophilic attack on the

CP C=C bond. Addition of an electrophile (H^+) to the CP C=C bond gives *endo*-unit C, which can undergo simultaneous hydride-shift transannular rearrangement to afford *exo*-unit D. In this case, if C acts as a propagating species then the polymer will incorporate unit 3 into its backbone. However, if rearrangement of C occurs before propagation, then D will be the active propagating species and the polymer will incorporate unit 4 into its backbone. Based on their IR and NMR spectral analyses, it has been shown that specific conditions (initiator, solvent, temperature, etc.) favor incorporation of certain structural units over others and that the microstructure of DCP polymers can be controlled to some extent. All DCP polymers synthesized by cationic homopolymerizations have possessed low molecular weights (M_n) ranging from 700-4,500 g/mol.[40-43]

Cationic Copolymerization of Soybean Oils and DCP. The presence of multiple C=C bonds in soybean oils allow their copolymerization into solid polymeric materials with other alkene comonomers via cationic polymerization. BFE has proved to be a very effective catalyst for cationic polymerizations.[33] However, the homopolymerization of SOY typically results in viscous fluids, which are of limited use.[45] In order to produce viable harder plastics, SOY has to be copolymerized with more rigid comonomers, such as ST and DVB.[18-20] Utilization of these relatively expensive aromatic comonomers (ST = ~ \$0.75/lb and DVB = ~ \$3.00/lb)[28] considerably improves the polymers' thermal and mechanical properties, but these improvements come at a price. Furthermore, the significant differences in reactivities between SOY and C_{100}SOY on the one hand, and ST and DVB on the other, require the use of BFE modifiers, such as NFO, to produce homogeneous polymers,[27] which further complicates the process. In contrast, DCP offers certain advantages over ST and DVB. It is an inexpensive diene (~ \$0.29/lb)[28] with a rigid bicyclic structure. Because of its structure, it

can act as a crosslinker in a cationic copolymerization and enhance the polymers' properties. Furthermore, knowing that its cationic polymerization proceeds through the formation of secondary or tertiary carbocation intermediates,[43] it is expected that DCP will exhibit reactivity comparable to SOY and C_{100}SOY. This, in turn, might allow one to eliminate the catalyst modifiers previously needed to achieve homogeneity.

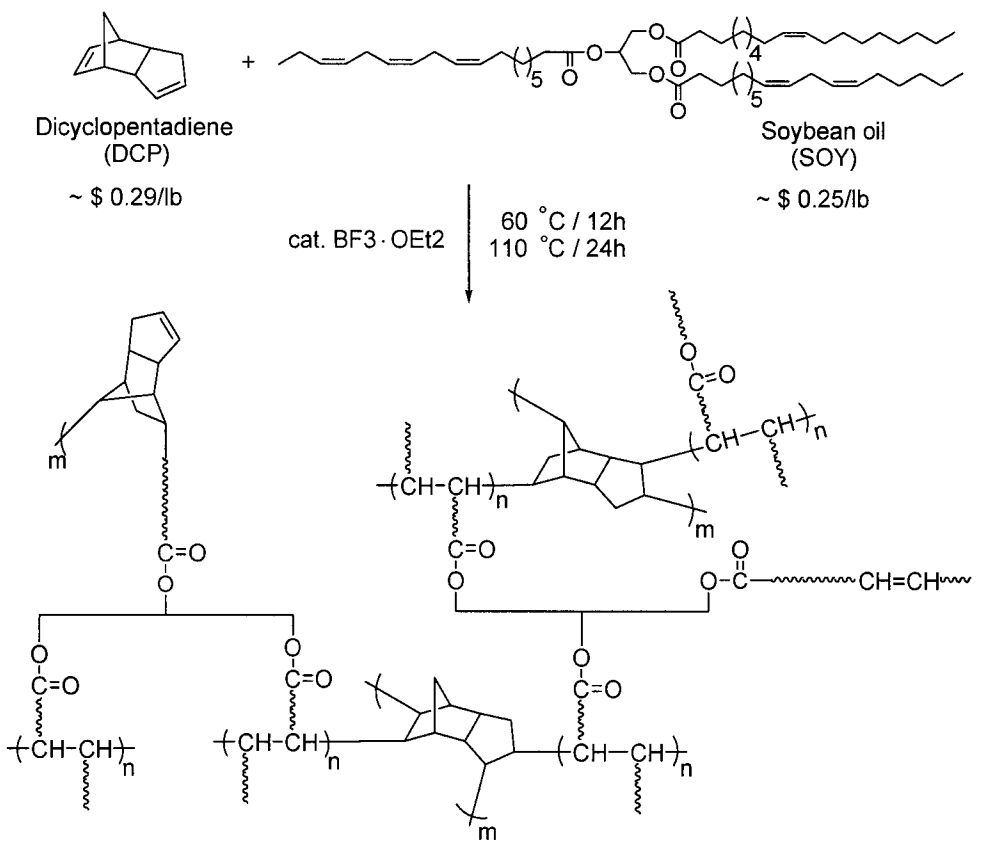

Scheme 2. Cationic copolymerization of SOY and C_{100}SOY with DCP.

SOY and C_{100}SOY have been cationically copolymerized with DCP using both NFO-modified and SOY- or C_{100}SOY-diluted BFE catalysts. Different catalytic systems have been used in order to determine whether NFO is really necessary as a modifier for optimum

polymer properties. It is worth mentioning that while completely soluble in NFO, the BFE catalyst has low solubility in both SOY and C_{100}SOY. Because of that, SOY- and C_{100}SOY-diluted BFE catalytic systems are heterogeneous solutions. However, they completely dissolve in bulk soybean oil-DCP solutions giving homogeneous clear brown reaction mixtures. The main reason for dilution of the BFE catalyst with soybean oil is to prevent excessive homopolymerization of the DCP, which can occur at room temperature causing the formation of white flakes of PDCP. Dilution of the BFE catalyst significantly reduces the formation of PDCP flakes and improves solubilization. Scheme 2 shows that soybean oil-DCP copolymerization proceeds through the formation and growth of a crosslinked copolymer network due to the presence of multiple C=C bonds in both the DCP and the soybean oils. The increase in the copolymers' molecular weight through crosslinking results in gelation, which is the irreversible transformation from a viscous liquid to an elastic gel. The gelation times are of great importance in establishing processing parameters. Gelation times for all soybean oil-DCP systems have been determined by measuring the time required for the liquid reactants to reach a certain viscosity at which the cessation of flow is observed. Beyond this point, the material is no longer able to flow easily and has limited processability. All gelation times are measured at 110 °C, since SOY-DCP systems failed to gel at either room temperature or 60 °C even after 48 hours. Table 1 summarizes the gelation times for all SOY-DCP and C_{100}SOY-DCP systems prepared with both NFO-modified and SOY- and C_{100}SOY-diluted BFE catalysts. Copolymer systems prepared using the NFO-modified BFE catalyst have shorter gelation times, which is presumably due to slightly better solubilization of the catalyst. The measured gelation times are in the range of 569 to 991 and 4 to 72 minutes for the SOY-DCP and C_{100}SOY-DCP systems respectively. The much shorter

Table 1. Gelation times and Soxhlet extraction data for soybean-DCP copolymers.

Copolymer	T_g (°C)[a,b]	Gelation times[b] (minutes)	Extraction Data (%)[b] Insoluble	Soluble
SOY50-DCP42-C8	39.9 (56.6)[c]	688 (707)[c]	73.7 (70.8)[c]	26.3 (29.2)[c]
SOY55-DCP37-C8	16.5 (14.4)[c]	715 (860)[c]	73.2 (70.9)[c]	26.8 (29.1)[c]
SOY60-DCP32-C8	2.9 (-0.2)[c]	505 (991)[c]	73.0 (70.4)[c]	27.0 (29.6)[c]
SOY65-DCP27-C8	-6.9 (-8.7)[c]	678 (698)[c]	72.5 (70.3)[c]	27.5 (29.7)[c]
SOY70-DCP22-C8	-13.0 (-10.8)[c]	646 (609)[c]	72.0 (70.1)[c]	28.0 (29.9)[c]
SOY75-DCP17-C8	-17.7 (-18.4)[c]	725 (569)[c]	69.7 (70.1)[c]	30.3 (29.9)[c]
C_{100}SOY55-DCP37-C8	18.7 (16.9)[d]	47 (63)[d]	84.2 (86.4)[d]	15.8 (13.6)[d]
C_{100}SOY60-DCP32-C8	1.0 (3.4)[d]	5 (72)[d]	83.4 (87.4)[d]	16.6 (12.6)[d]
C_{100}SOY65-DCP27-C8	-8.7 (-9.0)[d]	4 (25)[d]	83.0 (87.2)[d]	17.0 (12.8)[d]
C_{100}SOY70-DCP22-C8	-9.0 (-11.8)[d]	11 (22)[d]	82.8 (87.3)[d]	17.2 (12.7)[d]
C_{100}SOY75-DCP17-C8	-12.8 (-17.0)[d]	6 (28)[d]	82.4 (88.1)[d]	17.6 (11.9)[d]
C_{100}SOY80-DCP12-C8	-18.5 (-22.6)[d]	10 (31)[d]	82.4 (88.2)[d]	17.6 (11.8)[d]

[a] Glass transition temperatures represent the maxima of the tan δ curves obtained by DMA analysis. [b] The values outside of the parentheses correspond to samples prepared with the NFO-modified BFE catalyst, C8 = (NFO5-BFE3), while those in parentheses correspond to samples made with a SOY- or C_{100}SOY-modified BFE catalyst [[c] C8 = (SOY5-BFE3) or [d] C8 = (C_{100}SOY5-BFE3)].

gelation times for the C_{100}SOY-DCP systems are the direct consequence of the higher reactivity of the C_{100}SOY. When compared to the gelation times of the OIL-ST-DVB systems, the SOY-DCP and C_{100}SOY gelation times at room temperature are considerably

longer.[21,45] The main reason for this is the much lower reactivity of DCP when compared to the ST and DVB comonomers.

Molecular Structure Determination. The fully cured soybean oil-DCP copolymers have been obtained in essentially quantitative yield. Except for SOY50-DCP42-I8, where I8 is either NFO5-BFE3 or SOY5-BFE3, all other copolymers appear as dark brown rubbery materials at room temperature, which range from tough and ductile to very soft rubbers. The microstructures of these copolymers have been studied by Soxhlet extraction analysis with methylene chloride as a refluxing solvent. Table 1 summarizes the results obtained from these analyses. Typically, after overnight extraction, 70-74 and 82-88 wt % of insoluble materials are retained from the SOY-DCP and C_{100}SOY-DCP bulk materials, respectively. Due to the higher reactivity of the C_{100}SOY, the yield of the crosslinked materials from the C_{100}SOY-DCP systems is noticeably higher than that of the corresponding SOY-DCP systems. Interestingly, all of the values pertaining to a particular series are fairly similar and cover a very small range. For instance, an increase in SOY content from 50 to 75 wt % in the (SOY-DCP)92-(NFO5-BFE3) mixture only lowers the yield of the crosslinked polymer about 4%, whereas an increase in the C_{100}SOY content from 55 to 80 wt % in the (C_{100}SOY-DCP)92-(NFO5-BFE3) mixture lowers the yield of crosslinked polymer only 1.8%. We believe that these results are a direct consequence of the similar reactivities of the SOY and C_{100}SOY oils and DCP. That is to say that a significant change in the concentration of a slightly more reactive comonomer does not cause a drastic change in the yield of the crosslinked copolymer. The use of NFO as a catalyst modifier offers little advantage for the SOY-DCP system, since it results in only a 1-3% increase in the yield of the crosslinked polymer. On the other hand, its use in the C_{100}SOY-DCP system has the opposite effect,

causing a decrease in the yield of the crosslinked polymers by 2-4%. Interestingly, when C_{100}SOY is used as a catalyst diluent for the preparation of C_{100}SOY-DCP copolymers, the yields of the crosslinked copolymers slowly increase with increasing C_{100}SOY content in the initial composition. This suggests that in the absence of catalyst modifiers, the cationic initiator (H^+) has a preference for C_{100}SOY over DCP. Thus, in these systems C_{100}SOY is slightly more reactive than DCP. Solid state ^{13}C NMR analyses of the insoluble components remaining after Soxhlet extraction confirm the incorporation of both soybean oil and DCP units into the crosslinked network (Figure 2). This is evidenced by the presence of both C=O and C=C signals at 170 and 130 ppm respectively. A more detailed discussion will follow later in the text.

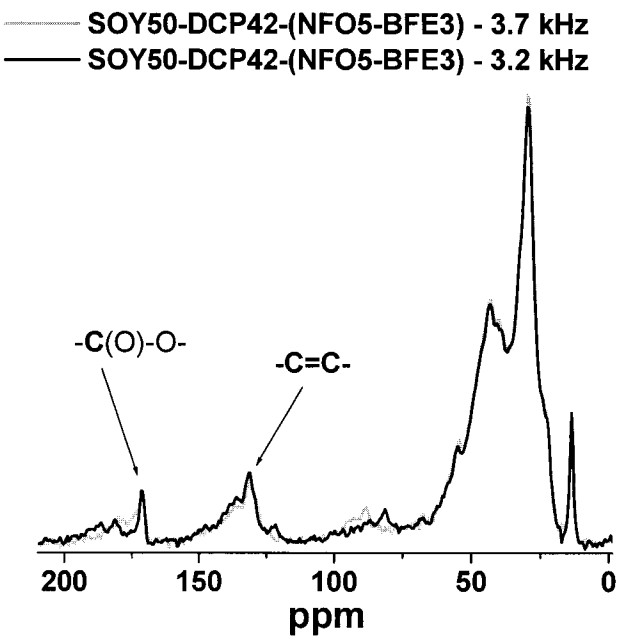

Figure 2. Solid state ^{13}C-NMR spectra of insoluble materials remaining after Soxhlet extraction of the SOY50-DCP42-(BFE3-NFO5) bulk copolymer.

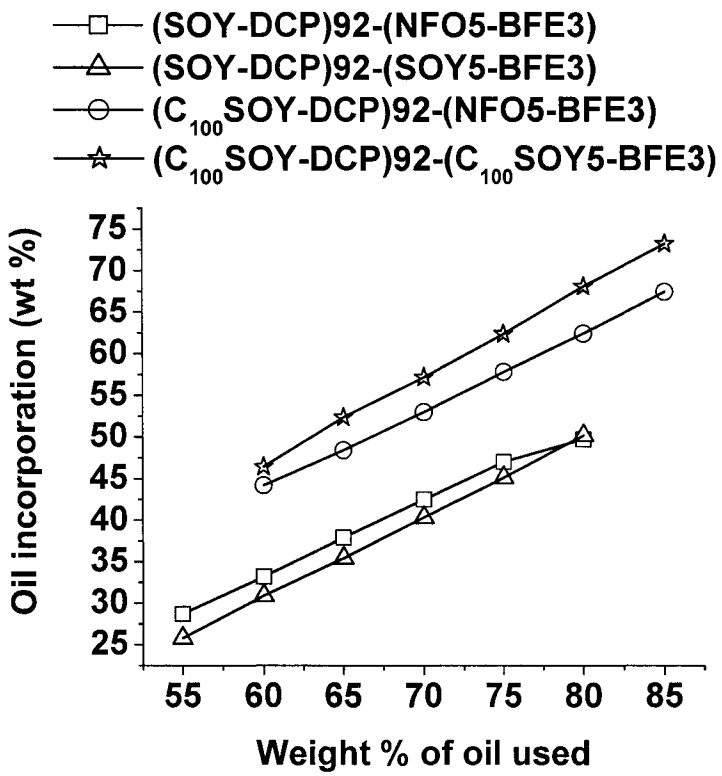

Figure 3. Dependence of the soybean oil incorporation on the wt % of oil in the initial composition.

It has also been noted that in all copolymers synthesized in this study, the incorporation of soybean oil in the crosslinked copolymer increases with increasing amounts of the oil in the initial composition. Figure 3 reveals an almost linear dependence of oil incorporation with the amount of oil. This is most likely due to the similar reactivities of DCP and both SOY and C_{100}SOY. The weight % of oil used in the initial composition is the sum of the oils used both as comonomers and diluents or modifiers. For example, the initial weight % of SOY in both SOY65-DCP27-(NFO5-BFE3) and SOY65-DCP27-(SOY5-BFE3)

is taken as 70 wt % (65 wt % of SOY + 5 wt % of NFO-modifier or SOY-diluent). Also, the calculation is based on the assumption that the soluble components consist solely of unreacted soybean oil. Although not completely correct, this assumption drastically simplifies the calculation and provides a good estimation. The higher C_{100}SOY incorporation into the C_{100}SOY-DCP copolymer is a direct consequence of its higher reactivity when compared to SOY. The use of NFO as a catalyst modifier in the SOY-DCP systems increases the SOY incorporation about 2%, while at the same time, it reduces the C_{100}SOY incorporation in the C_{100}SOY-DCP system about 5%.

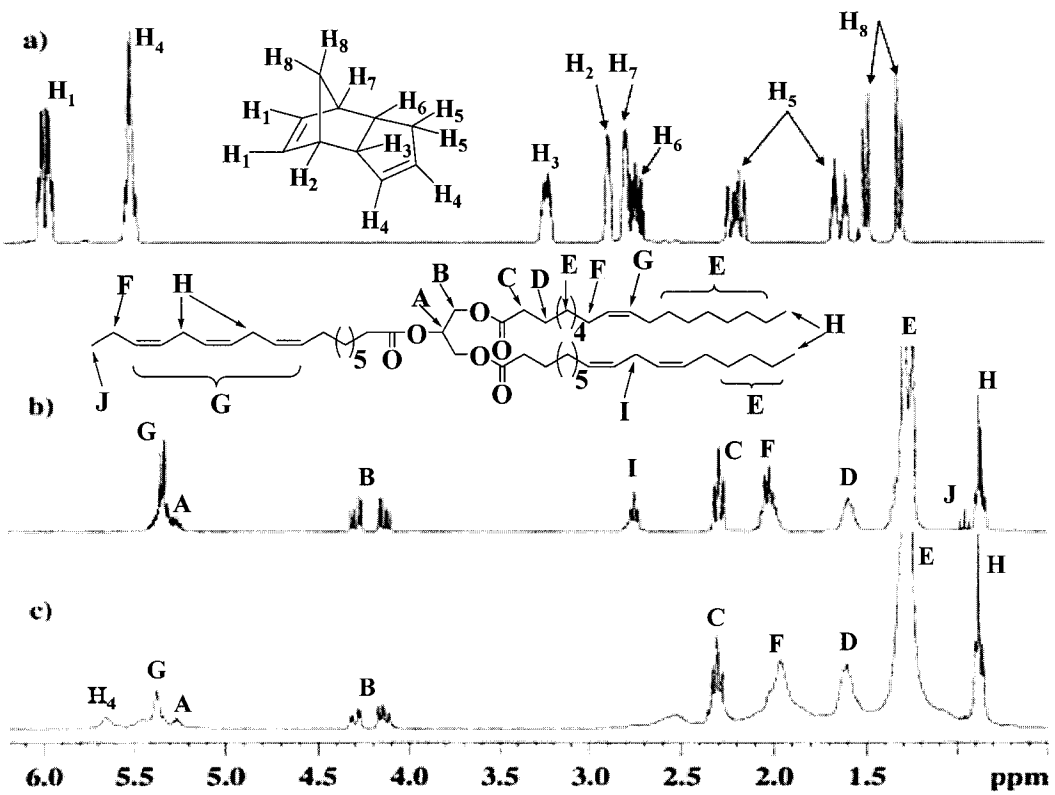

Figure 4. ^{1}H NMR spectra of a) pure DCP, b) pure SOY, and c) soluble extracts of the SOY50-DCP42-(SOY5-BFE3) copolymer.

Both the SOY-DCP and C_{100}SOY-DCP bulk materials consist of insoluble crosslinked materials plasticized with a certain amount of soluble components. The results summarized in Table 1 show that except in the (C_{100}SOY-DCP)92-(C_{100}SOY5-BFE3) system, the amount of soluble components increases slowly with increasing soybean oil content in the initial composition. ^{1}H NMR spectral analyses of these soluble materials confirm the presence of both soybean oil and DCP units, as evidenced by signals at 4.1-4.4 ppm and 5.5-5.6 ppm respectively (Figure 4). The former peaks correspond to the hydrogen atoms of the glycerol unit in the soybean oil, while the latter correspond to the olefinic hydrogens of DCP. The ^{1}H NMR spectra of pure SOY and DCP monomers are included for comparison purposes. It is important to note that the broad peak at 5.45 ppm also corresponds to the DCP unit. Additional proof that the latter two peaks (5.45 and 5.5-5.6 ppm) correspond to DCP is acquired through comparative ^{1}H NMR spectral analysis. Figure 5 shows a series of ^{1}H NMR spectra of soluble extracts of the (SOY-DCP)92-(SOY5-BFE3) copolymers. The results indicate that the intensities of the above-mentioned signals decrease with decreasing amounts of DCP in the initial composition, meaning that they are DCP-related. According to Peng *et al.*, these signals correspond to the hydrogen atoms of the unreacted CP C=C bonds in the DCP units.[43] Moreover, the absence of a signal at 5.9 ppm clearly indicates that all of the NB C=C bonds in DCP have reacted. Apparently, the opposite is true for the CP C=C bonds. However, the CP C=C bonds that do react during the cationic copolymerization, along with the NB C=C bonds, form effective crosslinks in the bulk materials. Based on ^{1}H NMR spectral analyses of the soluble extracts, we believe that the reaction of the NB C=C bonds most likely results in incorporation of *exo*-units 2 (Scheme

1) into the crosslinked copolymer matrix. Unfortunately, ^{1}H NMR spectral analysis does not provide us with enough data to make analogous judgment about the CP C=C bonds.

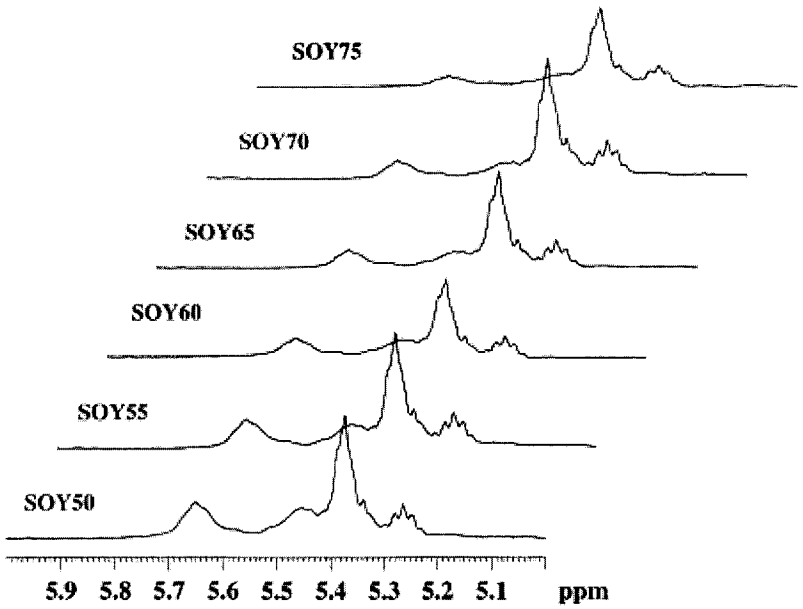

Figure 5. ^{1}H NMR spectra of (SOY-DCP)92-(SOY5-BFE3) extracts in $CHCl_3$.

In order to determine the molecular weight distribution of these soluble materials, they have been subjected to GPC analysis. Figure 6 shows a series of chromatographs of soluble extracts from the SOY-DCP copolymers. The results indicate that each extract consists of several components of different molecular weights (MW). For example, peaks A, B, C, D, and E shown in Figure 6, correspond approximately to 420, 750, 1400, 2800, and 5000-10000 g/mol molecular weights respectively. Comparative GPC analysis of pure SOY reveals that its molecular weight corresponds to that of peak C. Thus, it is not surprising that the intensity of peak C increases with increasing SOY content in the initial (SOY-DCP)92-(NFO5-BFE3) copolymer composition. This molecular weight (~1400 g/mol) is obviously much higher than the real molecular weight (880 g/mol) obtained by calculation based on the

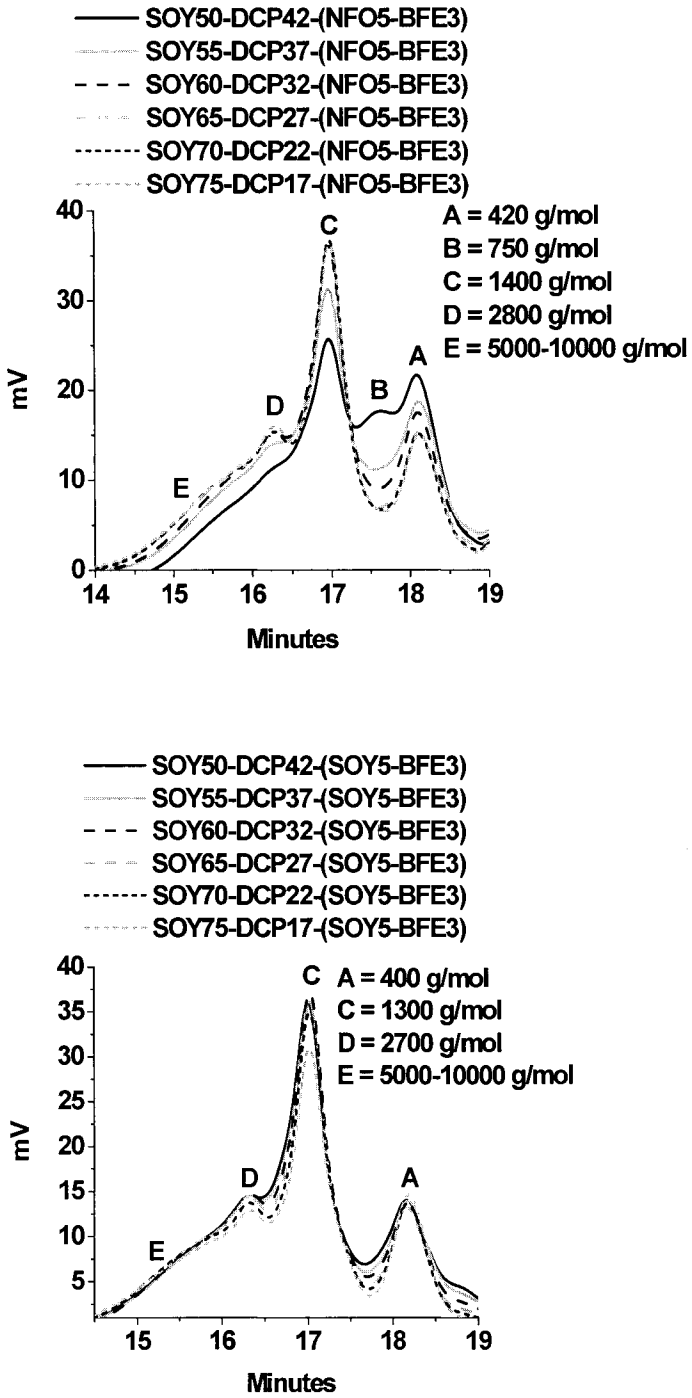

Figure 6. GPC chromatograms of SOY-DCP soluble extracts.

soybean oil fatty acid composition.[26] This deviation is most likely due to the higher hydrodynamic volume of SOY relative to linear polystyrene of the same molecular weight, which is used for calibration.[46] We believe that the lowest molecular weight components (peak A, Figure 6) correspond to NFO (an ethyl ester of Norway fish oil),[47] SOY monoglycerides, SOY diglycerides, or fatty acid fractions formed via acid-catalyzed hydrolysis during the copolymerization process.[48] Peak B, on the other hand, is obviously DCP-related since its intensity diminishes with decreasing amounts of DCP in the initial composition. This peak most likely corresponds to soluble DCP-oligomers. Peak E represents a higher molecular weight shoulder of peak C in the soluble extracts of the SOY50-DCP42-(NFO5-BFE3) copolymers. However, its intensity tends to increase with increasing SOY content in other (SOY-DCP)92-(NFO5-BFE3) copolymer samples. We believe that both peaks D and E correspond to either soluble SOY homopolymers or SOY-DCP oligomers. Similar results have been obtained for extracts of the corresponding (C_{100}SOY-DCP)92-(NFO5-BFE3) copolymers (Figure 7). Interestingly, copolymers prepared without the NFO-modifier show no evidence of peak B in their chromatograms (the right hand spectra in both Figures 6 and 7). However, the existence of peak A in each of these chromatograms confirms that the lowest molecular weight components in all other extracts indeed consist of SOY or C_{100}SOY related mono- or diglyceride fragments.

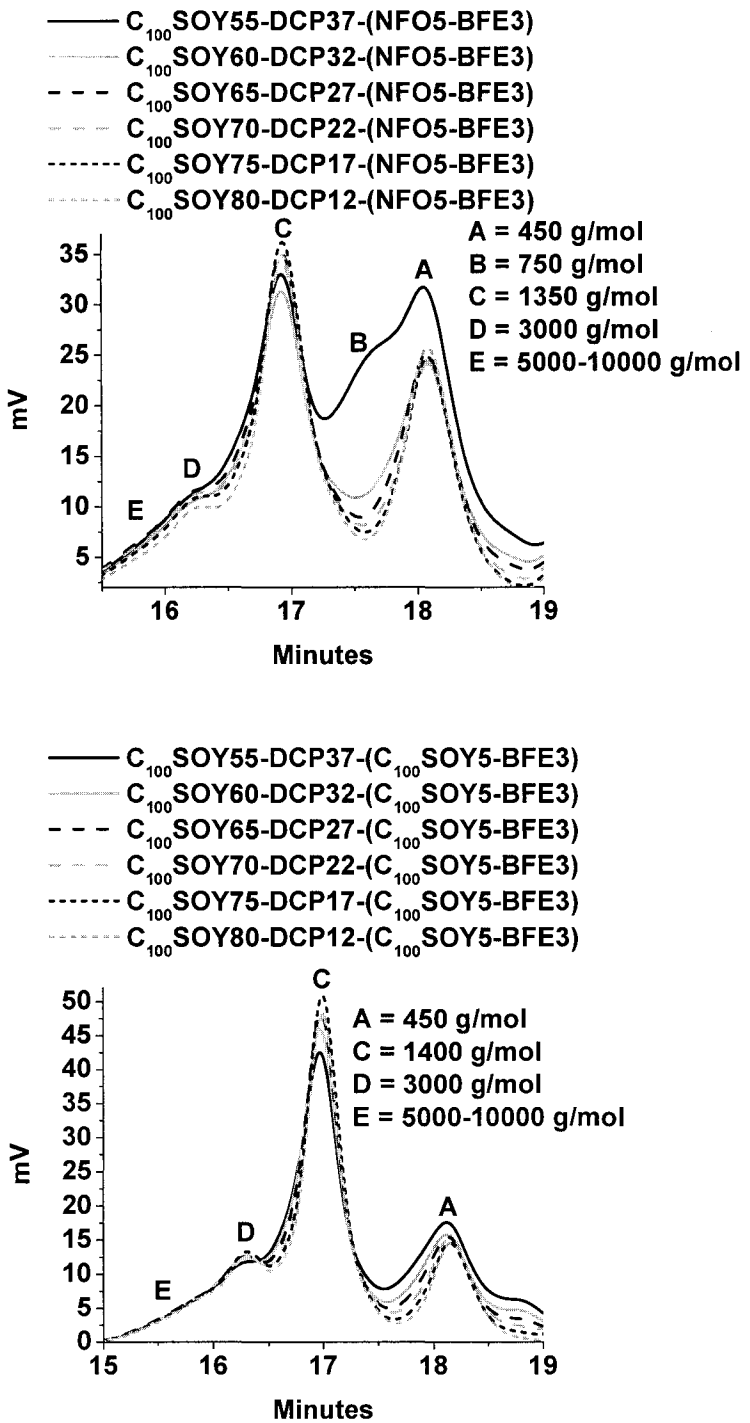

Figure 7. GPC chromatograms of C_{100}SOY-DCP soluble extracts.

Table 2. Thermal properties of the (SOY-DCP)92-(BFE3-NFO5) copolymers.

Copolymer	ν_e	TGA Data (°C)		
	$(mol/m^3)^a$	$T_{10}{}^d$	$T_{50}{}^e$	$(T_{max})^f$
SOY50-DCP42-C8	1034 (501)[b]	333 (284)[b]	549 (472)[b]	569 (492)[b]
SOY55-DCP37-C8	282 (369)[b]	332 (293)[b]	539 (476)[b]	565 (503)[b]
SOY60-DCP32-C8	336 (223)[b]	323 (289)[b]	537 (473)[b]	564 (495)[b]
SOY65-DCP27-C8	119 (436)[b]	331 (286)[b]	541 (480)[b]	564 (500)[b]
SOY70-DCP22-C8	154 (339)[b]	334 (289)[b]	535 (474)[b]	560 (479)[b]
SOY75-DCP17-C8	128 (145)[b]	330 (280)[b]	529 (470)[b]	548 (479)[b]
C_{100}SOY55-DCP37-C8	865 (1295)[c]	337 (364)[c]	548 (542)[c]	581 (549)[c]
C_{100}SOY60-DCP32-C8	858 (984)[c]	330 (355)[c]	529 (539)[c]	561 (550)[c]
C_{100}SOY65-DCP27-C8	710 (1342)[c]	338 (363)[c]	542 (554)[c]	553 (567)[c]
C_{100}SOY70-DCP22-C8	996 (1340)[c]	325 (349)[c]	511 (528)[c]	537 (542)[c]
C_{100}SOY75-DCP17-C8	470 (974)[c]	340 (366)[c]	530 (544)[c]	550 (562)[c]
C_{100}SOY80-DCP12-C8	745 (1117)[c]	335 (372)[c]	532 (536)[c]	547 (554)[c]

[a] Crosslink densities have been calculated at temperatures 100 °C above the corresponding T_g. The values outside the parentheses correspond to samples prepared with the NFO-modified BFE catalyst, C8 = (NFO5-BFE3), while those within the parentheses correspond to samples made with the SOY- or C_{100}SOY-modified BFE catalyst [b] C8 = (SOY5-BFE3) or [c] C8 = (C_{100}SOY5-BFE3). [d] 10 % Weight loss temperature. [e] 50 % Weight loss temperature. [f] Temperature of maximum thermal degradation.

Thermal Properties. Table 2 summarizes the glass transition temperatures, crosslink densities, and thermogravimetric data for all soybean oil-DCP copolymers synthesized in this study. The glass transition temperatures (T_g) of the copolymers have been calculated from the peaks of the tan delta curves obtained by DMA analysis. The crosslink densities have

been calculated from the storage moduli at temperatures 100 °C above the corresponding T_g temperatures. The calculations are based on rubber elasticity theory and the detailed procedure has been described in our previous work.[22,26] Thermogravimetric data include 10 and 50% weight loss temperatures (T_{10} and T_{50}), and the temperatures of maximum thermal degradation (T_{max}).

The glass transition temperatures of the soybean oil-DCP copolymers range from -18.4 to 56.6 °C. Except for the samples SOY50-DCP42-I8 (I8 = NFO5-BFE3 and SOY5-BFE3), all other copolymers have T_g's which are below ambient temperature and, therefore, are in their rubbery state. The glass transition temperatures of all copolymers gradually decrease with increasing amounts of soybean oil in the initial composition. This is mainly due to higher incorporation of the more flexible triglyceride molecules into the crosslinked copolymer structure with increasing amounts of oil in the initial copolymer compositions. Also, copolymers prepared with SOY- or C_{100}SOY-diluted catalysts tend to have slightly lower T_g's than those prepared using the NFO-modified catalyst. This is in agreement with the Soxhlet extraction data and % C_{100}SOY incorporation results (Figure 3) for the C_{100}SOY-DCP copolymers, since the elimination of NFO results in higher C_{100}SOY incorporation into the crosslinked structure and, thus, slightly higher flexibilities and lower T_g values. The same is not true for the SOY-DCP copolymers. At this moment, we are unable to explain this behavior. The crosslink densities, on the other hand, do not show such a regular dependence in all cases. For instance, while the crosslink densities of the SOY-DCP copolymers show a clear tendency to decrease with decreasing amounts of DCP in the initial composition, the crosslink densities of the C_{100}SOY-DCP copolymers do not show any dependence on the DCP amounts in the initial composition. However, they do have slightly

higher values than those of the SOY-DCP copolymers, presumably due to the higher reactivity of the C_{100}SOY. The crosslink densities for the SOY-DCP and C_{100}SOY-DCP copolymers are in the range 119-1034 mol/m^3 and 470-1295 mol/m^3 respectively. These values are much lower than those of the SOY-DVB and SOY-ST-DVB copolymers reported earlier by our group,[22,26,27] which accounts for their rubbery nature. Additionally, our initial results show that the tan delta values of these copolymers are in the range of 0.7-1.2, which suggests that these rubbers might be used as damping materials below ambient temperatures. More detailed dynamic mechanical analysis is underway and will be reported in due time.

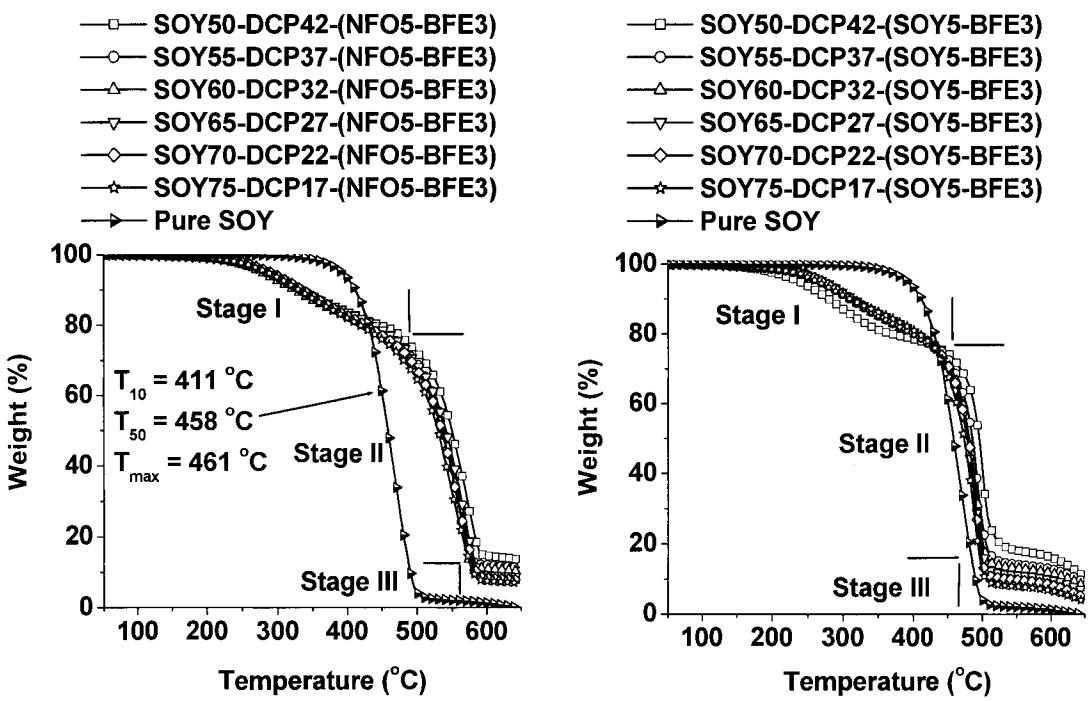

Figure 8. Thermal degradation of the SOY-DCP copolymers in air.

Thermogravimetric analysis reveals that all soybean oil-DCP bulk polymers are thermally stable in air below 200 °C and exhibit a three-stage thermal degradation above this temperature (Figures 8 and 9). The first stage degradation (200-450 °C) is attributed to evaporation and decomposition of the unreacted oil and other soluble components in the bulk material. The second stage (450-550 °C) is the fastest degradation stage and corresponds to degradation and char formation of the crosslinked polymer structure, while the last stage (>550 °C) corresponds to gradual oxidation of the char residue. The second degradation stage is further characterized by T_{max} values determined from the minima of the corresponding derivative % weight loss curves.[18,26]

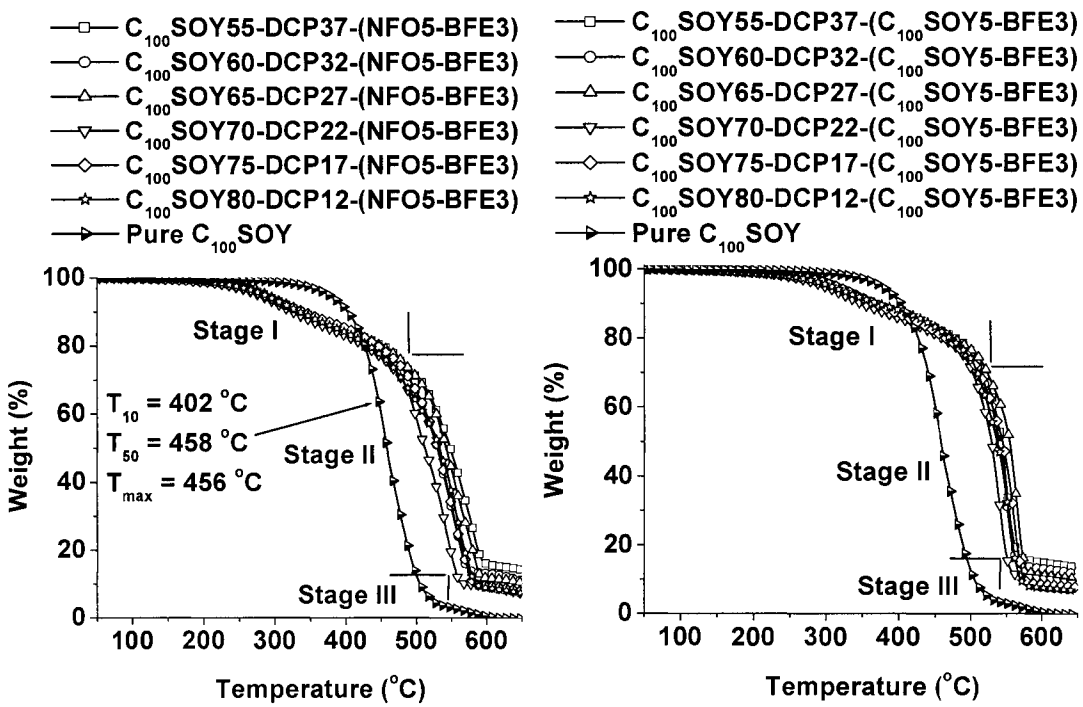

Figure 9. Thermal degradation of the C_{100}SOY-DCP copolymers in air.

The thermal degradation behavior of all SOY-DCP and C_{100}SOY-DCP copolymers is shown in Figures 8 and 9 respectively. Thermograms of pure SOY and C_{100}SOY are also included in these graphs for comparison purposes. The TGA data summarized in Table 2 show that the SOY-DCP and C_{100}SOY-DCP copolymers lose 10% of their weight at temperatures ranging from 280–334 °C and 325–372 °C respectively. The higher reactivity of C_{100}SOY over that of SOY is expected to result in higher T_{10} values for the C_{100}SOY-DCP copolymers. Interestingly, the use of NFO as a catalyst modifier seems to diminish this influence, causing all soybean oil copolymers to have similar T_{10} values (see Table 2, T_{10} values outside the parentheses). In contrast, the copolymers prepared with SOY- and C_{100}SOY-diluted catalysts show completely opposite thermal properties, with C_{100}SOY-DCP copolymers having 62-92 °C higher T_{10} values from those of the SOY-DCP copolymers (see Table 2, T_{10} values in parentheses). We are inclined to believe that this behavior is due to the enhanced solubility of the modified catalyst in the bulk oil-DCP solution, which in turn causes significant differences in formation of the crosslinked copolymer network. A more detailed explanation of this effect is based on two factors: catalyst homogeneity and differences in reactivities between SOY, C_{100}SOY, and DCP. While the NFO-modified catalyst is completely homogeneous, neither the SOY- nor the C_{100}SOY-diluted BFE catalysts are. Also, when the NFO-modified BFE catalyst is added to the bulk oil-DCP solution, it dissolves instantly giving a dark-brown reaction mixture without the formation of any precipitate. However, when the SOY- or C_{100}SOY-diluted BFE catalysts are added to the bulk solution, we notice formation of white flakes of PDCP, which dissolve in the bulk solution after a couple of minutes. Thus, the addition of 8 wt % of SOY-diluted catalyst to the 92 wt % of bulk SOY-DCP solution initially consumes more DCP due to its higher

reactivity over that of SOY. This in turn has two important consequences. First, the crosslinked SOY-DCP copolymer structure is significantly different from that formed with the NFO-modified catalyst, and second, it results in a higher amount of unreacted SOY and other soluble components after Soxhlet extraction (Table 1). This second consequence directly translates to lower T_{10} values for the (SOY-DCP)92-(SOY5-BFE3) copolymers. On the other hand, the addition of 8 wt % of the C_{100}SOY-diluted catalyst to the 92 wt % of bulk C_{100}SOY-DCP solution initially consumes more C_{100}SOY due to its slightly higher reactivity over that of DCP, as previously suggested. This, in turn, reduces the amount of unreacted C_{100}SOY and other soluble components in the bulk copolymers and gives more homogeneous crosslinked copolymer structures. The further consequence is, of course, an increase in T_{10} values for the (C_{100}SOY-DCP)92-(C_{100}SOY5-BFE3) copolymers versus those of the (C_{100}SOY-DCP)92-(NFO5-BFE3) copolymers. As previously mentioned, the 10% wt loss temperatures correspond to first stage thermal degradation. Keeping in mind that the initial weight loss of pure SOY and C_{100}SOY occurs at 350 °C and that their T_{10} values are 411 and 402 °C respectively (Figures 8 and 9), it is obvious that the initial decomposition of the soybean oil-DCP copolymers cannot be ascribed solely to unreacted soybean oil, but rather to evaporation and decomposition of the low molecular weight soluble fractions mentioned earlier.

The T_{50} values for the SOY-DCP and C_{100}SOY-DCP copolymers are in the range 470-549 °C and 511–554 °C respectively. The use of NFO has the same effect on the T_{50} values as it does on the T_{10} values. When employed as a catalyst modifier, NFO causes all copolymers to have almost the same T_{50} values (see Table 2, T_{50} values outside the parentheses). Quite the contrary, the copolymers prepared with the SOY- and C_{100}SOY-

diluted catalyst show just the opposite thermal properties. Thus, the C_{100}SOY-DCP copolymers have 48-81 °C higher T_{50} values (see Table 2, T_{50} values in parentheses). The T_{50} values correspond to the second thermal degradation stage which, as previously suggested, corresponds to degradation and char formation of the crosslinked polymer structure. This hypothesis is supported through a comparison of the second stage degradations of pure SOY and C_{100}SOY with their corresponding copolymers. It has been experimentally determined that pure SOY and C_{100}SOY have much lower T_{50} values (Figures 8 and 9), which indicates that their decomposition alone cannot account for the high thermal stability of their corresponding copolymers. Evidently, the incorporation of rigid bicyclic DCP units into the copolymer structures considerably increases their thermal stability and thereby proves that the second stage indeed corresponds to degradation of the crosslinked copolymer structure. At the very end of this stage, a certain amount of char is also formed. Our TGA results indicate that the amount of the char formed is directly proportional to the initial amount of DCP (Figures 8 and 9). Thus, copolymers with high initial amounts of DCP have the highest char yields. Besides the T_{50} values, the second stage degradation is also characterized by T_{max} values, which are in the range of 479-569 °C and 537-581 °C for the SOY-DCP and C_{100}SOY-DCP copolymers, respectively. Similar to our explanations pertaining to the T_{10} and T_{50} values, the T_{max} values show almost the same dependence on both the type of the catalyst and the initial composition of the reaction mixture.

Conclusions

The cationic copolymerizations of SOY and C_{100}SOY with DCP catalyzed by NFO-modified and SOY- and C_{100}SOY-diluted BFE catalysts provide a series of novel thermosetting copolymers ranging from tough and ductile to very soft rubbers. It has been

shown that the homogeneity of the catalysts used for the copolymerization have different effects on the copolymer properties. While the NFO-modified BFE-catalyst is homogeneous, the SOY- and C_{100}SOY-diluted BFE catalysts are not. The results indicate that NFO can be completely omitted as a catalyst modifier during synthesis of the C_{100}SOY-DCP copolymers, while its use for the synthesis of SOY-DCP copolymers results in a small enhancement of copolymer properties. Regardless of the catalyst used, all copolymerization reactions appear homogeneous in nature. As opposed to ST and DVB, all monomers used in this study have comparable reactivities, with the order being C_{100}SOY > DCP > SOY. Our analyses show that the nature of the catalyst and the monomers' reactivity have a significant influence on the copolymers' thermal properties.

All copolymers appear as dark brown polymers with a slight odor. The gelation times of the reactions vary from 4 to 991 minutes at 110 °C and show no dependence on the initial stoichiometry. The yields of the soybean oil-DCP copolymers are essentially quantitative. On the other hand, the yields of the crosslinked copolymers which remain after Soxhlet extraction range from 69-88% and depend on the monomer stoichiometry and the type of catalyst used. ^{1}H NMR spectral and Soxhlet extraction analysis show that the bulk copolymers consist of a crosslinked soybean oil-DCP network interpenetrated with certain amounts of soluble components, such as soybean oil-DCP copolymers, free oil, and some low molecular weight oil fragments, such as mono- and diglycerides or fatty acids. GPC analysis confirms that the molecular weights of these soluble fractions are in the range 400-10,000 g/mol based on polystyrene standards. The bulk copolymers have T_g's ranging from -22.6-56.6 °C. Except for the T_g of SOY50-DCP42-I8, the T_g's of all copolymers are below ambient temperature and are comparable to those of commercially available rubbery

materials. Initial DMA analysis reveals that their tan delta values are in the range 0.7-1.2, suggesting that these materials show promise as damping materials below ambient temperature.[24,49] All soybean oil-DCP copolymers are thermally stable below 200 °C. Their 10% weight loss temperatures are in the range 280-372 °C, while their 50% weight loss temperatures are in the range 470-554 °C.

These novel thermosetting copolymers have been prepared using 50-85 weight % of biorenewable materials. Their properties suggest that they may prove useful alternatives for current petroleum-based plastics and find certain utility. In the years to come, biobased polymers will most likely continue to play an important role and help set our society on a more sustainable and environmentally responsible path.

Acknowledgements

The authors gratefully acknowledge the Iowa Energy Center, the USDA, Archer Daniels Midland, and the Illinois-Missouri Biotechnology Alliance for their generous financial support. We also thank Dr. Vladimir Tsukruk and his graduate student, Sergiy Peleshanko, of the Material Science and Engineering Department, Dr. Surya K. Mallapragada and her graduate students, Michael Determan and Sim-Siong Wong, of the Department of Chemical Engineering, as well as Dr. Jay-Lin Jane and Dr. Perminus Mungara of the Department of Food Science and Human Nutrition at Iowa State University for valuable discussions and use of their facilities.

References and Notes

(1) Bozell, J. J. *Chemicals and Materials from Renewable Resources*; ACS Symposium Series; Oxford University Press, 2001.

(2) *Feedstocks for the Future: Renewables for the Production of Chemicals and Materials*; Bozell, J. J.; Patel, M., Eds.; ACS Symposium Series, 2005, in press.

(3) Byrom, D. *Biomaterials - Novel Materials from Biological Sources;* Stockton Press: New York, 1992.

(4) Wool, R. P.; Sun, X. S. *Bio-Based Polymers and Composites*; Elsevier Press, 2005.

(5) *Natural Fibers, Biopolymers, and Biocomposites*; Mohanty, A. K.; Misra, M.; Drzal, L. T., Eds.; CRC Press Taylor & Fransis Group: Boca Raton, FL, 2005.

(6) Kaplan, D. L. *Biopolymers from Renewable Resources*; Springer Verlag: New York, 1998.

(7) Kumar, G. S. *Biodegradable Polymers: Prospects and Progress*; New York: Marcel Dekker, 1987.

(8) Vert, M. *Biodegradable Polymers and Plastics*; Cambridge, England: Royal Society of Chemistry, 1992.

(9) O'Brien, R. D. *Fats and Oil – Formulating and Processing for Applications*, 2nd ed.; CRC Press, 2004.

(10) Eckey, E. W. *Vegetable Fats and Oils*; The ACS Monograph Series, New York: Reinhold Publishing Co., 1954.

(11) Salunkhe, D. K.; Chavan, J. K.; Adsule, R. N.; Kadam, S. S. *World Oilseeds: Chemistry, Technology and Utilization*; New York: Van Nostrand Reinhold, 1991.

(12) The Freedonia Group, *Soy Products & Markets, US Industry Study with Forecast to 2007 and 2012*; Study #1699, September 2003.

(13) Wang, C.; Erhan, S. *J. Am. Oil Chem. Soc.* **1999**, *76*, 1211-1216.

(14) Gunstone, F. D. *Industrial Uses of Soybean Oil for Tomorrow*; Special Report '96, Iowa State University and the Iowa Soybean Promotion Board, 1995.

(15) Ash, M.; Dohlman, E. *Oil Crops Situation and Outlook Yearbook*; Economic Research Service, USDA, OSC-2005, p. 10, May 2005.

(16) Fehr, W. R.; Hammond, E. G. U.S. Patent 5,750, 845, 1998.

(17) Zeeland Farm Services, Inc. ZFS Newsletter, Spring 2005; p 7.

(18) Andjelkovic, D. D.; Li, F.; Larock, R. C. *Novel Polymeric Materials from Soybean Oils – Synthesis, Properties and Potential Applications;* In *Feedstocks for the Future: Renewables for the Production of Chemicals and Materials*; Bozell, J. J.; Patel, M., Eds.; ACS Symposium Series, 2005, in press.

(19) Li, F.; Larock, R. C. In *Natural Fibers, Biopolymers, and Their Biocomposites*; Mohanty, A. K.; Misra, M.; Drzal, L. T., Eds.; CRC Press: Boca Raton, FL, 2005; p. 727-750.

(20) Larock, R. C.; Hanson, M. U.S. Patent 6,211,315, 2001.

(21) Li, F.; Larock, R. C. *J. Appl. Polym. Sci.* **2001**, *80*, 658-670.

(22) Li, F.; Larock, R. C. *J. Polym. Sci. Part B: Polym. Phys.* **2000**, *38*, 2721-2738.

(23) Li, F.; Larock, R. C. *J. Polym. Sci. Part B: Polym. Phys.* **2001**, *39*, 60-77.

(24) Li, F.; Larock, R. C. *Polym. Adv. Tech.* **2002**, *13*, 436-449.

(25) Li, F.; Larock, R. C. *J. Appl. Polym. Sci.* **2002**, *84*, 1533-1543.

(26) Andjelkovic, D. D.; Valverde, M.; Henna, P.; Li, F.; Larock, R. C. *Polymer* **2005**, *46*, 9674-9685.

(27) Li, F.; Hanson, M. V.; Larock, R. C. *Polymer* **2001**, *42*, 1567-1579.

(28) Chemical Market Reporter, March 21, 2005.

(29) Larock, R. C.; Dong, X.; Chung, S.; Reddy, Ch. K.; Ehlers, L. E. *J. Am. Oil. Chem. Soc.* **2001**, *78*, 447-453.

(30) Sacchi, R.; Addeo, F.; Paolillo, F. *Magn. Reson. Chem.* **1997**, *35*, S133-S145.

(31) Guillen, M. D.; Ruiz, A. *Eur. J. Lipid Sci. Technol.* **2003**, *105*, 688-696.

(32) Miyake, Y.; Yokomizo, K.; Matsuzaki, N. *J. Am. Oil. Chem. Soc.* **1998**, *75*, 1091-1094.

(33) *Cationic Polymerization: Mechanisms, Synthesis, and Applications*; Matyjaszewski, K., Ed.; New York: Marcel Dekker, Inc., 1996.

(34) Kenedy, J. P. *Cationic Polymerization of Olefins: A Critical Inventory*; John Willey & Sons, Inc.: NY, 1975; Chapter 1.

(35) Li, F.; Larock, R. C. *J. Polym. Environ.* **2002**, *10*, 59-67.

(36) de Kock, R. J.; Veermans, A. *Die Makromolekulare Chemie* **1966**, *95*, 179-186.

(37) Kuntz, I. In *Concise Encyclopedia of Polymer Science and Engineering*; 2nd Ed., Kroschwitz, J. I., Ed.; Wiley-Interscience: NY, 1990; p. 237-238.

(38) Vredenburgh, W.; Foley, K. F.; Scarlati, A. N. In *Concise Encyclopedia of Polymer Science and Engineering*; 2nd Ed., Kroschwitz, J. I., Ed.; Wiley-Interscience: NY, 1990; p. 456-458.

(39) Fink, J. K. *Reactive Polymers Fundamentals and Applications – A Concise Guide to Industrial Polymers*; William Andrew Publishing: NY, 2005; Chapter 1.

(40) Kenedy, J. P.; Makowski, H. S. *J. Macromol. Sci.* **1967**, *A1(3)*, 345-349.

(41) Corner, T.; Foster, R. G.; Hepworth, P. *Polymer* **1969**, *10*, 393-397.

(42) Cesca, S.; Priola, A.; Santi, G. *Polym. Lett.* **1970**, *8*, 585-588.

(43) Peng, Y. X.; Liu, J. L.; Cun, L. F. *J. Polym. Sci. Part A: Polym. Chem.* **1996**, *34*, 3527-3530.

(44) Becker, G.; Roth, W. A. *Ber. Dtsch. Chem. Ges.* **1934**, *67*, 627-633.

(45) Li, F.; Larock, R. C. *Polym. Int.* **2003**, *52*, 126-132.

(46) Matyjaszewski, K.; Miller, J. P.; Pyun, J.; Kickelbick, G.; Diamanti, S. *Macromolecules* **1999**, *32*, 6526-6535.

(47) Li, F.; Perrenoud, A.; Larock, R. C. *Polymer* **2001**, *42*, 10133-10145.

(48) This assumption is previously confirmed during GPC analysis of the soluble extracts from the (SOY-DVB)92-(NFO5-BFE3) copolymers, which were synthesized earlier by our group (see reference 26). These soluble components were devoid of DVB, as evidenced by the complete absence of aromatic signals in the ^{1}H NMR spectra of these extracts. Thus, they must be composed of unreacted NFO (MW ~ 360 g/mol, see reference 45) and SOY-related components, such as SOY oligomers (3000-5000 g/mol), unreacted SOY (1300 g/mol), and low MW SOY fragments (390 and 900 g/mol), presumably mono- and diglycerides. The presence of NFO is actually confirmed by the presence of a quartet at ~4.1 ppm in the ^{1}H NMR spectra of these extracts, which corresponds to methylene protons in the -OCH_2CH_3 group of the NFO ethyl ester.

(49) *Sound and Vibration Damping with Polymers*; Corsaro, R. D.; Sperling, L. H., Eds.; ACS Symposium Series 424; American Chemical Society: Washington, DC, 1990.

CHAPTER 6. ELUCIDATION OF STRUCTURAL ISOMERS FROM THE HOMOGENEOUS RHODIUM-CATALYZED ISOMERIZATION OF VEGETABLE OILS

A paper submitted to the Journal of Food and Agricultural Chemistry.

Dejan D. Andjelkovic, Byungrok Min, Dong Ahn and Richard C. Larock

Abstract

The structural isomers formed by the homogeneous rhodium-catalyzed isomerization of several vegetable oils have been elucidated. A detailed study of the isomerization of the model compound methyl linoleate has been performed to correlate the distribution of conjugated isomers, the reaction kinetics, and the mechanism of the reaction. It has been shown that $[RhCl(C_8H_8)_2]_2$ is a highly efficient and selective isomerization catalyst for the production of highly conjugated vegetable oils with a high conjugated linoleic acid (CLA) content, which is highly desirable in the food industry. The combined fraction of the two major CLA isomers [(9*Z*,11*E*)-CLA and (10*E*,12*Z*)-CLA] in the overall CLA mixture is in the range from 76.2 to 93.4%. The high efficiency and selectivity of this isomerization method along with the straightforward purification process renders this approach highly promising for the preparation of conjugated oils and CLA. Proposed improvements in catalyst recovery and reusability will only make this method more appealing to the food, paint, coating, and polymer industries in the future.

Introduction

The isomerization of vegetable oils has been the subject of increasing numbers of scientific studies in recent years. While the initial interest in the conjugation of vegetable oils was driven by the improved drying characteristics of the conjugated oils for coating and paint applications (*1-3*), the current focus of the research also involves the synthesis of more reactive comonomers for the preparation of bioplastics via cationic and free-radical copolymerizations (*4, 5*), as well as the synthesis of conjugated linoleic acids (CLA) (*6, 7*).

Irrespective of the type of polymerization method used, conjugated oils have proven to be much more reactive monomers than regular oils, resulting in higher vegetable oil incorporation in the resulting copolymers (*4, 5*). For instance, cationic copolymerization of conjugated vegetable oils with a variety of alkene comonomers has been shown to produce thermosetting materials with improved thermal and mechanical properties when compared to their non-conjugated analogues (*4, 5*). Furthermore, these bioplastics also exhibit excellent damping (*8*) and shape memory (*9*) properties, which are highly desirable in a variety of applications in the aircraft, automobile and machinery industries.

CLA is a general term which describes a group of positional and geometric isomers of linoleic (*cis*-9,*cis*-12-octadecadienoic) acid. Due to its beneficial properties, which include anticarcinogenesis (*10*), antiatherosclerosis (*11*), enhancement of immune functions (*12*) and body fat reduction (*13*), CLA has been used in a variety of nutritional, therapeutic and pharmacologic applications (*11*). Thus, it is not surprising that the synthesis of CLA has received considerable attention in recent years (*6, 7*). For this reason, the conjugation of vegetable oils rich in linoleic fatty acid, such as soybean (51%), cottonseed (53%), corn

(57%), walnut (62%), sunflower (64%), grapeseed (70%) and safflower (75%) oils (*6*), represents a promising route to CLA.

There exist numerous reports on the homogeneous isomerization of fatty acid double bonds. Many of those methods are based on transition-metal catalysis utilizing a variety of chromium (*14*), ruthenium (*15, 16*) and rhodium (*17-20*) complexes. In the course of our research in this area, we have recently developed a homogeneous rhodium-catalyzed isomerization procedure for the synthesis of highly conjugated vegetable oils and esters of fatty acids under mild conditions (*21*). For example, the utilization of as little as 0.1 mol % of $[RhCl(C_8H_{14})_2]_2$ (C_8H_{14} = cyclooctene), 0.4 mol % of (p-$CH_3C_6H_4)_3P$ (TTP) and 0.8 mol % of $SnCl_2 \cdot 2H_2O$ (with respect to the amount of vegetable oil) in absolute ethanol at 60 °C for 24 h produces >90% conjugated soybean oil and works well for other natural oils. Herein, we wish to elucidate the structural isomers of the fatty acid methyl esters of CLA obtained from the homogeneous rhodium-catalyzed isomerization of various vegetable oils and subsequent transesterification, and to determine the suitability of this method for the synthesis of CLA.

Experimental Section

Materials. The vegetable oils used in this study were Planters peanut (PNT), Mazola corn (COR), Wesson soybean (SOY), Low Saturation Soybean oil (LSS), Hain safflower (SAF) and Superb linseed (LIN) oils. All of the oils were purchased in local supermarkets, except the Superb linseed and Low Saturation Soybean (Select Oil®) oils, which were supplied by Archer Daniels Midland Co. (Decatur, IL) and Zeeland Food Service, Inc. (Zeeland, MI) respectively. All of the oils were used without further purification. The $RhCl_3 \cdot 3H_2O$ was provided by Kawaken Fine Chemicals Co. Ltd. (Japan) and used as

received. The (p-$CH_3C_6H_5)_3P$ and absolute ethanol were purchased from Aldrich Chemical Company and used as received. The CLA gas chromatography (GC) standards, methyl *cis,cis*-9,12-octadecadienoate (9*Z*,12*Z*)-CLA, methyl *cis,trans*-9,11-octadecadienoate (9*Z*,11*E*)-CLA, methyl *trans,cis*-10,12-octadecadienoate (10*E*,12*Z*)-CLA, methyl *cis,cis*-9,11-octadecadienoate (9*Z*,11*Z*)-CLA, methyl *trans,trans*-9,11-octadecadienoate (9*E*,11*E*)-CLA, and *cis,trans*-11,13-octadecadienoic acid (>97% purity) were purchased from Matreya Inc. (Pleasant Gap, PA). Prior to GC analysis, *cis,trans*-11,13-octadecadienoic acid was converted to its methyl ester by acid-catalyzed esterification in methanol to afford methyl *cis,trans*-11,13-octadecadienoate (11*Z*,13*E*)-CLA. The methyl esters of palmitoleic (C16:1), oleic (C18:1), vaccinic (*t*-C18-1), and all saturated fatty acid standards were obtained from NuChek Prep, Inc. (Elysian, MN). The chlorobis(cyclooctene)rhodium dimer, $[RhCl(C_8H_{14})_2]_2$, was synthesized according to a previously published procedure (*22*). Standard grade silica gel (porosity 60 Å, particle size 32-63 μm, surface area 500-600 m^2/g) was purchased from Sorbent Technologies (Atlanta, GA) and used as received. SPEX certiprep Rh standard ($RhCl_3$ in a matrix of 10% HCl) has been used as a calibration standard for ICP-MS analysis.

Characterization. All ^1H NMR spectroscopic analyses of the conjugated vegetable oils and other compounds were recorded in $CDCl_3$ using a Varian Unity spectrometer at 300 MHz. The methyl esters of CLA were separated and quantified using an HP6890 series gas chromatograph (Hewlett Packard Co., Wilmington, DE) equipped with an autosampler and flame ionization detector. A SUPELCOWAX^{TM}-10 capillary column (30 m × 0.25 mm × 0.25 μm film thickness, Supelco, Bellefonte, PA) was used for separation. ICP-MS analysis was performed on a Hewlett Packard 4500 series ICP-MS spectrometer. The experimental

conditions, such as the forward power (1200 W), carrier gas flow (1.2 l/min), sample flow rate (250 μL/min), and sampling depth (7.8 mm), were set for optimal sensitivity.

General Conjugation Procedure. To 10 g (34 mmol) of methyl linoleate in 5 mL of absolute EtOH was added 25 mg (0.034 mmol, 0.1 mol %) of $[RhCl(C_8H_{14})_2]_2$, 41.4 mg (0.136 mmol, 0.4 mol %) of $(p\text{-}CH_3C_6H_5)_3P$, and 62 mg (0.272 mmol, 0.8 mol %) of $SnCl_2 \bullet 2H_2O$. The reaction flask was evacuated and refilled with Ar three times and the solution stirred in an oil bath at 60 °C for 24 h. After removal of the ethanol under vacuum, the remaining mixture was dissolved in *n*-pentane and purified by flash chromatography on silica gel. The product obtained in almost quantitative yield was 87.1% conjugated (Figure 1, b). ^{1}H NMR spectrum of conjugated methyl linoleate ($CDCl_3$): δ 0.88 (t, 3 H, CH_3CH_2), 1.18-1.43 (m, 14 H, $CH_2CH_2CH_2CH_3$ and $OCCH_2CH_2(CH_2)_4$), 1.53-1.68 (m, 2 H, $OCCH_2CH_2$), 2.00-2.20 (m, 4 H, allylic), 2.23-2.32 (t, 2 H, $OCCH_2$), 2.70-2.80 (t, signal for residual bis-allylic protons), 3.65 (s, 3 H, OCH_3), 5.22-6.33 (m, 4 H, CH=CH-CH=CH).

Conjugation of Methyl Linolenate. The methyl ester of linolenic acid with 92% conjugation was obtained in quantitative yield according to the above described procedure. ^{1}H NMR spectrum of conjugated methyl linolenate ($CDCl_3$): δ 0.81-1.05 (m, 3 H, CH_3CH_2), 1.20-1.50 (m, 12 H, $CH_2CH_2CH_3$ and $OCCH_2CH_2(CH_2)_4$), 1.53-1.68 (m, 2 H, $OCCH_2CH_2$), 1.90-2.23 (m, 6 H, 4 H, allylic and 2 H, $OCCH_2$ overlapped) , 2.70-2.80 (t, signal for residual bis-allylic protons), 3.65 (s, 3 H, OCH_3), 5.20-5.50 (m, 2 H, vinylic), 5.55-5.73 (m, 1 H, vinylic), 5.80-6.21 (m, 2 H, vinylic), 6.23-6.54 (m, 1 H, vinylic).

Conjugation of the Vegetable Oils. Conjugated PNT, COR, SOY, SAF, and LIN oils with >95% conjugation were obtained in >99% yield according to the above described

procedure. The ^{1}H NMR spectra of all conjugated vegetable oils correspond closely to the previously reported spectra (*21*).

Kinetic Study. Aliquots were taken at different times during the conjugation reaction and subjected to the same workup as previously described. Samples were analyzed by both ^{1}H NMR spectroscopy and GC-MS in order to determine the progress of the reaction.

CLA Analysis by GC. Approximately 20 mg of triglyceride, 1 ml of 3N methanolic-HCl (Supelco Co., Bellefonte, PA), and 150 µl of hexane were added to a test tube, tightly capped, and incubated in a water bath at 65 °C for 50 minutes. After cooling to room temperature, 1 ml of hexane and 8 ml of water were added to the test tube, mixed thoroughly, and left overnight at room temperature for phase separation. The hexane solution containing the CLA methyl esters was separated and quantified by gas chromatography. In order to improve the separation and reduce the separation time, the following oven temperature program was used: step 1 – temperature ramp from 180 °C to 200 °C at 5 °C/min, step 2 – isothermal hold at 200 °C for 6 minutes, step 3 – temperature ramp from 200 °C to 220 °C at 10 °C/min, step 4 – temperature ramp from 220 °C to 230 °C at 5 °C/min, and step 5 – isothermal hold at 230 °C for 6 minutes. Helium (He) gas was used as a carrier gas and the column flow rate was 1.0 ml/min. The temperatures of the inlet and detector were 280 °C and 320 °C respectively. The flow rates of air, hydrogen gas, and make-up gas (He) at the detector were 350, 35, and 38.3 ml/min, respectively. The area of each peak was integrated by Chemstation software (Hewlett Packard Co., Wilmington, DE), and the peak areas were used to calculate the fatty acid composition.

Sample Preparation and ICP-MS Analysis. The conjugated vegetable oils have been purified by flash chromatography on silica gel using *n*-pentane as a solvent. After

removal of the ethanol from the crude reaction mixture under reduced pressure, 150 ml of conjugated oil was diluted with 300 mL of *n*-pentane and passed through a glass frit packed with 60, 90, or 120 g of silica gel to obtain dark red, orange, or yellow solutions respectively. The solvents were removed under reduced pressure and the remaining solution was used for ICP-MS analysis in order to determine the Rh and Sn content. Based on the initial concentrations of Rh and Sn, 1 mg/mL samples were prepared by mixing a small amount of conjugated oil with 1% HNO_3 in 50 mL volumetric flasks. The flasks were shaken vigorously to facilitate dissolution of the Rh and Sn salts in water and used for analysis the next day. A blank sample (1 mg/mL) was prepared by mixing regular SOY and DI water in a volumetric flask. After the run, the blank signal was subtracted from all of the subsequent data. The Rh and Sn content in the samples were calculated using a calibration curve obtained from the analysis of $RhCl_3$ and $SnCl_4$ standard solutions. The original concentration of the standard (1000 ppm) was diluted volumetrically to 100 ppb, 10 ppb, and 1 ppb with DI water and the resulting solutions were used for the calibration.

Results and Discussion

Calculation of the Percent Conjugation. The percent conjugation (% C) for methyl linoleate, methyl linolenate, and all vegetable oils was determined by ^{1}H NMR spectroscopic analysis. Figure 1 shows the ^{1}H NMR spectra of the methyl esters of regular and conjugated linoleic acids along with their representative structures and peak assignments. The structure on the top right represents (9*Z*,11*E*)-CLA, which is only one of several possible structural isomers of the methyl ester of CLA. The signal at 3.65 ppm (**A**) in both spectra corresponds to protons in the methoxy group of the methyl ester. The vinylic hydrogens (**F**) of the non-conjugated ester (Figure 1, a) are typically detected at 5.2-5.4 ppm, while the methylene

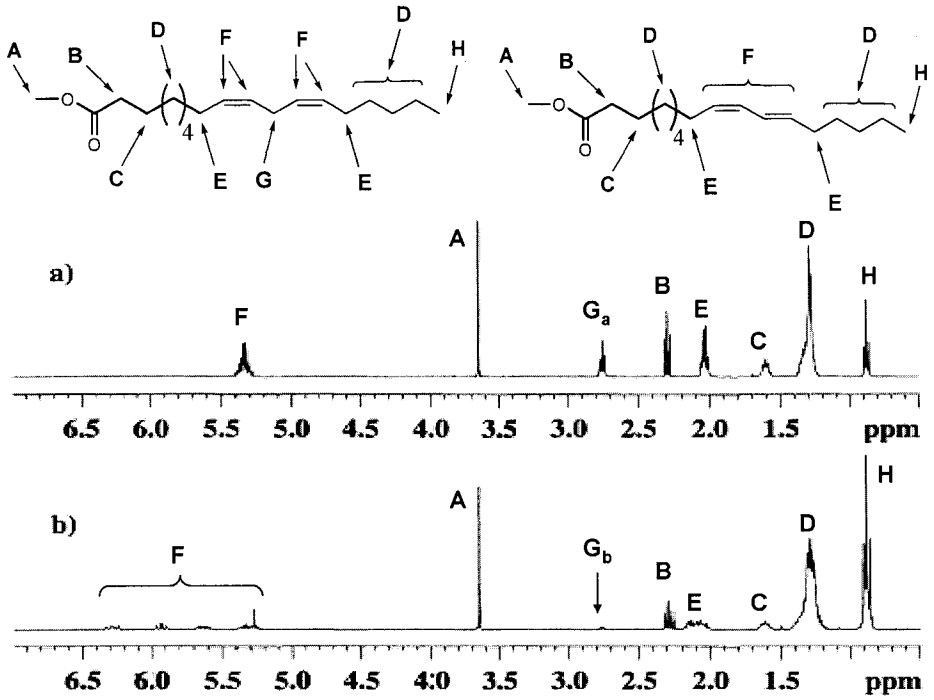

Figure 1. ^{1}H NMR spectra of the methyl esters of a) regular and b) conjugated linoleic acids with their representative structures and corresponding peak assignments.

protons positioned between the two C=C bonds, also know as the bis-allylic protons (**G**), are observed at 2.7-2.8 ppm. The signal for the bis-allylic protons indicates that the C=C bonds in the methyl ester are non-conjugated. Conversely, the vinylic hydrogens (**F**) of the conjugated ester (Figure 1, b) are detected in the 5.2-6.4 ppm range as a group of four multiplets, which indicate the existence of conjugation in the diene system. Furthermore, the significantly reduced intensity of the peak due to the bis-allylic protons (**G**) at 2.7-2.8 ppm confirms the existence of conjugation. It is this difference in the intensities of the bis-allylic peaks in the spectra of the conjugated and non-conjugated esters that allows us to calculate

the percent conjugation in these esters, as well as in all of the vegetable oils used in this study. The percent conjugation (% C) was calculated according to the following equation:

$$\% C = 100 - (100G_b / G_a)$$

where G_a and G_b represented the integrated areas of the bis-allylic peaks in the regular and conjugated esters respectively (Figure 1). The same method was used for calculation of the % C of all vegetable oils.

Homogeneous Rhodium-catalyzed Isomerization of Model Compounds. Linoleic and linolenic acids are the major polyunsaturated fatty acids in most vegetable oils, including the oils used in this study. Because of that, we began our study by elucidating the structural isomers obtained from the rhodium-catalyzed isomerization of two model compounds, the methyl esters of linoleic and linolenic acids. However, due to a lack of GC standards for the conjugated methyl linolenate isomers, we focused on analysis of the isomers of conjugated methyl linoleate. Furthermore, out of the eighteen most likely isomers of methyl linoleate, two of them, (9*Z*,11*E*)-CLA and (10*E*,12*Z*)-CLA, are of particular importance, since they represent derivatives of two CLAs, which have been shown to exhibit numerous important biological activities (*7*). Thus, our analysis focused primarily on these isomers.

The isomerization of the methyl esters of linoleic and linolenic acids was performed using as little as 0.1 mol % of the $[RhCl(C_8H_{14})_2]_2$ catalyst according to the procedure described in the experimental section. Aliquots were taken at specific times during the reaction and analyzed by ^1H NMR spectroscopy and GC, monitoring changes in the bis-allylic signal intensities (**G**, Figure 1), which are indicative of the isomerization progress and directly relate to disappearance of the starting material. Figure 2a shows these changes for the methyl ester of linoleic acid over a period of 24 hours. Comparison of the peak

intensities before and after the reaction calculates to 87.1% conjugation of the final product. Figure 2b, on the other hand, shows changes in both the intensities and appearances of the vinylic signals (**F**, Figure 1). These changes also confirm the progress of the isomerization reaction, but are not appropriate for the straightforward calculation of the % C.

a)

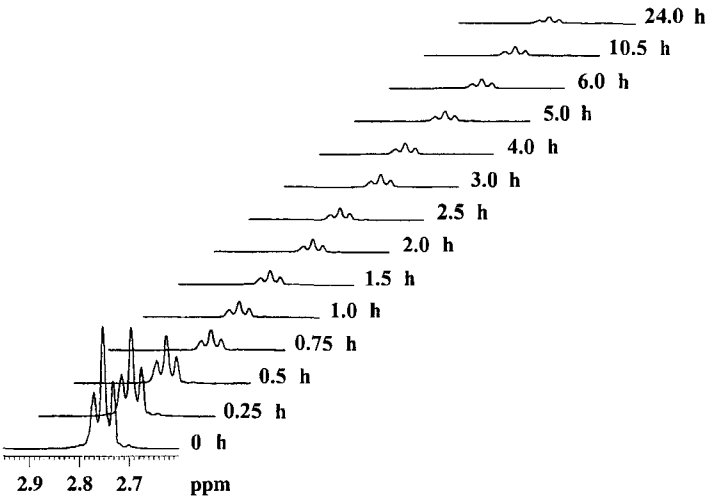

b)

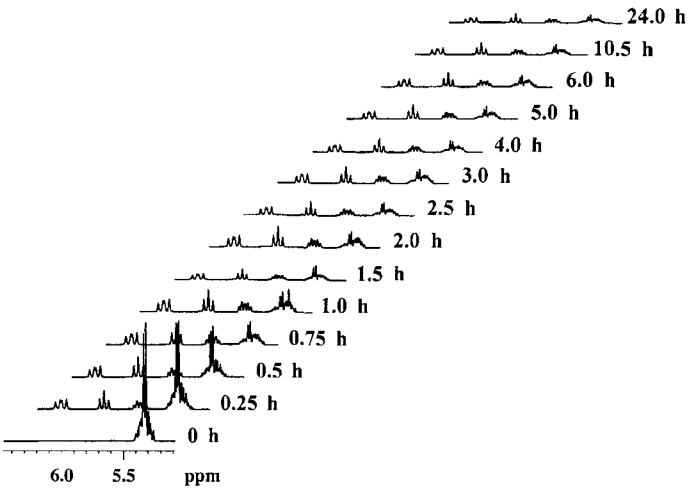

Figure 2. Progress of the isomerization of methyl linoleate monitored by ^{1}H NMR spectroscopic analysis of the a) bisallylic and b) vinylic regions.

It has been observed that the intensity of the bis-allylic signal rapidly decreases with increasing conversion in the first two hours of the reaction. At that point, 83.4% of the methyl linoleate has already been conjugated. The initial rate of the reaction exhibits a first order dependence on the concentration of methyl linoleate (Figure 3, black squares). However, in the next 22 hours the % C only improves 14.6% with obvious retardation in the reaction rate and deviation from the initial first order kinetics. A closer analysis of the reaction mechanism reveals several reasons for such behavior. The initial rate constant (k) was calculated to be 6 x 10^{-4} s^{-1}. While fairly constant in the first two hours of the reaction, the rate constant rapidly decreased through the rest of the isomerization reaction (Figure 3, black stars).

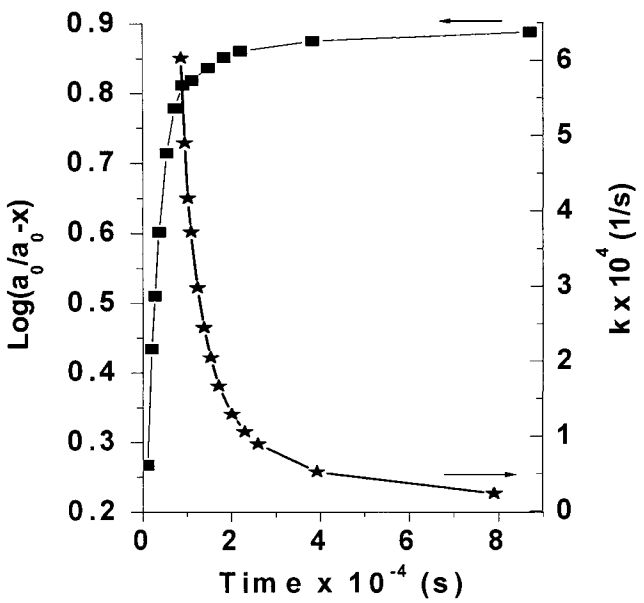

Figure 3. Kinetic study of the isomerization of methyl linoleate.

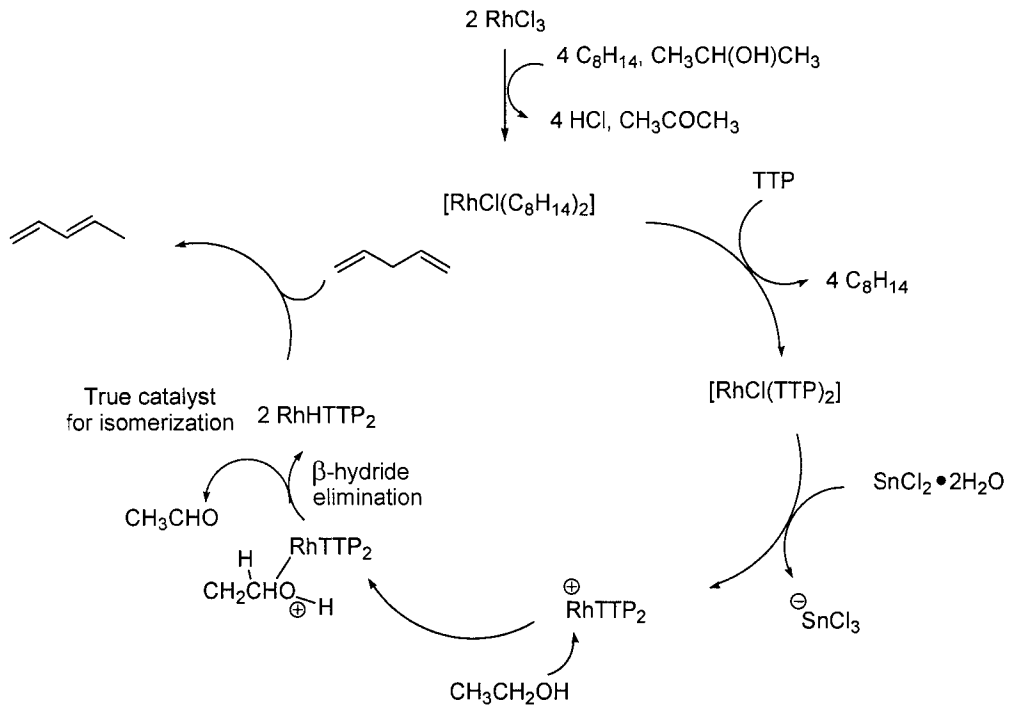

Scheme 1. Proposed mechanism for homogeneous rhodium-catalyzed isomerization.

A proposed mechanism for formation of the isomerization catalyst is outlined in Scheme 1. The rhodium(I) dimeric catalyst precursor is readily synthesized from $RhCl_3 \bullet 3H_2O$ and cyclooctene in isopropanol as the solvent (*22*). The labile cyclooctene ligands are susceptible to fast exchange with the tri-*p*-tolylphosphine (TTP) ligands under the reaction conditions to give $RhCl(TTP)_2$. The $SnCl_2 \bullet 2H_2O$ then acts as a Lewis acid and generates an electron-deficient $[Rh(TTP)_2]^+$ intermediate, which, upon coordination of the ethanol oxygen, undergoes β-hydride elimination to generate a Rh hydride, which is the true isomerization catalyst. Isomerization of the model compounds and vegetable oils is then accomplished presumably by an addition-elimination mechanism (*23*) or rearrangement through a transitory π-allyl complex (*24*). While iron and some palladium-catalyzed isomerizations proceed by a π-allyl complex (*25-27*), most other metal-catalyzed

isomerizations, including at least one previous rhodium-catalyzed isomerization (*24*), appear to proceed by an addition-elimination mechanism. The presumed mechanism for the rhodium hydride-catalyzed isomerization of methyl linoleate to the corresponding conjugated isomers is shown in Scheme 2. It has been shown that an open coordination site in the metal complex and a transition state involving a *syn*-coplanar arrangement of the α- and β-carbons, the β-hydrogen and the metal center is a prerequisite for the addition-elimination mechanism (*28*). Thus, the mechanism proceeds via three distinct steps: 1) coordination of the Rh-hydride to the olefin, 2) Rh-hydride addition to the double bond, and 3) Rh-hydride elimination by an alternative β-hydrogen to regenerate the Rh-hydride catalyst.

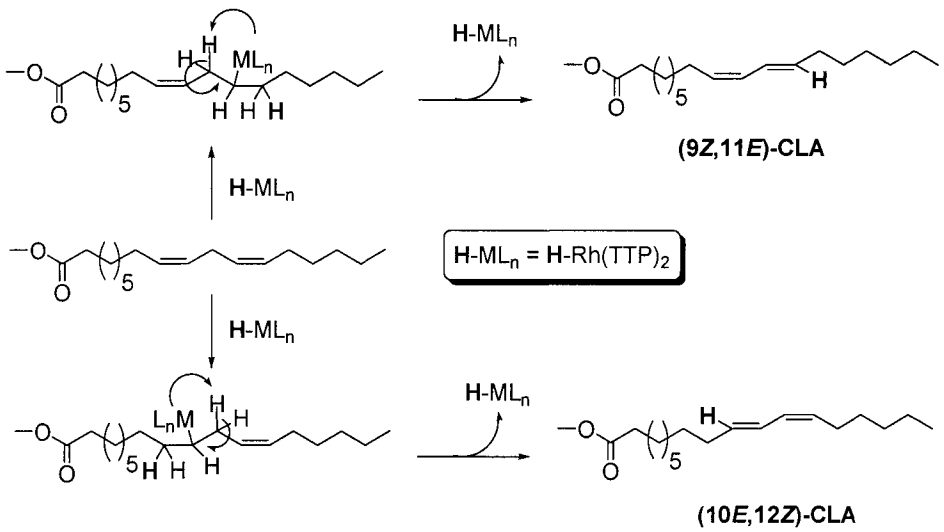

Scheme 2. Addition-elimination mechanism for the isomerization of methyl linoleate.

During the initial stages of the reaction, the concentration of the starting, non-conjugated materials is high and the reaction follows approximately first order kinetics, as shown by the initial linear dependence (Figure 3). However, with increasing conversion, the concentration of the conjugated species increases to such an extent that such species start to

compete effectively with the starting material for the catalyst in the isomerization reaction. The existence of other positional isomers of CLA suggests that even the conjugated species undergo further isomerization in the presence of the Rh-hydride catalyst (see Table 1 later in the text). These isomerization reactions account for the formation of the thermodynamically more favorable isomers (9*Z*,11*E*)-CLA and (10*E*,12*Z*)-CLA, as well as other positional isomers, which result from the shift of the conjugated system up or down the fatty acid carbon chain. This is one of the main reasons for the deviation from the first order kinetics in the later stages of the reaction. Another reason might be slow catalyst decomposition under the reaction conditions. For example, acetaldehyde, which is formed during the initial ethanol rhodium β-hydride elimination step, is known to undergo decarbonylation in the presence of Rh catalysts (*29-33*).

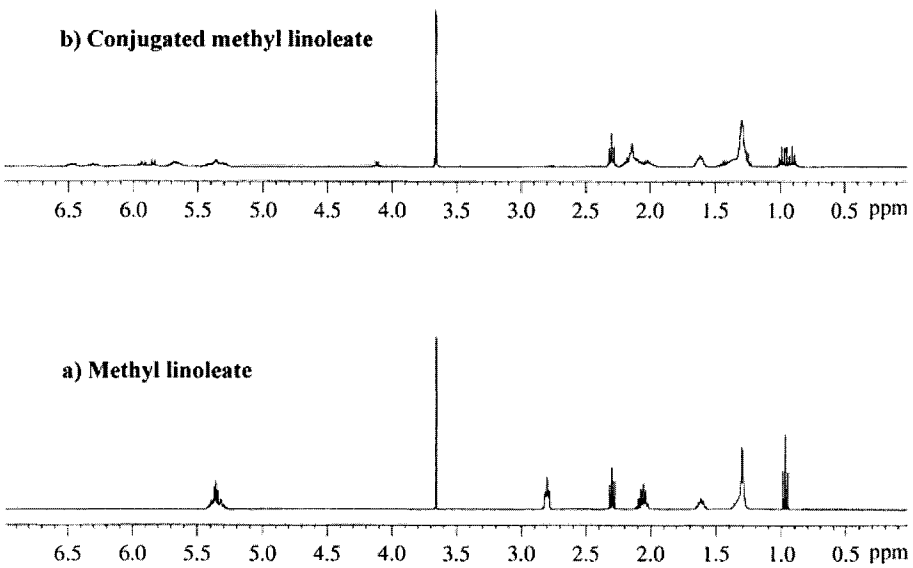

Figure 4. ^{1}H NMR spectra of a) conjugated and b) regular methyl linolenate.

The progress of the methyl linolenate isomerization was followed in the same manner as that of methyl linoleate. Figure 4 shows the ^{1}H NMR spectra of regular and conjugated methyl linolenate. Our calculations indicate 98% conjugation of the final product as evidenced by the complete disappearance of the bis-allylic signal in the spectrum of the conjugated product.

Table 1. CLA compositions of samples taken during the isomerization of methyl linoleate as determined by GC analysis.

Fatty acid	Linoleic acid (C18:0)	(9*Z*,11*E*)-CLA	(10*E*,12*Z*)-CLA	(9*E*,11*E*)-CLA	(9*Z*,11*Z*)-CLA	Total
0 h	100.0	-	-	-	-	100.0
0.25 h	61.5	13.9	22.7	1.0	0.9	100.0
0.5 h	41.0	23.1	33.6	1.2	1.0	100.0
0.75 h	37.1	25.6	34.6	1.5	1.3	100.0
1 h	27.5	28.0	41.5	1.6	1.5	100.0
1.5 h	26.5	28.5	41.8	1.6	1.6	100.0
2 h	24.9	29.6	42.1	1.7	1.6	100.0
2.5 h	22.8	31.2	42.6	1.7	1.6	100.0
3 h	21.7	31.8	43.0	1.8	1.6	100.0
4 h	20.5	32.4	43.6	1.9	1.7	100.0
5 h	19.1	33.3	43.9	1.9	1.8	100.0
6 h	18.3	33.7	44.2	1.9	1.9	100.0
10.5 h	17.2	34.3	44.5	2.0	1.9	100.0
24 h	17.2	33.8	45.1	2.0	1.9	100.0

Elucidation of the Structural Isomers from the Conjugation of Methyl Linoleate. Aliquots taken during the conjugation of methyl linoleate were subjected to GC analysis in order to determine their CLA compositions and to monitor the progress of the reaction. Table 1 lists the CLA compositions for 13 samples taken during a 24 hour-long isomerization reaction. The time intervals at which these samples were acquired are shown on Figure 2a. Six commercially available GC standards were used for this analysis: methyl linoleate (9*Z*,12*Z*)-LA, (9*Z*,11*E*)-CLA, (10*E*,12*Z*)-CLA, (9*Z*,11*Z*)-CLA, (9*E*,11*E*)-CLA, and (11*Z*,13*E*)-CLA. The results indicate that two major CLA isomers are formed during the conjugation reaction, (9*Z*,11*E*)-CLA (33.8%) and (10*E*,12*Z*)-CLA (45.1%). Their retention times (rt) are 10.58 and 10.81 respectively (Figure 5). These two isomers account for approximately 79% of all species in the mixture (unreacted methyl linoleate plus all CLA isomers), which translates to 95.2% of all CLA isomers formed during conjugation (Table 1). Two other CLA isomers, (9*E*,11*E*)-CLA (rt = 11.69 min, 2.1%) and (9*Z*,11*Z*)-CLA isomer (rt = 11.18 min, 1.9%) are also formed, although in much smaller amounts. The (11*Z*,13*E*)-CLA isomer (rt = 10.69 min) could not be accounted for, presumably due to overlap with the signals of the two major CLA isomers, (9*Z*,11*E*)-CLA and (10*E*,12*Z*)-CLA. The existence of a peak for methyl linoleate (rt = 8.71 min) clearly indicates that there is 17.2% of unreacted methyl linoleate in the mixture. Thus, based on the GC analysis, the % C is calculated to be 82.9%. When compared to the ^{1}H NMR spectroscopic data, this value is approximately 4-5% lower. At this point, we are not able to account for the discrepancies between the two methods used for % C analysis. Also, when compared to the methyl linolenate results (% C = 98% by ^{1}H NMR), the % C value for methyl linoleate (87.1% by ^{1}H NMR) is also lower. The reason for such discrepancies is unclear to us at the moment. However, from our

experience, we know that a small 10-30% increase in the Rh-catalyst load can push the % C to almost quantitative in all cases. It is also important to mention that hydrogenation products are not observed at any time during the isomerization of this model compound.

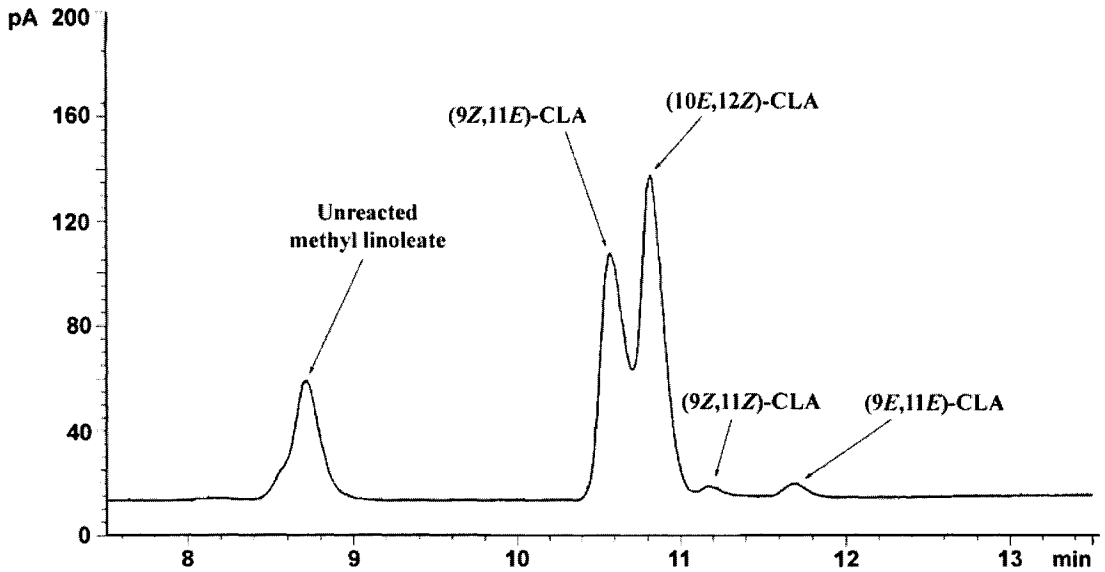

Figure 5. Gas chromatogram of conjugated methyl linoleate (Table 1, sample after 24h).

Elucidation of the Structural Isomers from the Isomerization of Various Vegetable Oils. The conjugation of SOY and other oils was monitored in a manner similar to that described above. In this case, the CLA isomer analysis was more difficult to perform due to the existence of a large number of saturated and other unsaturated fatty acid esters. Table 2 lists the CLA and other fatty acid compositions for 11 samples taken during the 24 hour-long isomerization of SOY. Figure 6 shows the progress of the isomerization of SOY monitored by ^{1}H NMR spectroscopic analysis along with the time intervals at which these samples were acquired. Figure 7 shows a GC chromatogram of the conjugated SOY (CSOY) at the end of the isomerization reaction (see Table 2, sample after 24 hours) with complete

Table 2. CLA compositions of samples taken during the isomerization of SOY as determined by GC analysis.

Fatty acid	0 h	0.5 h	1 h	1.5 h	2 h	2.5 h	3 h	3.5 h	4.5 h	5.5 h	10 h	24 h
(C14:0)	0.1	0.1	0.1	0.1	0.1	0.1	0.1	0.1	0.2	0.2	0.2	0.1
(C16:0)	11.4	12.5	12.9	12.9	12.7	13.1	13.2	13.3	13.4	13.3	13.3	12.9
(C16:1)	0.1	0.1	0.1	0.1	0.1	0.1	0.1	0.1	0.2	0.1	0.2	0.1
(C18:0)	3.8	4.1	4.2	4.3	4.3	4.3	4.3	4.3	4.3	4.3	4.3	4.4
(C18:1)	20.8	20.9	21.3	21.4	21.4	21.5	21.7	21.6	21.6	21.5	21.5	21.7
(tC18:1)	1.5	1.5	1.5	1.5	1.5	1.5	1.5	1.5	1.5	1.5	1.5	1.5
(C18:2)	53.8	23.4	13.9	9.7	6.9	5.5	4.5	3.9	2.9	2.5	1.3	0.7
(C18:3)	8.5	0.8	0.3	0.2	0.1	-	-	-	-	-	-	-
(9*Z*,11*E*)-CLA	-	11.0	13.9	16.0	17.3	17.7	18.0	18.3	18.6	18.7	19.3	19.7
(10*E*,12*Z*)-CLA	-	11.8	16.0	17.4	18.7	19.3	19.5	19.6	20.1	20.4	20.5	20.8
(9*Z*,11*Z*)-CLA	-	0.3	0.4	0.5	0.5	0.5	0.6	0.6	0.5	0.5	0.5	0.6
(9*E*,11*E*)-CLA	-	5.6	6.7	7.1	7.6	7.6	7.7	7.9	8.0	8.1	8.6	8.7
CLN [a]	-	7.8	8.5	8.8	8.7	8.7	8.7	8.8	8.7	8.8	8.8	8.8
Total	100	100	100	100	100	100	100	100	100	100	100	100

The following non-conjugated fatty acids have been used as GC standards: Myristic (C14:0), Palmitic (C16:0), Palmitoleic (C16:1), Stearic (C18:0), Oleic (C18:1), Vaccinic (tC18:1), Linoleic (C18:2) and Linolenic (C18:3). [a] Isomers of the conjugated methyl linolenate (based on the GC analysis of 92% conjugated methyl linolenate and subsequent retention time comparisons).

peak assignments. Based on the ^{1}H NMR spectroscopic analysis of its bisallylic peaks, the conjugated SOY sample was 99% conjugated. During the conjugation reaction, the 53.8% of linoleic acid present in the regular SOY was almost quantitatively converted into its conjugated isomers. Again, the two major CLA isomers were (9*Z*,11*E*)-CLA (19.7%) and (10*E*,12*Z*)-CLA (20.9%), which account for approximately 81.3% of all CLA isomers in the mixture. The rest of the CLA mixture was composed primarily of (9*E*,11*E*)-CLA (8.7%) and a small amount of (9*Z*,11*Z*)-CLA (0.6%). When compared with the data obtained from the analysis of methyl linolenate (95.2%), the overall fraction of the two major CLA isomers, (9*Z*,11*E*)-CLA and (10*E*,12*Z*)-CLA, was much lower (81.3%). On the other hand, the fraction of the (9*E*,11*E*)-CLA isomer was dramatically increased, while the fraction of the thermodynamically less favorable (9*Z*,11*Z*)-CLA isomer remained low. The observed differences might be a consequence of the lower effective concentration of the linoleic fatty acid in the SOY triglyceride system when compared to the pure methyl linolenate model system. According to the GC data (see Tables 1 and 2), the isomerization of the linoleic fatty acid in the SOY triglyceride system proceeds much faster than that of the pure methyl linolenate model system. It is possible that once produced, the CLA isomers in the SOY system have more time to isomerize further and yield higher amount(s) of other thermodynamically more favorable CLA isomers, such as (9*E*,11*E*)-CLA (Table 2). The GC results further confirm that the initial 8.5% of linolenic fatty acid present in the pure SOY was quantitatively converted into a mixture of conjugated isomers (CLN entry in Table 2). The retention times of these peaks have been confirmed by comparison with the retention times of the peaks observed in the GC chromatogram of the 98% conjugated methyl linolenate. Based on these results, the overall % C of the conjugated SOY has been

calculated to be 99.9%. This is in excellent agreement with the value obtained from the ^{1}H NMR spectroscopic analysis.

a)

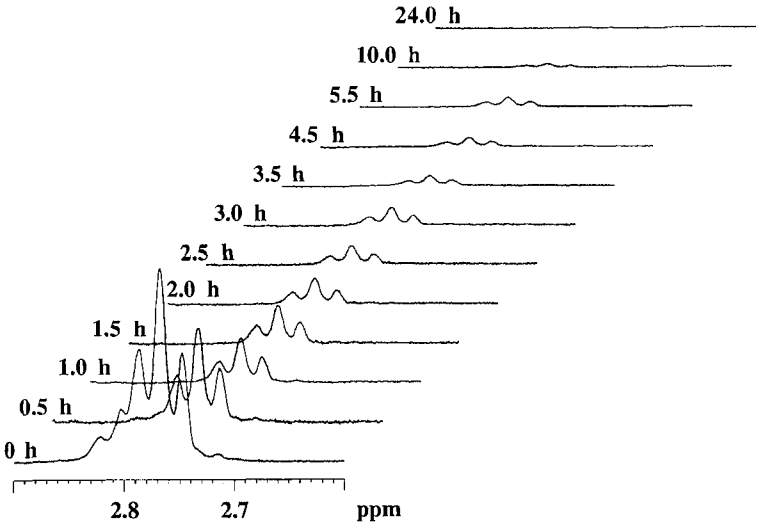

b)

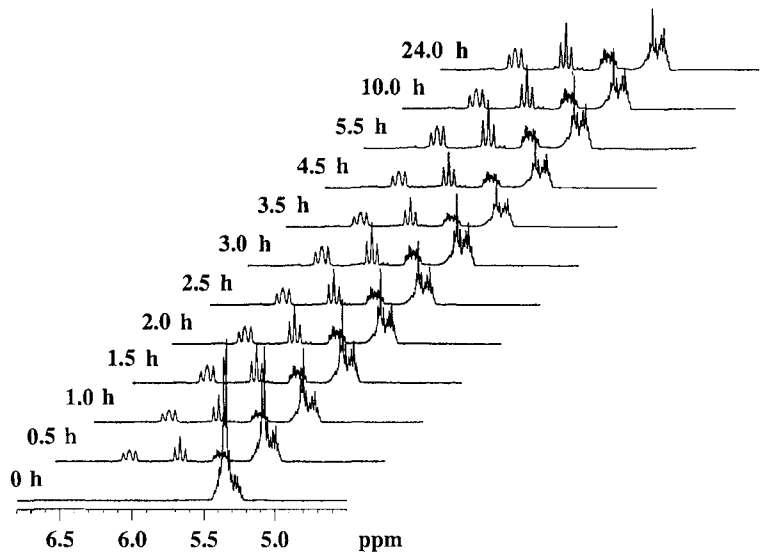

Figure 6. Progress of the isomerization of SOY monitored by ^{1}H NMR spectroscopic analysis of the a) bisallylic and b) vinylic regions.

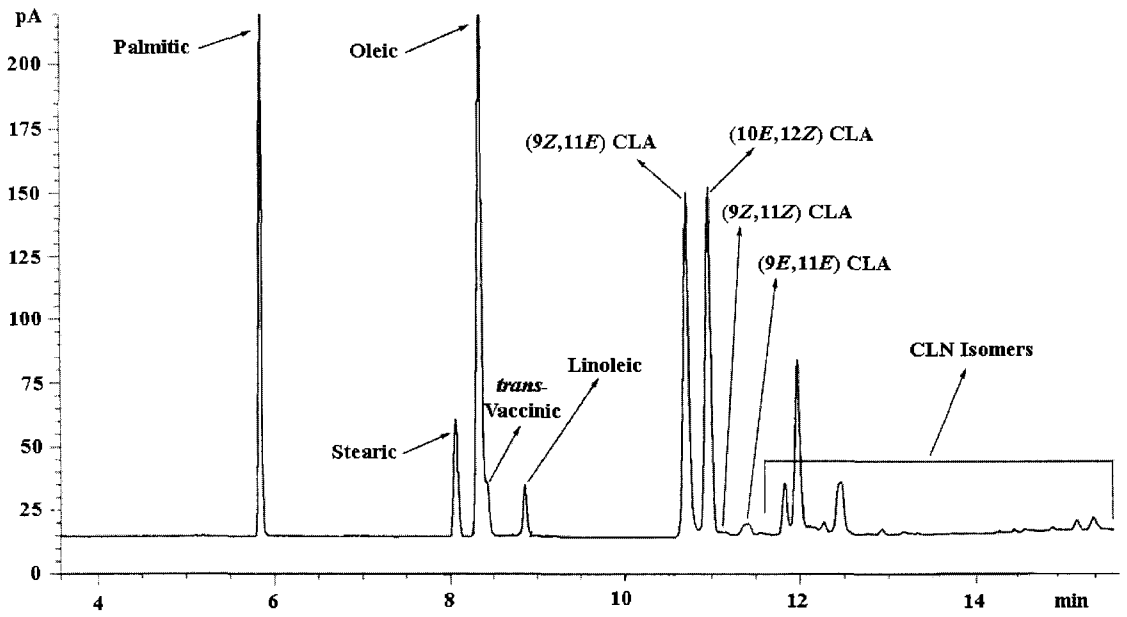

Figure 7. Gas chromatogram of conjugated SOY (Table 2, sample after 24 hours).

The results summarized in Table 3 also show that the amount of all CLA isomers formed during the reaction (49.8%) is approximately 4% lower than the initial amount of linoleic fatty acid in the pure SOY. This is distributed among the more saturated fatty acid components (stearic and oleic acids) as shown by the small increase in their content. Although minor, this suggests that hydrogenation is a possible concomitant side reaction. However, contrary to these facts, a small increase (~1.5%) in the palmitic acid (C16:0) content is also observed. Since chain scission is fairly unlikely to occur during the isomerization process, this suggests that experimental error may be responsible for the observed discrepancies and that hydrogenation may not occur at all. At this moment we are uncertain as to the extent of hydrogenation. Anyhow, if present at all, its contribution is fairly small and it does not change drastically the overall efficiency of the isomerization process.

Table 3. Fatty acid composition comparisons for several regular vegetable oils and their conjugated analogues as determined by GC analysis.

Fatty acid	LIN	CLIN	PNT	CPNT	SOY	CSOY
Myristic (C14:0)	-	-	-	-	0.1	0.2
Palmitic (C16:0)	5.5	6.5	12.4	12.7	11.5	12.9
Palmitoleic (C16:1)	0.1	0.2	0.2	0.3	0.1	0.2
Stearic (C18:0)	3.5	4.2	2.5	2.7	3.8	4.8
Oleic (C18:1)	20.0	23.4	52.0	52.1	19.9	24.0
t-Vaccinic (C18:1)	0.9	0.8	0.8	1.0	1.4	2.1
Linoleic (C18:2)	17.0	-	32.0	0.7	55.6	3.2
Linolenic (C18:3)	53.0	-	-	-	7.6	-
(9*Z*,11*E*)-CLA	-	8.1	-	13.3	-	20.7
(10*E*,12*Z*)-CLA	-	8.5	-	14.2	-	21.9
(9*Z*,11*Z*)-CLA	-	1.0	-	-	-	1.1
(9*E*,11*E*)-CLA	-	3.0	-	3.0	-	4.1
CLN [a]	-	44.4	-	-	-	4.9
Total	100.0	100.0	100.0	100.0	100.0	100.0
% C	-	100.0	-	100.0	-	99.9
% Major CLAs [b]	-	80.8	-	90.3	-	89.1
% (9*E*,11*E*)-CLA [c]	-	14.6	-	9.7	-	8.6
% (9*Z*,11*Z*)-CLA [d]	-	4.6	-	0	-	2.3

[a] Isomers of the conjugated methyl linolenate (based on the GC analysis of 92% conjugated methyl linolenate and subsequent retention time comparisons). [b] The % fraction of both major CLA isomers [(9*Z*,11*E*) and (10*E*,12*Z*)] in the overall CLA mixture. [c] The % fraction of the (9*E*,11*E*)-CLA isomer in the overall CLA mixture. [d] The % fraction of the (9*Z*,11*Z*)-CLA isomer in the overall CLA mixture.

Table 3. Continued.

Fatty acid	COR	CCOR	LSS	CLS	SAF	CSAF
Myristic (C14:0)	-	-	-	0.1	0.1	0.2
Palmitic (C16:0)	11.6	11.6	4.38	4.6	7.7	8.2
Palmitoleic (C16:1)	0.1	0.2	0.10	0.1	0.1	0.1
Stearic (C18:0)	1.8	2.0	3.25	3.5	2.1	2.2
Oleic (C18:1)	26.9	28.1	19.16	20.6	13.7	14.5
t-Vaccinic (C18:1)	0.8	0.8	1.11	1.2	0.8	0.8
Linoleic (C18:2)	57.5	0.8	63.50	0.6	75.3	2.1
Linolenic (C18:3)	1.3	-	8.50	-	0.2	-
(9*Z*,11*E*)-CLA	-	24.6	-	27.5	-	26.8
(10*E*,12*Z*)-CLA	-	26.5	-	29.5	-	27.5
(9*Z*,11*Z*)-CLA	-	0.8	-	1.0	-	0.8
(9*E*,11*E*)-CLA	-	2.8	-	4.1	-	16.2
CLN [a]	-	1.8	-	7.2	-	0.5
Total	100.0	100.0	100.0	100.0	100.0	100.0
% C	-	100.0	-	100.0	-	100.0
% Major CLAs [b]	-	93.4	-	91.7	-	76.2
% (9*E*,11*E*)-CLA [c]	-	5.1	-	6.6	-	22.7
% (9*Z*,11*Z*)-CLA [d]	-	1.5	-	1.7	-	1.1

[a] Isomers of the conjugated methyl linolenate (based on the GC analysis of 92% conjugated methyl linolenate and subsequent retention time comparisons). [b] The % fraction of both major CLA isomers [(9*Z*,11*E*) and (10*E*,12*Z*)] in the overall CLA mixture. [c] The % fraction of the (9*E*,11*E*)-CLA isomer in the overall CLA mixture. [d] The % fraction of the (9*Z*,11*Z*)-CLA isomer in the overall CLA mixture.

Table 3 lists fatty acid compositions for several commercially available vegetable oils and their conjugated analogues prepared by our homogeneous rhodium-catalyzed isomerization process over the course of 24 hours. The vegetable oils shown in the table are arranged according to their initial linoleic fatty acid content. The isomerization results indicate that all oils are essentially quantitatively converted into their corresponding conjugated isomers. Again, the major CLA isomers formed are the (9*Z*,11*E*)-CLA and (10*E*,12*Z*)-CLA isomers. Their total content in the overall CLA mixture varies from 80.8% in CLIN to 93.3% in CCOR. It appears that the highest fraction of these two isomers is found in vegetable oils which have intermediate amounts of both linoleic and linolenic fatty acids. For instance, the intermediate cases, CCOR (93.4%) and CLS (91.7%) oils, have the highest content of the two major CLA isomers. This suggests that the presence of a certain amount of linolenic acid in the pure oil favors the formation of the two major CLA isomers. On the other hand, its excess (LIN, 80.8%, has 53.0% of linolenic acid) or scarcity (SAF, 76.2%, has 0.2% of linolenic acid) show the opposite effect. At the same time, the fraction of the thermodynamically more stable (9*E*,11*E*)-CLA isomer follows the opposite trend. While relatively low for CSOY, CCOR and CLS oils (8.6%, 5.1% and 6.7% respectively), the (9*E*,11*E*)-CLA content in the CLIN and CSAF oils increases substantially (14.6% and 22.7% respectively). Conversely, the fraction of the thermodynamically less stable (9*Z*,11*Z*)-CLA isomer remains low in all samples.

With regard to our previous discussion of hydrogenation, we noticed that the isomerization of LIN oil resulted in a 9% decrease in conjugated linolenic acid content (initial 53.0% content vs 44.4% CLN content, Table 3). Closer inspection revealed that this amount was redistributed among the CLA isomers, as well as stearic and oleic acids, in the

CLIN upon conjugation. The magnitude of the discrepancy in this case strongly suggests the existence of hydrogenation as a side reaction, which accounts for the conversion of linolenic fatty acid into more saturated C18-fatty acids in the CLIN sample and, therefore, leads to their fractional increase. However, on the basis of the results with other oils, we noticed that the contribution of hydrogenation in other oils was either drastically lower or it did not exist at all. This suggests that the high content of linolenic fatty acid in LIN enhances the hydrogenation side reaction.

Product Purification and ICP-MS Analysis. In order to be useful for any food applications, conjugated oils and CLAs need to be devoid of any toxic metals or other organics. Therefore, the ease and efficiency of their purification is an important issue. During the course of our investigation, we observed that simple flash chromatography of the conjugated model compounds and vegetable oils on silica gel with *n*-pentane as the solvent was an efficient and straightforward purification method. The amount of silica gel needed for complete removal of the toxic metals (Rh and Sn) and organics (TTP) was optimized by performing flash chromatography using silica gel beads made with varying amounts of silica gel (see the experimental section). The untreated solution of conjugated oils and catalyst mixture had a dark red color, which was indicative of a high content of transition metal. With an increase in the amount of silica gel used in the purification, the color of the resulting solution changed from red to orange to yellow. The final yellow color, of course, closely resembled the natural color of most of the vegetable oils. In order to determine the content of both Rh and Sn in each of these colored solutions, we subjected them to ICP-MS analysis. For that purpose, an ICP-MS calibration curve (Figure 8) was generated using standard solutions of $RhCl_3$ and $SnCl_4$. For example, the results obtained from the analysis of the

CSOY solutions are shown in Table 4. The data indicate that the red solution of CSOY contained 13.4 ppb of Rh and 1.4 ppb of Sn (Table 4, entry 3), while the orange solution contained 8.51 ppb and 0.86 ppb of Rh and Sn respectively (Table 4, entry 2). The yellow solution obtained after purification on the largest silica gel bed (Table 4, entry 1) had 0.78 and 0.57 ppb of Rh and Sn respectively. The concentrations of these two metals are therefore at the threshold level set by the Food and Drug Administration (FDA) in July 1995 (*34*) and should not raise any toxicological issues.

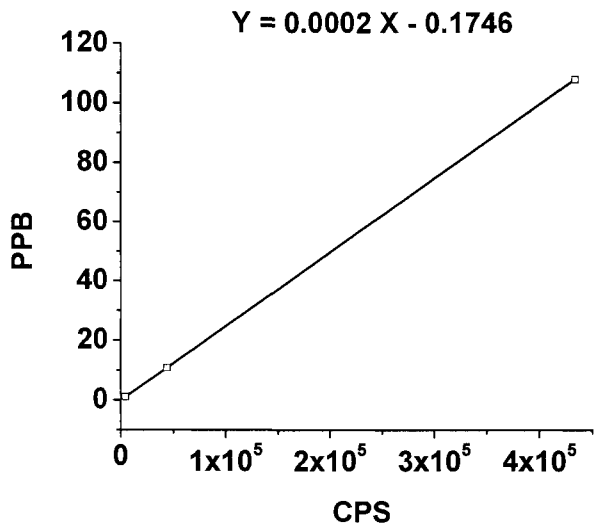

Figure 8. ICP-MS calibration curve for Rh.

Table 4. Concentrations of Rh and Sn in three separate CSOY samples.

Entry	CPS[a] (Rh)	C_{Rh} (ppb)[b]	CPS[a] (Sn)	C_{Sn} (ppb)[b]
1	4700	0.78	3745	0.57
2	43432	8.51	5170	0.86
3	68048	13.43	7658	1.36

[a] CPS = counts per second. [b] ppb = parts per billion.

Conclusions

Based on these findings, we conclude that homogeneous rhodium-catalyzed isomerization represents an extremely efficient and selective method for the conjugation of both model compounds and vegetable oils. This method preserves the original structure of the substrates and only causes rearrangement of the carbon-carbon double bonds in the system. It offers certain advantages over the alkali-based methods (*7*), because it does not cause hydrolysis of the final product. In fact, it yields highly conjugated products, which are of considerable interest in the paint, coating and polymer industries (*1-5*). Also, straightforward flash chromatographic purification affords an easy way to obtain very pure conjugated products devoid of any major amounts of residual catalyst and thus eliminates numerous issues raised by contamination. This approach is also very interesting from the food industry standpoint, because it mainly produces (9*Z*,11*E*)-CLA and (10*E*,12*Z*)-CLA isomers. The fraction of these two important isomers in the overall CLA mixture of conjugated oils is in the range from 76.2% to 93.4%.

Due to this high conversion and selectivity, this approach offers tremendous potential for CLA preparation. However, in order to determine the suitability of this method for the industrial production of food-grade CLA, one must consider the overall economics of the process. The main concern is, of course, the high cost of the Rh catalyst, which, aside from its high efficiency and selectivity, renders this process more expensive than the existing alkali-based processes. Recycling of the catalyst is known to reduce the overall cost significantly and it still represents one of the main considerations in the design of highly efficient processes (*35-39*). One approach towards fast and efficient catalyst recovery would be immobilization on a solid support (*40*). The main disadvantage of this method lies in the

fact that catalyst efficiency usually decreases significantly after a couple of cycles due to leakage from the solid support. Another approach, first developed by Horvath (*41*), takes advantage of the limited miscibility of partially or fully fluorinated compounds with nonfluorinated ones in fluorous biphasic systems (FBS). For instance, a typical FBS consists of a fluorous phase containing a dissolved catalyst and some other nonfluorous phase, which can be any organic or inorganic solvent with limited or no solubility in the fluorous phase. Usually, the fluorous phase consists of a perfluorinated hydrocarbon and a fluorous phase compatible catalyst. For that purpose the catalyst often contains fluorinated ligands in order to enhance its solubility in the fluorous media. The chemical transformations in these systems then occur either in the fluorous phase or at the interface of the two phases. In their original work (*41*), Horvath and coworkers have demonstrated efficient extraction of a rhodium catalyst from toluene after catalytic hydroformylation of olefins. The successful catalyst recovery under the mild conditions coupled with retention of the catalyst's efficacy offers huge potential for industrial application of homogeneous catalysis in the future. This approach has been reviewed extensively and proven useful in numerous catalytic processes (*42-48*).

In the near future, we intend to utilize this approach and optimize the overall isomerization process. We believe that these improvements may render this homogeneous rhodium-catalyzed isomerization industrially applicable for the production of CLA.

Acknowledgements

The authors gratefully acknowledge the Iowa Soybean Promotion Board for financial support. We also thank Dr. Robert S. Houk and his graduate student Cory T. Gross of the

Chemistry Department at Iowa State University for their assistance with the ICP-MS analysis.

Literature Cited

1. Turner, G. P. A. In *Introduction to Paint Chemistry and Principles of Paint Technology*, 3rd Ed., Chapman and Hall: London, 1988.

2. Bentley, J. The Use of Oils and Fatty Acids in Paints and Surface Coatings. In *Lipid Technologies and Applications*, Gunstone, F. D., Padley, F. B., Eds.; Marcel Dekker: New York, 1997; pp. 711-736.

3. Lin, K. F. Paints, Varnishes, and Related Products. In *Bailey's Industrial Oil and Fat Products*, Hui, Y. H., Eds.; John Wiley: New York, 1996; Vol. 5, pp. 227-274.

4. Andjelkovic, D. D.; Li, F.; Larock, R. C. Novel Polymeric Materials from Soybean Oils –Synthesis, Properties and Potential Applications. In *Feedstocks for the Future: Renewables for the Production of Chemicals and Materials*. Bozell, J. J., Patel, M., Eds.; ACS Symposium Series 921, ACS Press: Washington DC, 2006; Chapter 6, pp. 67-81.

5. Li, F.; Larock, R. C. Synthesis, Properties and Potential Applications of Novel Thermosetting Biopolymers from Soybean and Other Natural Oils. In *Natural Fibers, Biopolymers, and Their Biocomposites*, Mohanty, A. K., Misra, M., Drzal, L. T., Eds.; CRC Press: Boca Raton, FL, 2005; pp. 727-750.

6. *Advances in Conjugated Linoleic Acid Research*, Yurawecz, M. P., Mossoba, M. M., Kramer, J. K. G., Pariza, M. W., Nelson, G. J., Eds.; American Oil Chemists Society Press: Champaign, IL, 1999, Vol. 1.

7. Raeney, M. J.; Liu, Y.-D.; Wescott, N. D. Method for commercial preparation of conjugated linoleic acid. U.S. Patent 6,420,577 (2002) and references cited therein.

8. Li, F.; Larock, R. C. New soybean oil-styrene-divinylbenzene thermosetting copolymers. IV. Good damping properties. *Polym. Adv. Technol.* **2002**, *13*, 436-449.

9. Li, F.; Larock, R. C. New soybean oil-styrene-divinylbenzene thermosetting copolymers. V. Shape memory effect. *J. Appl. Polym. Sci.* **2002**, *84*, 1533-1543.

10. Ip, C.; Chin, S. F.; Scimeca, A.; Pariza, M. W. Mammary cancer prevention by conjugated dienoic derivative of linoleic acid. *Cancer Res.* **1991**, *51*, 6118-6124.

11. Saebo, A.; Skarie, C.; Jerome, D. Isomer enriched conjugated linoleic acid compositions. U.S. Patent 6,225,486 (2001) and references cited therein.

12. Whigham, L. D.; Cook, M. E.; Atkinson, R. L. Conjugated linoleic acid: implications for human health. *Pharm. Res.* **2000**, *42*, 503-510.

13. Gnadig, S.; Rickert, R.; Sebedio, J. L.; Steinhart, H. Conjugated linoleic acid (CLA): physiological effects and production. *Eur. J. Lipid Sci. Technol.* **2001**, *103*, 56-61.

14. Frankel, E. N. Homogeneous catalytic conjugation of polyunsaturated fats by chromium carbonyls. *J. Am. Oil Chem. Soc.* **1970**, *47*, 33-36.

15. Sleeter, R. T. Method of conjugating double bonds in drying oils. U.S. Patent 5,719,301 (1998).

16. Krompiec, S.; Jerzy, J.; Majewski, J.; Grobelny, J. Isomerization of vegetable oils catalyzed by ruthenium complexes. *Pol. J. Appl. Chem.* **1998**, *42*, 43-48.

17. DeJarlais, W. J.; Gast, L. E. Conjugation of polyunsaturated fats: activity of some group VIII metal compounds. *J. Am. Oil Chem. Soc.* **1971**, *48*, 21-24.

18. Singer, H.; Stein, W.; Lepper, H. Catalytic isomerization of olefinically unsaturated compounds to conjugated double-bonded structures. German Patent 2,049,973 (1972).

19. Singer, H.; Seibel, R.; Mess, U. The isomerization of linoleic acid methyl esters with rhodium complexes. *Fette Seifen Anstrichm.* **1977**, *4*, 147-150.

20. Basu, A.; Bhaduri, S.; Kasar, J. G. Isomerization catalysts for manufacture of conjugated polyunsaturated fatty acid derivatives. Indian Patent 162,553 (1998).

21. Larock, R. C.; Dong, X.; Chung, S.; Reddy, C. K.; Ehlers, L. Preparation of conjugated soybean and other natural oils and fatty acids by homogeneous transition metal catalysis. *J. Am. Oil Chem. Soc.* **2001**, *78*, 447-453.

22. Van der Ent, A.; Onderdelinden, A. L. Chlorobis(cyclooctene)rhodium(I) and iridium(I) complexes. *Inorg. Synth.* **1990**, *28*, 90-92.

23. Cramer, R. Olefin coordination compounds of rhodium. III. The mechanism of olefin isomerization. *J. Am. Chem. Soc.* **1966**, *88*, 2272-2282.

24. Morrill, T. C.; D'Souza, C. A. Efficient hydride-assisted isomerization of alkenes via rhodium catalysis. *Organometallics* **2003**, *22*, 1626-1629.

25. Harrod, J. F.; Chalk, A. J. Homogeneous catalysis. I. Double bond migration in *n*-olefins, catalyzed by group VIII metal complexes. *J. Am. Chem. Soc.* **1964**, *86*, 1776-1779.

26. Harrod, J. F.; Chalk, A. J. Homogeneous catalysis. III. Isomerization of deuterio olefins by group VIII metal complexes. *J. Am. Chem. Soc.* **1966**, *88*, 3491-3497.

27. Davies, N. R. Palladium-catalyzed olefin isomerization. *Nature* **1964**, *201*, 490-491.

28. Collmann, J. P.; Hegedus, L. S.; Norton, J. R.; Finke, R. C. *Principles and Applications of Organotransition Metal Chemistry*, 2nd ed.; University Science Books: Mill Valley, CA, 1987.

29. Baird, M. C.; Nyman, C. J.; Wilkinson, G. The decarbonylation of aldehydes by tris(triphenylphosphine)chloro-rhodium(I). *J. Chem. Soc.* 1968, **A**, 348.

30. Ohno, K.; Tsuji, J. Organic synthesis by means of noble metal compounds. XXXV. Novel decarbonylation reactions of aldehydes and acyl halides using rhodium complexes. *J. Am. Chem. Soc.* 1968, **90,** 99-107.

31. Walborsky, H. M.; Allen, L. E. Stereochemistry of tris(triphenylphosphine)rhodium chloride decarbonylation of aldehydes. *J. Am. Chem. Soc.* 1971, **93,** 5465-5468.

32. Tsuji, J.; Ohno, K. Decarbonylation reactions using transition metal compounds. *Synthesis* 1969, **1,** 157-170.

33. Suggs, J. W. Isolation of stable acylrhodium(III) hydride intermediate formed during aldehyde decarbonylation. Hydroacylation. *J. Am. Chem. Soc.* 1978, **100,** 640-641.

34. Cheeseman, M. A.; Machuga, E. J.; Bailey, A. B. A tiered approach to threshold of regulation. *Food Chem. Toxicol.* **1999**, *37*, 387-412.

35. Knapen, J. W. J.; van der Made, A. W.; de Wilde, J. C.; van Leeuwen, P. W. N. M.; Wijkens, P.; Grove, D. M.; van Koten, G. Homogeneous catalysts based on silane dendrimers functionalized with arylnickel(II) complexes. *Nature* **1994**, *372*, 659-663.

36. Chauvin, Y.; Mussmann, L.; Olivier, H. A novel class of versatile solvents for two-phase catalysis: hydrogenation, isomerization, and hydroformylation of alkenes catalyzed by rhodium complexes in liquid 1,3-dialkylimidazolium salts. *Angew. Chem., Int. Ed. Engl.* **1995**, *34*, 2698-2700.

37. Cornlis, B.; Herrmann, W. A. In *Applied Homogeneous Catalysis with Organometallic Compounds*, Cornlis, B., Herrmann, W. A., Eds.; Weinheim: New York, 1996; Chapter 3.1, pp. 577-600.

38. Cornlis, B.; Herrmann, W. A. In *Applied Homogeneous Catalysis with Organometallic Compounds*, Cornlis, B., Herrmann, W. A., Eds.; Weinheim: New York, 1996; Chapter 4.1, pp. 1167-1197.

39. Cole-Hamilton, D. J. Homogeneous catalysis - new approaches to catalyst separation, recovery, and recycling. *Science* **2003**, *299*, 1702-1706.

40. McNamara, C. A.; Dixon, M. J.; Bradley, M. Recoverable catalysts and reagents using recyclable polystyrene-based supports. *Chem. Rev.* **2002**, *102*, 3275-3300.

41. Horvath, I. T.; Rabai, J. Facile catalyst separation without water: fluorous biphase hydroformylation of olefins. *Science* **1994**, *266*, 72-75.

42. Cornils, B. Fluorous biphase systems - the new phase-separation and immobilization technique. *Angew. Chem., Int. Ed. Engl.* **1997**, *36*, 2057-2059.

43. Hughes, R. P. Organo-transition metal compounds containing perfluorinated ligands. *Adv. Organomet. Chem.* **1990**, *31*, 183-267.

44. de Wolf, E.; van Koten, G.; Deelman, B.-J. Fluorous phase separation techniques in catalysis. *Chem. Soc. Rev.* **1999**, *28*, 37-41.

45. Rutherford, D.; Juliette, J. J. J.; Rocaboy, C.; Horvath, I. T.; Gladysz, J. A. Transition metal catalysis in fluorous media: application of a new immobilization principle to rhodium-catalyzed hydrogenation of alkenes. *Catalysis Today* **1998**, *42*, 381-388.

46. Hope, E. G.; Kemmitt, R. D. W.; Paige, D. R.; Stuart, A. M. The rhodium catalyzed hydrogenation of styrene in the fluorous biphase. *J. Fluorine Chem.* **1999**, *99*, 197-200.

47. Juliette, J. J. J.; Rutherford, D.; Horvath, I. T.; Gladysz, J. A. Transition metal catalysis in fluorous media: practical application of a new immobilization principle to rhodium-catalyzed hydroborations of alkenes and alkynes. *J. Am. Chem. Soc.* **1999**, *121*, 2696-2704.

48. Richter, B.; Spek, A. L.; van Koten, G.; Deelman, B.-J. Fluorous versions of Wilkinson's catalyst. Activity in fluorous hydrogenation of 1-alkenes and recycling by fluorous biphasic separation. *J. Am. Chem. Soc.* **2000**, *122*, 3945-3951.

CHAPTER 7. GENERAL CONCLUSIONS

General Conclusions for Part I

The first part of this dissertation explored the synthesis and characterization of a new class of high-performance polymeric materials, HFIP-linked benzophenone polymers. These novel materials have combined the structural features of PBPs and HFIP-polymers. This combination may extend their utility to applications that were previously inaccessible. The development of these novel materials was accomplished through the application of basic principles of macromolecular design and synthetic organic chemistry. The unique structures of these new polymers make them interesting candidates for coatings, gas separation membranes, and electronics applications, such as nonvolatile organic memory.

This work further demonstrates the utility and versatility of the Ni(0)-catalyzed polymerization approach to the synthesis of new isomeric HFIP-containing polymers. Functional group tolerance and mild reaction conditions make this Ni(0)-catalyzed coupling approach very attractive for the synthesis of functionalized HFIP polymers. In particular, the results show the efficiency of the Ni(0)-catalyzed polymerization of difunctional monomers for the synthesis of HFIP-linked benzophenone polymers. For that purpose, novel functionalized bistriflate and bischloride monomers have been developed and polymerized. Chloride and triflate functionalities were the end-groups of choice in this study due to their high reactivity and ready availability.

Poor film forming properties of PBP homopolymers have also been addressed. A new method based on the Ni(0)-catalyzed copolymerization of bistriflate monomers with newly developed polyfunctional comonomers (crosslinkers) has been described. Our results

have confirmed the efficiency of this method for the synthesis of higher molecular weight HFIP-linked benzophenone polymers with optimized properties. Specifically, the thermal, mechanical and film forming properties of these new copolymers have been improved when compared to their homopolymer analogues. This enabled the preparation of tough and more flexible films for subsequent analyses. For example, DMA analysis of these films shows a noticeable improvement in the mechanical properties of these new copolymers.

To fully examine these materials in gas membrane applications, detailed gas permeability measurements are needed. Due to the similarity between the backbones of these new HFIP-linked benzophenone polymers and their parent HFIP polymers (**PDTFE**) developed earlier in our group,[1-3] it is expected that these new materials will exhibit similar, if not improved, selectivities and efficiencies to the **PDTFE** material. Information obtained from these analyses will help us establish necessary structure-property relationships and improve the materials' efficiencies through subsequent synthetic modification or composite fabrication approaches.

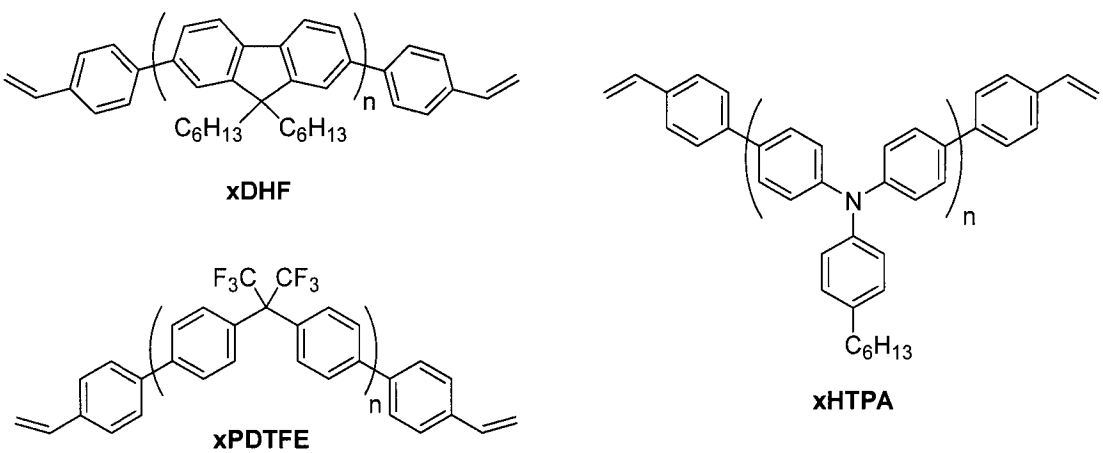

Scheme 1. Crosslinkable materials used to fabricate electronic devices.

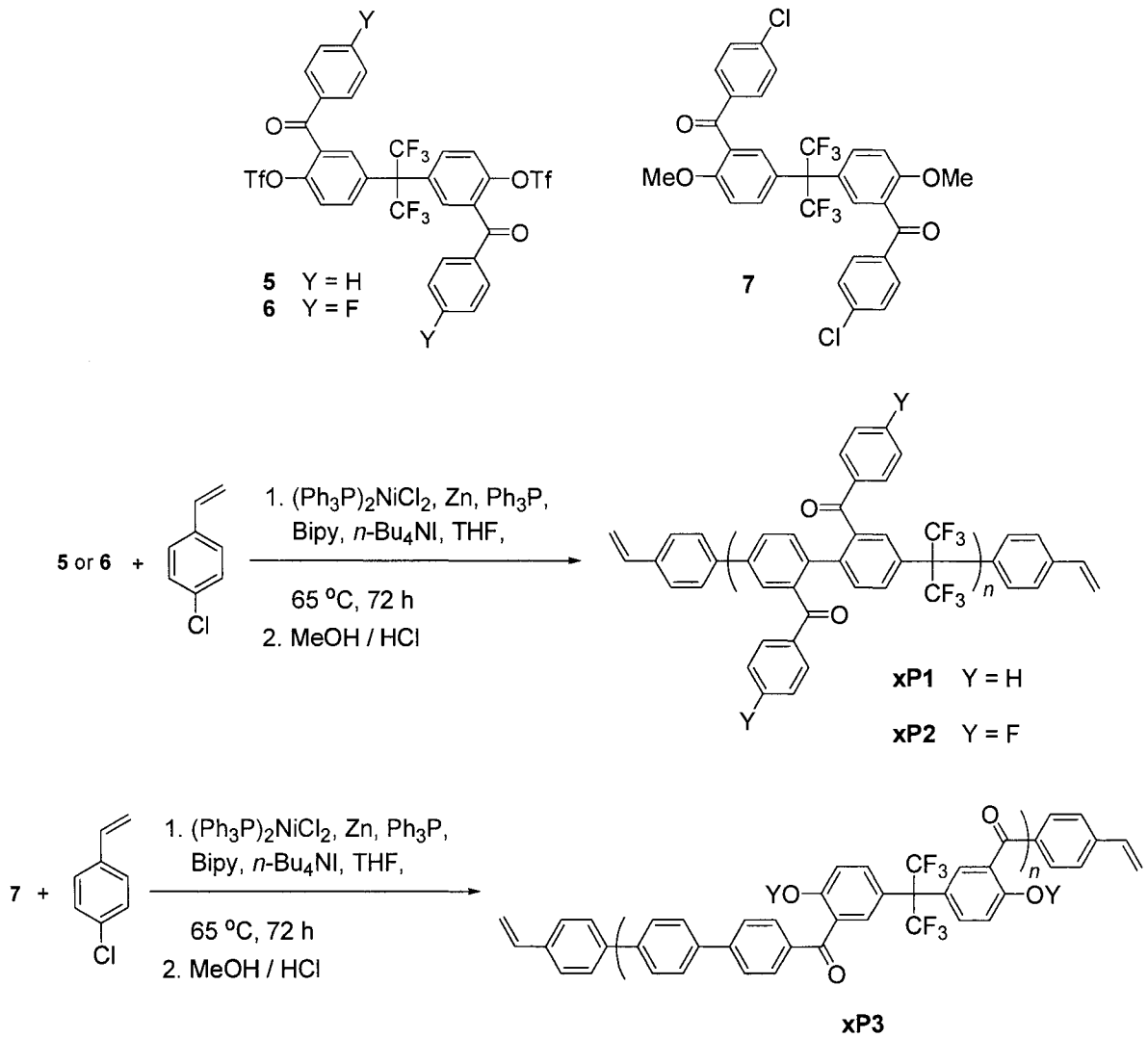

Scheme 2. Proposed synthesis of isomeric styrene-endcapped HFIP-linked benzophenone polymers for organic memory device fabrication.

The unique structural features of these new HFIP materials make them potentially interesting in electrical applications, where wide band gap materials with low current density, good electron/hole mobility, and good thermal and oxidative stability are required.[4,5] Recent work by Carter and coworkers have shown that **PDTFE**-based crosslinked materials (**xPDTFE**) demonstrate more stability, in terms of their lifetime and thermal stability, than

poly(9,9-di-*n*-hexylfluorene) (**xDHF**) and poly-[(4-*n*-hexyltriphenyl)amine]-based (**xHTPA**) diode-type devices (**Scheme 1**).[6] Therefore, it would be interesting to use novel HFIP-linked benzophenone materials in a similar manner and determine their utility and efficiency for organic memory device applications. In order to do that, crosslinkable styrene functionalities must be introduced by carefully endcapping the growing polymer chains of the HFIP-linked benzophenones with *p*-chlorostyrene during the Ni(0)-coupling copolymerization, as shown in **Scheme 2**. This will allow us to synthesize several HFIP-linked benzophenone polymers suitable for electronic device fabrication. Prepared electronic devices will then be evaluated for their efficiencies and results compared to the performances of currently available materials.

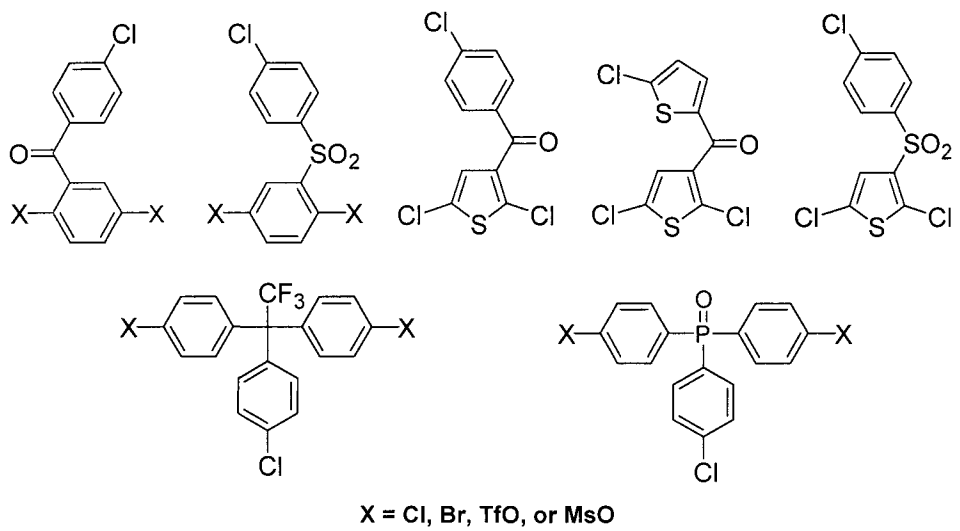

Scheme 3. Proposed structures of trifunctional comonomers for Ni(0)-catalyzed copolymerization.

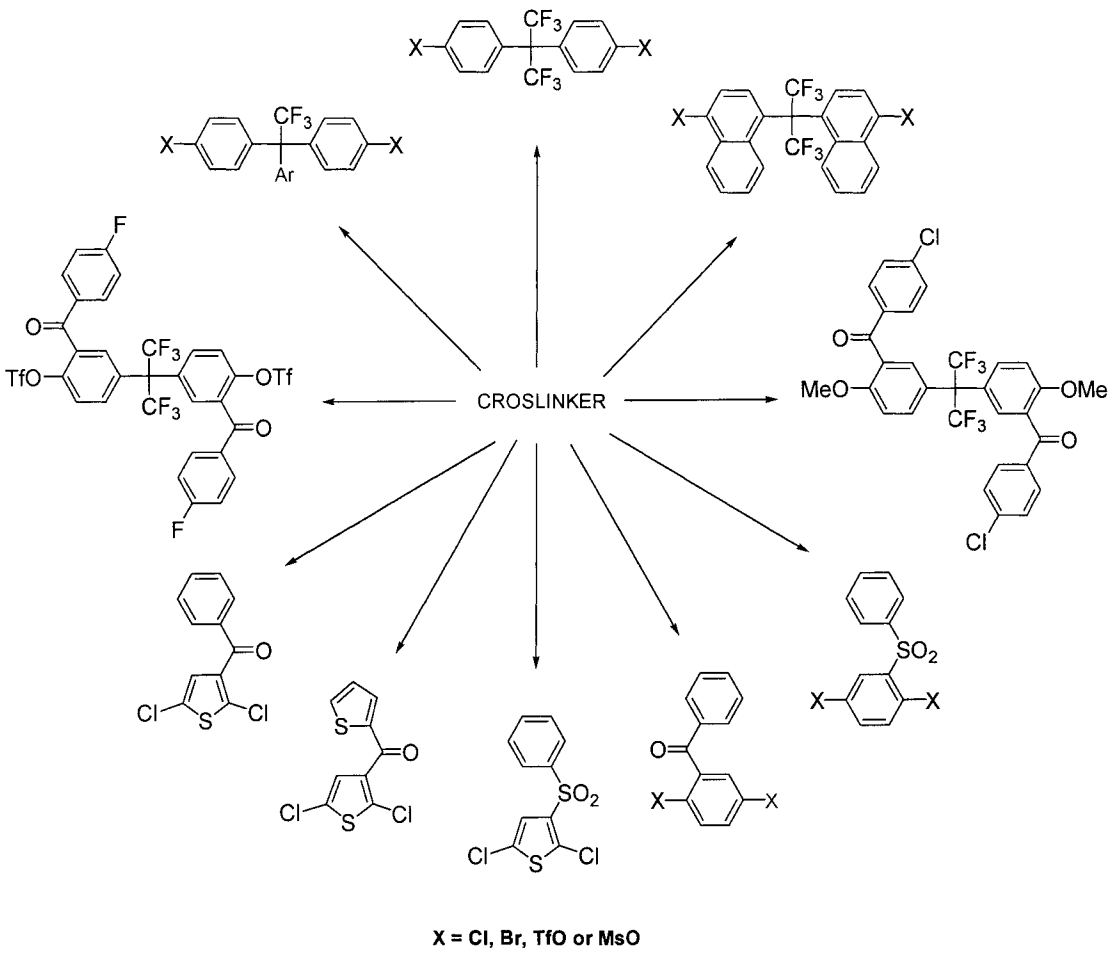

Scheme 4. Potential Ni(0)-catalyzed copolymerization avenues.

Future work in this area will focus on two additional projects. The first one will involve an extension of the Ni(0)-catalyzed crosslinking methodology described in chapter 2. As a viable route for the optimization of the polymers' properties, this method can be extended through the development of a wide range of polyfunctional comonomers and their subsequent application in adequate copolymerization processes. As mentioned earlier, chloride and triflate groups represent the best choice when lower cost and higher reactivities are needed. Additionally, mesylate functional groups are also worth exploring due to their even lower cost and proven efficiency in polymerization processes.[7,8] **Scheme 3** lists several

other types of trifunctional crosslinkers, which can easily be developed. These comonomers can then be utilized in numerous copolymerization processes to further extend the range of available HFIP-containing and HFIP-free high performance materials (**Scheme 4**).

The second project will focus on the development of new HFIP-containing ladder polymers for potential gas membrane and electronic applications.[9] These polymers can be prepared through the intramolecular electrophilic cyclization of reduced adjacent benzophenone units in **P1** and **P2** homo and copolymers (**Scheme 5**). These materials are known to possess very high thermal and oxidative stabilities due to their fused aromatic polycyclic structures. Furthermore, their structural similarities with **PDTFE** polymers make them good candidates for organic nonvolatile electrical bistable storage device applications.[6]

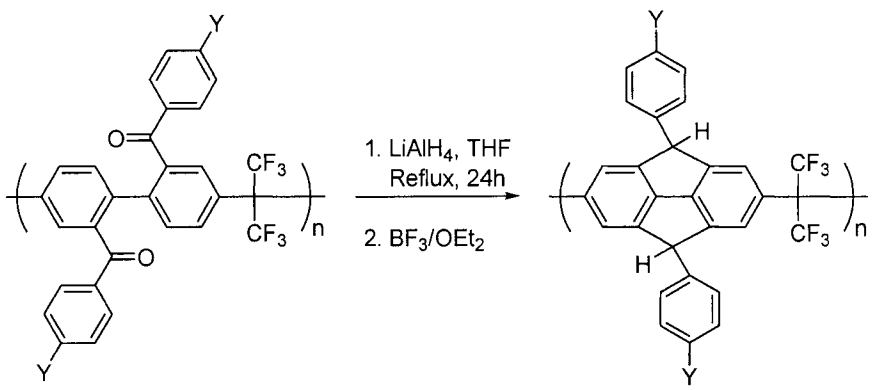

Scheme 5. Proposed synthesis of HFIP-containing ladder polymers.

General Conclusions for Part II

The second part of this dissertation focuses on the design and synthesis of novel agricultural oil-based materials, which are of interest in the polymer, paint, coatings and food

industries. Biobased materials have received considerable attention over the past decade due to their low cost, ready availability and environmental compatibility. Application of such materials has a huge potential market due to the present emphasis on sustainable technologies.

Chapter 4 focuses on the utilization of a wide range of commercial agricultural oils for the cationic copolymerization with ST and DVB. More specifically, twelve agricultural oils of differing degrees of unsaturation were cationically copolymerized with ST and DVB into a series of terpolymers. In this study, the only variable was the type of oil, while the amounts of ST and DVB were kept constant. The results gathered from detailed structure-property relationship analyses confirm that the cationic polymerization, which is effective for soybean, corn, tung, and fish oils, can be extended to the polymerization of other readily available vegetable oils. Furthermore, the data indicates that the polymers' properties can be tailored to suit targeted applications by a simple choice of vegetable oil type and stoichiometry in the final resin.

While our earlier work on soybean oils showed that a variety of polymeric materials can be prepared by cationic copolymerization, it also pointed out the fundamental flaw, which relates to the drastically different reactivities of vegetable oils on the one hand, and ST and DVB as the alkene comonomers on the other hand. Additionally, the high cost of DVB ($3.00/lb) as a crosslinker renders the whole approach less attractive from an economic standpoint. Luckily, there exists a variety of other petroleum-based comonomers, which should have similar reactivities to vegetable oils, simply based on their structural features. For instance, readily available and inexpensive dicyclopentadiene (DCP, $0.29/lb) represents an excellent alternative to DVB and effectively addresses some of the above-mentioned

issues. The synthesis and characterization of a range of novel biobased rubbers prepared by the cationic copolymerization of regular (SOY) and 100% conjugated (C_{100}SOY) soybean oils with DCP is the focus of chapter 5 of this dissertation. The results obtained from detailed chemical, microstructural, thermal, and mechanical analyses confirm that this approach offers a simple and inexpensive route to a range of new biobased rubbers. Due to their low softening temperatures and good damping ability, these materials show promise as replacements for petroleum-based materials in sound and vibration damping and asphalt additive applications.

The isomerization of vegetable oils is the subject of the following chapter. The emphasis is placed on elucidation of the structural isomers from the homogeneous rhodium-catalyzed isomerization of model compounds and several agricultural oils. This work establishes the relationship between the distribution of conjugated isomers, the reaction kinetics and the reaction mechanism. The results based on NMR, GC, and ICP-MS analyses show that $[RhCl(C_8H_{14})_2]_2$ represents a highly efficient and selective isomerization catalyst for the production of highly conjugated vegetable oils with a high content of CLA isomers [(9*Z*,11*E*) CLA and (10*E*, 12*Z*) CLA], which are highly desirable in the food industry. The combined fraction of these two major CLA isomers in the overall CLA mixture of all conjugated products is in the range from 76.2 to 93.4%. The high efficiency and selectivity of this isomerization method along with a straightforward purification process renders this approach highly promising for conjugated oils and CLA preparation. Furthermore, based on the distribution of conjugated linoleic acid (CLA) isomers in the conjugated products, the

overall utility of this process for industrial CLA production is evaluated. The end of the chapter also lists several suggestions for improvements in the overall process.

Future work in the area of biobased materials will focus on the commercialization of current technology and development of new materials and methods for broader manipulation of renewable resources. Current cationic polymerization methodology has been very effective for the production of a wide range of thermosetting polymers from vegetable oils. However, an exceedingly long curing process, the high cost of some crosslinkers, and environmental and health issues related to the BFE catalyst, are major shortcomings of this process for the commercial production of these promising materials. Therefore, future efforts will be directed toward finding appropriate solutions for these problems.

Curing times must be reduced significantly to industrially acceptable levels. One way to accomplish this is through the adjustment of resin compositions in order to enhance their overall reactivities and gelation processes. This work will require close examination of the polymerization kinetics, gelation points and cure times for a variety of promising vegetable oil-alkene compositions.[10,11] For example, the vegetable oil-ST-DVB resins[12] have much lower gelation times and cure much faster than the corresponding vegetable oil-DCP resins.[13] However, the high cost of the divinylbenzene crosslinker makes these resins economically less attractive. Thus, improvements in the oil-DCP systems are highly desirable. In order to decrease gelation times for these systems and speedup the curing process, we intend to adjust the reactivity of these resins by the addition of a small (10-20 wgt %) amount of inexpensive ST, *n*-butyl vinyl ether (nBVE) or other reactive comonomer, at the expense of the DCP. Due to their higher reactivities, these comonomers will most likely increase the overall reactivity of the resin and cut the gelation times to industrially acceptable levels. Alternative

carbocationic catalysts, which include various Lewis acid catalysts, such as $SnCl_4$ or $ZnCl_2$, will also be examined for this purpose.

Another approach will rely on the addition of thickeners. For example, our preliminary results show that the addition of as little as 1-5 wgt % of high molecular weight polybutadiene (PBD, $M_w \sim$ 300-500 kg/mol) results in a drastic increase in the viscosity of the oil-ST-DVB resins. Since the gelation process is related to the viscosity increase during the curing process, this should reduce the gelation times of the OIL-DCP-based resins still further. Also, the addition of such small amounts of PBD does not alter the thermo-mechanical properties of the final thermosetting materials. Due to the presence of C=C double bonds in its backbone, PBD serves as a crosslinker just like the vegetable oil triglycerides.

The copolymerization of vegetable oils and their derivatives can also be extended to other types of polymerization processes. This will require synthetic modifications of agricultural oils in order to furnish them with appropriate functionalities compatible with a chosen polymerization process. For instance, the ring-opening metathesis polymerization (ROMP) of synthetically modified agricultural oils represents another very promising approach for the preparation of industrially-promising bioplastics. Earlier work on ROMP has provided a range of useful polymers, including polynorbornadienes (PNBD), polycyclooctenes, polyacetylenes,[14,15] and their derivatives.[16] Furthermore, ROMP has been successfully applied to the industrial scale production of inexpensive and highly unsaturated polymers, such as Norsorex and Vestenamer.[17] Thus, ROMP is a practical approach to industrially-useful polymers.

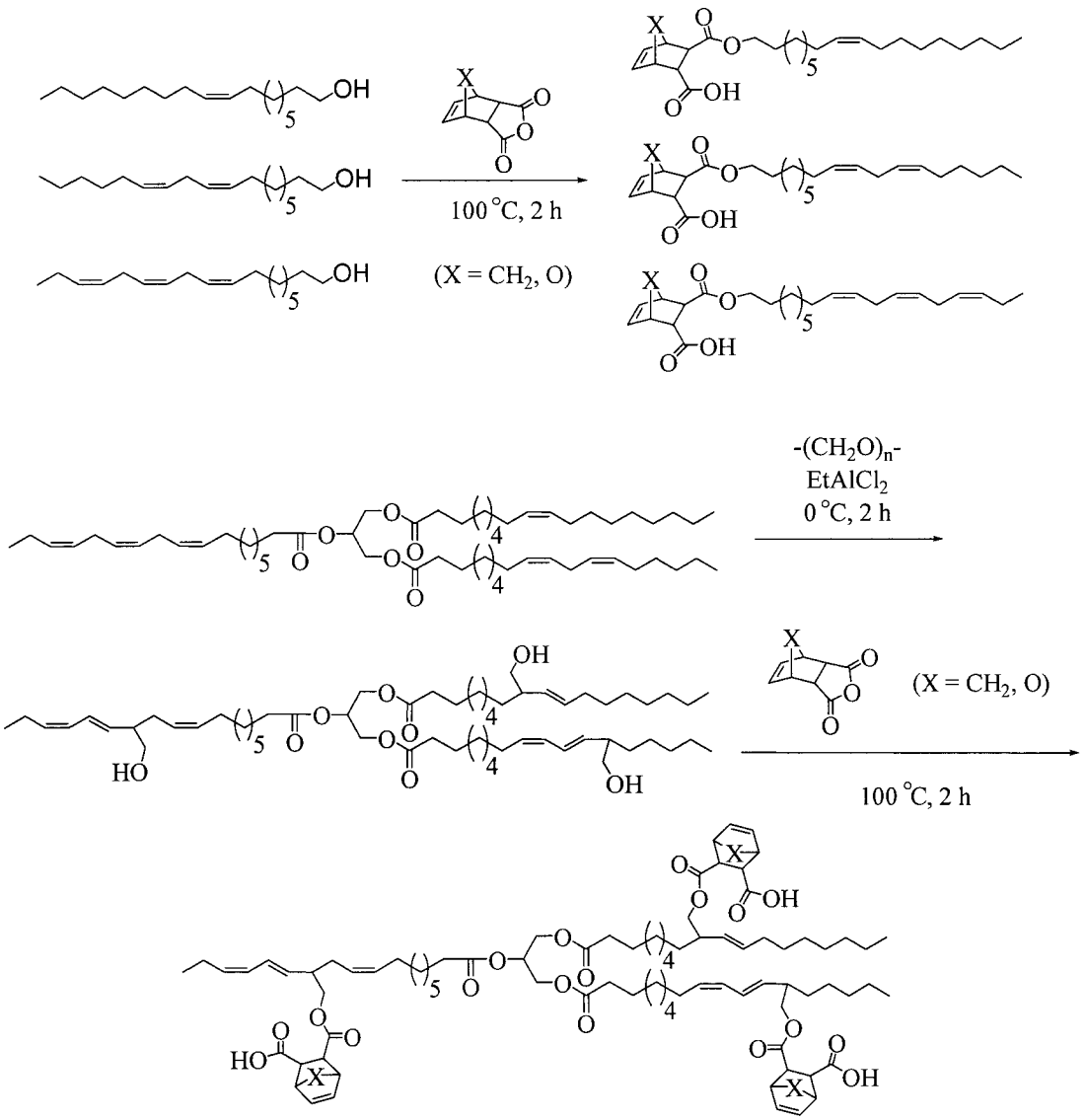

Scheme 6. Synthesis of vegetable oil-based ROMP monomers.

A range of commercially-promising vegetable oil precursors can easily be prepared by simple esterification of fatty alcohols,[18,19] diglycerides,[20-23] or hydroxymethylated oils[24] by commercially available and inexpensive carboxylic acid anhydrides, such as bicyclo[2.2.1]hept-5-ene-2,3-dicarboxylic anhydride or the corresponding 7-oxa analogue (**Scheme 6**). Furthermore, Diels-Alder adducts of vegetable oils and cyclopentadiene are also well known in industry (**Scheme 7**)[25] and are commercially available through Archer

Daniels Midland Co., which produces linseed oil-DCPD prepolymers (ML-189) for a range of commercial applications. These modified oils contain bicyclic rings, which should be readily crosslinked by either homopolymerization or copolymerization with a wide range of inexpensive and commercially available alkenes at room temperature in a matter of minutes using only catalytic amounts of a variety of ROMP catalysts.

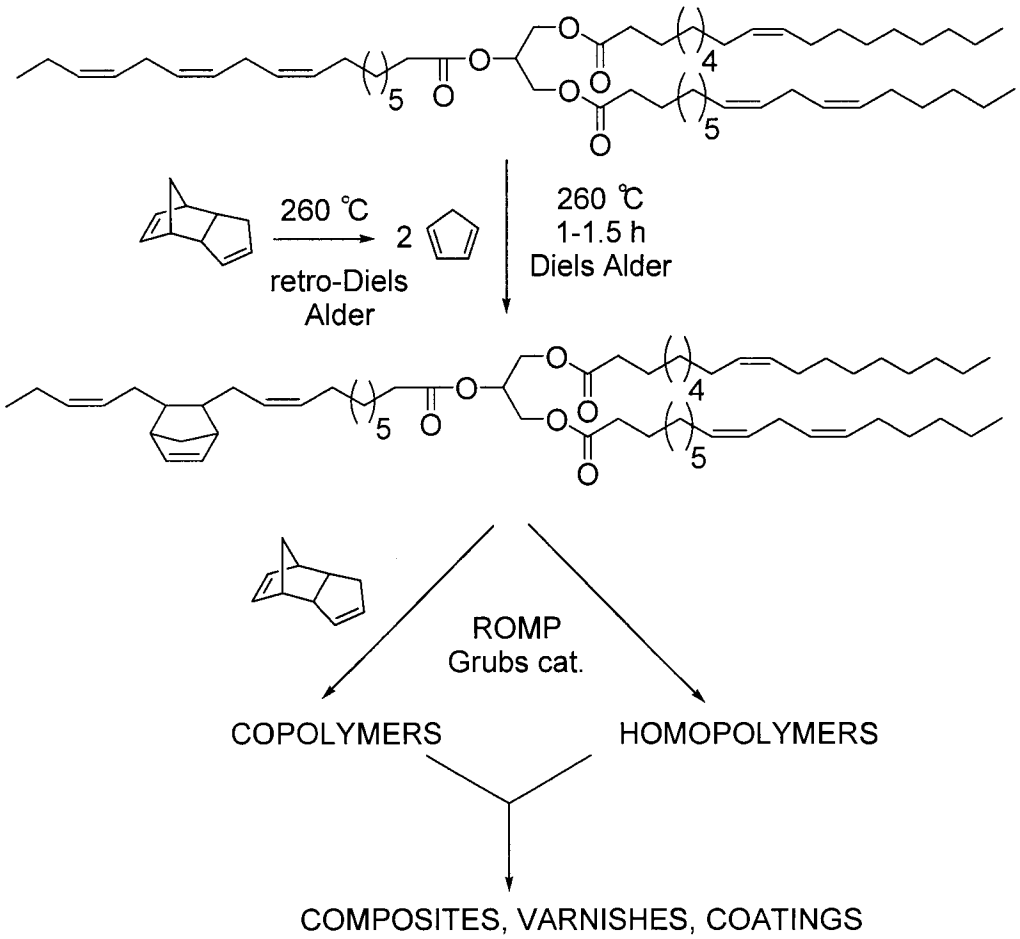

Scheme 7. Synthesis of vegetable oil-DCP adducts for ROMP polymerization.

Furthermore, this ROMP approach can also be used for the development of practical waterborne agricultural oil-based coatings through the utilization of emulsion or suspension polymerization techniques. This research should develop new and improved applications for

agricultural oils as paints and coatings, and increase the value of these crops as raw materials for the manufacture of various coatings. The resulting coatings should be inexpensive, practical, bio-based, waterborne, and VOC-free, with excellent thermal and mechanical properties, providing major advantages over present petroleum-based materials.

References

1. Havelka, P. A.; Kazukiyo N.; Freeman, B. D.; Sheares, V. V. *Macromolecules* **1999**, *32*, 6418-6424.
2. Havelka, P. A.; Kazukiyo, N.; Freeman, B. D.; Sheares, V. V. *PMSE Preprints* **1999**, *81*, 533-534.
3. Sheares, V. V. (Iowa State University Research Foundation, Inc.). U.S. Patent 6,515,101, February 4, 2003.
4. Ma, L.; Pyo, S.; Ouyang, J.; Xu, Q.; Yang, Y. *Appl. Phys. Lett.* **2003**, *82*, 1419-1421.
5. Ma, L.; Liu, J.; Pyo, S.; Xu, Q.; Yang, Y. *Mol. Cryst. Liq. Cryst. Sci. Technol., Sect. A* **2002**, *378*, 185-189.
6. Beinhoff, M.; Bozano, L. D.; Scott, J. C.; Carter, K. R. *Macromolecules* **2005**, *38*, 4147-4156.
7. Percec, V.; Bae, J.-Y.; Zhao, M.; Hill, D. H. *Macromolecules* **1995**, *28*, 6726-6734.
8. Percec, V.; Bae, J.-Y.; Zhao, M.; Hill, D. *J. Org. Chem.* **1995**, *60*, 176-185.
9. Qiu, S.; Lu, P.; Liu, X.; Shen, F.; Liu, L.; Ma. Y.; Shen. J. *Macromolecules* **2003**, *36*, 9823-9829.
10. Li, F.; Larock, R. C. *Polym. Int.* **2003**, *52*, 126-132.
11. Gillham, J. K. *Proc. N. Amer. Thermal Anal. Soc. Ann. Conf. (NATAS 2005),* September, 2005.

12. Li, F.; Larock, R. C. *J. Appl. Polym. Sci.* **2001**, *80*, 658-670.

13. Andjelkovic, D. D.; Larock, R. C. *Biomacromolecules* **2005**, *93*, 927-936.

14. Grubbs, R. H.; Woodson Jr., C. S. (California Institute of Technology). U. S. Patent 5,728,785, 1998.

15. Woodson, C. S.; Grubbs, R. H. (California Institute of Technology). U. S. Patent 6,020,443, 2000.

16. Grubbs, R. H.; Scherman, O. A.; Kim, H. M. (California Institute of Technology). U. S. Patent 6,884,859, 2005.

17. Breslow, D. S. *Prog. Polym. Sci.* **1993**, *18*, 1141-1175.

18. Westfechtel, A.; Huebner, N.; Friesenhagen, L.; Pelzer, G.; Klein, N.; Behler, A.; Downing, T. B.; Kennedy, S. A.; Blewett, C. W. (Cognis Deutschland GmbH & Co. KG). U. S. Patent 6,548,717, 2003.

19. Demmering, G.; Friesenhagen, L.; Heck, S.; Kubersky, H. (Henkel Kommanditgesellschaft auf Aktien). U. S. Patent 6,683,225, 2004.

20. Jacobs, L.; Lee, I.; Poppe, G. PCT Int. Appl. 2003029392, 2003.

21. Lee, I.; Poppe, G. PCT Int. Appl. 2003014271, 2003.

22. Wool, R. P.; Küsefoglu, S.; Palmese, G.; Khot, S.; Zhao, R. (University of Delaware). U. S. Patent 6,121,398, 2000.

23. Can, E.; Küsefoglu, S.; Wool, R. P. *J. Appl. Polym. Sci.* **2001**, *81*, 69-77.

24. Eren, T.; Küsefoglu, S. H. *J. Appl. Polym. Sci.* **2004**, *91*, 4037-4046.

25. Kodali, D. R. (Cargill Inc.). U. S. Patent 6,420,322, 2002.

APPENDIX A. SUPPLEMENTAL DATA FOR CHAPTER 2

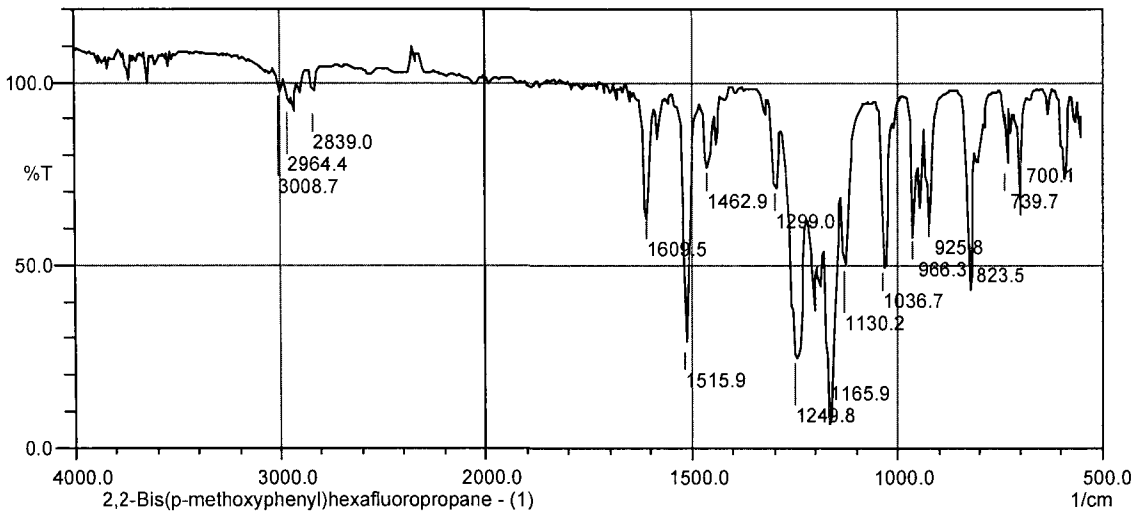

FT-IR spectrum of 2,2-Bis(*p*-methoxyphenyl)hexafluoropropane (**1**).

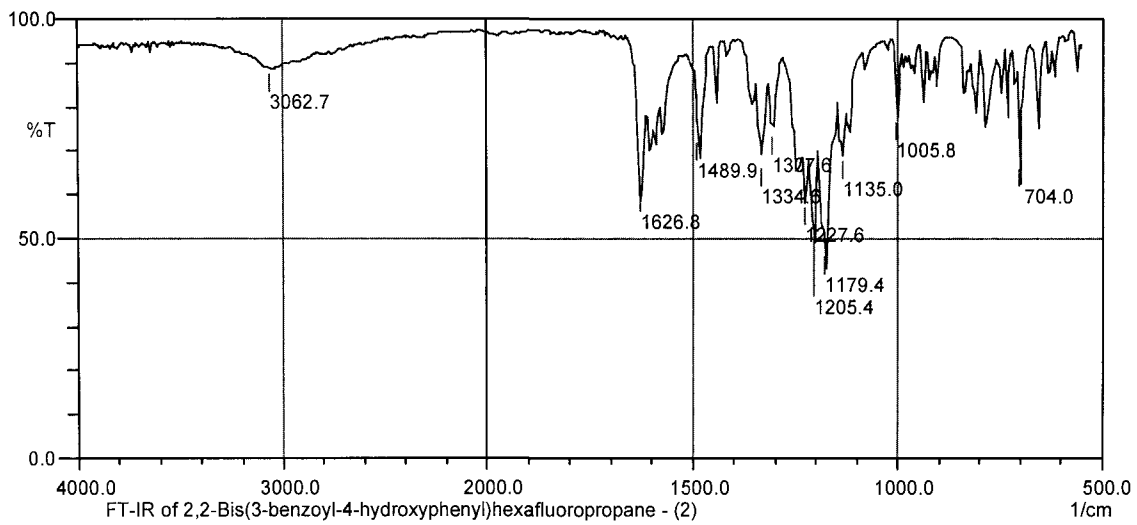

FT-IR spectrum of 2,2-Bis(3-benzoyl-4-hydroxyphenyl)hexafluoropropane (**2**).

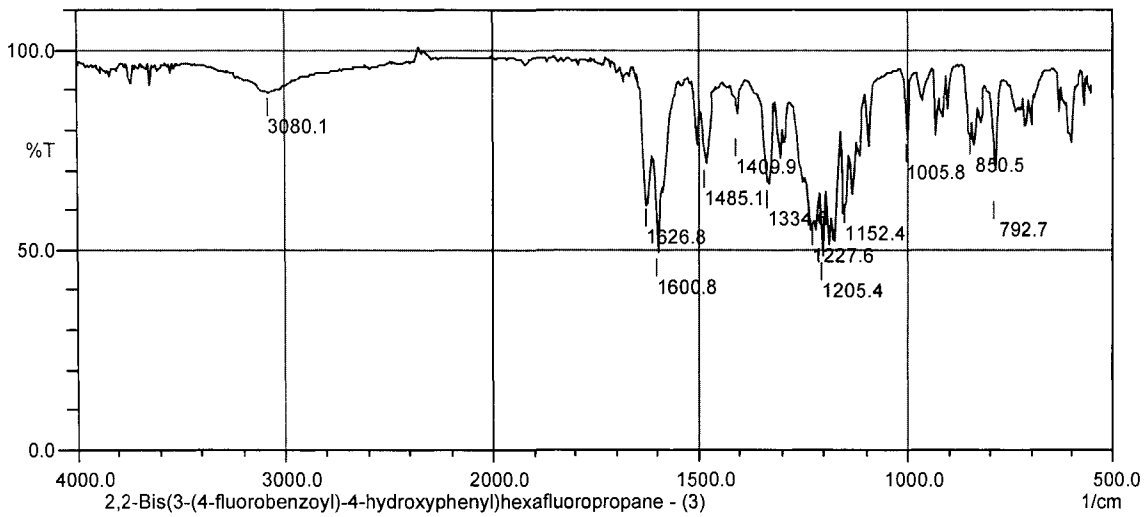

FT-IR spectrum of 2,2-Bis(3-(4-fluorobenzoyl)-4-hydroxyphenyl)hexafluoropropane (**3**).

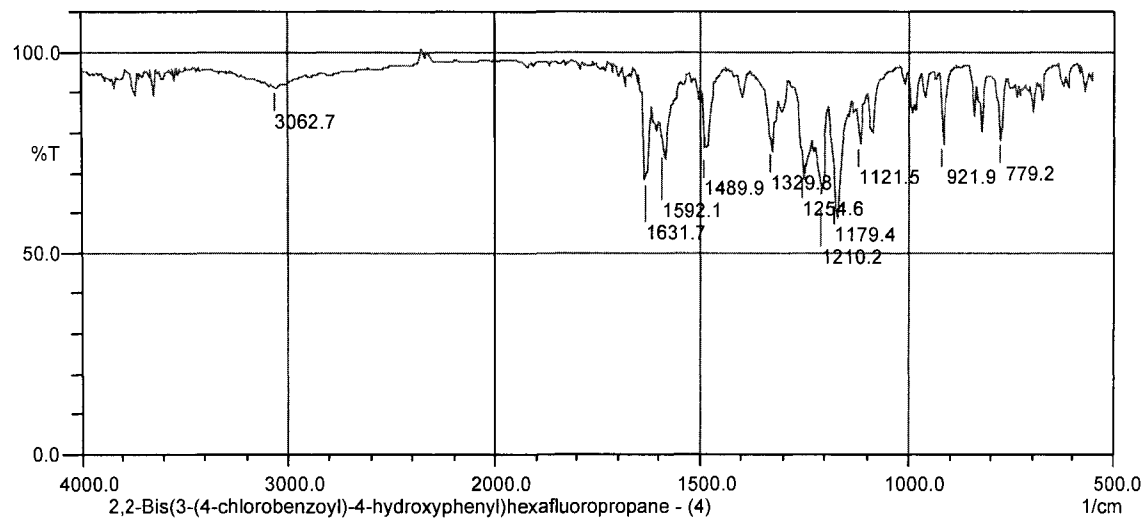

FT-IR spectrum of 2,2-Bis(3-(4-chlorobenzoyl)-4-hydroxyphenyl)hexafluoropropane (**4**).

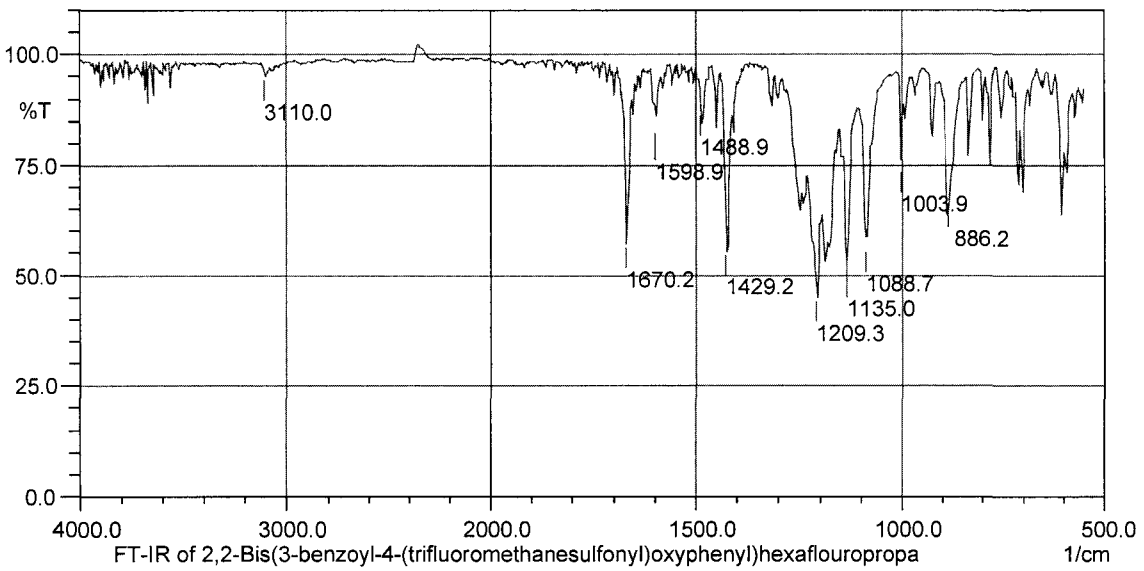

FT-IR spectrum of 2,2-Bis(3-benzoyl-4-(trifluoromethanesulfonyl)oxyphenyl) hexafluoropropane (**5**).

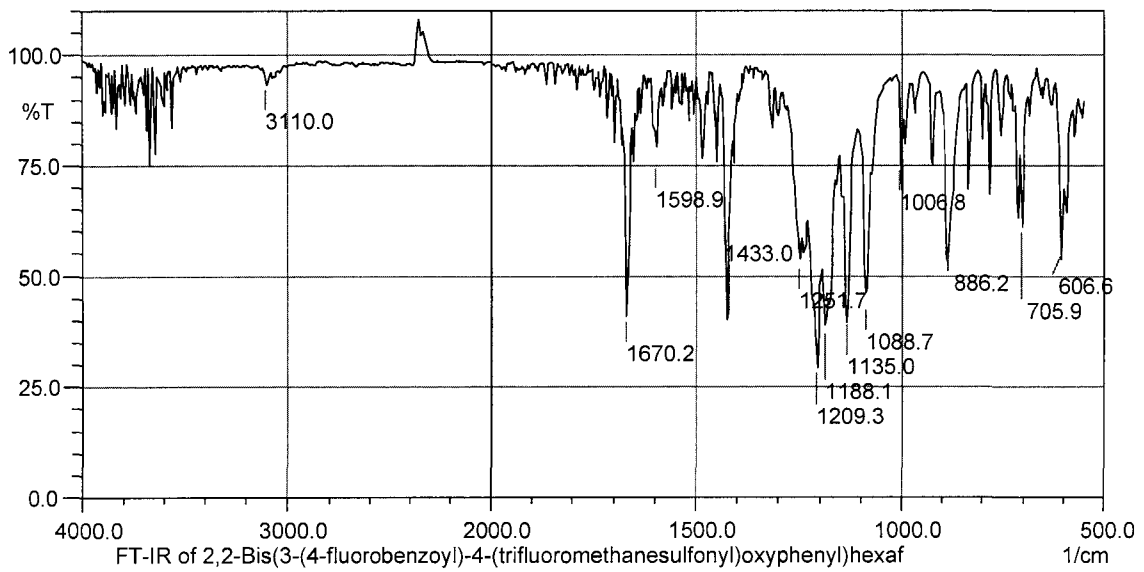

FT-IR spectrum of 2,2-Bis(3-(4-fluorobenzoyl)-4-(trifluoromethanesulfonyl)oxyphenyl) hexafluoropropane (**6**).

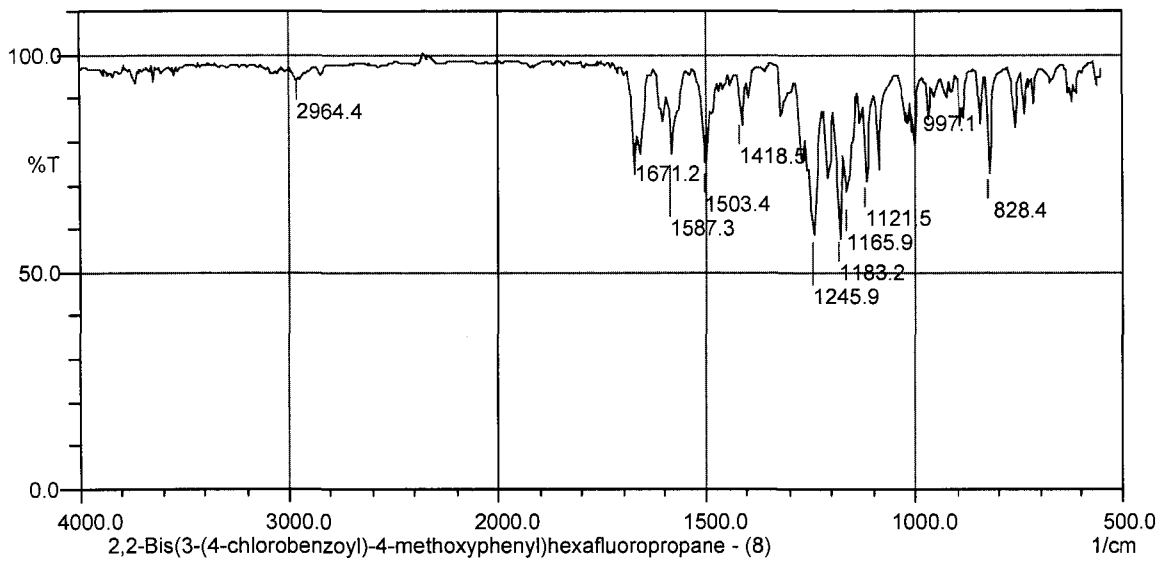

FT-IR spectrum of 2,2-Bis(3-(4-chlorobenzoyl)-4-(methoxyphenyl)hexafluoropropane (7).

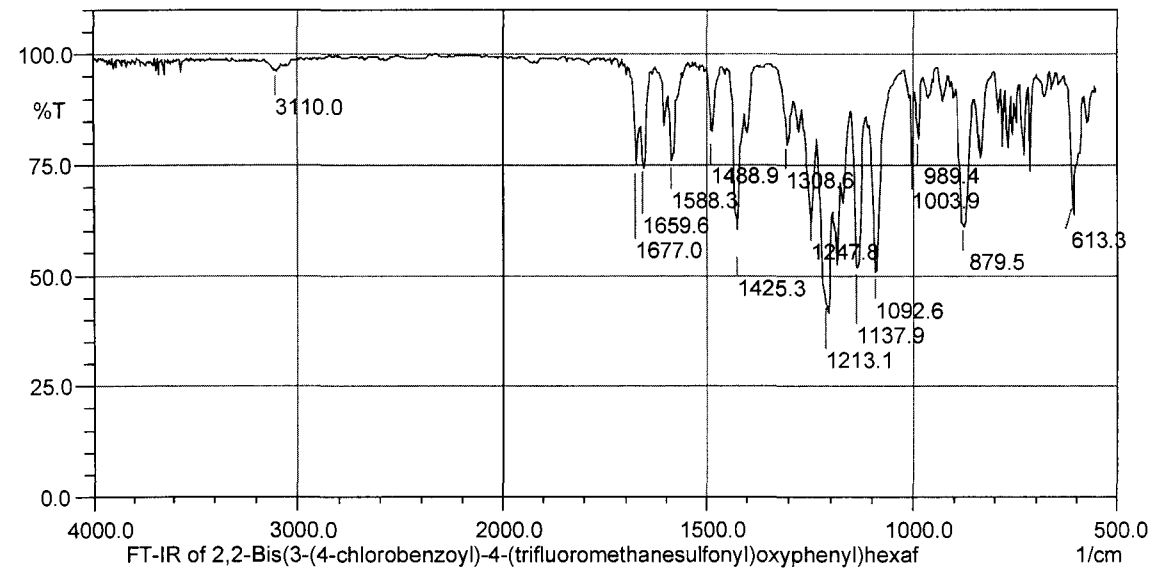

FT-IR spectrum of 2,2-Bis(3-(4-chlorobenzoyl)-4-(trifluoromethanesulfonyl)oxyphenyl) hexafluoropropane **CRS**.

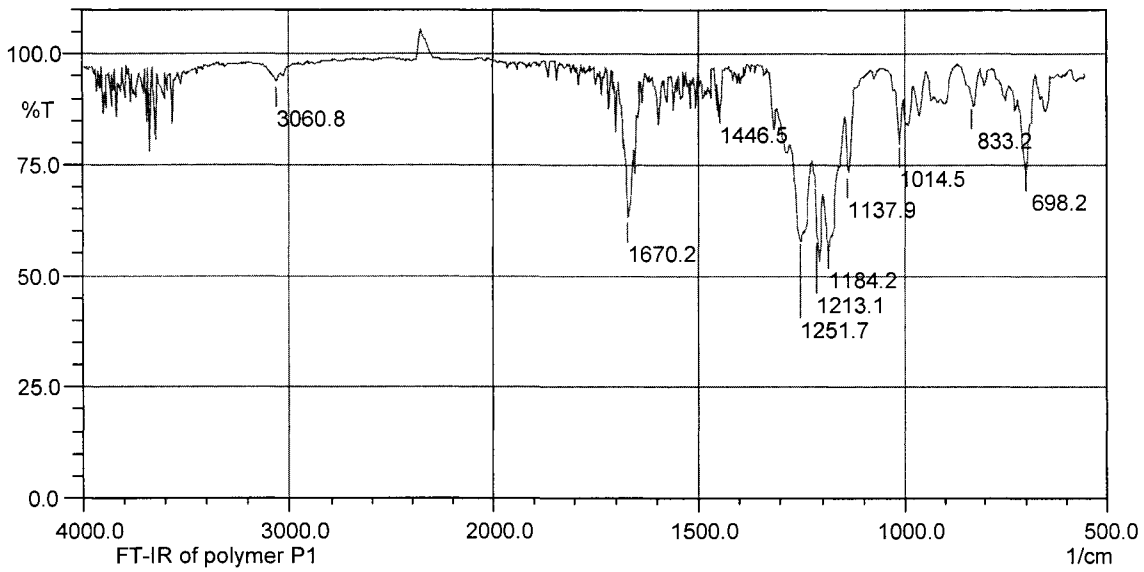

FT-IR spectrum of polymer **P1**.

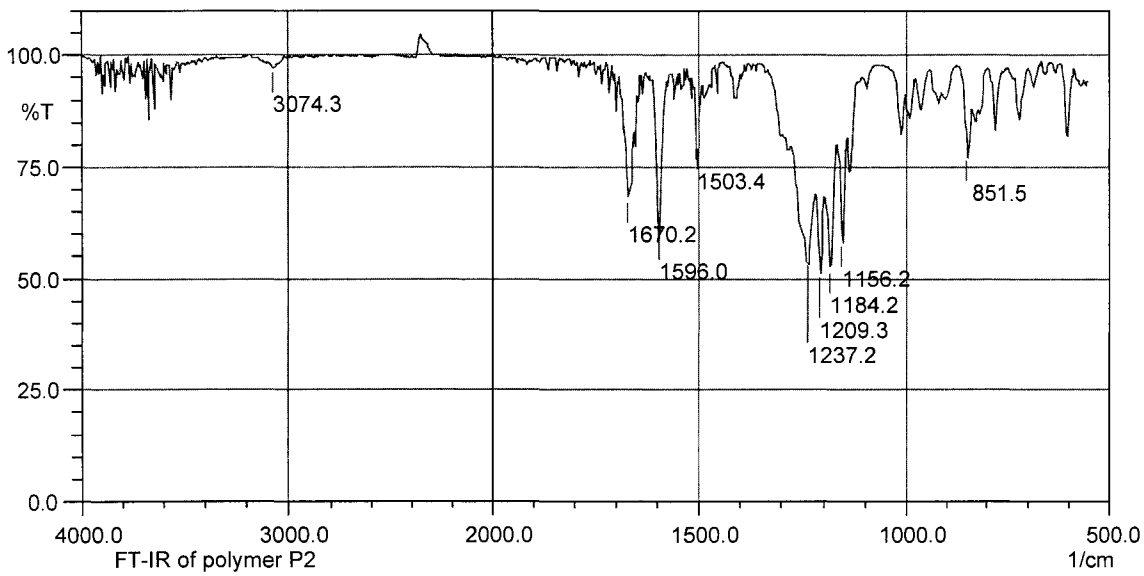

FT-IR spectrum of polymer **P2**.

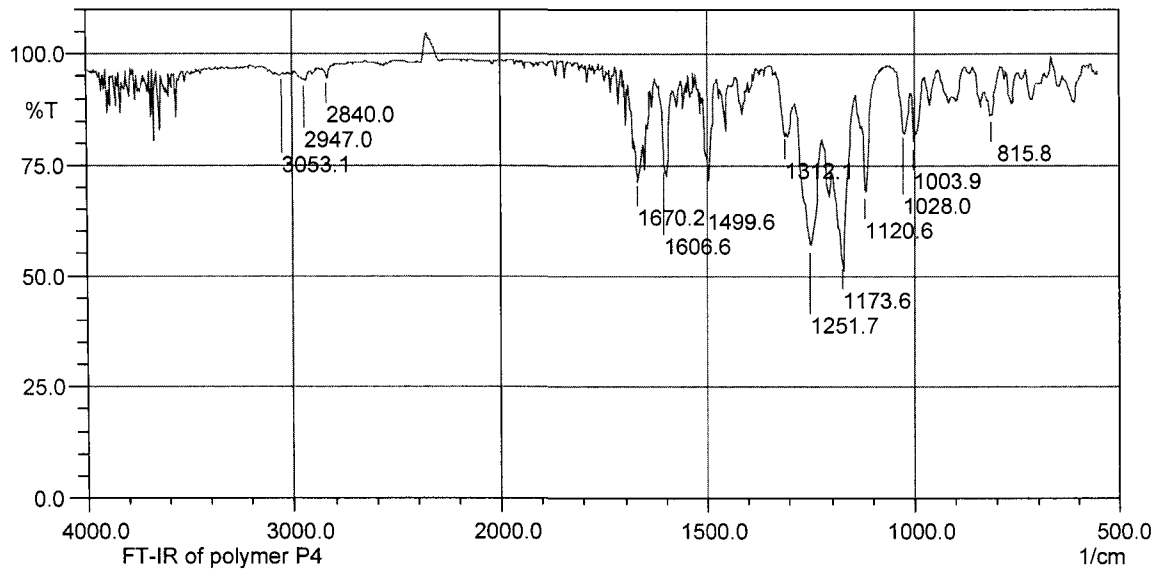

FT-IR spectrum of polymer **P3**.

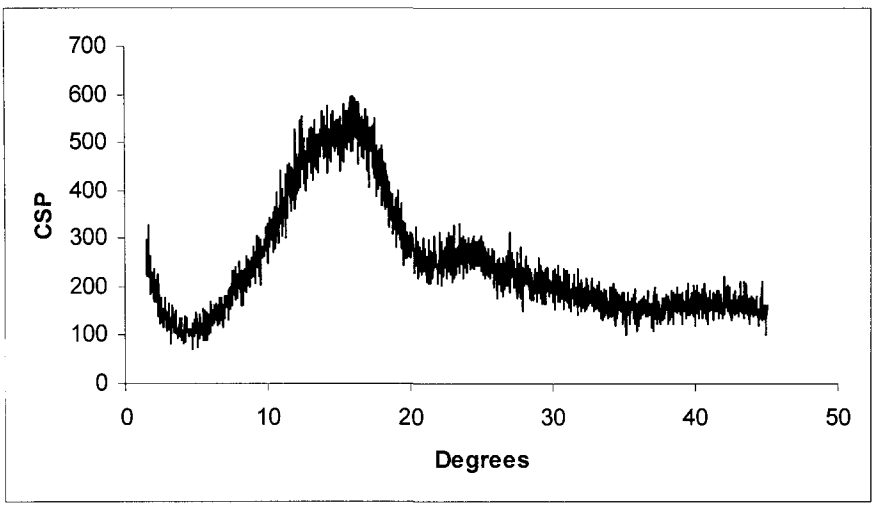

Powder X-Ray diffraction pattern of polymer **P1**.

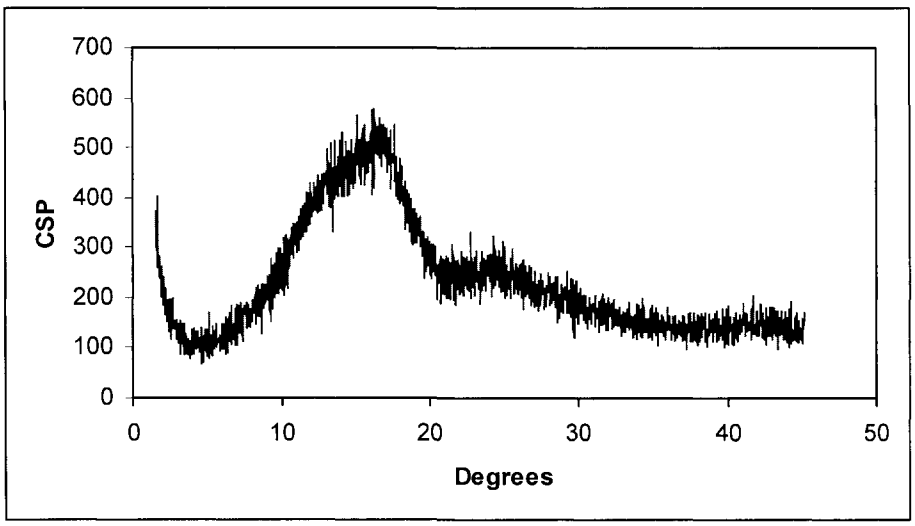

Powder X-Ray diffraction pattern of polymer **P2**.

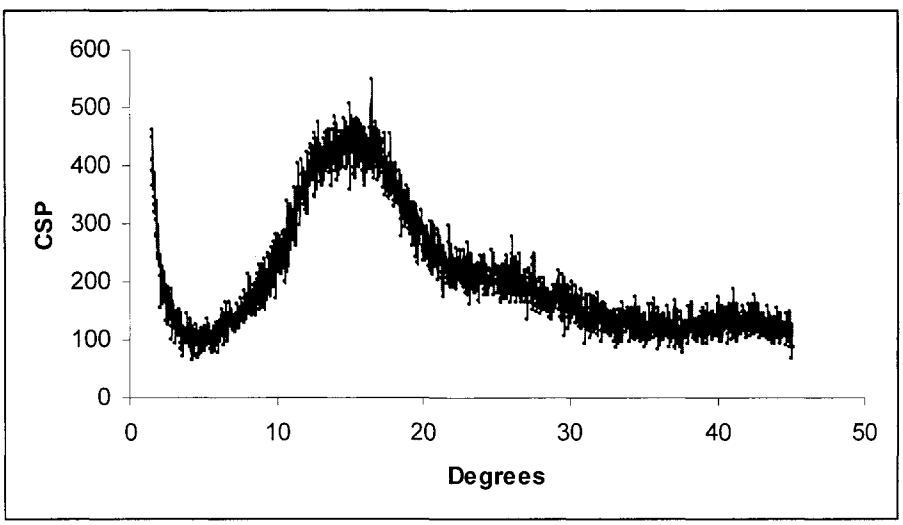

Powder X-Ray diffraction pattern of polymer **P3**.

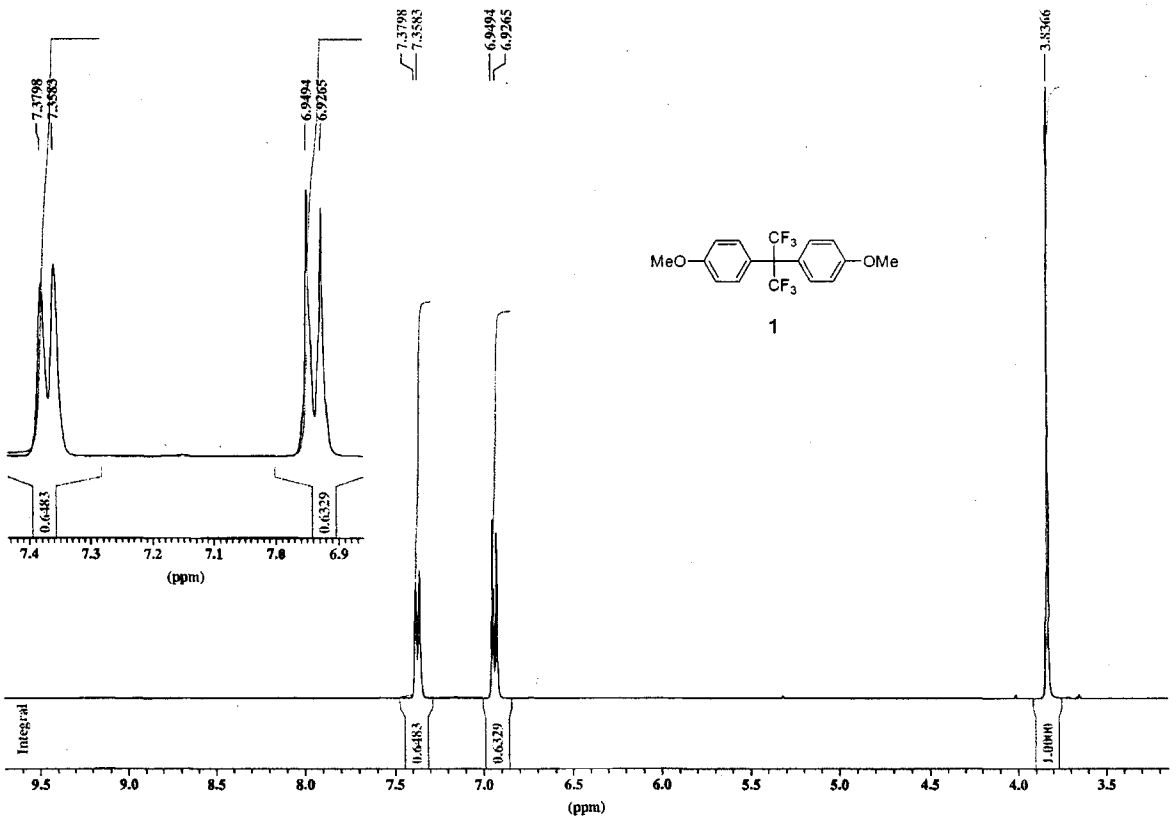

^{1}H NMR spectrum of 2,2-Bis(*p*-methoxyphenyl)hexafluoropropane (**1**).

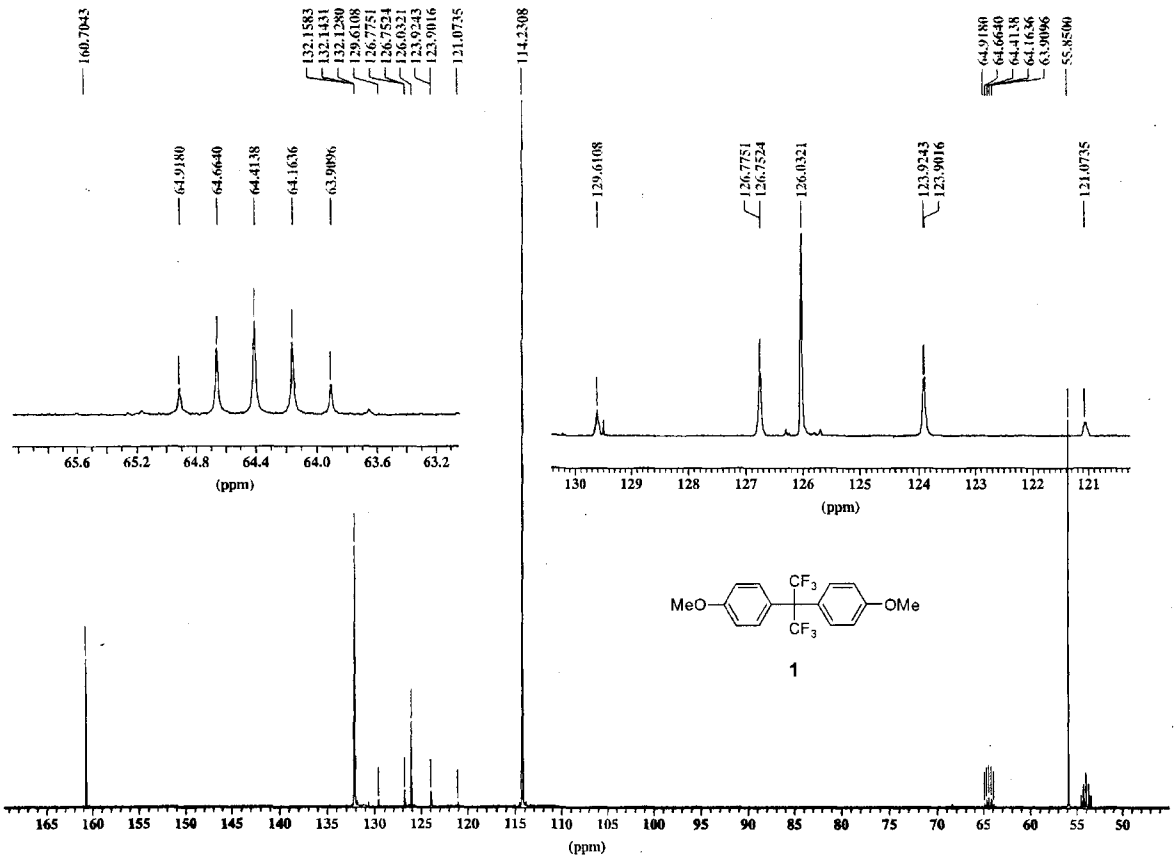

^{13}C NMR spectrum of 2,2-Bis(*p*-methoxyphenyl)hexafluoropropane (**1**).

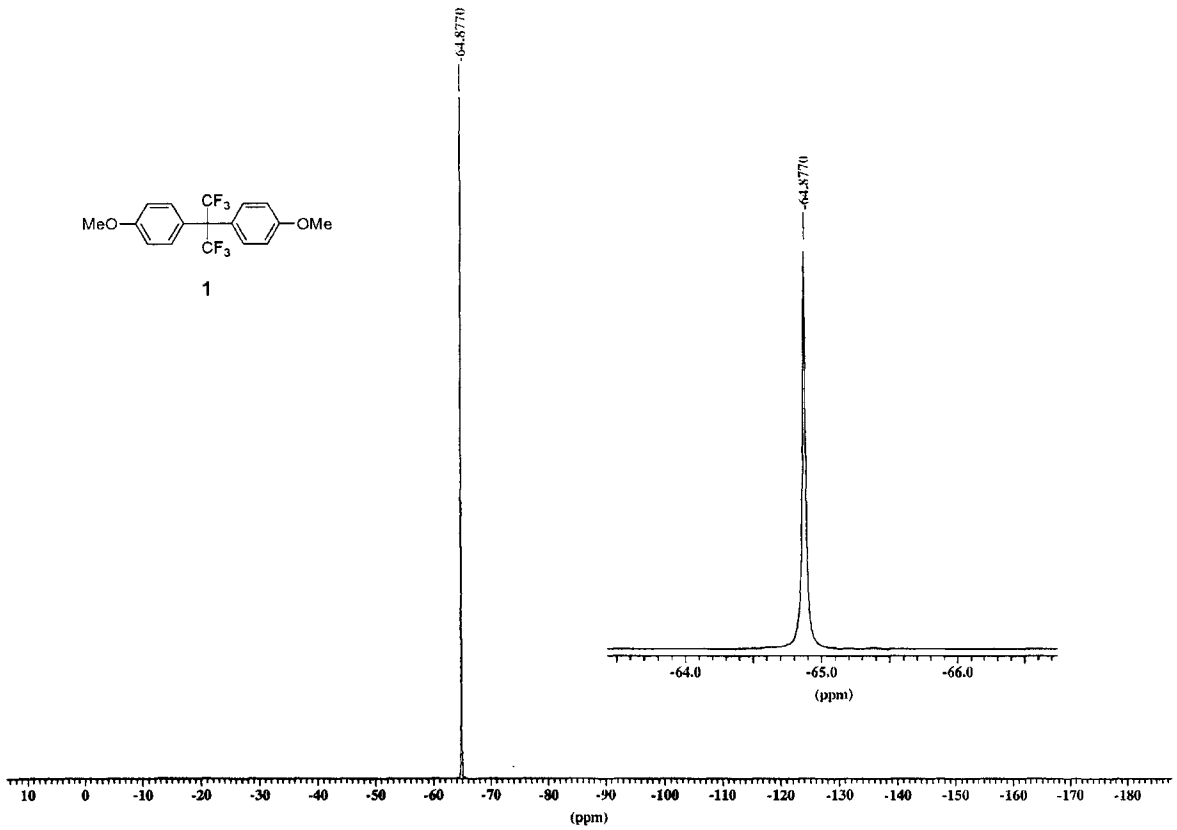

^{19}F NMR spectrum of 2,2-Bis(*p*-methoxyphenyl)hexafluoropropane (**1**).

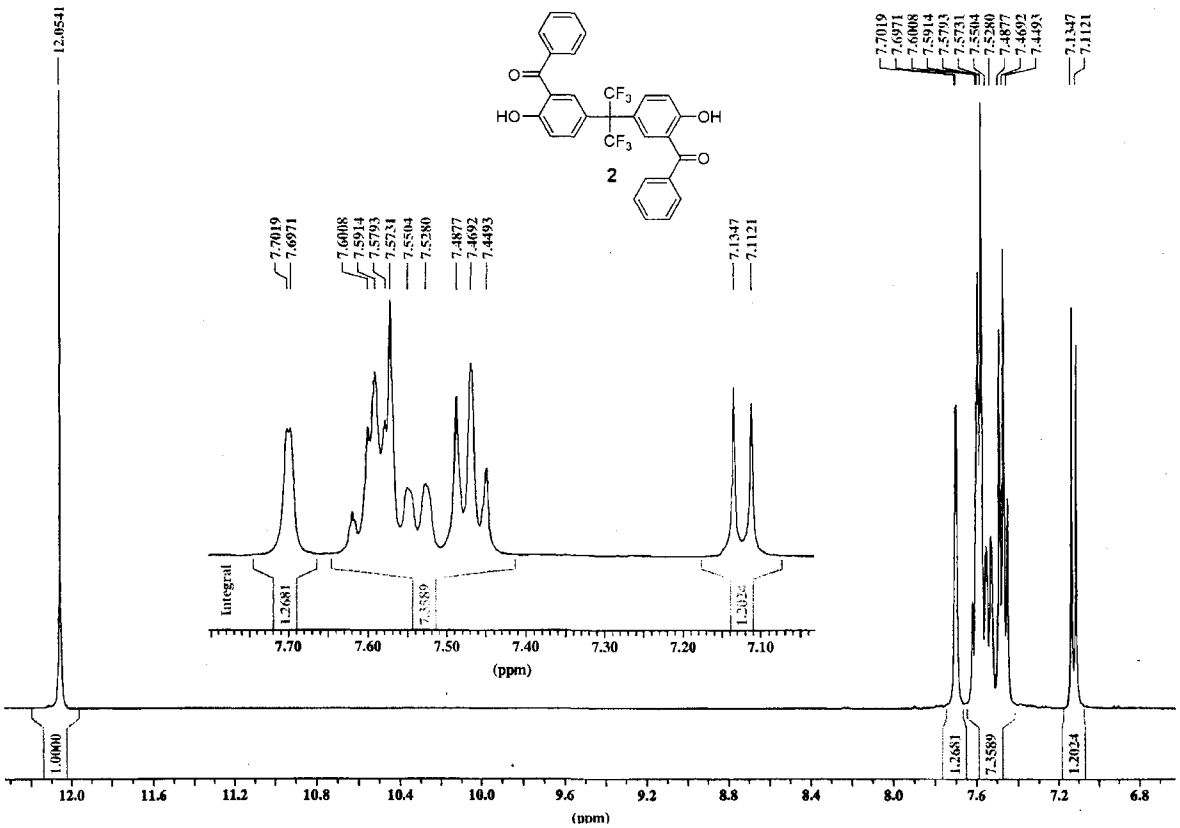

^{1}H NMR spectrum of 2,2-Bis(3-benzoyl-4-hydroxyphenyl)hexafluoropropane (**2**).

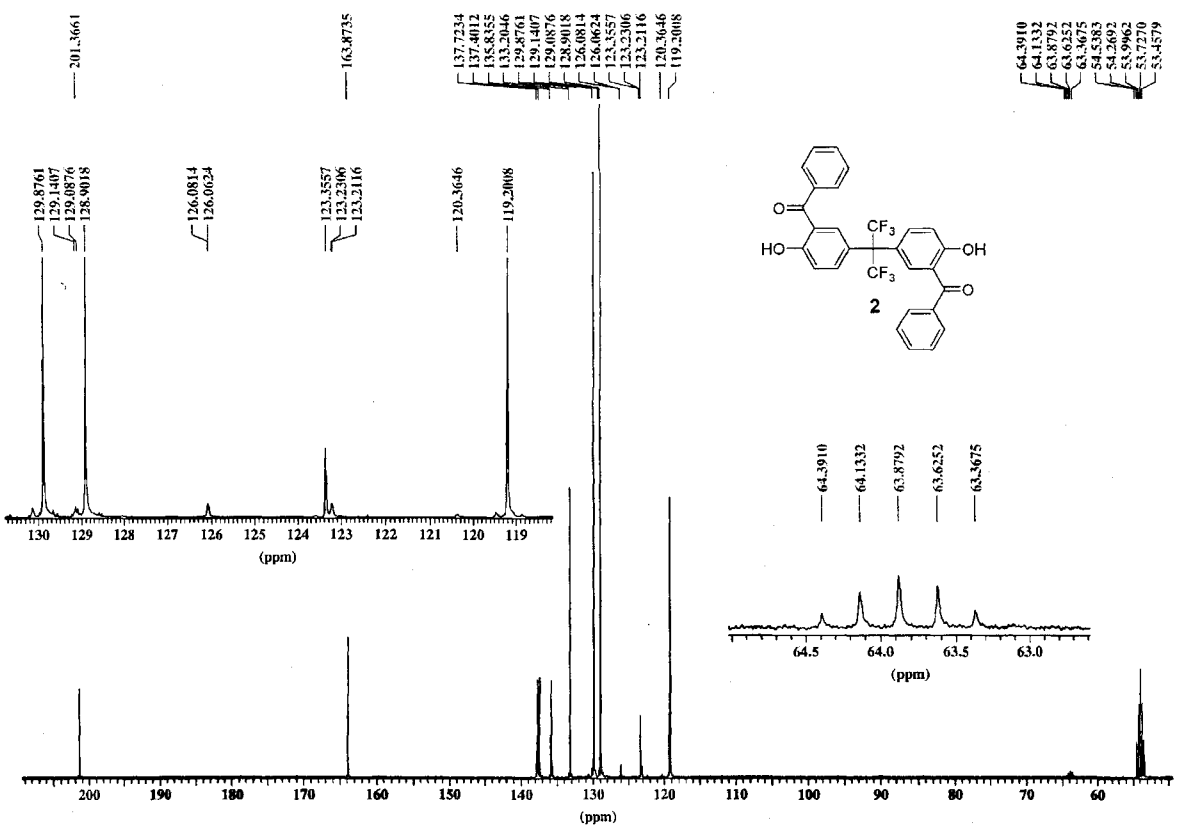

^{13}C NMR spectrum of 2,2-Bis(3-benzoyl-4-hydroxyphenyl)hexafluoropropane (**2**).

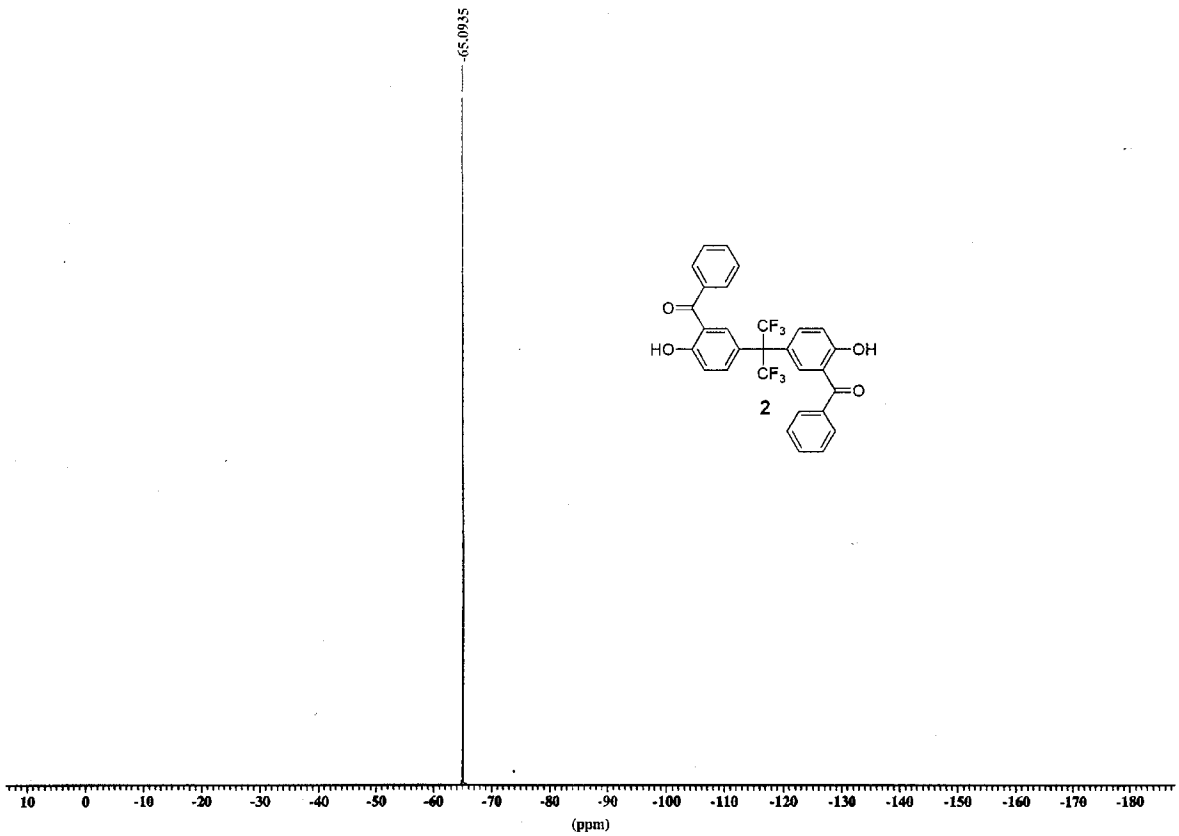

^{19}F NMR spectrum of 2,2-Bis(3-benzoyl-4-hydroxyphenyl)hexafluoropropane (**2**).

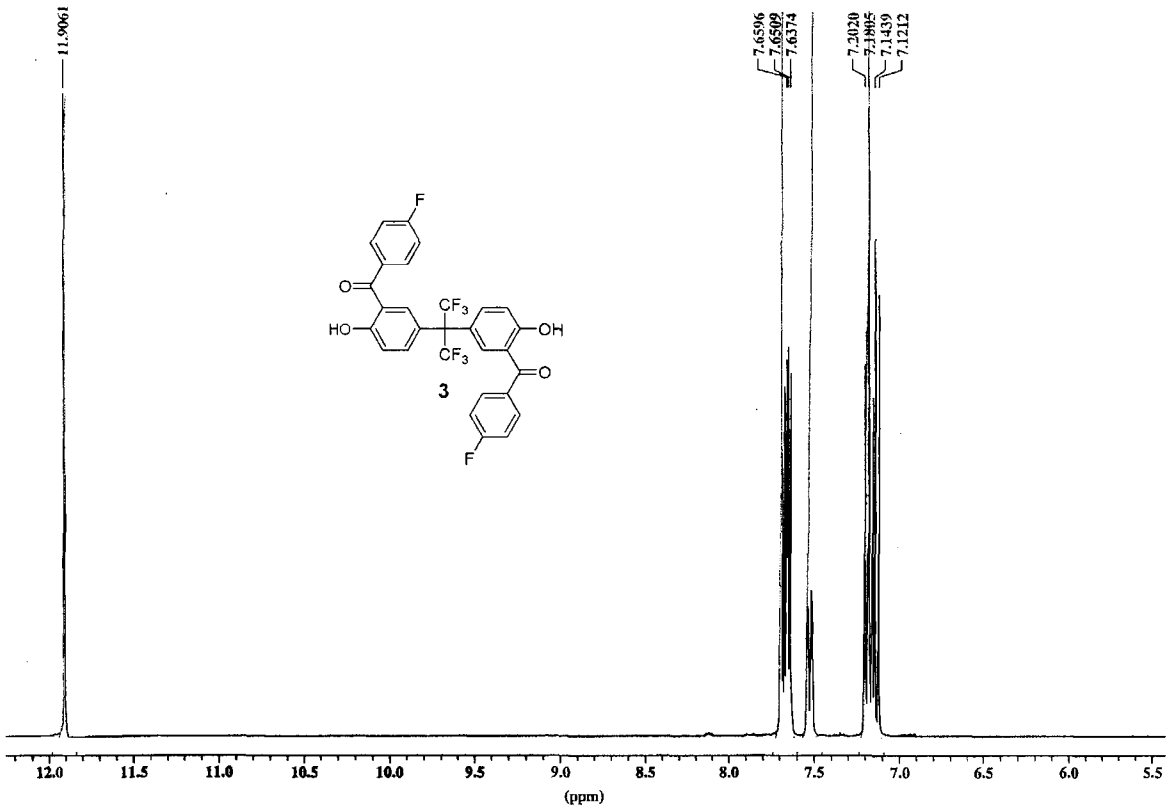

^{1}H NMR spectrum of 2,2-Bis(3-(4-fluorobenzoyl)-4-hydroxyphenyl)hexafluoropropane (**3**).

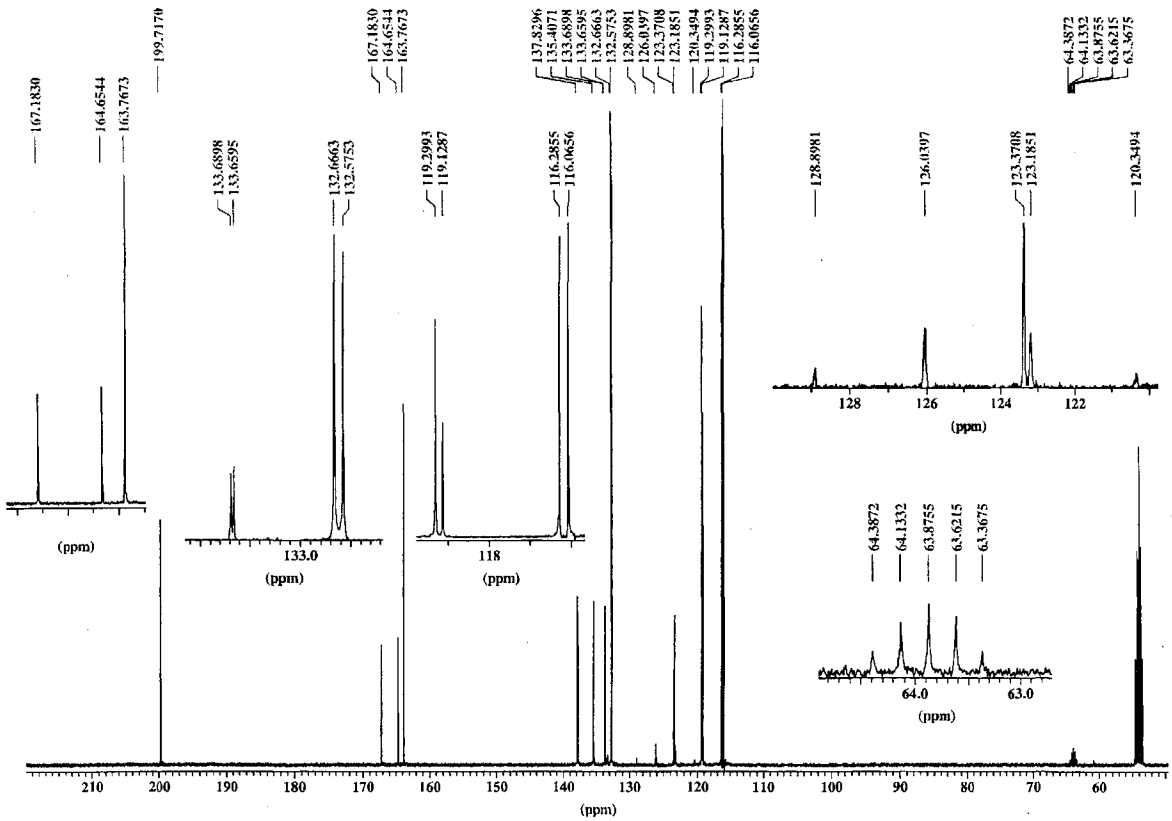

^{13}C NMR spectrum of 2,2-Bis(3-(4-fluorobenzoyl)-4-hydroxyphenyl)hexafluoropropane (**3**).

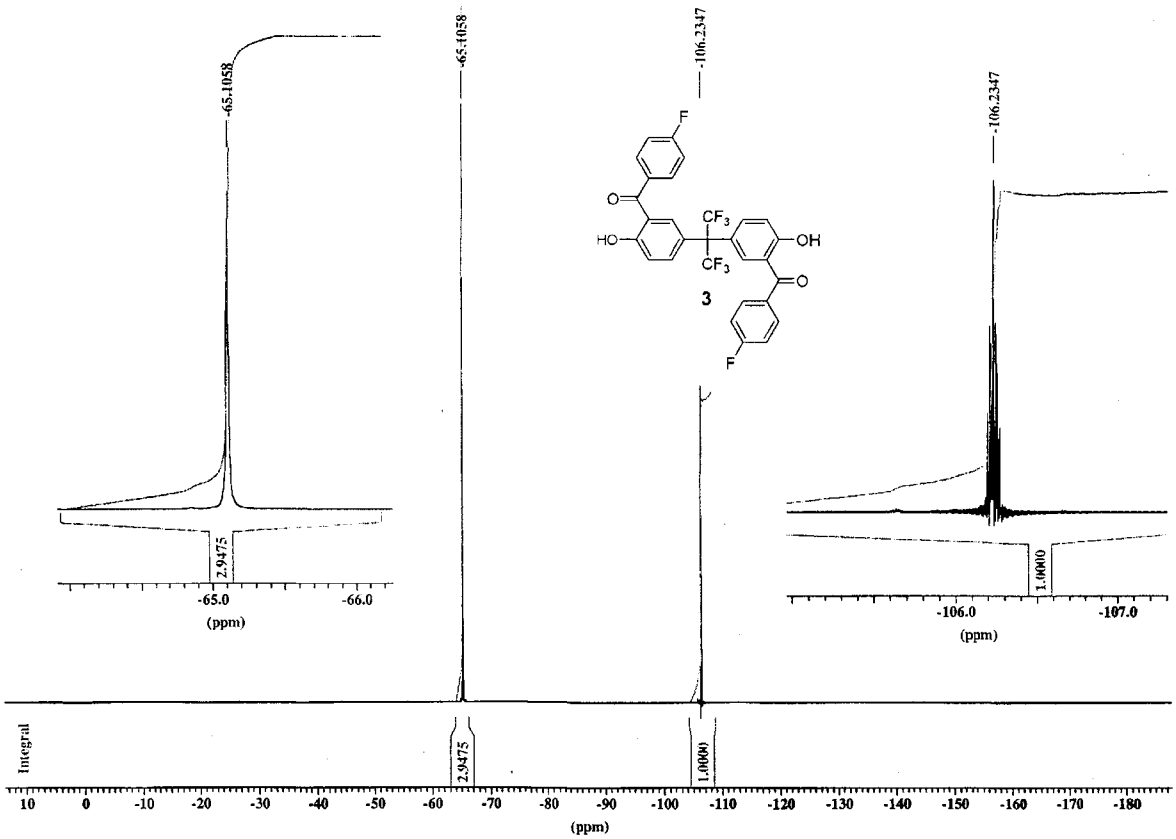

^{19}F NMR spectrum of 2,2-Bis(3-(4-fluorobenzoyl)-4-hydroxyphenyl)hexafluoropropane (**3**).

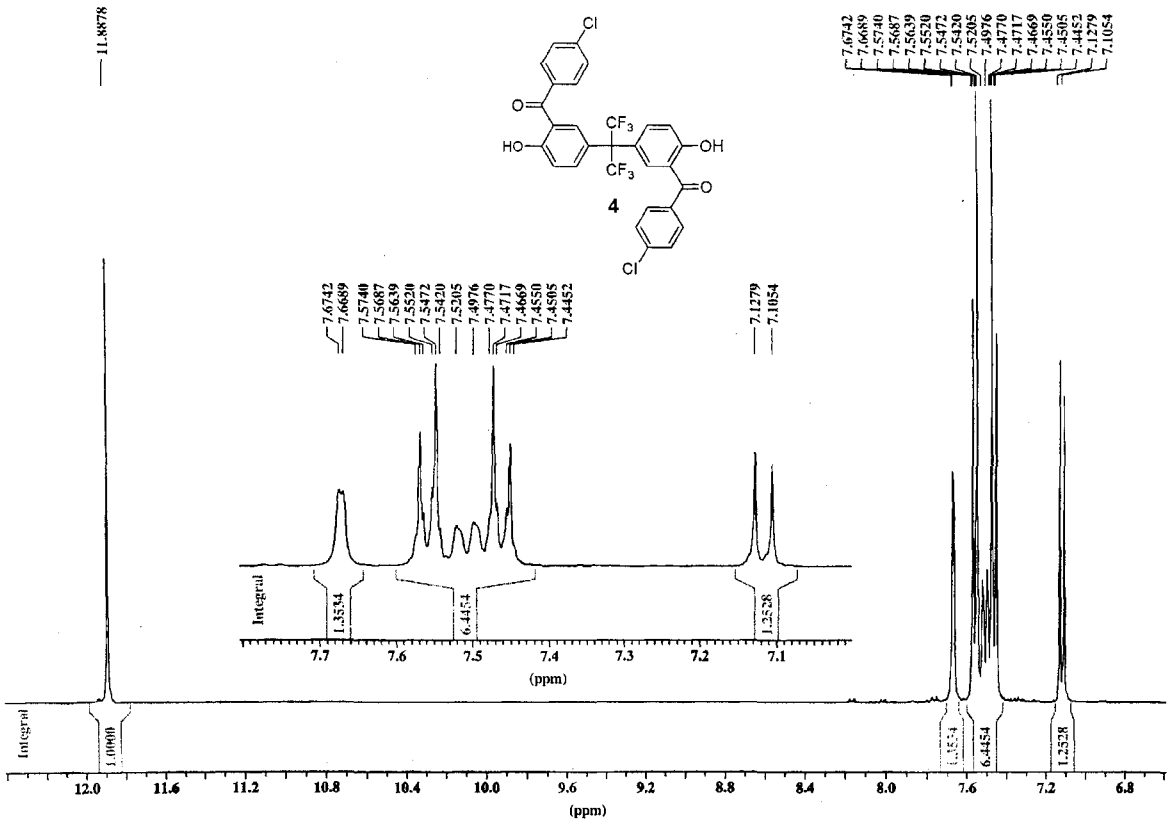

^{1}H NMR spectrum of 2,2-Bis(3-(4-chlorobenzoyl)-4-hydroxyphenyl)hexafluoropropane (**4**).

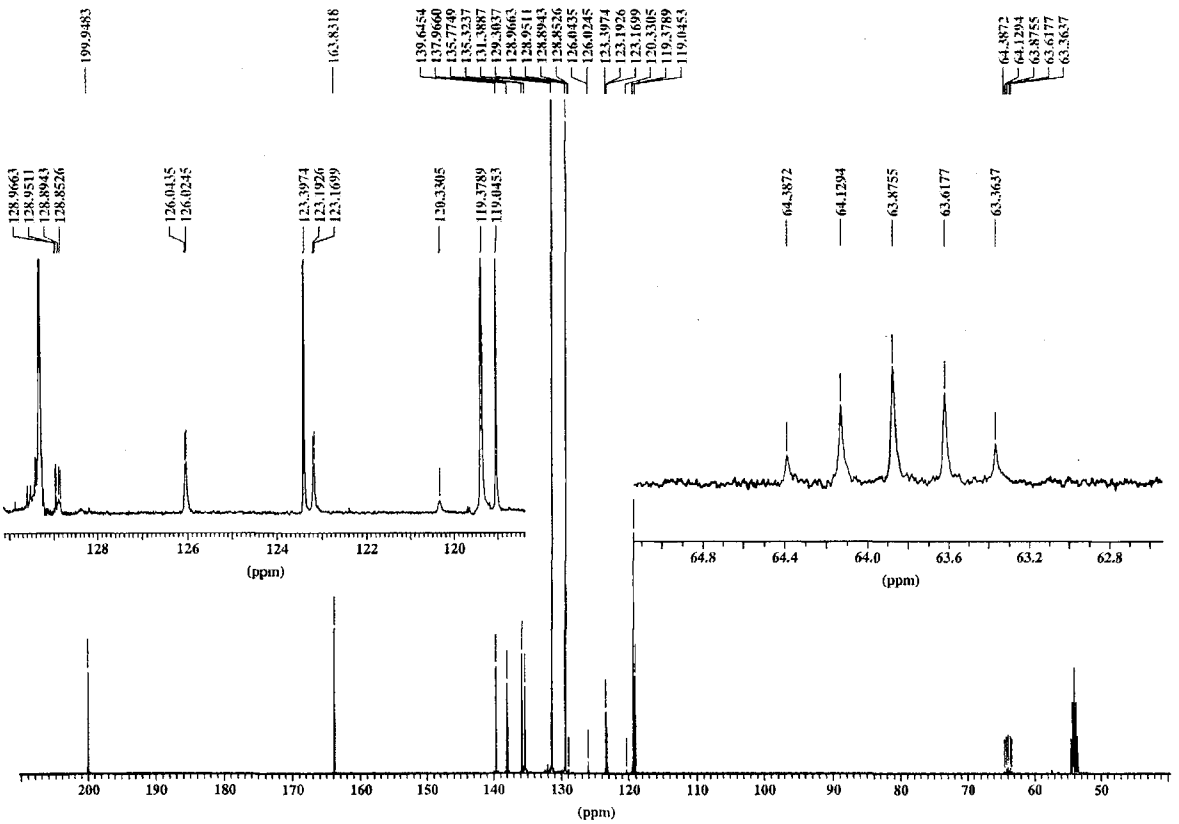

^{13}C NMR spectrum of 2,2-Bis(3-(4-chlorobenzoyl)-4-hydroxyphenyl)hexafluoropropane (**4**).

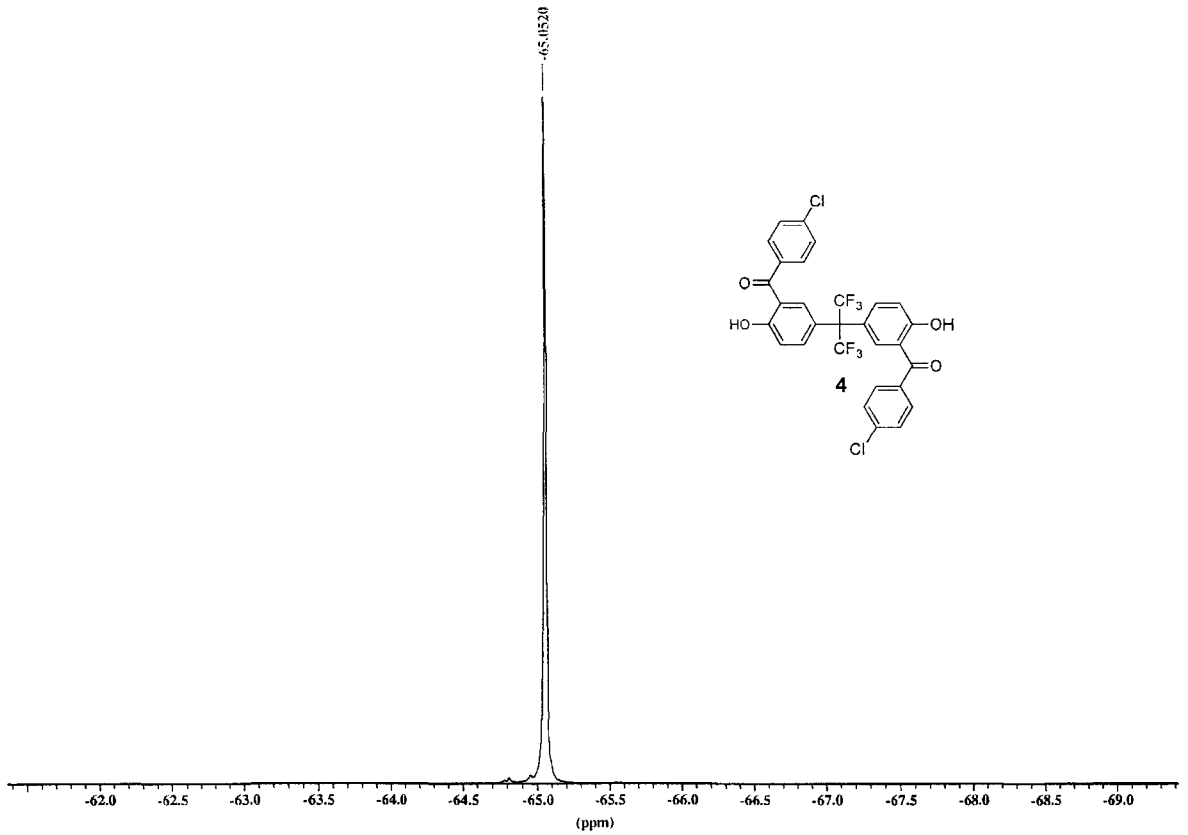

^{19}F NMR spectrum of 2,2-Bis(3-(4-chlorobenzoyl)-4-hydroxyphenyl)hexafluoropropane (**4**).

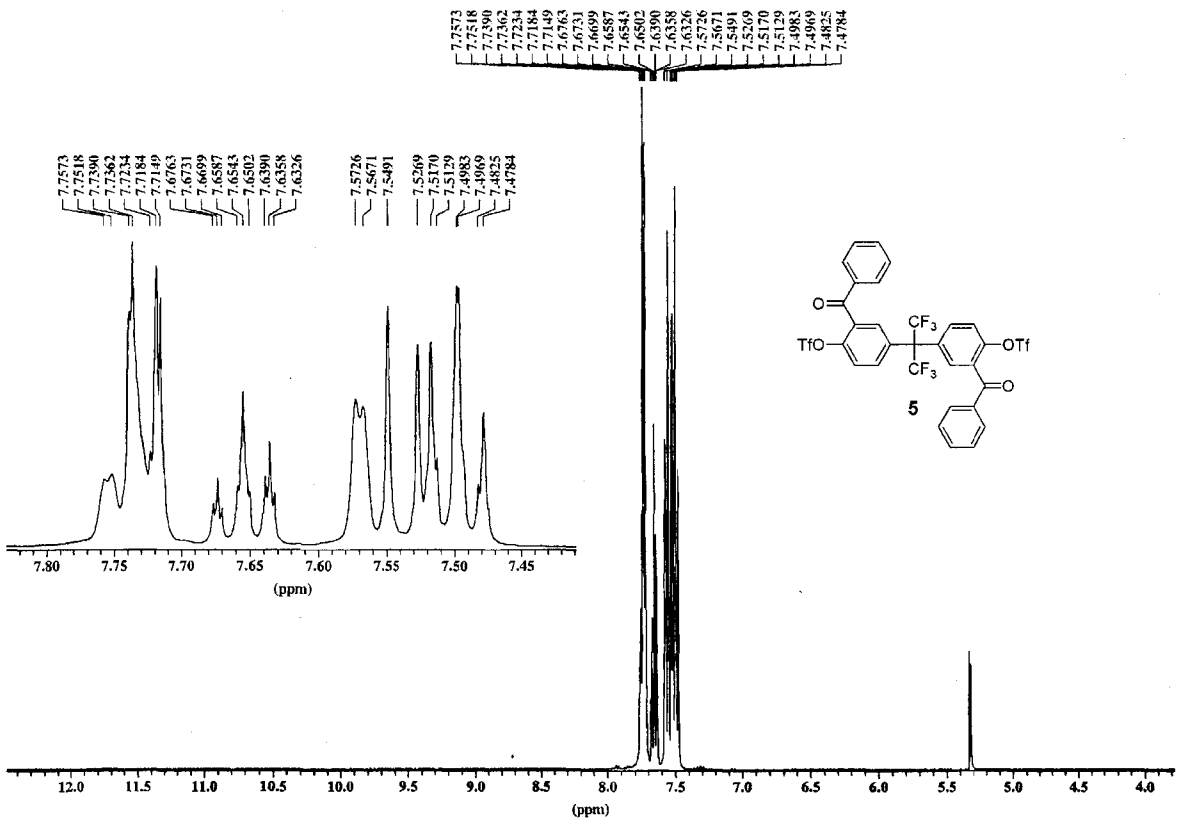

^{1}H NMR spectrum of 2,2-Bis(3-benzoyl-4-(trifluoromethanesulfonyloxy)phenyl) hexafluoropropane (**5**).

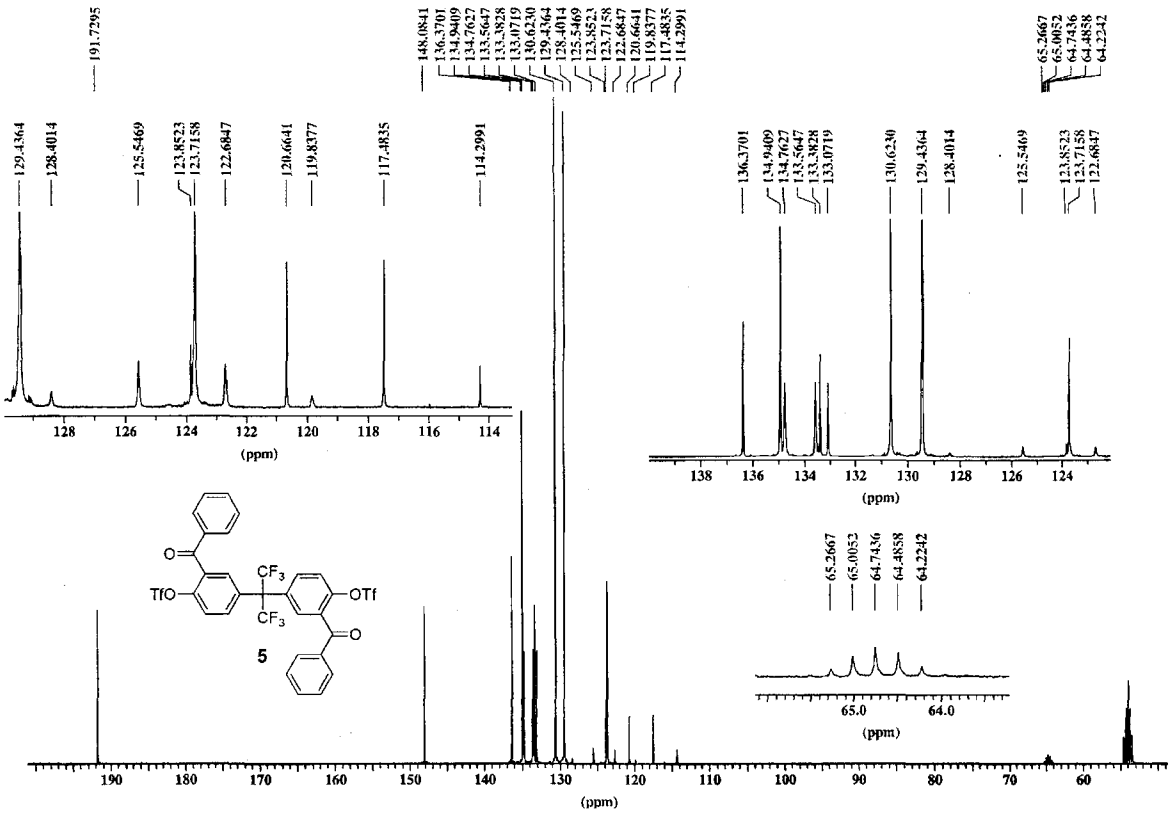

^{13}C NMR spectrum of 2,2-Bis(3-benzoyl-4-(trifluoromethanesulfonyloxy)phenyl) hexafluoropropane (**5**).

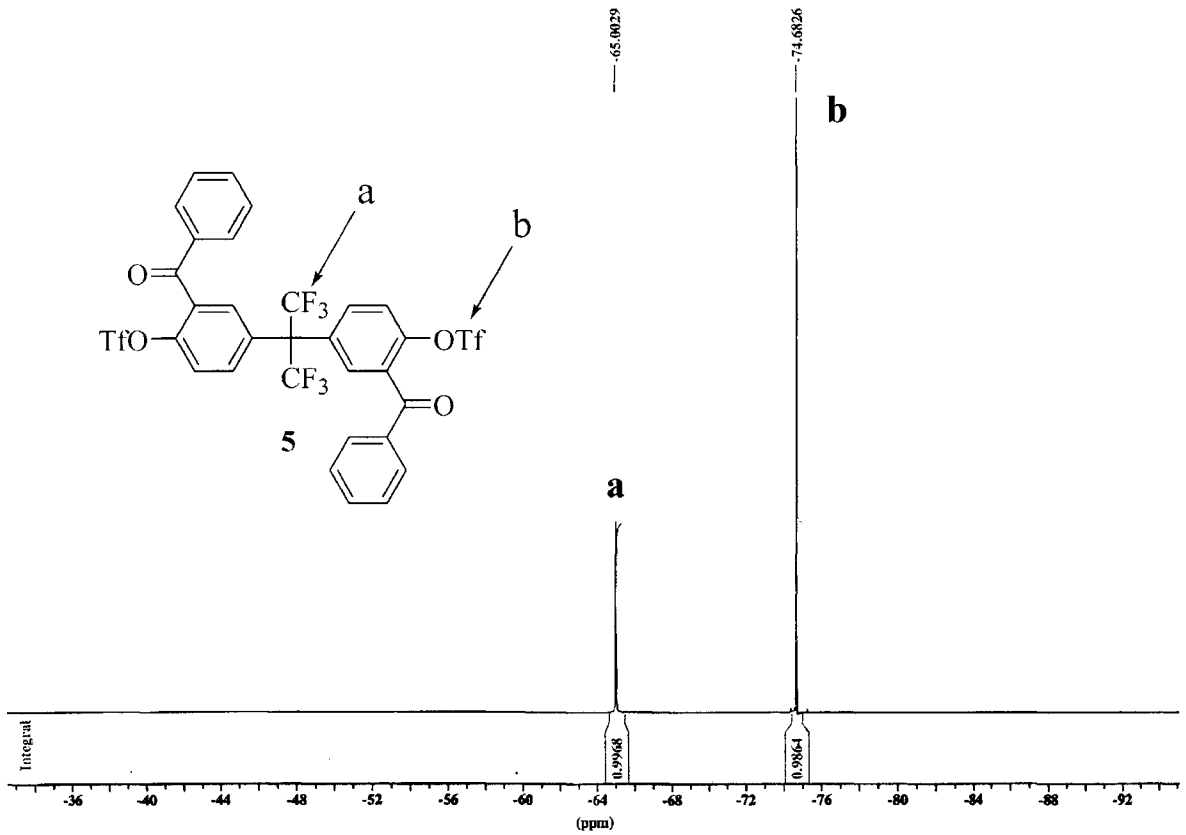

^{19}F NMR spectrum of 2,2-Bis(3-benzoyl-4-(trifluoromethanesulfonyloxy)phenyl) hexafluoropropane (**5**).

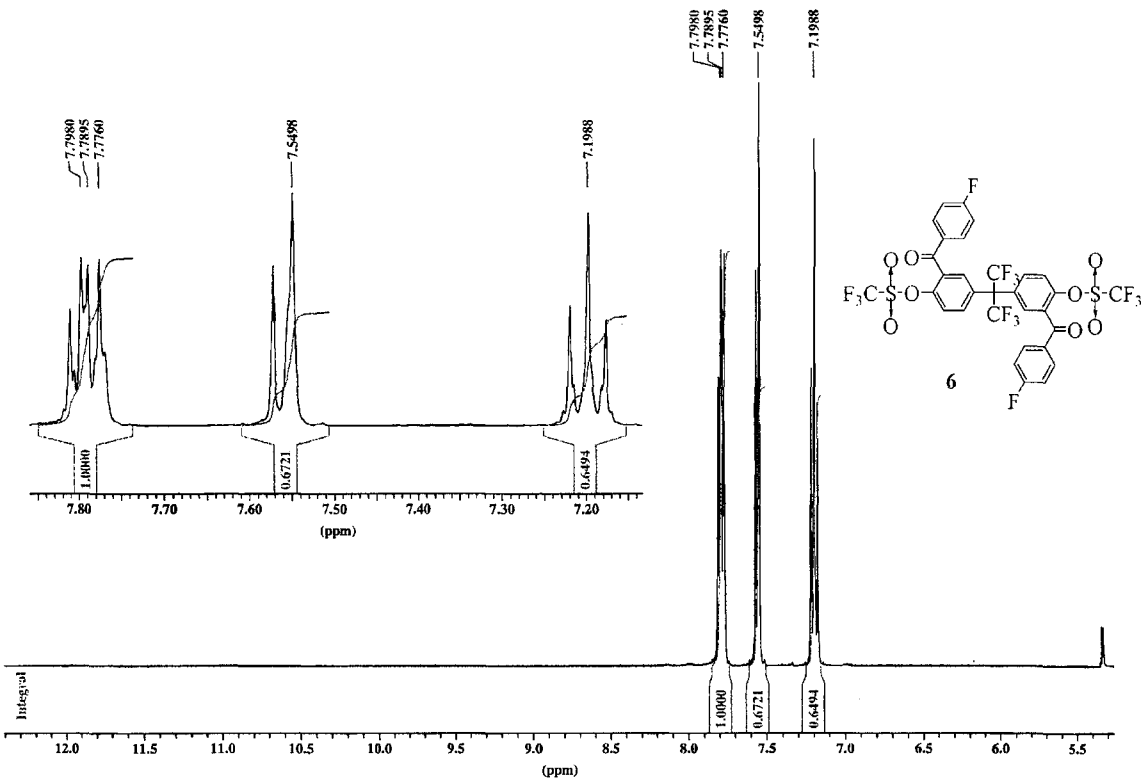

^{1}H NMR spectrum of 2,2-Bis(3-(4-fluorobenzoyl)-4-(trifluoromethanesulfonyloxy)phenyl) hexafluoropropane (**6**).

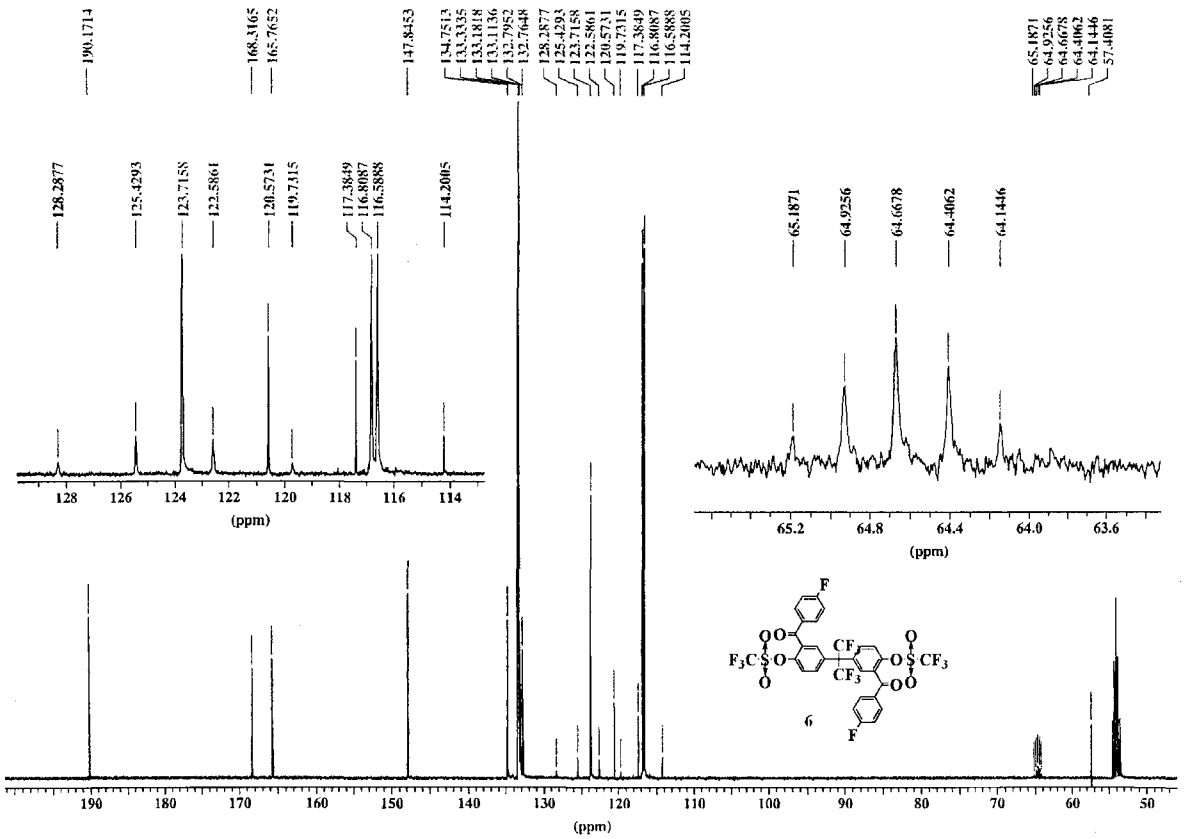

^{13}C NMR spectrum of 2,2-Bis(3-(4-fluorobenzoyl)-4-(trifluoromethanesulfonyloxy)phenyl) hexafluoropropane (**6**).

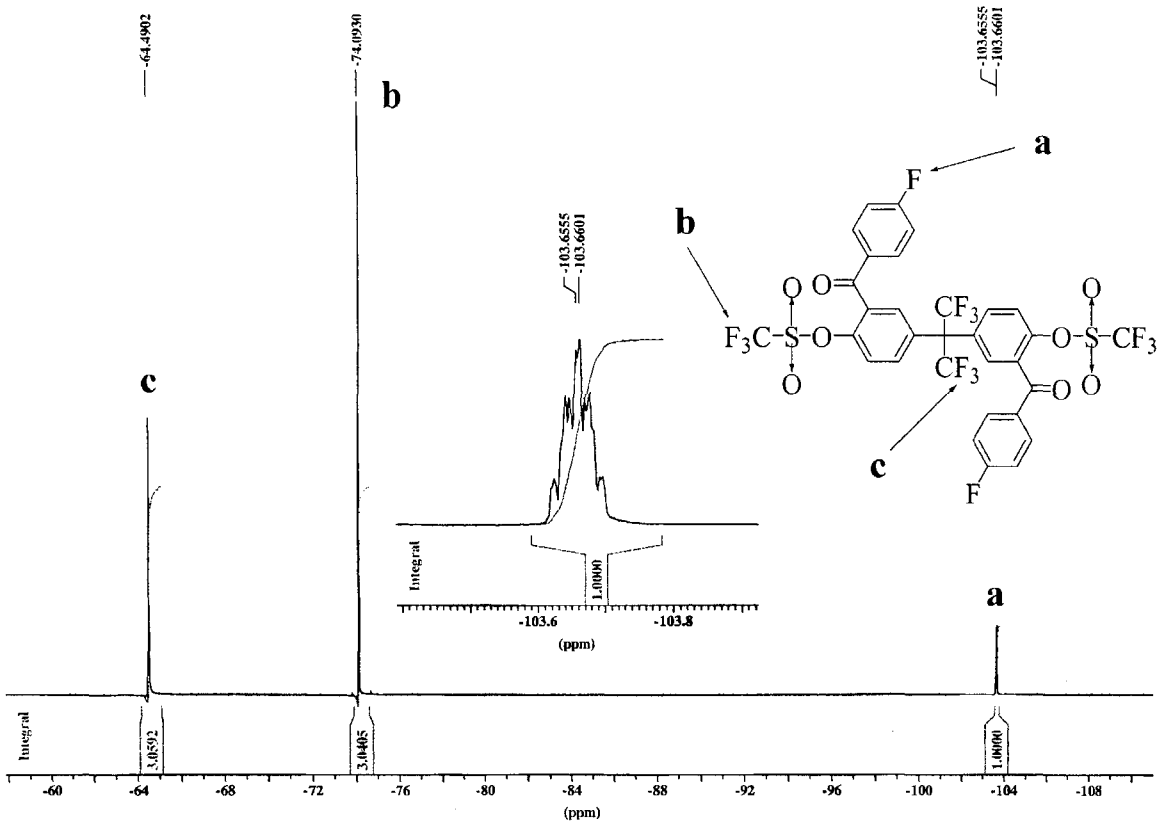

^{19}F NMR spectrum of 2,2-Bis(3-(4-fluorobenzoyl)-4-(trifluoromethanesulfonyloxy)phenyl) hexafluoropropane (**6**).

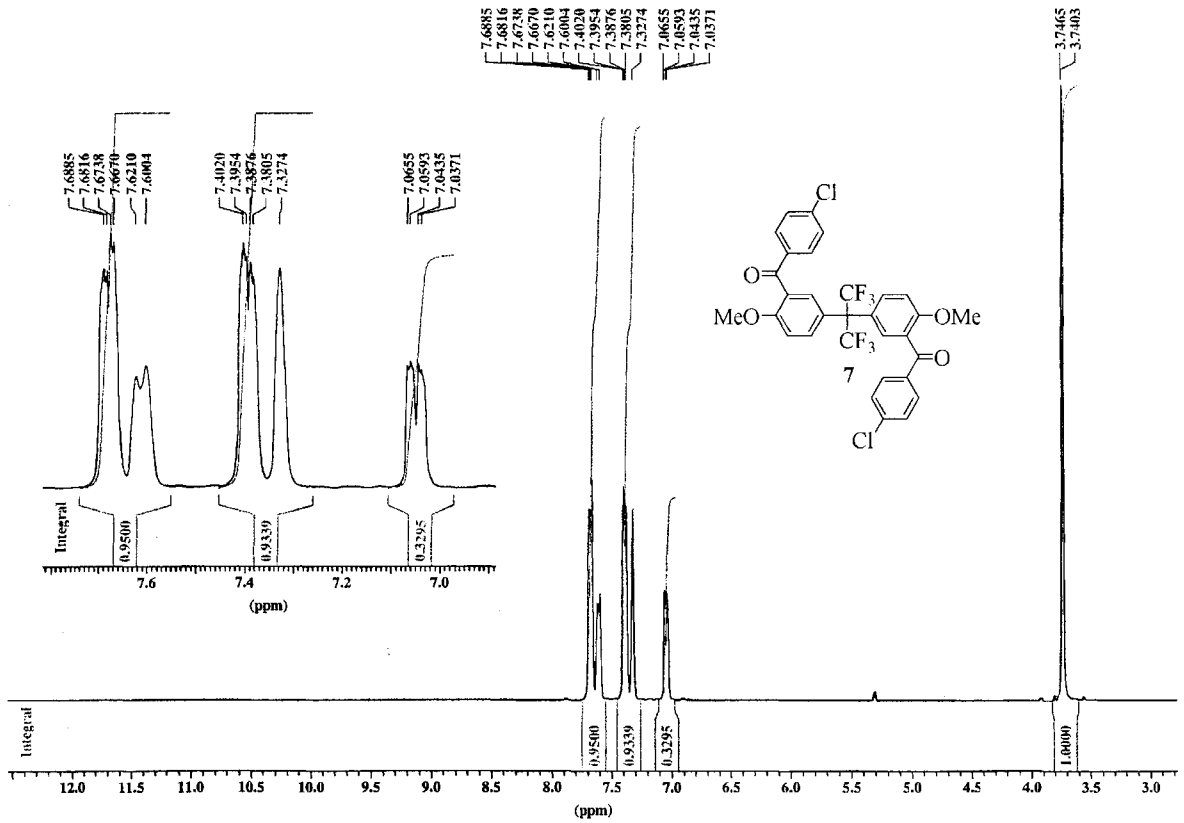

^{1}H NMR spectrum of 2,2-Bis(3-(4-chlorobenzoyl)-4-(methoxyphenyl)hexafluoropropane (**7**).

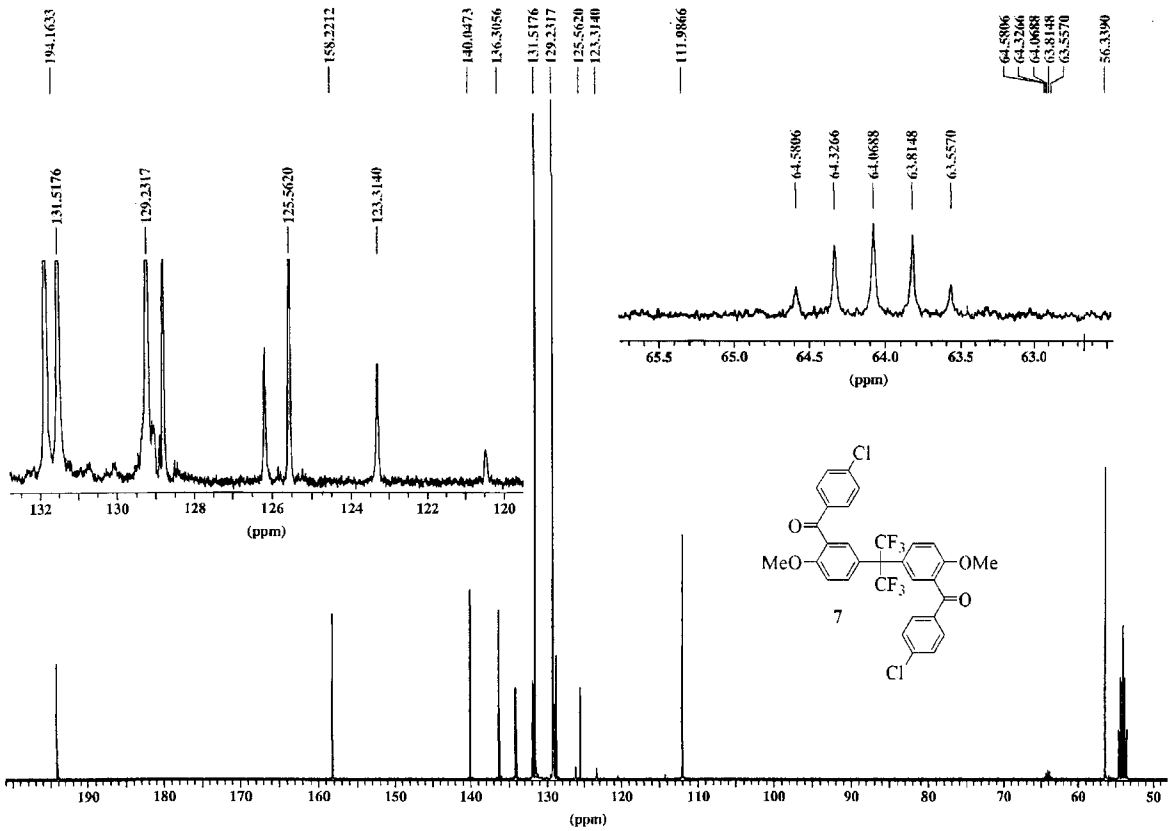

^{13}C NMR spectrum of 2,2-Bis(3-(4-chlorobenzoyl)-4-(methoxyphenyl)hexafluoropropane (7).

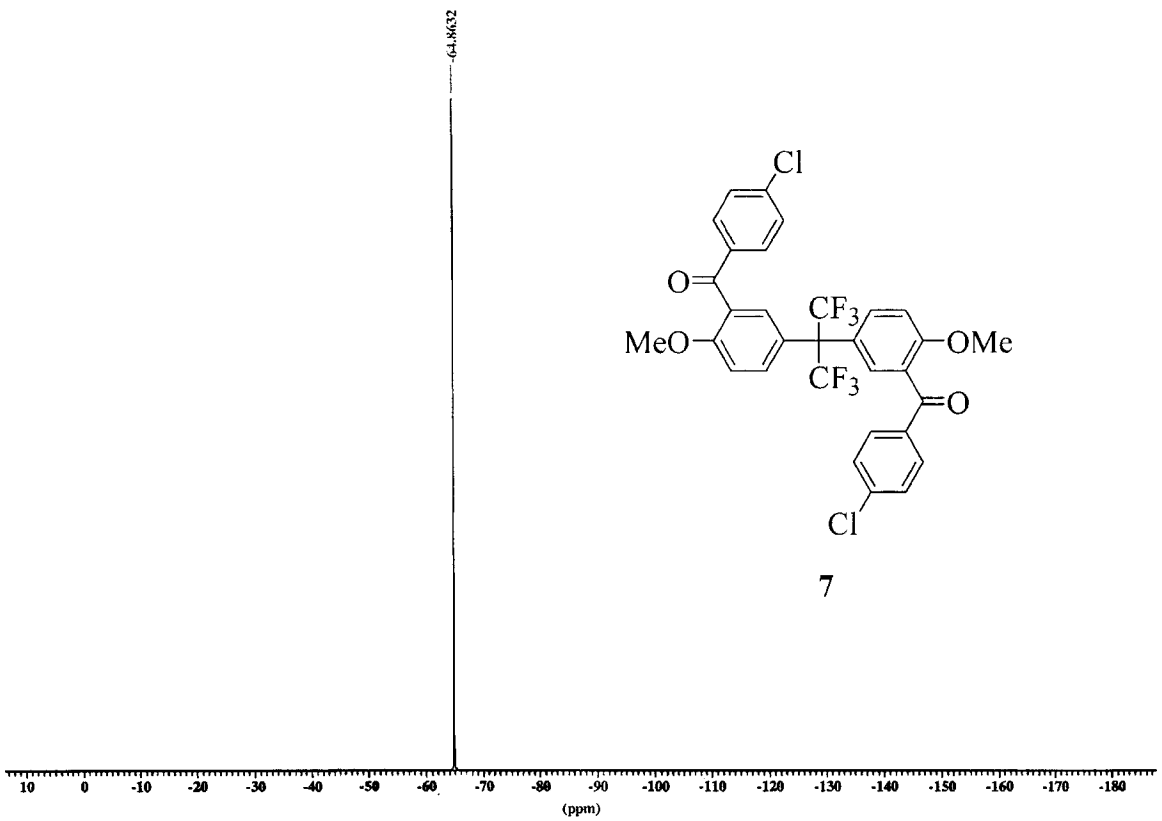

7

^{19}F NMR spectrum of 2,2-Bis(3-(4-chlorobenzoyl)-4-(methoxyphenyl)hexafluoropropane (**7**).

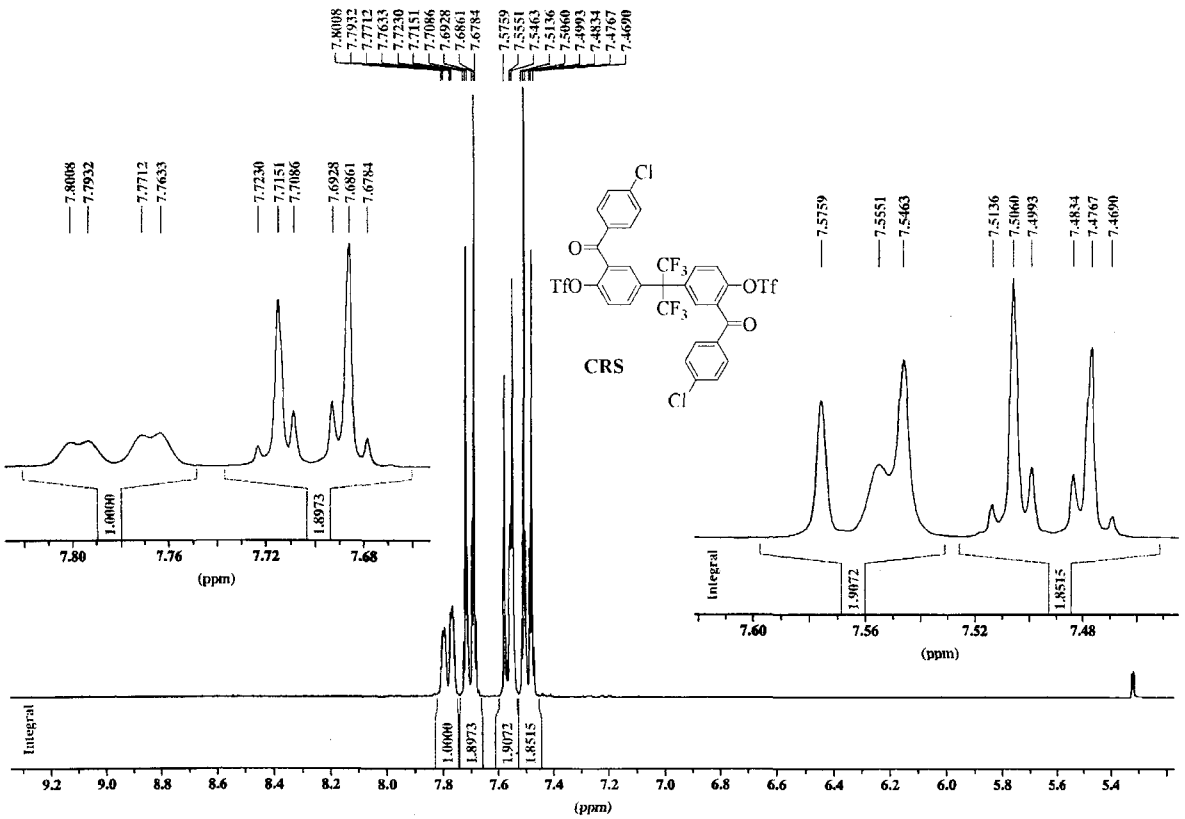

^{1}H NMR spectrum of 2,2-Bis(3-(4-chlorobenzoyl)-4-(trifluoromethanesulfonyloxy)phenyl) hexafluoropropane **CRS**.

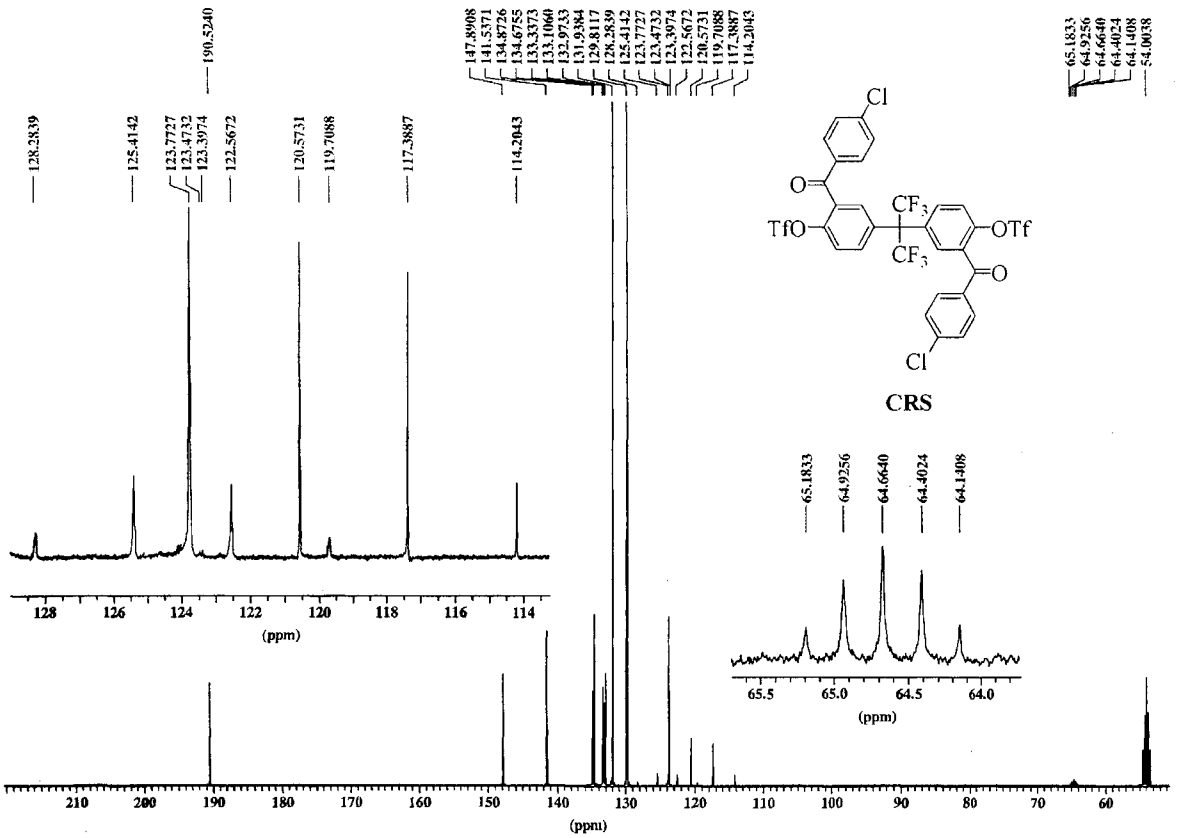

^{13}C NMR spectrum of 2,2-Bis(3-(4-chlorobenzoyl)-4-(trifluoromethanesulfonyloxy)phenyl) hexafluoropropane **CRS**.

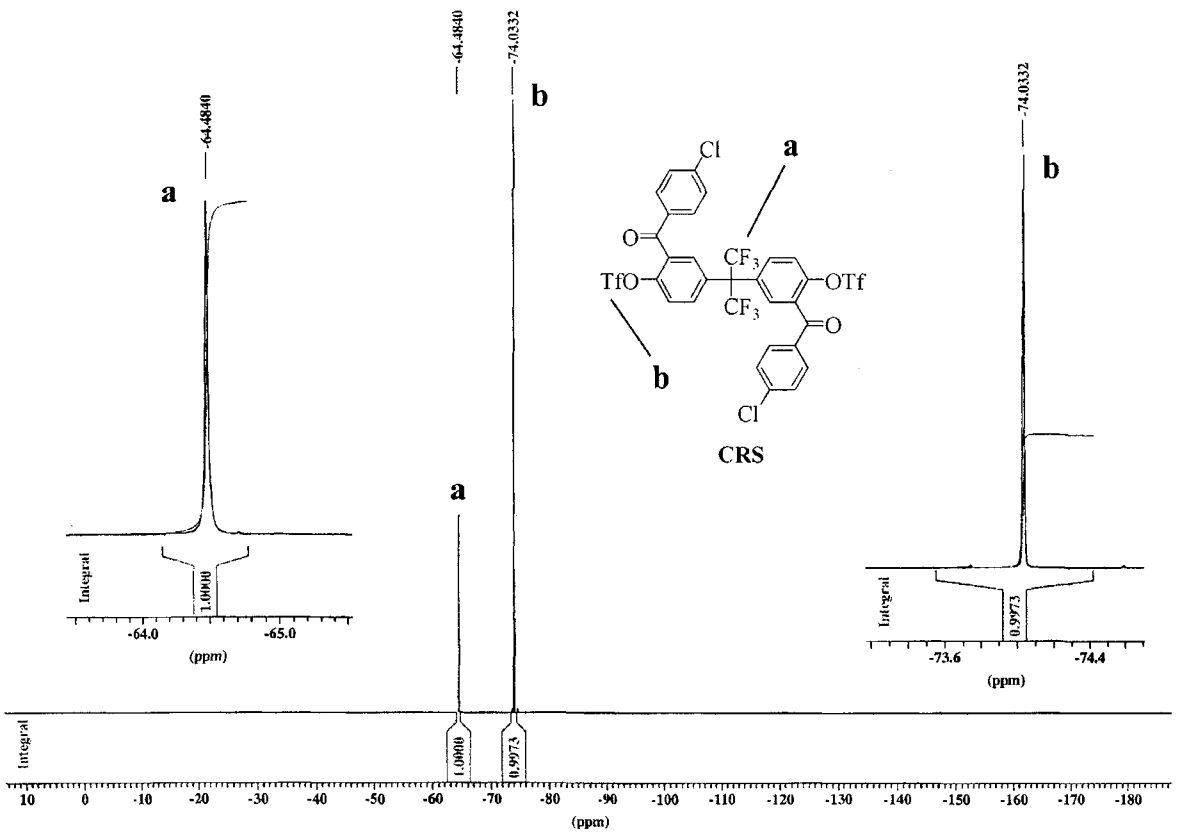

^{19}F NMR spectrum of 2,2-Bis(3-(4-chlorobenzoyl)-4-(trifluoromethanesulfonyloxy)phenyl) hexafluoropropane **CRS**.

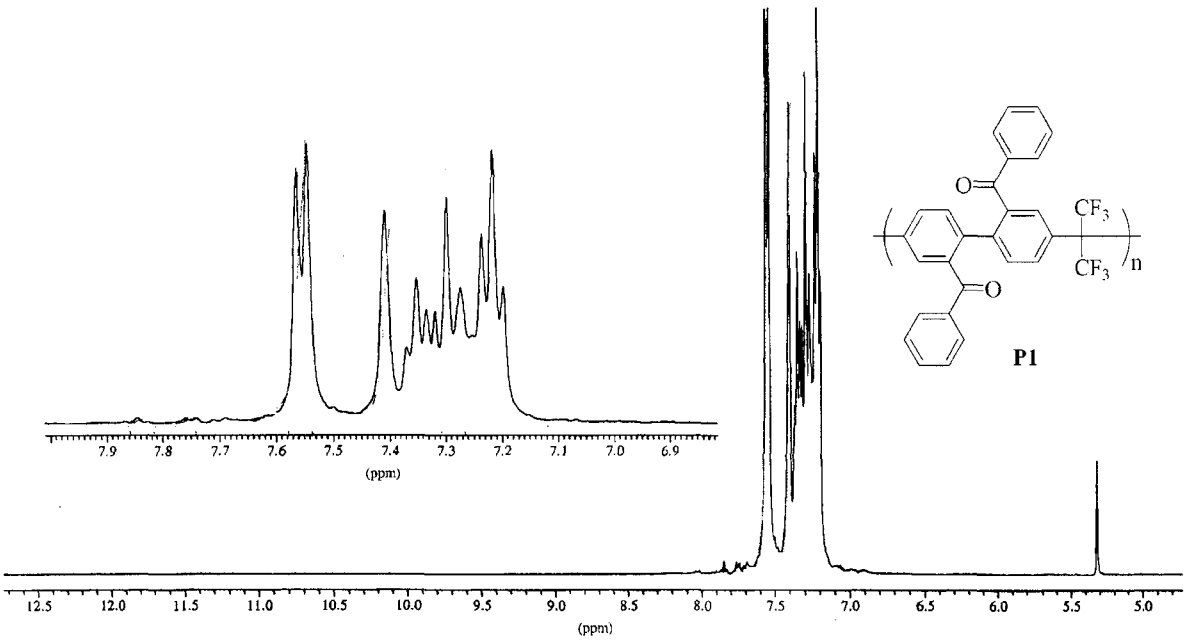

^{1}H NMR spectrum of polymer **P1**.

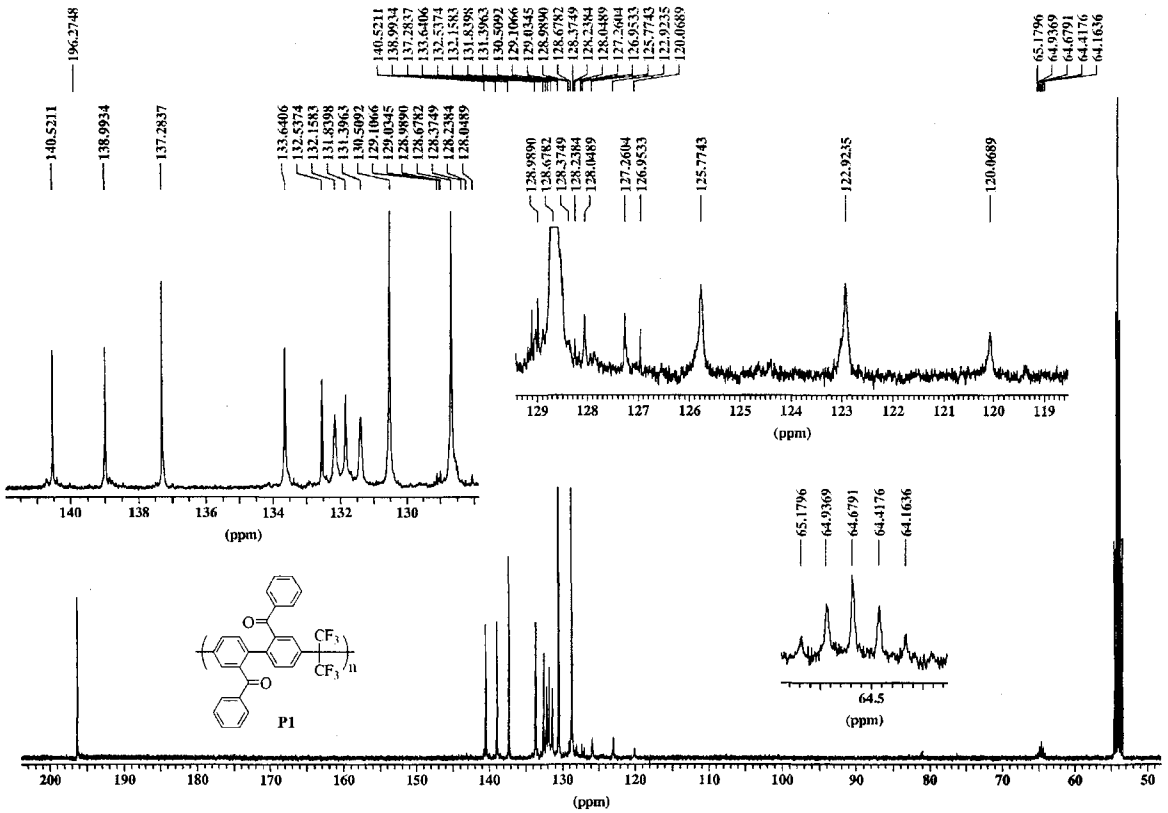

^{13}C NMR spectrum of polymer **P1**.

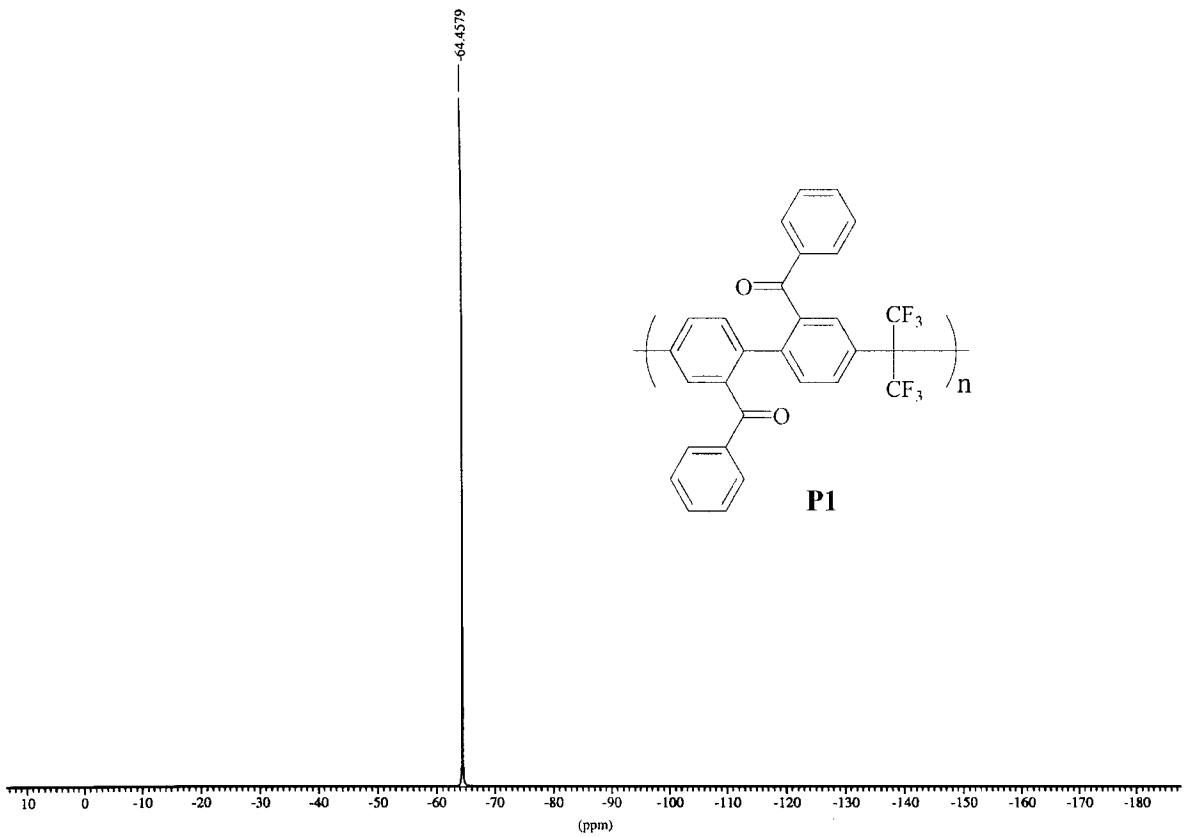

^{19}F NMR spectrum of polymer **P1**.

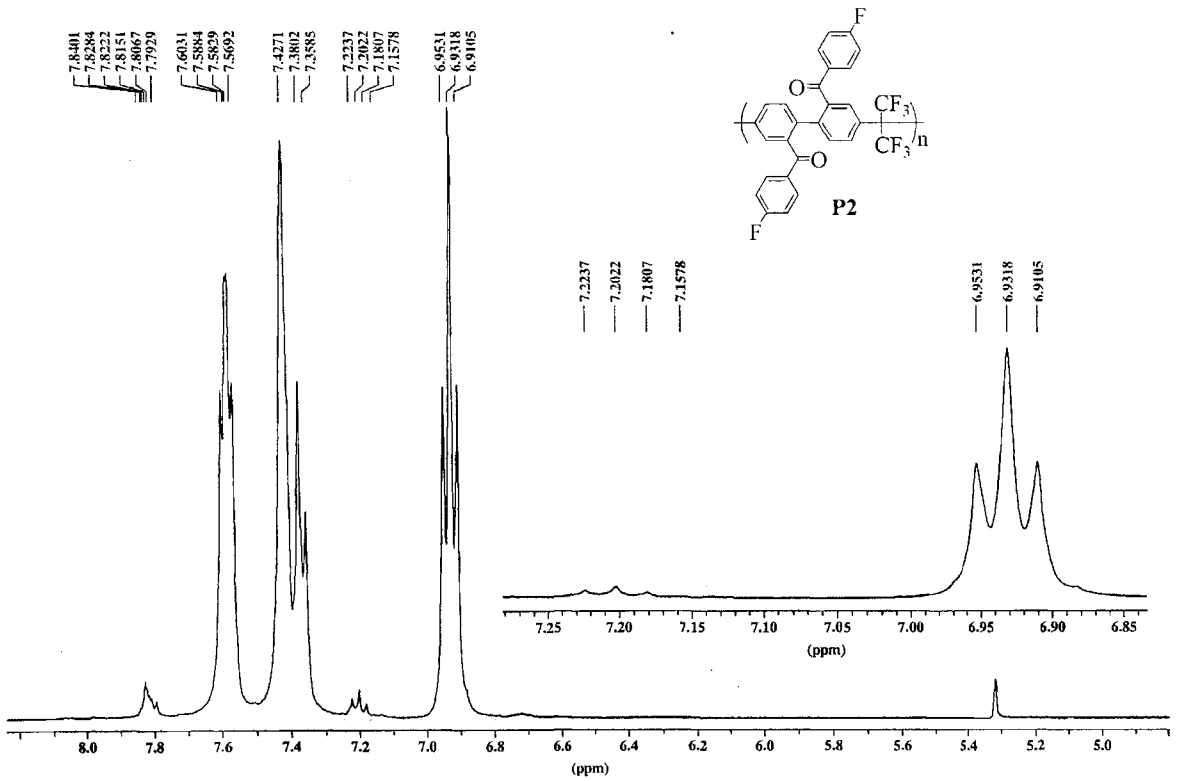

^{1}H NMR spectrum of polymer **P2**.

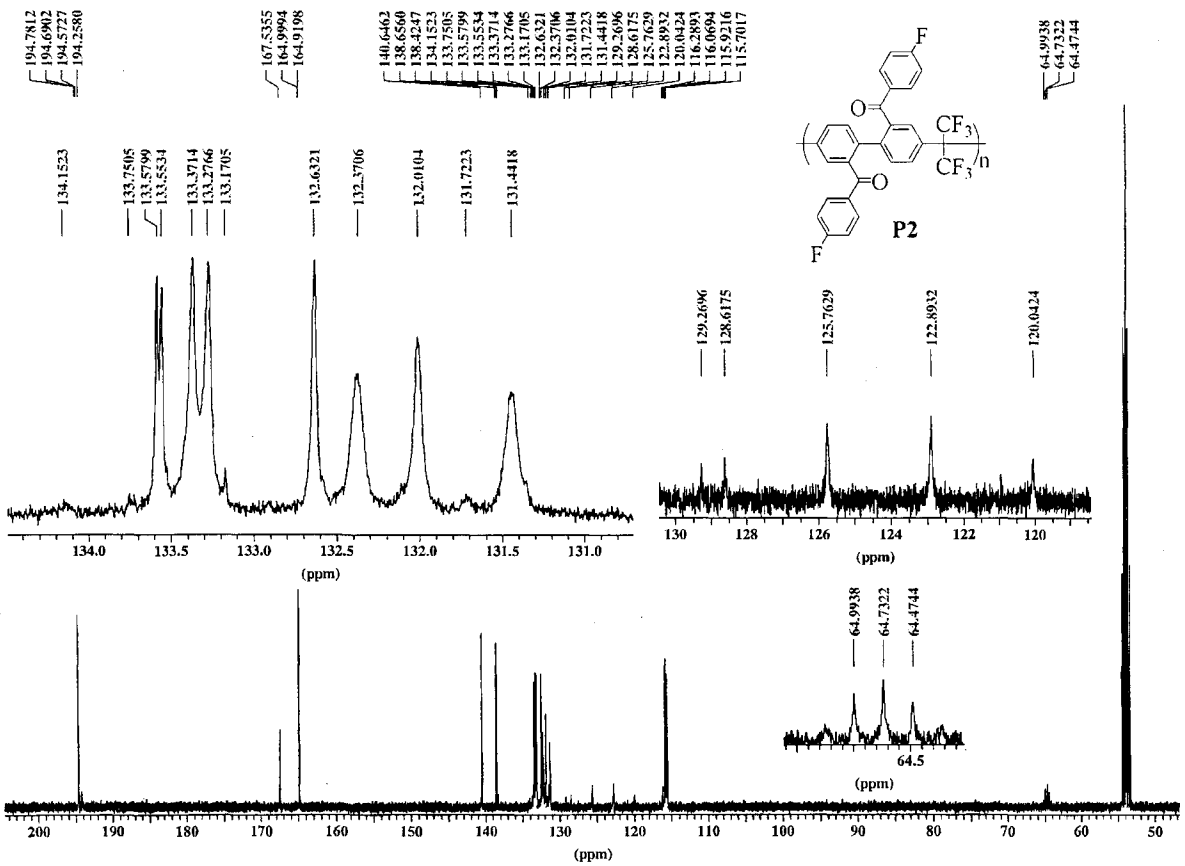

^{13}C NMR spectrum of polymer **P2**.

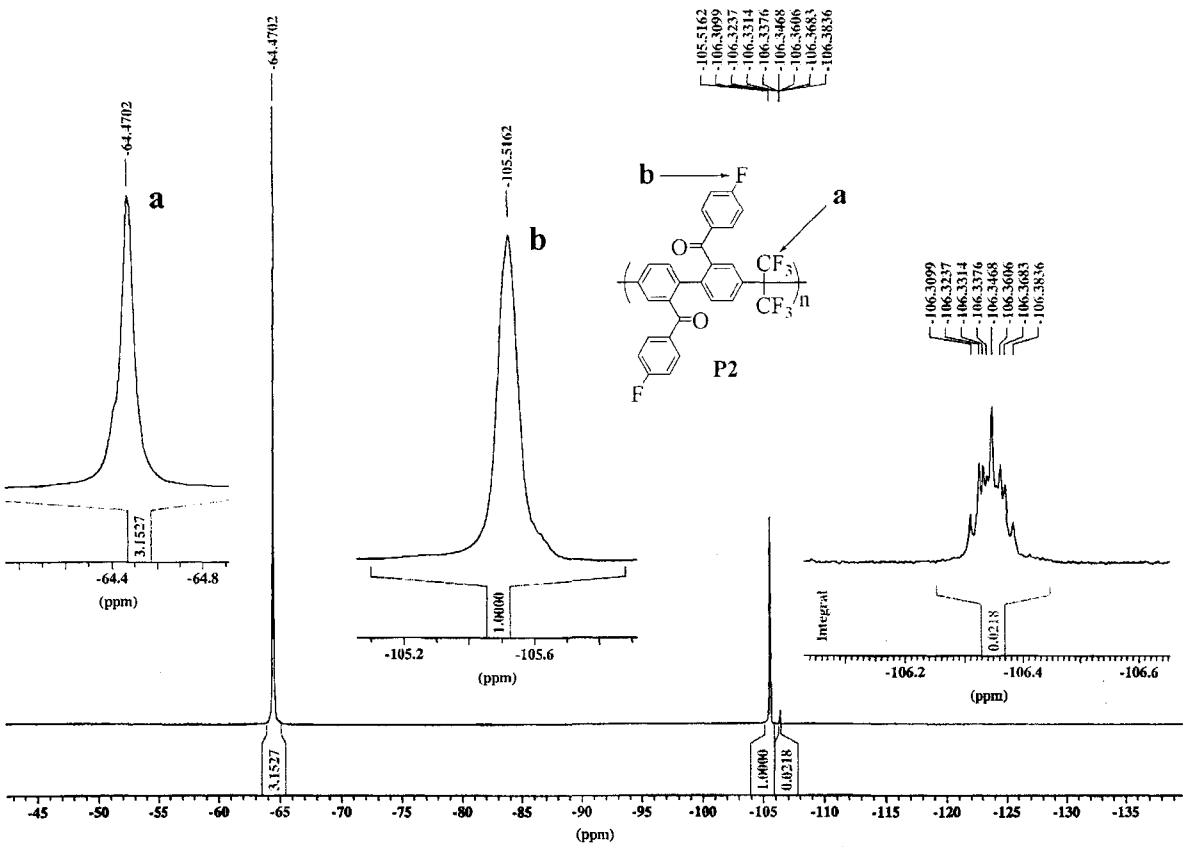

^{19}F NMR spectrum of polymer **P2**.

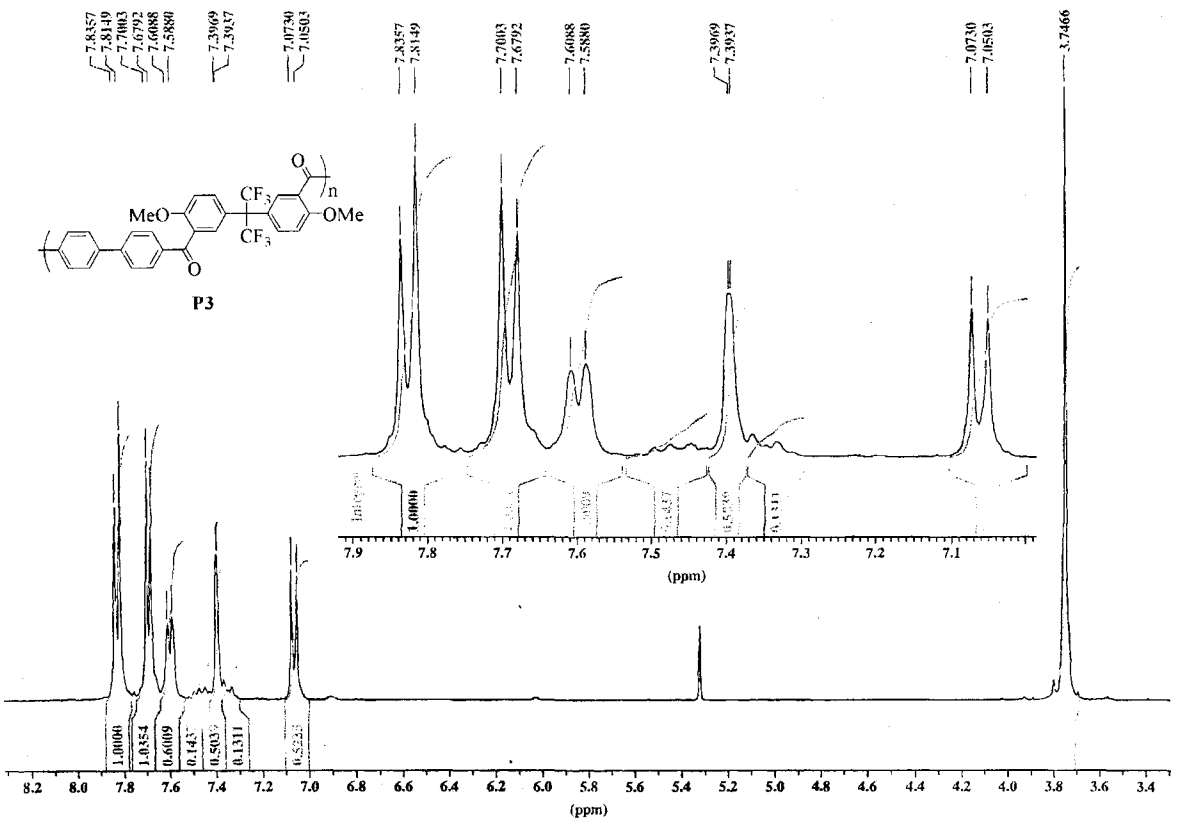

^{1}H NMR spectrum of polymer **P3**.

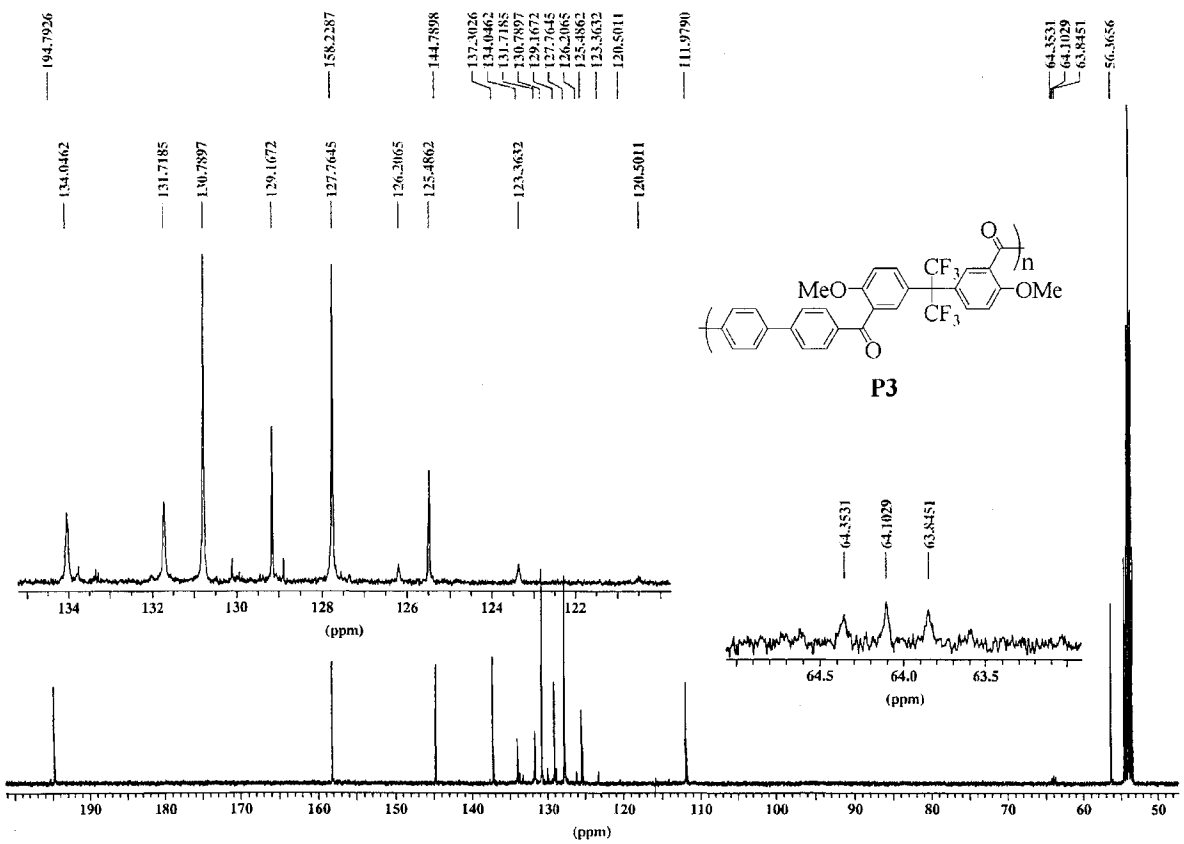

^{13}C NMR spectrum of polymer **P3**.

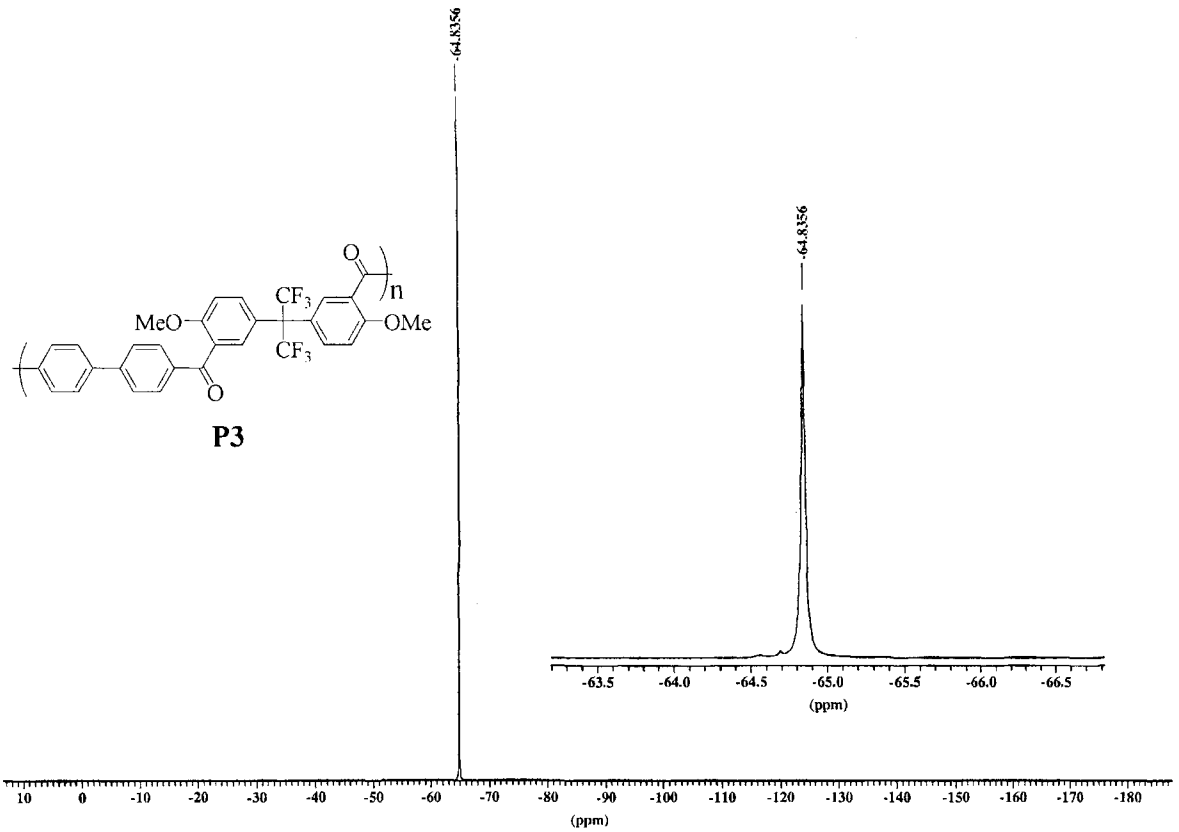

P3

^{19}F NMR spectrum of polymer **P3**.

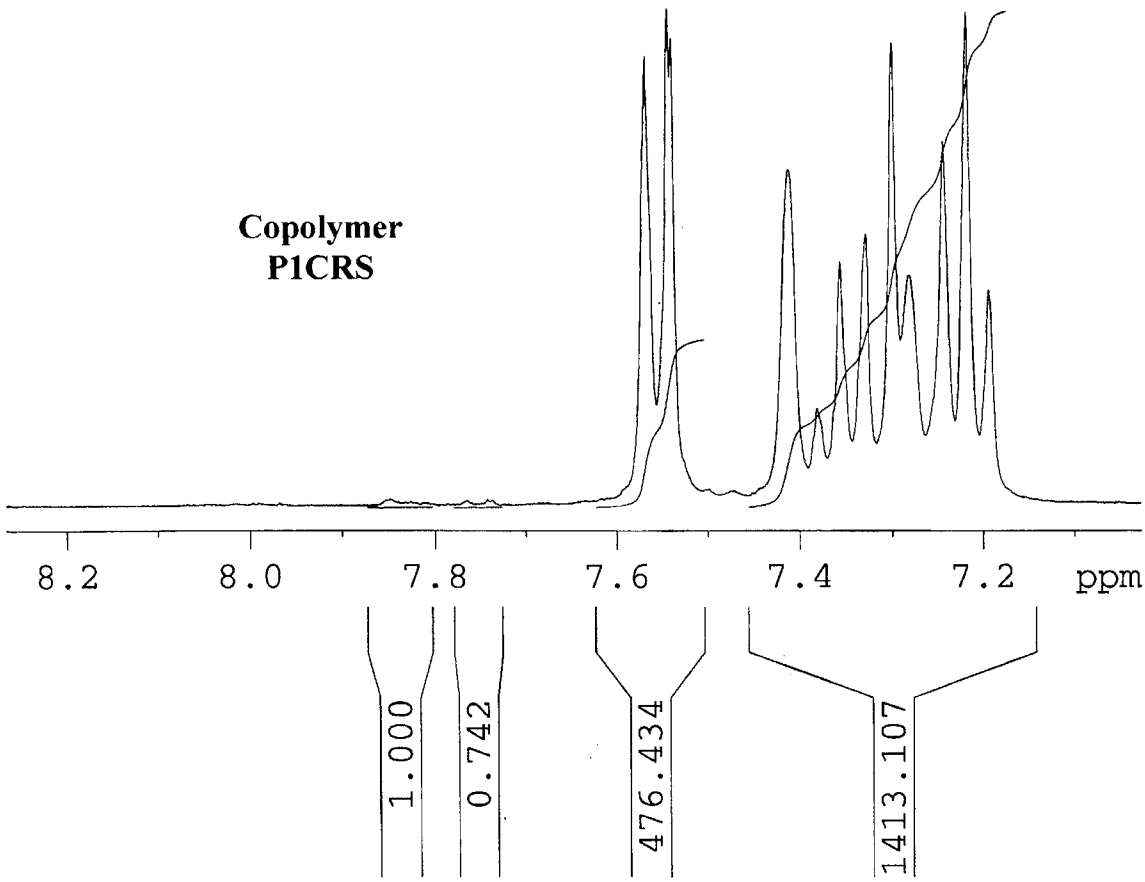

^{1}H NMR spectrum of copolymer **P1CRS**.

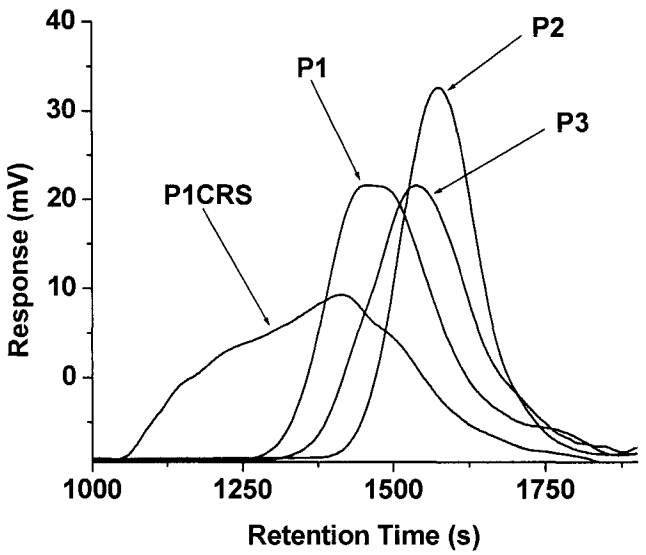

GPC chromatograms of isomeric HFIP-linked benzophenone polymers.

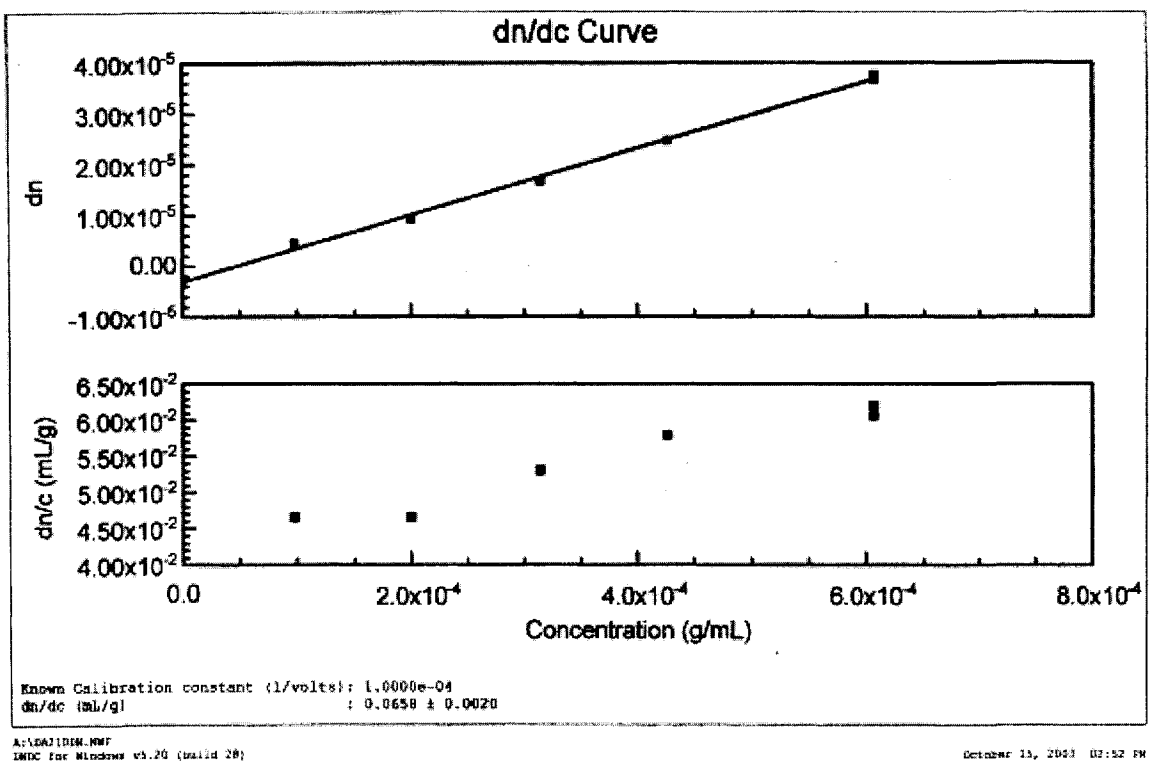

Calculation of dn/dc value for **P1**.

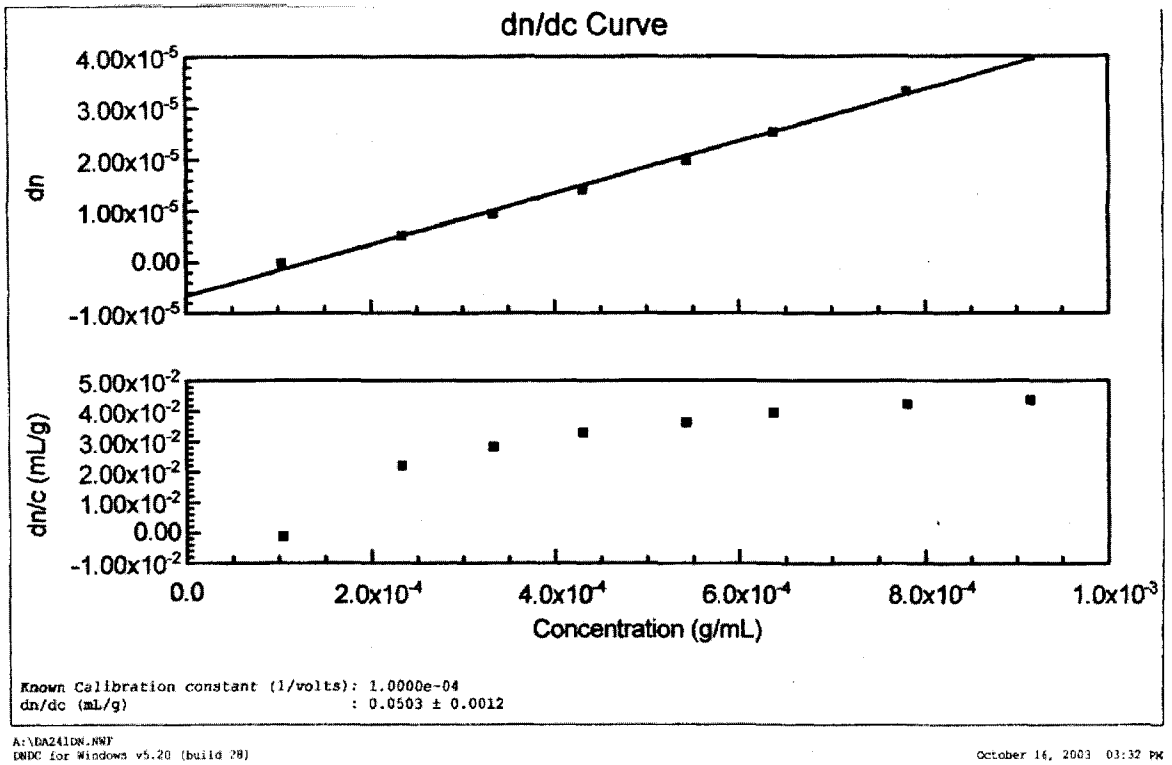

Calculation of dn/dc value for **P2**.

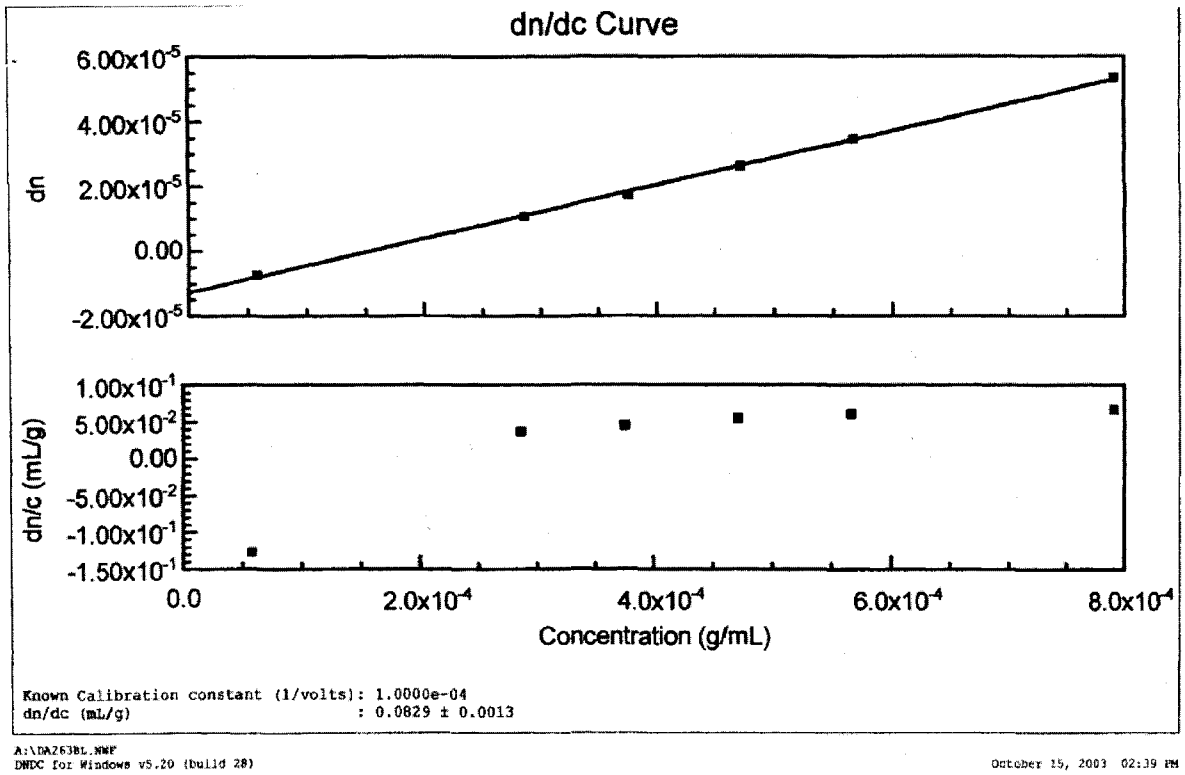

Calculation of dn/dc value for **P3**.

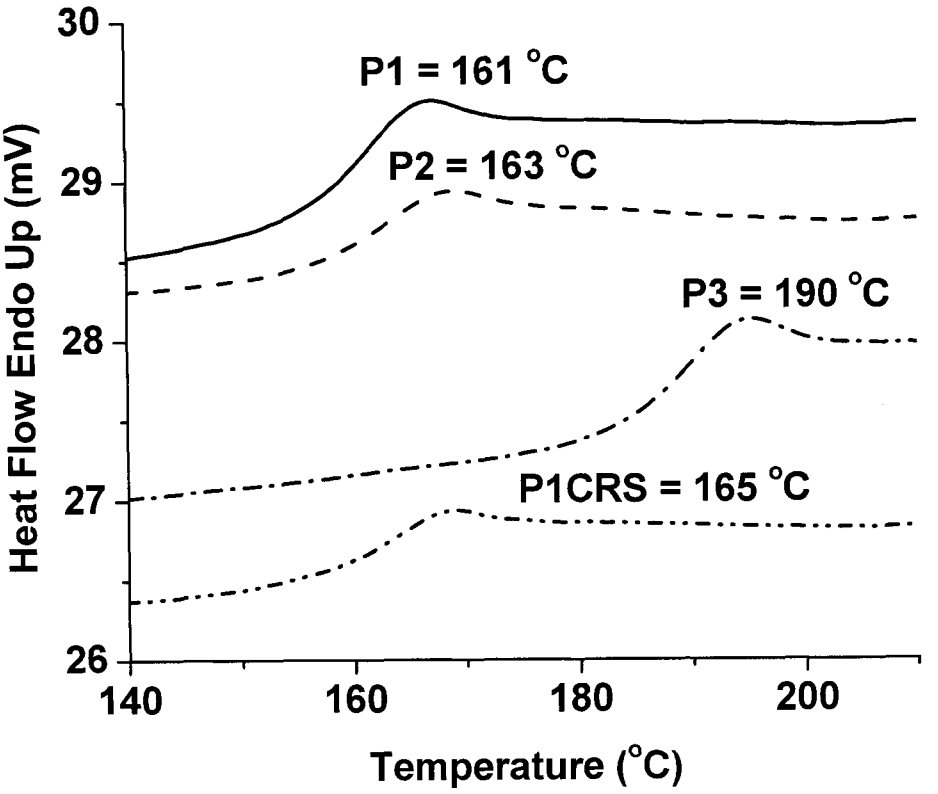

DSC traces of the isomeric HFIP-linked benzophenone polymers.

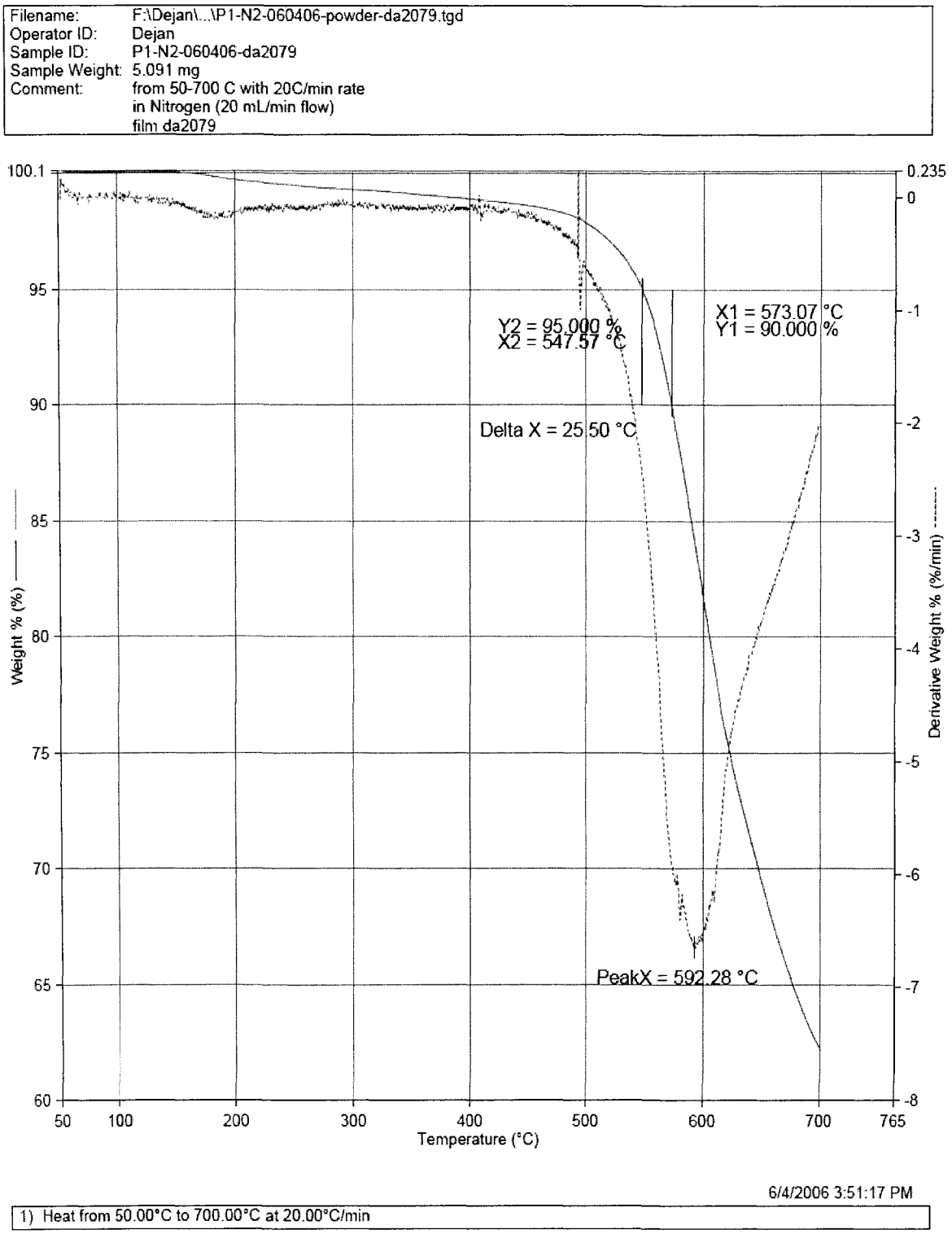

TGA thermogram of polymer **P1** in nitrogen atmosphere.

Filename:	F:\Dejan...\P2F-N2-060406-powder-da2041.tgd
Operator ID:	Dejan
Sample ID:	P2F-N2-060406-da2041
Sample Weight:	4.794 mg
Comment:	from 50-700 C with 20C/min rate in Nitrogen (20 mL/min flow) film da2041

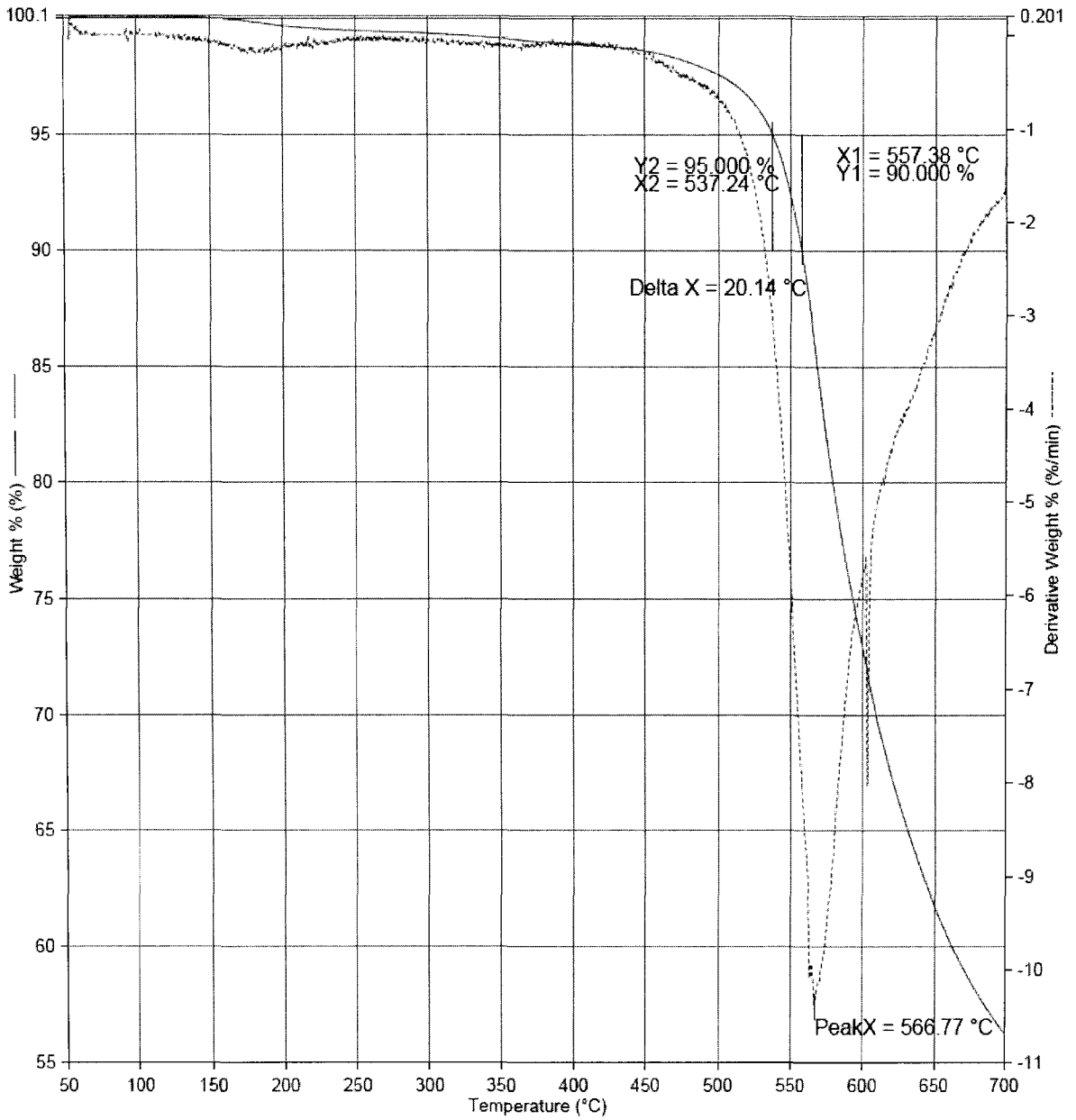

TGA thermogram of polymer **P2** in nitrogen atmosphere.

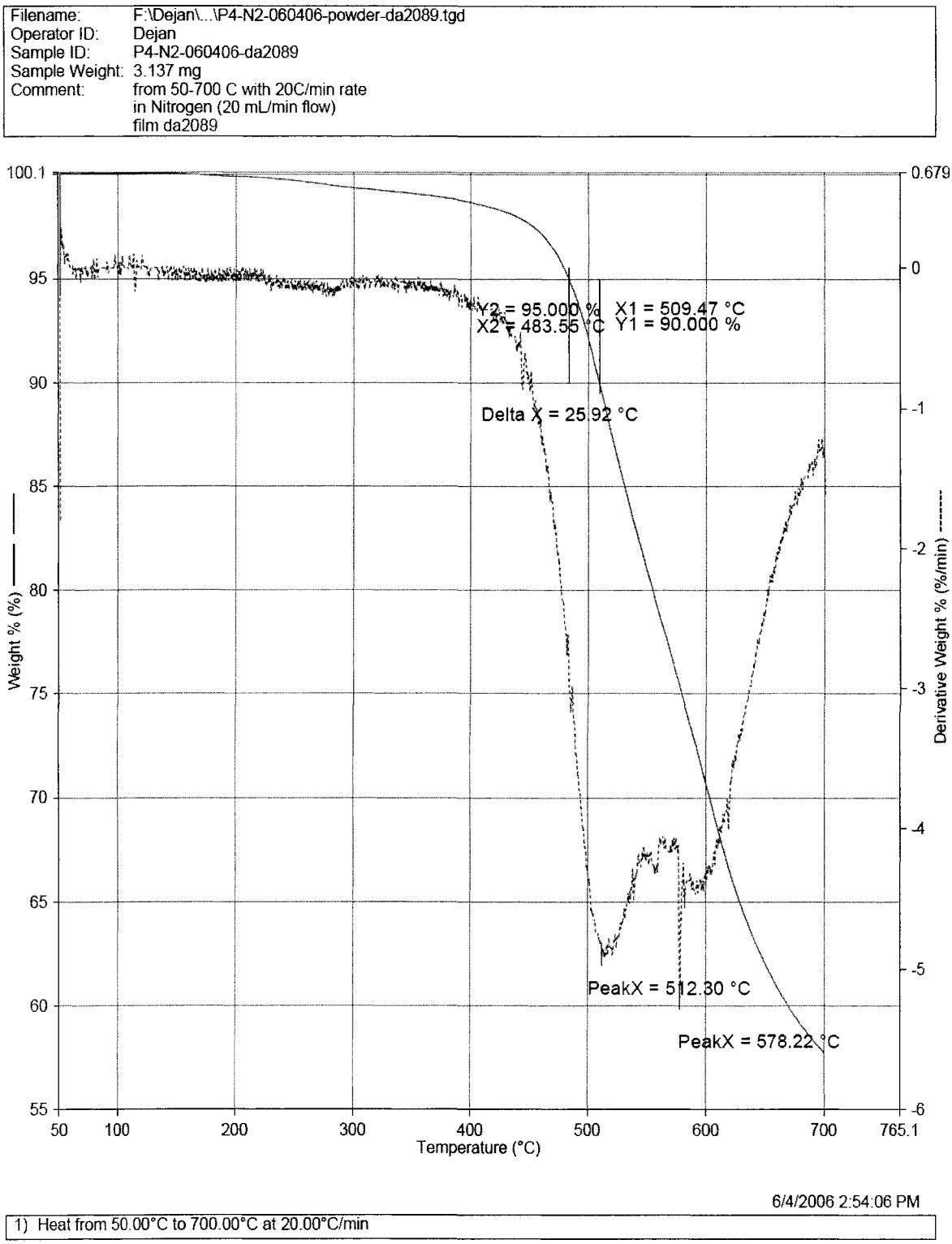

TGA thermogram of polymer **P3** in nitrogen atmosphere.

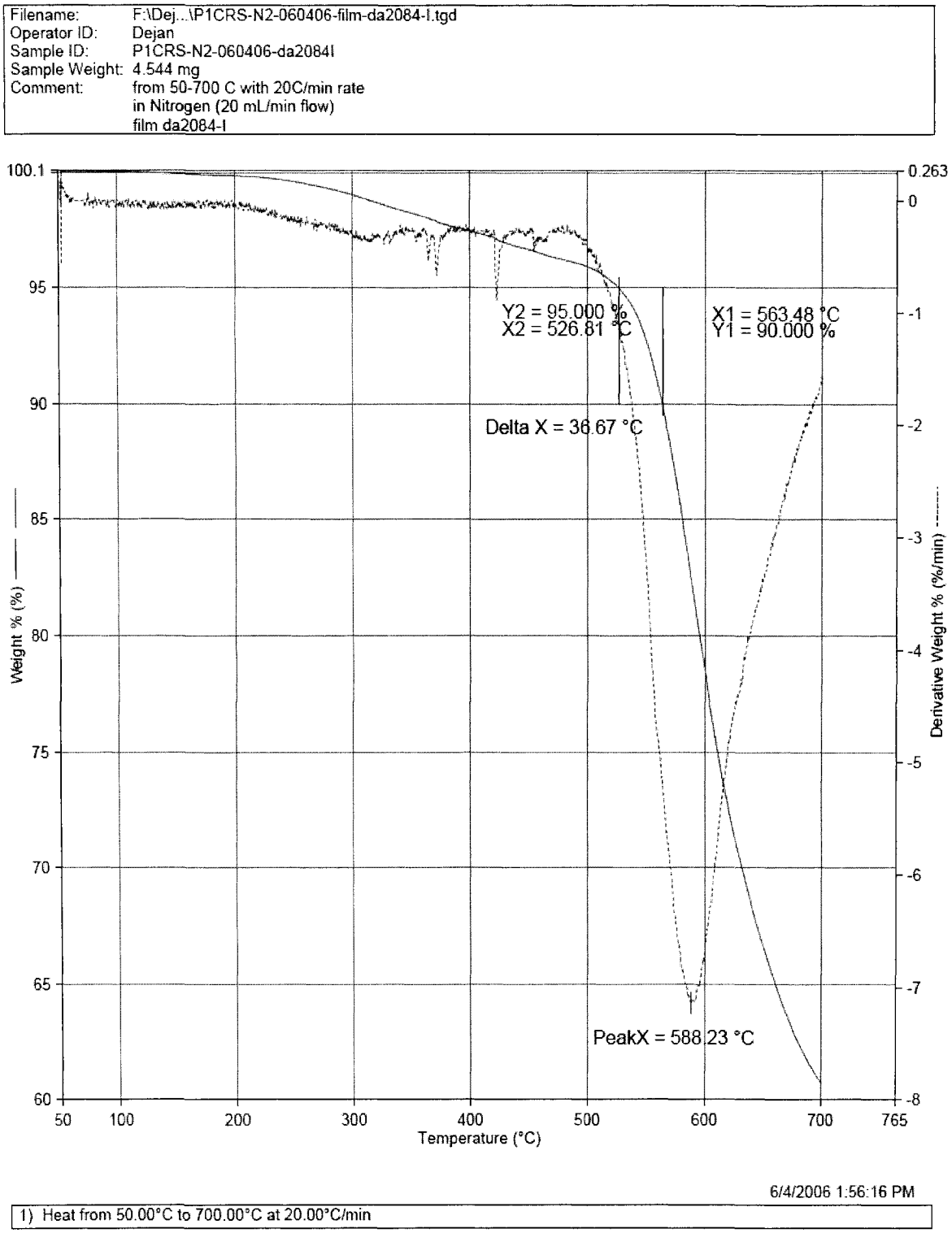

TGA thermogram of copolymer **P1CRS** in nitrogen atmosphere.

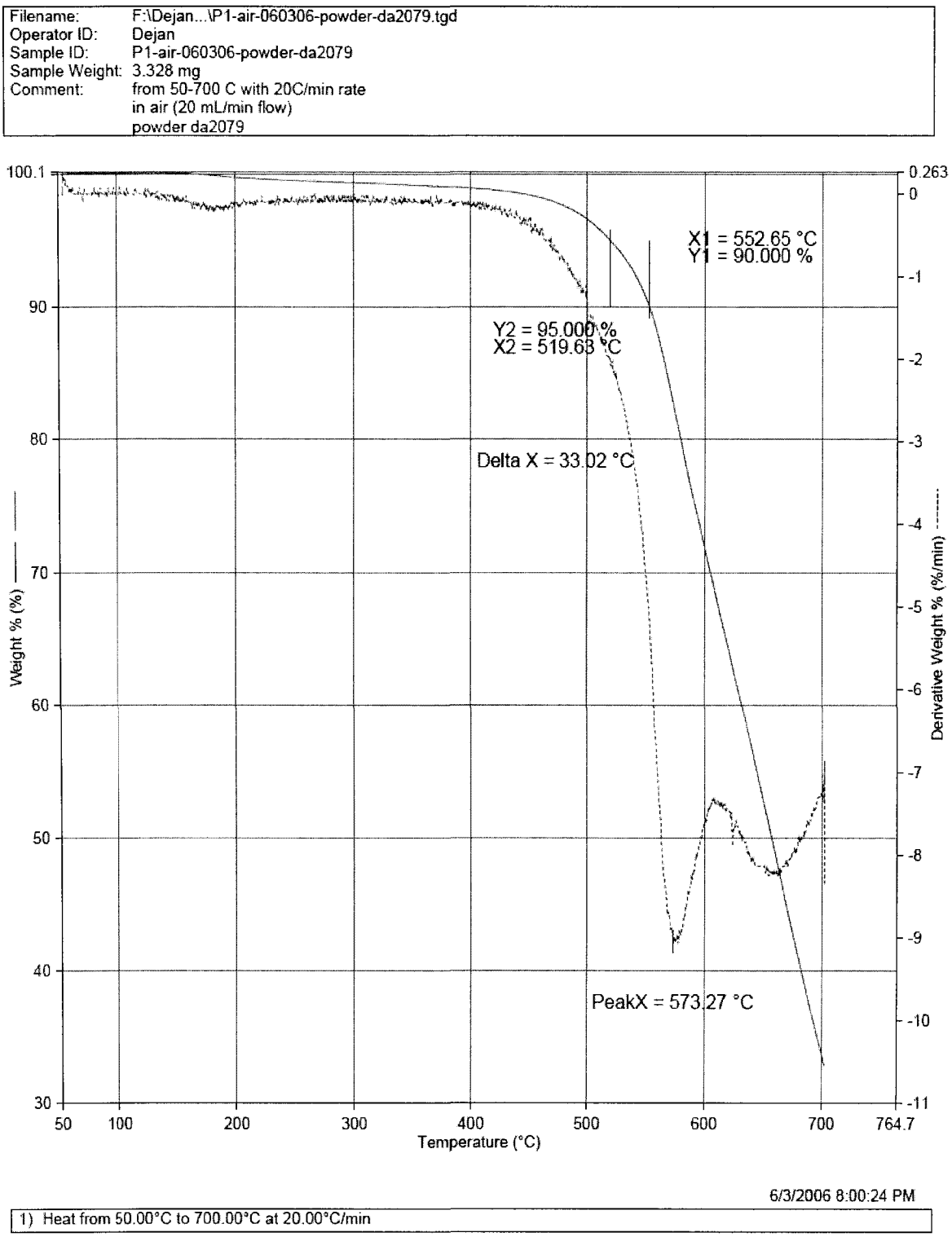

TGA thermogram of polymer **P1** in air.

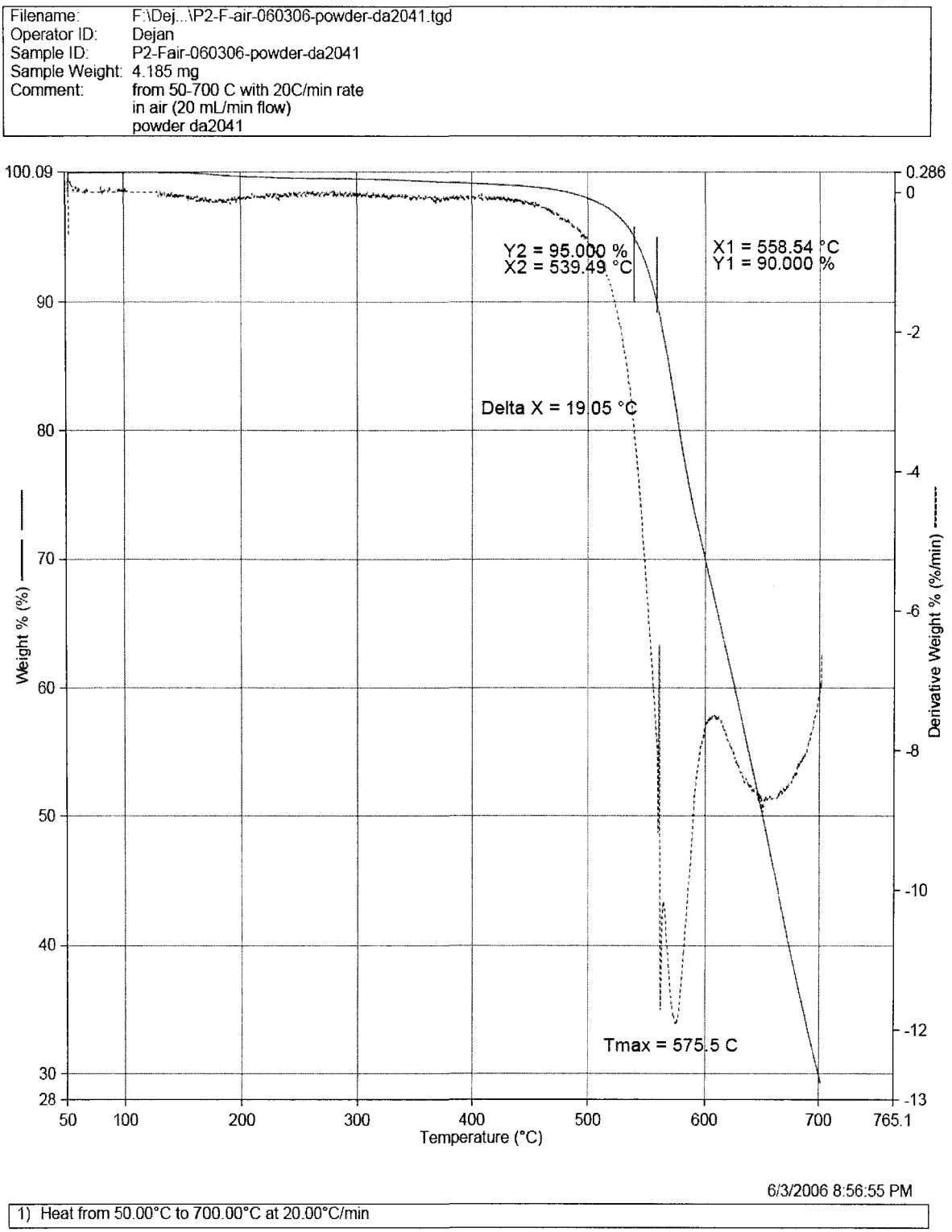

TGA thermogram of polymer **P2** in air.

Filename:	F:\Dejan\TGA da...\P4-air-060306-powder.tgd
Operator ID:	Dejan
Sample ID:	P4-air-060306-powder
Sample Weight:	3.203 mg
Comment:	from 50-700 C with 20C/min rate in air (20 mL/min flow) powder da2089

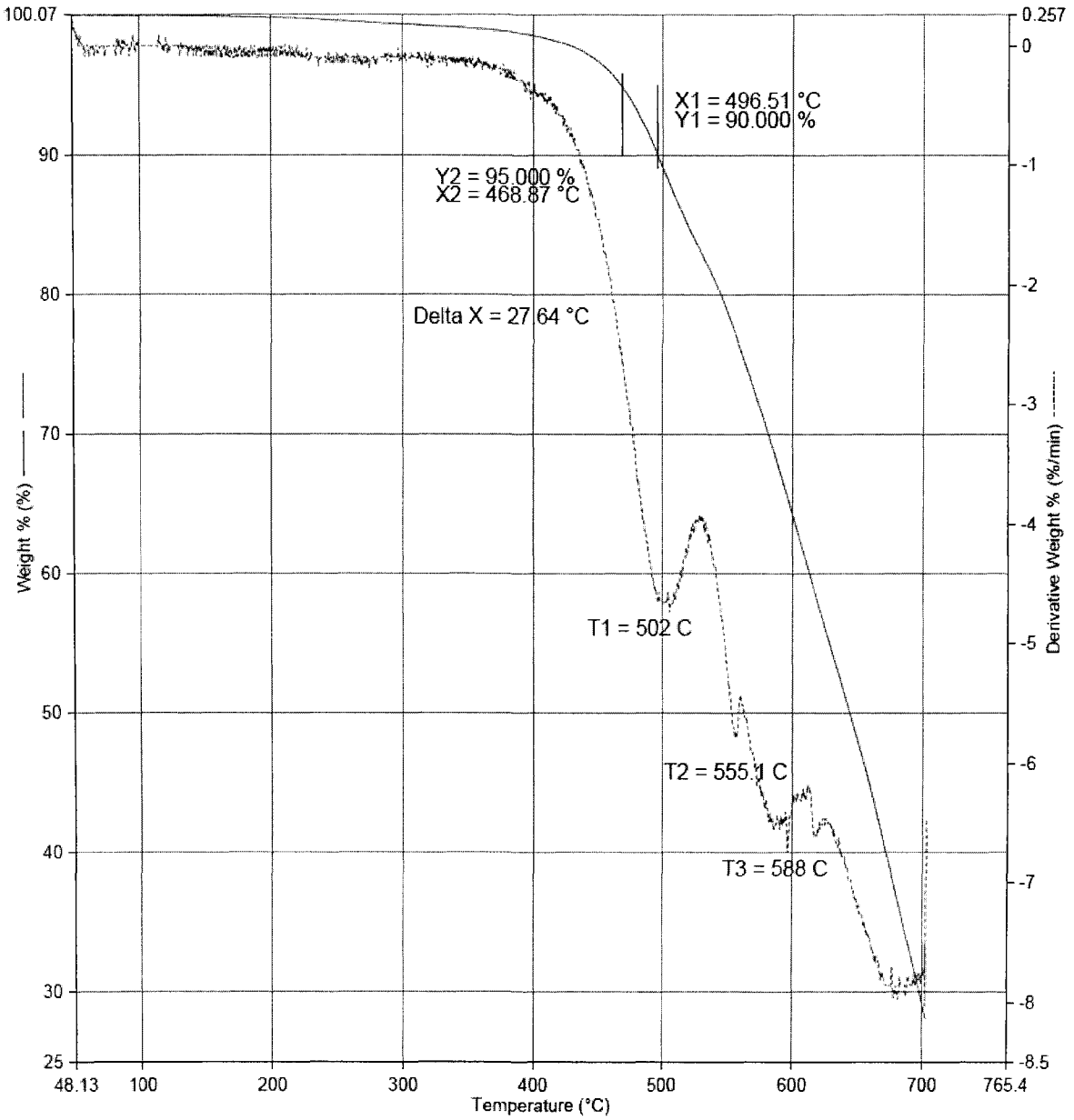

TGA thermogram of polymer **P3** in air.

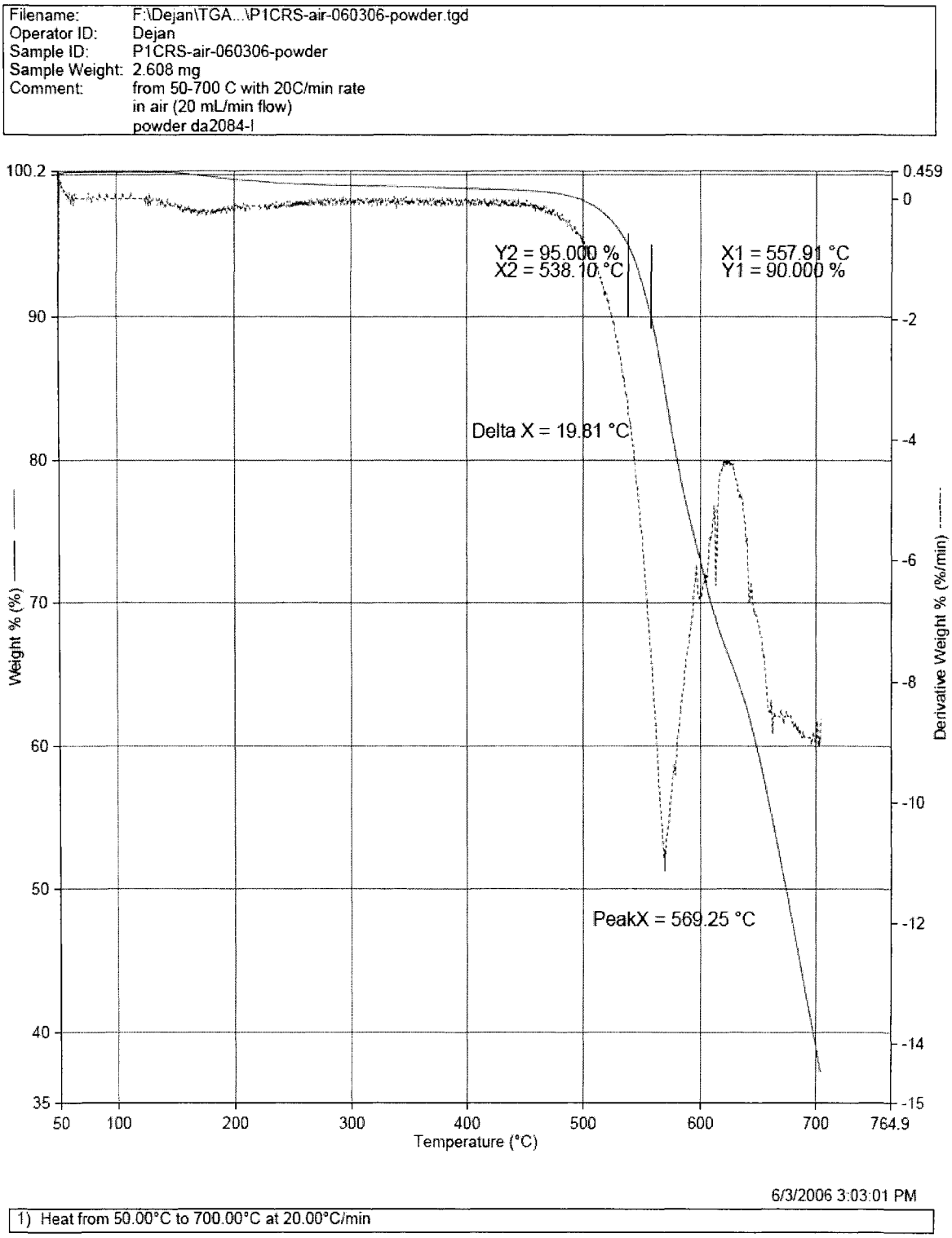

TGA thermogram of copolymer **P1CRS** in air.

APPENDIX B. SUPPLEMENTAL DATA FOR CHAPTER 4

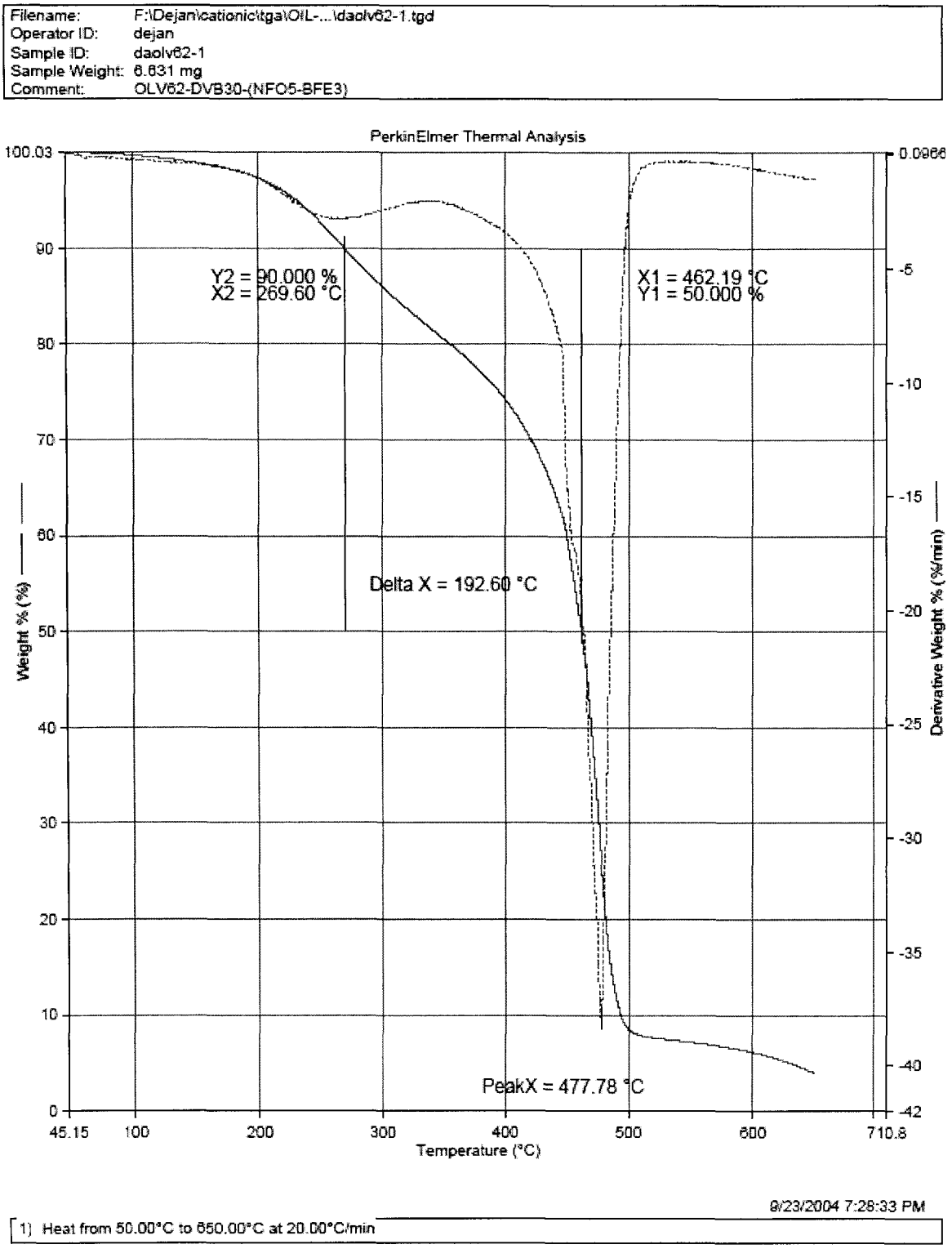

TGA thermogram of copolymer OLV62-DVB30-(NFO5-BFE3) in air.

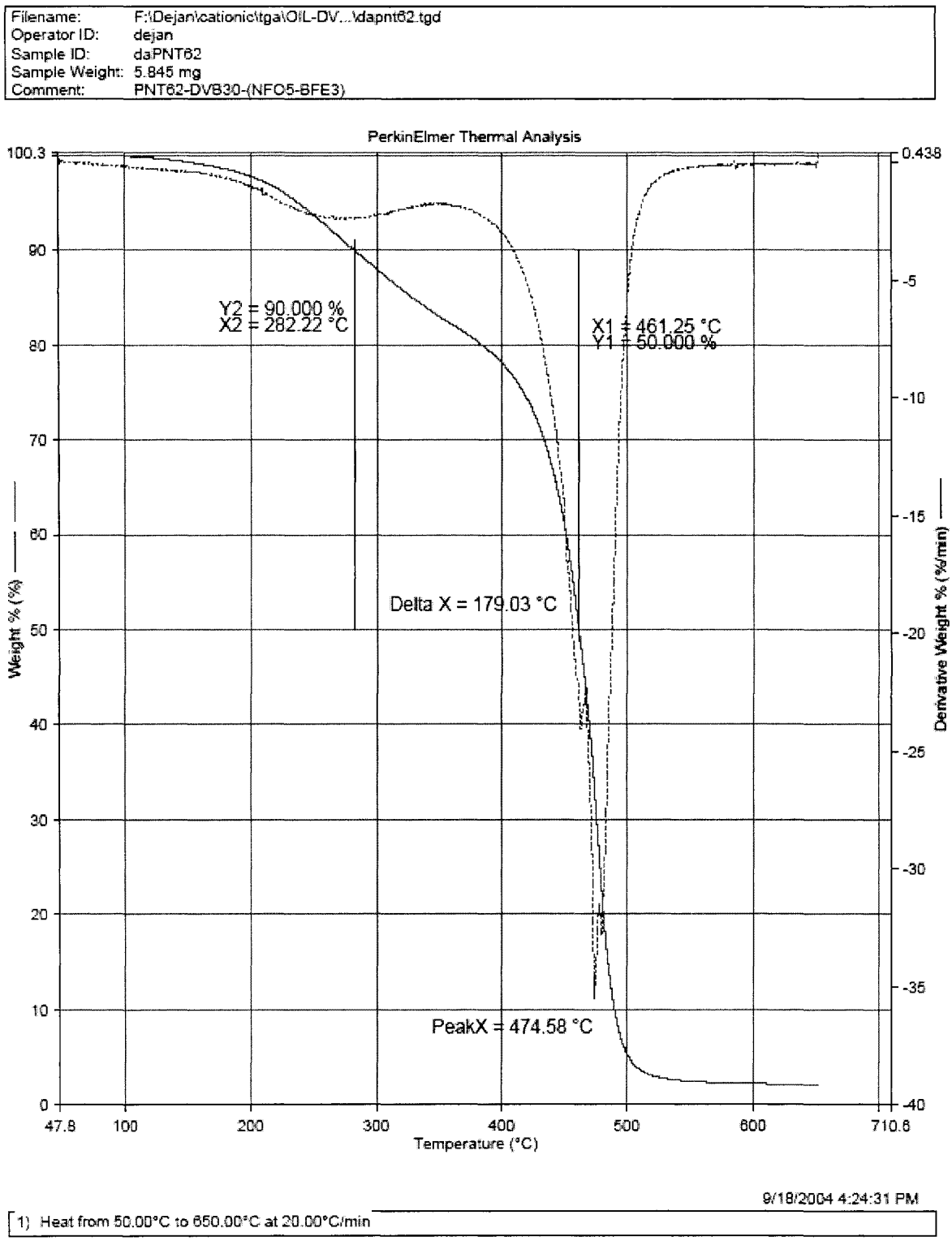

TGA thermogram of copolymer PNT62-DVB30-(NFO5-BFE3) in air.

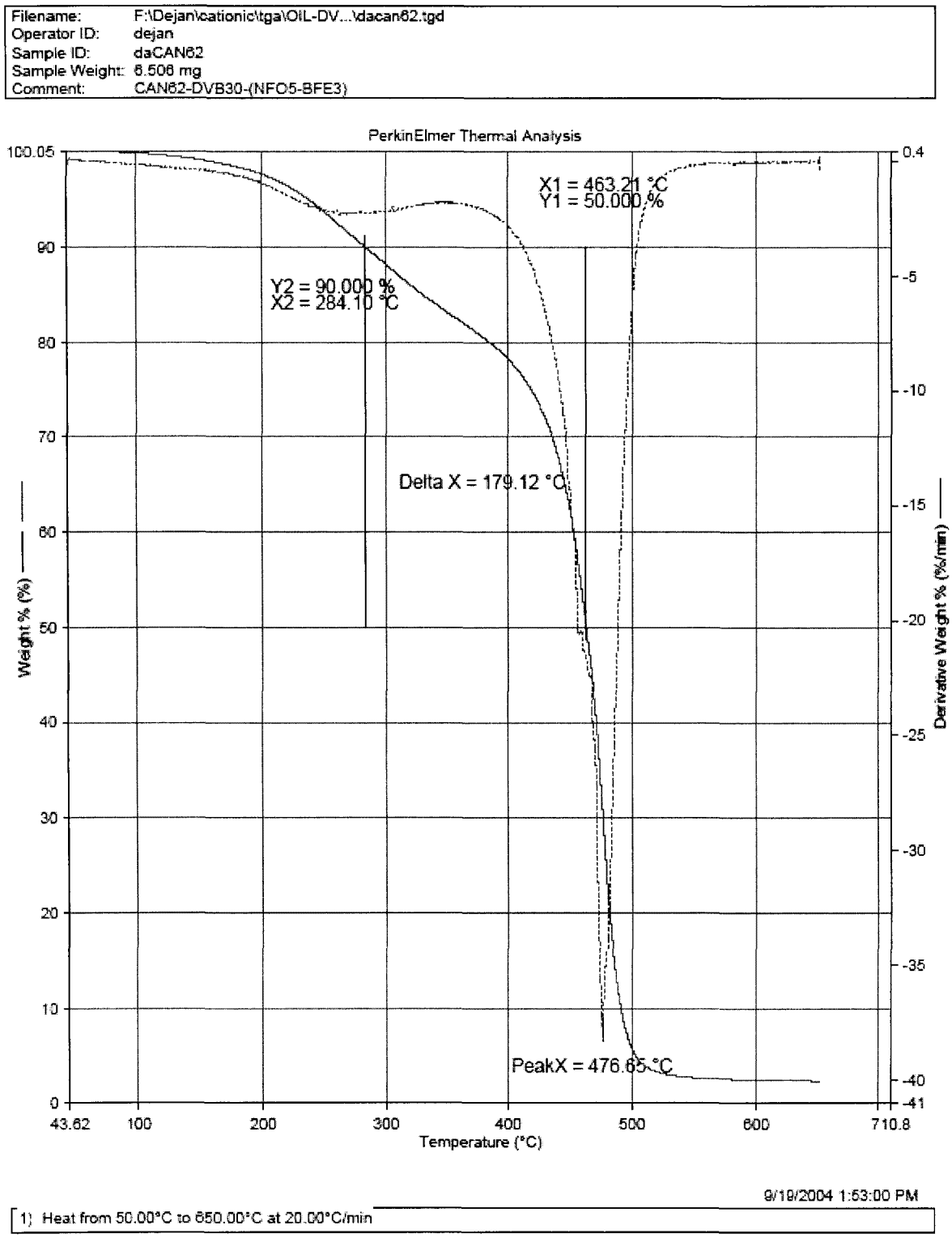

TGA thermogram of copolymer CAN62-DVB30-(NFO5-BFE3) in air.

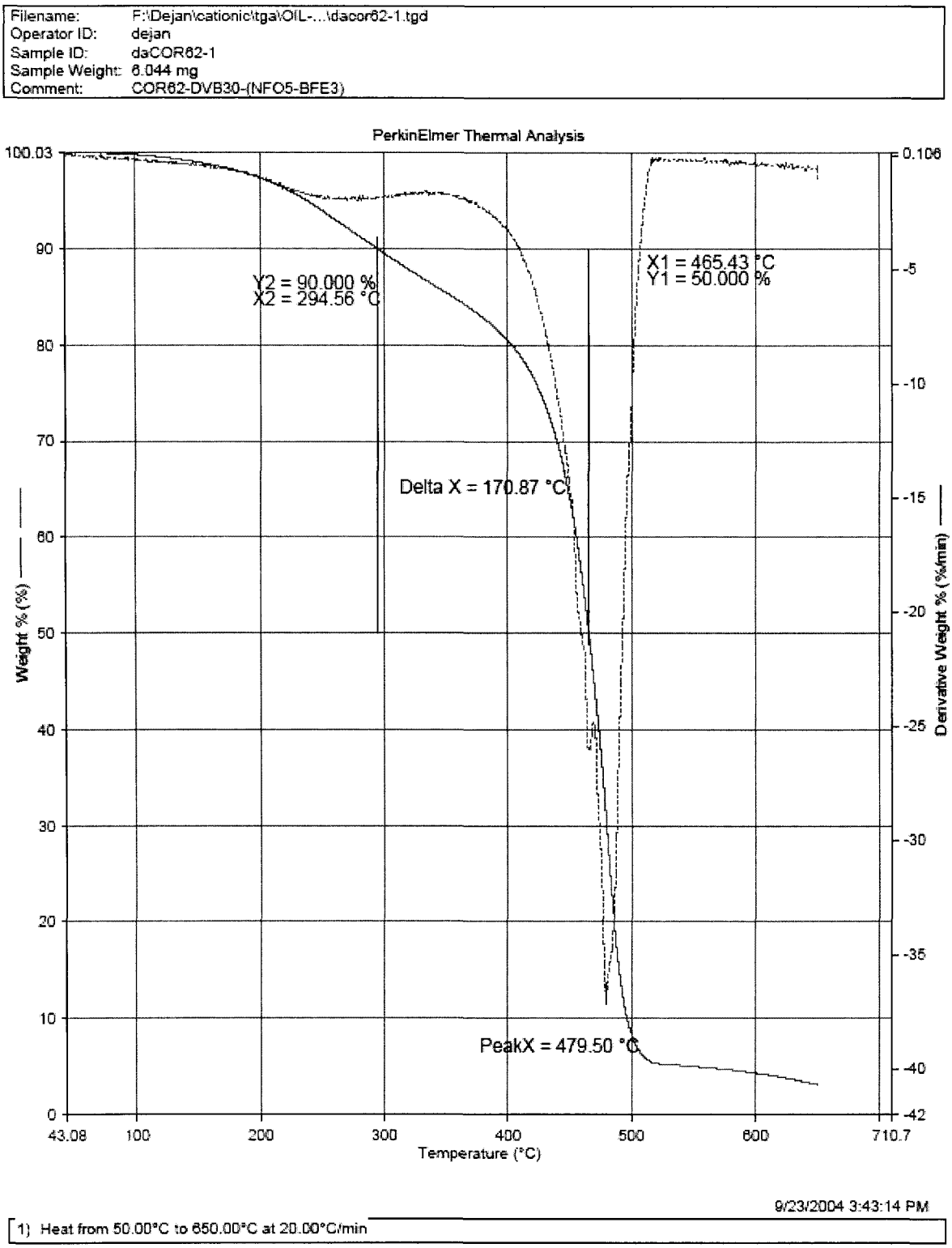

TGA thermogram of copolymer COR62-DVB30-(NFO5-BFE3) in air.

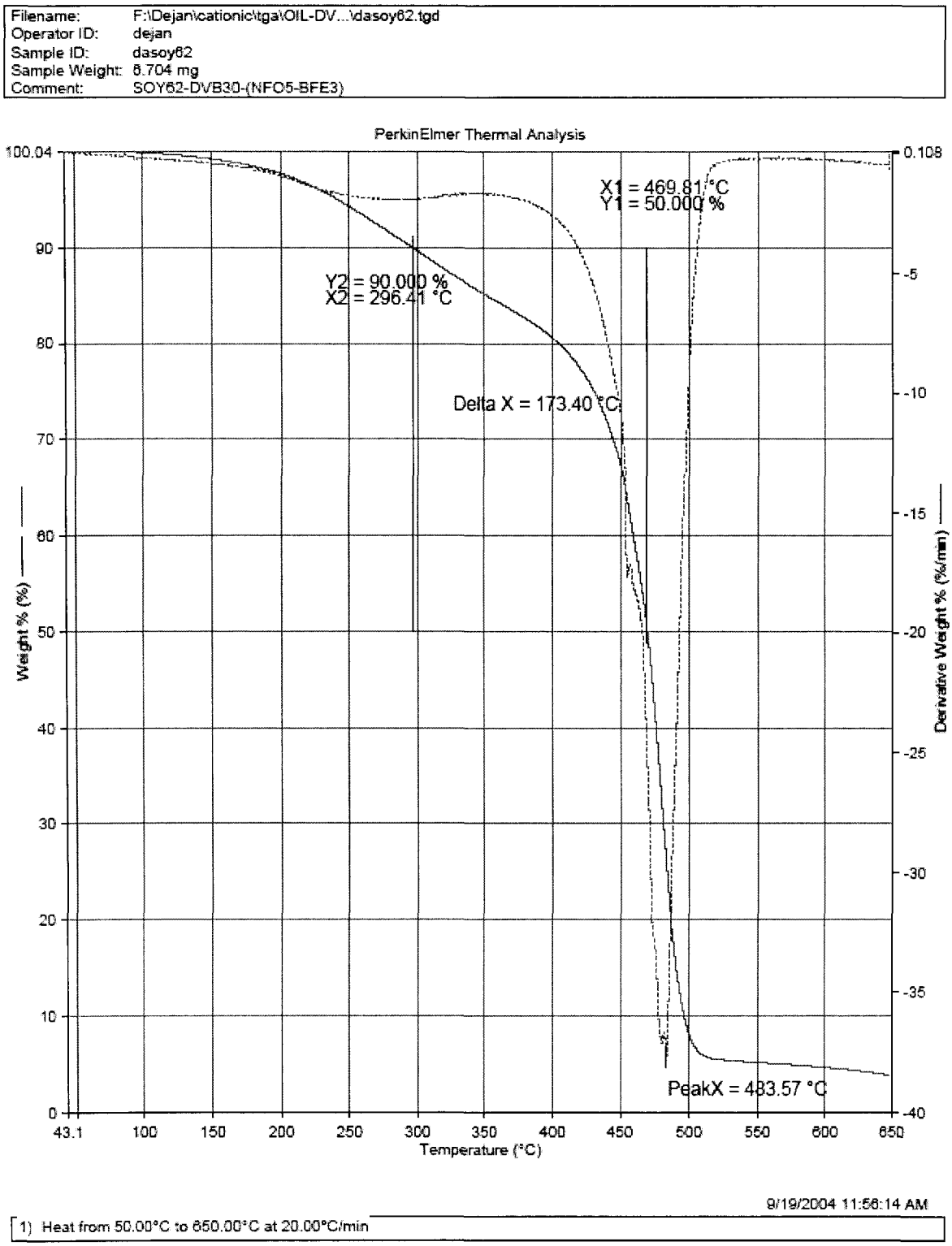

TGA thermogram of copolymer SOY62-DVB30-(NFO5-BFE3) in air.

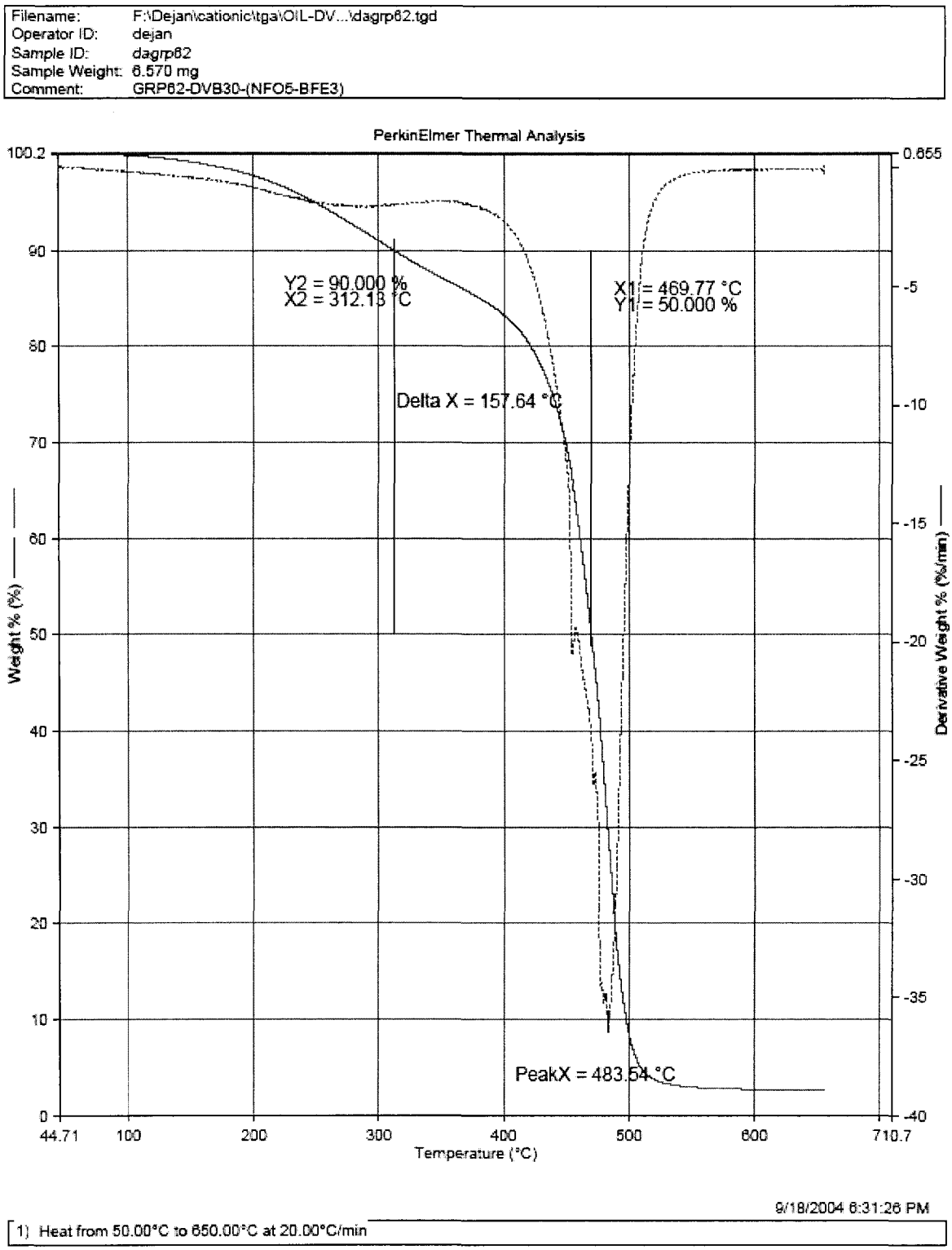

TGA thermogram of copolymer GRP62-DVB30-(NFO5-BFE3) in air.

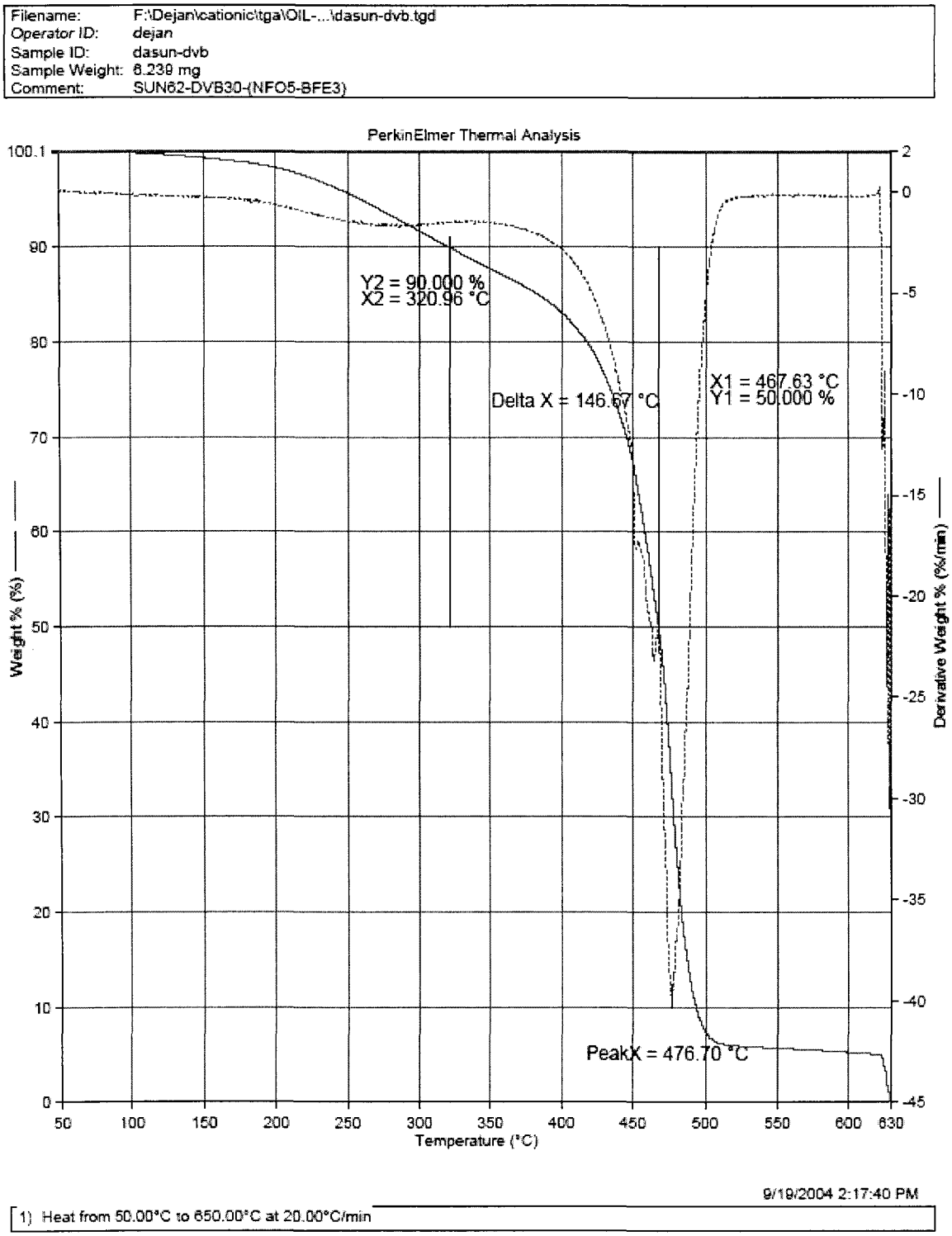

TGA thermogram of copolymer SUN62-DVB30-(NFO5-BFE3) in air.

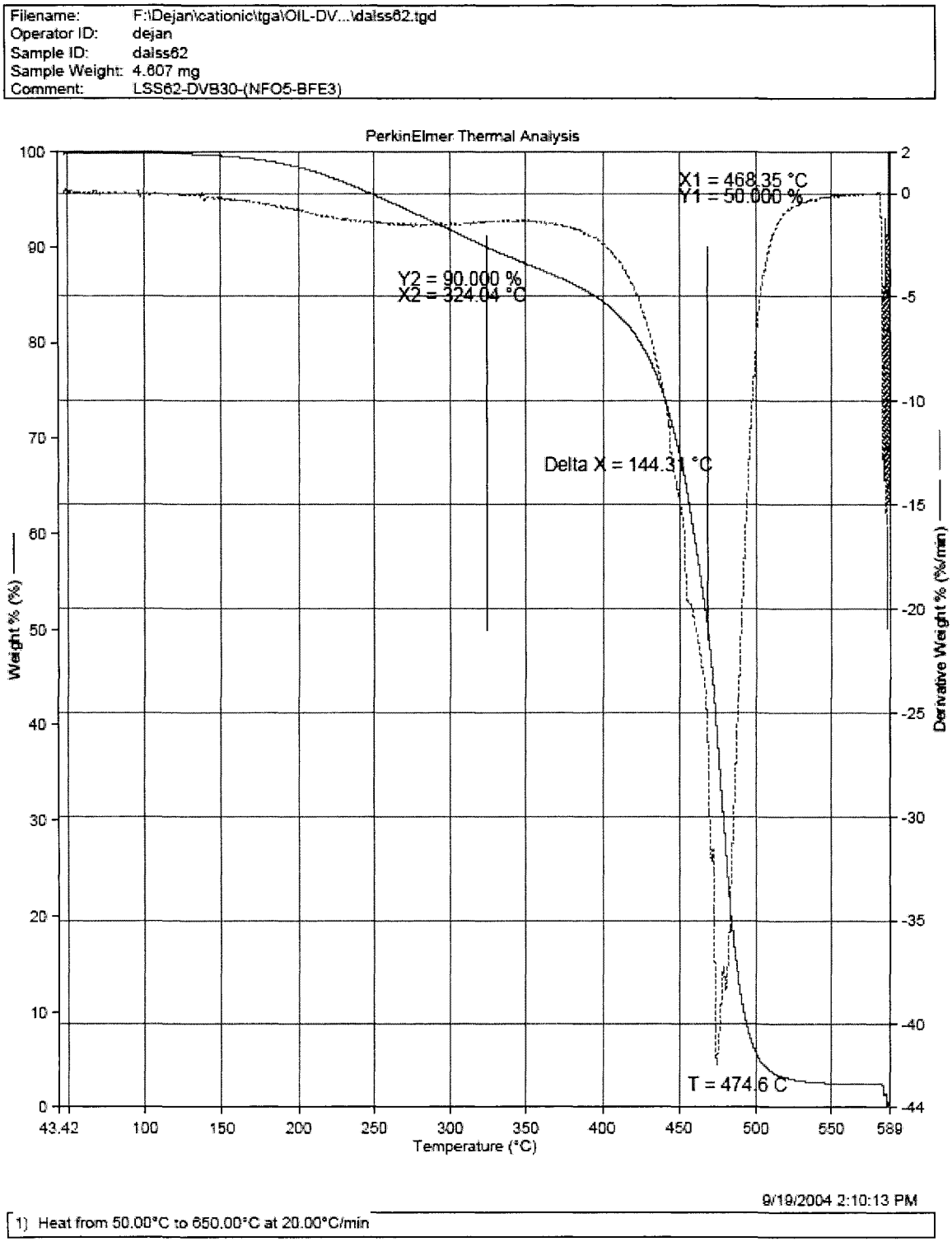

TGA thermogram of copolymer LSS62-DVB30-(NFO5-BFE3) in air.

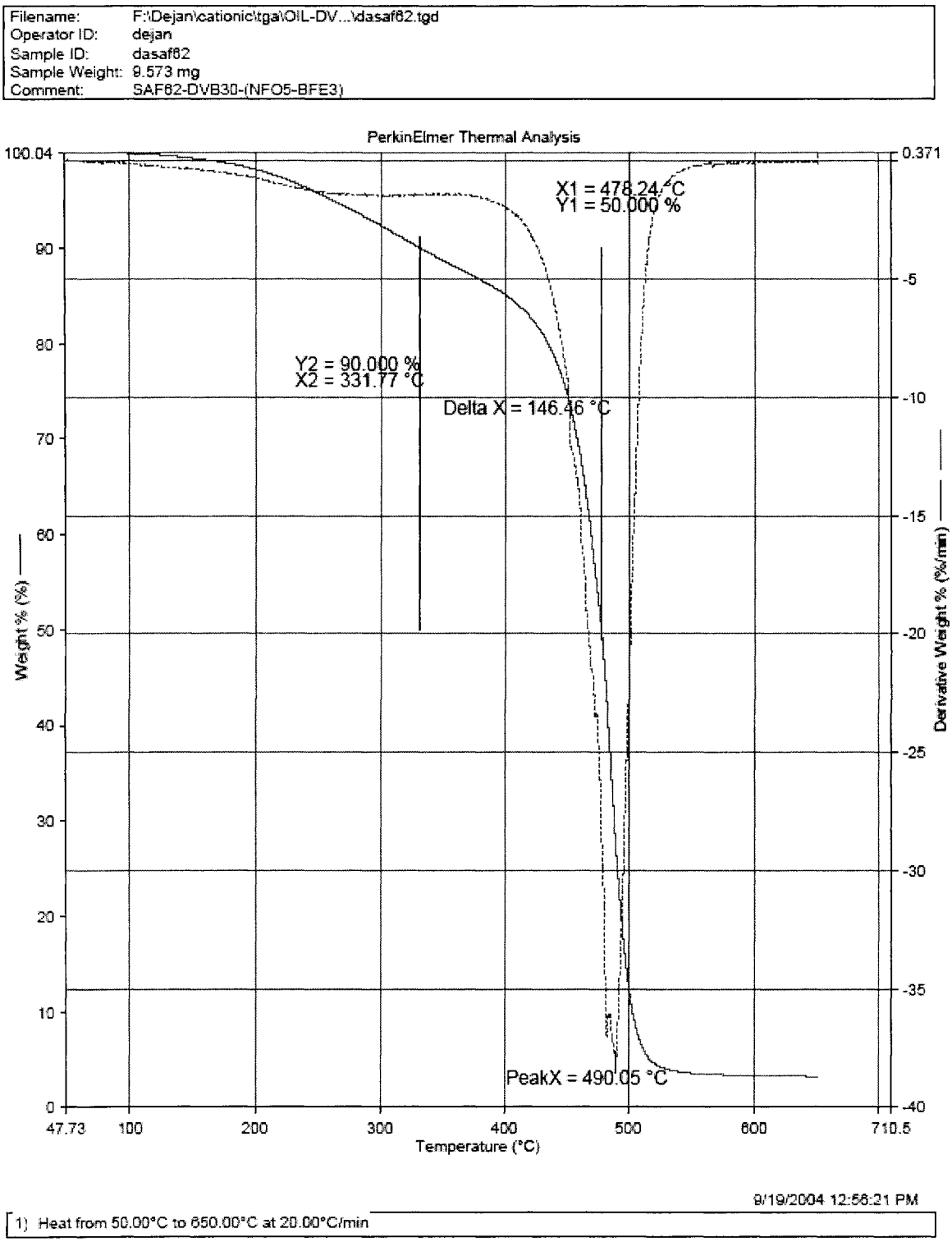

TGA thermogram of copolymer SAF62-DVB30-(NFO5-BFE3) in air.

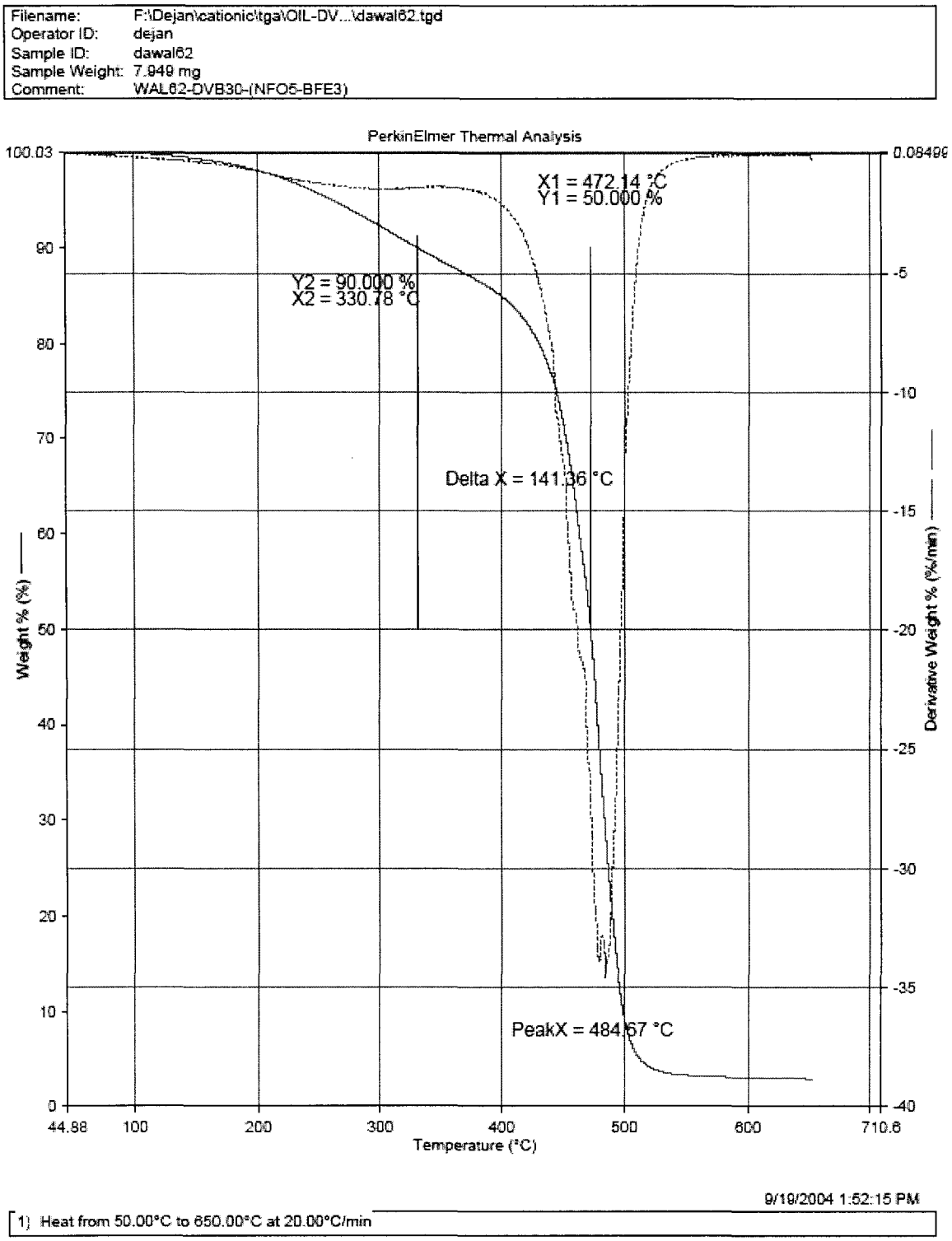

TGA thermogram of copolymer WNT62-DVB30-(NFO5-BFE3) in air.

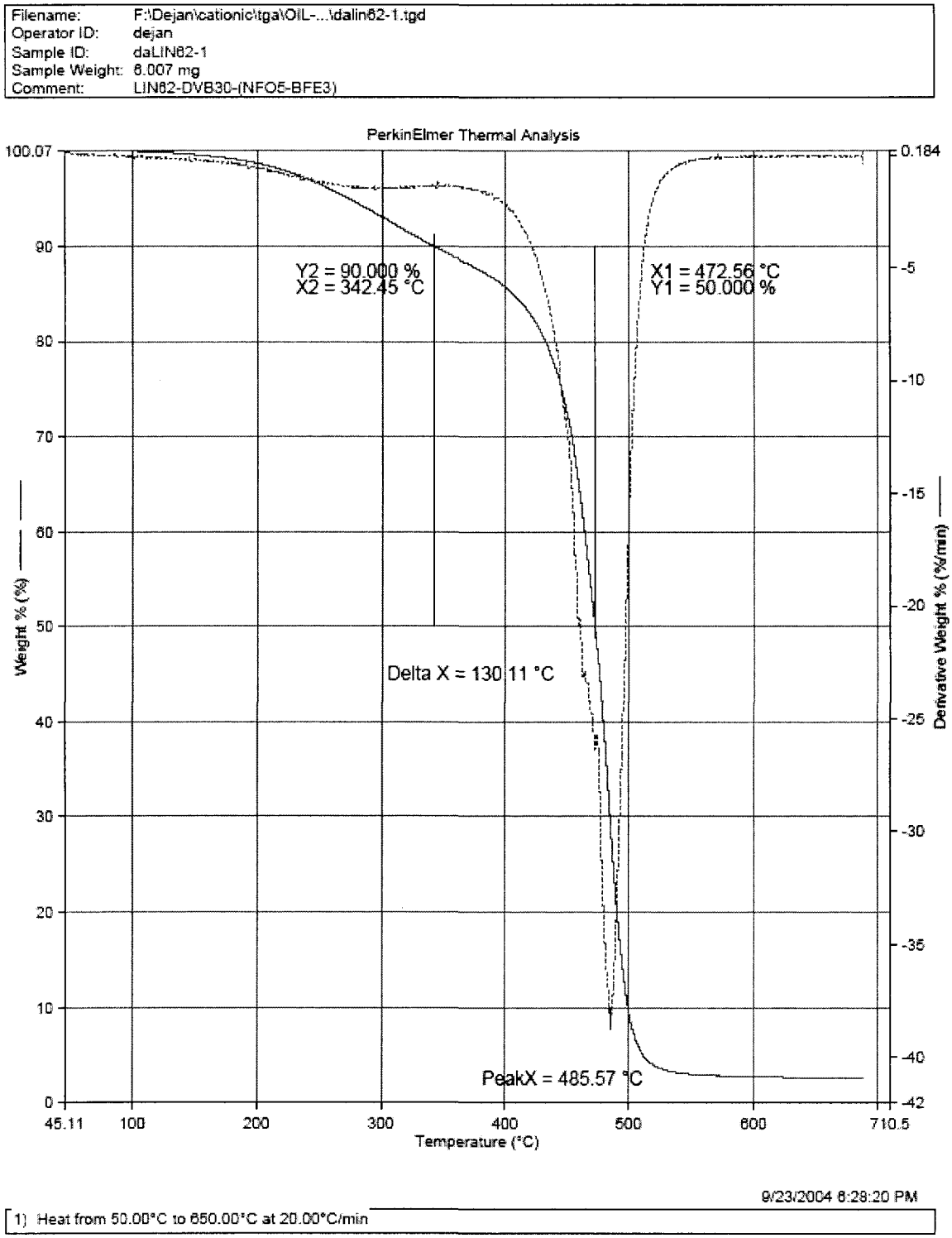

TGA thermogram of copolymer LIN62-DVB30-(NFO5-BFE3) in air.

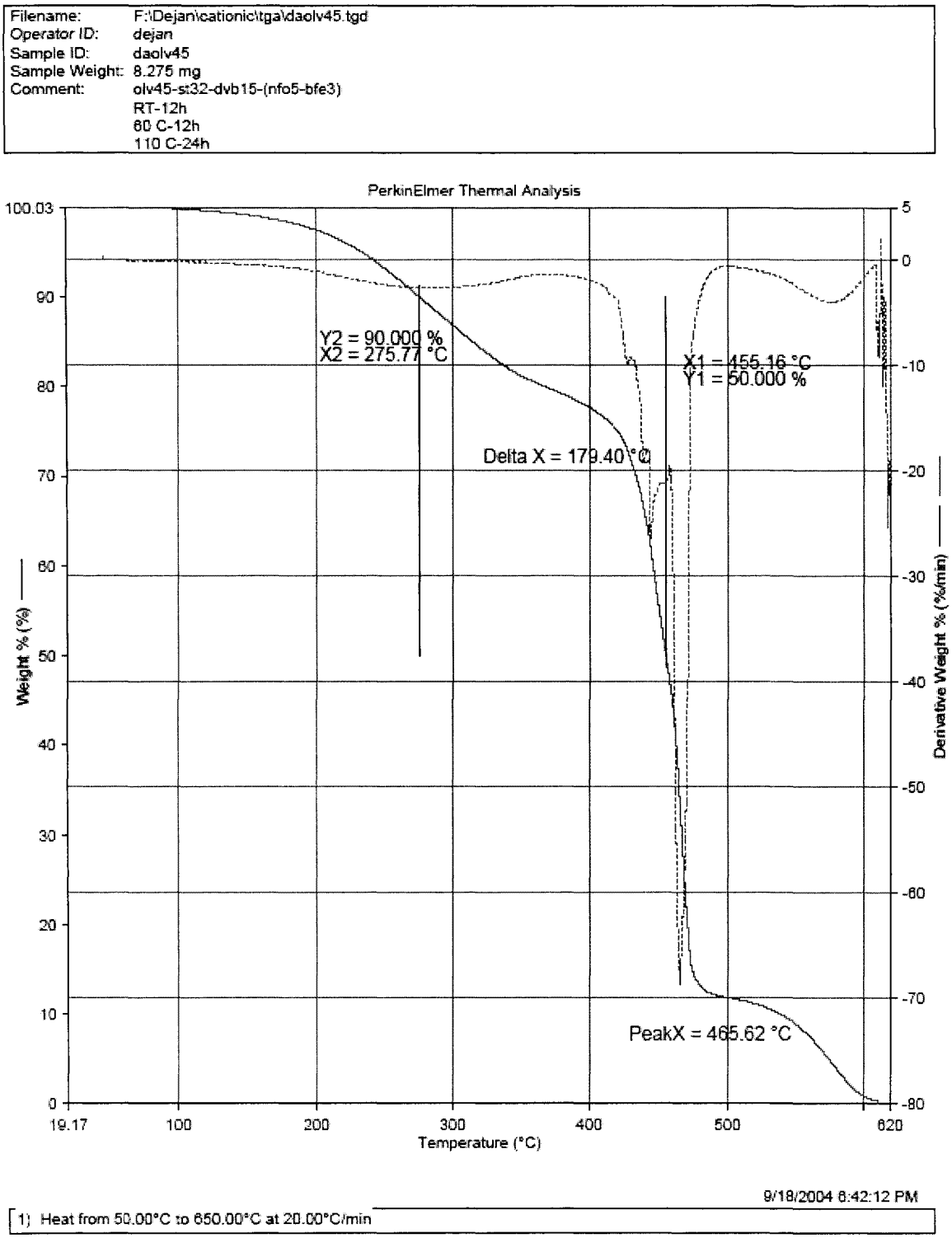

TGA thermogram of copolymer OLV45-ST32-DVB15-(NFO5-BFE3) in air.

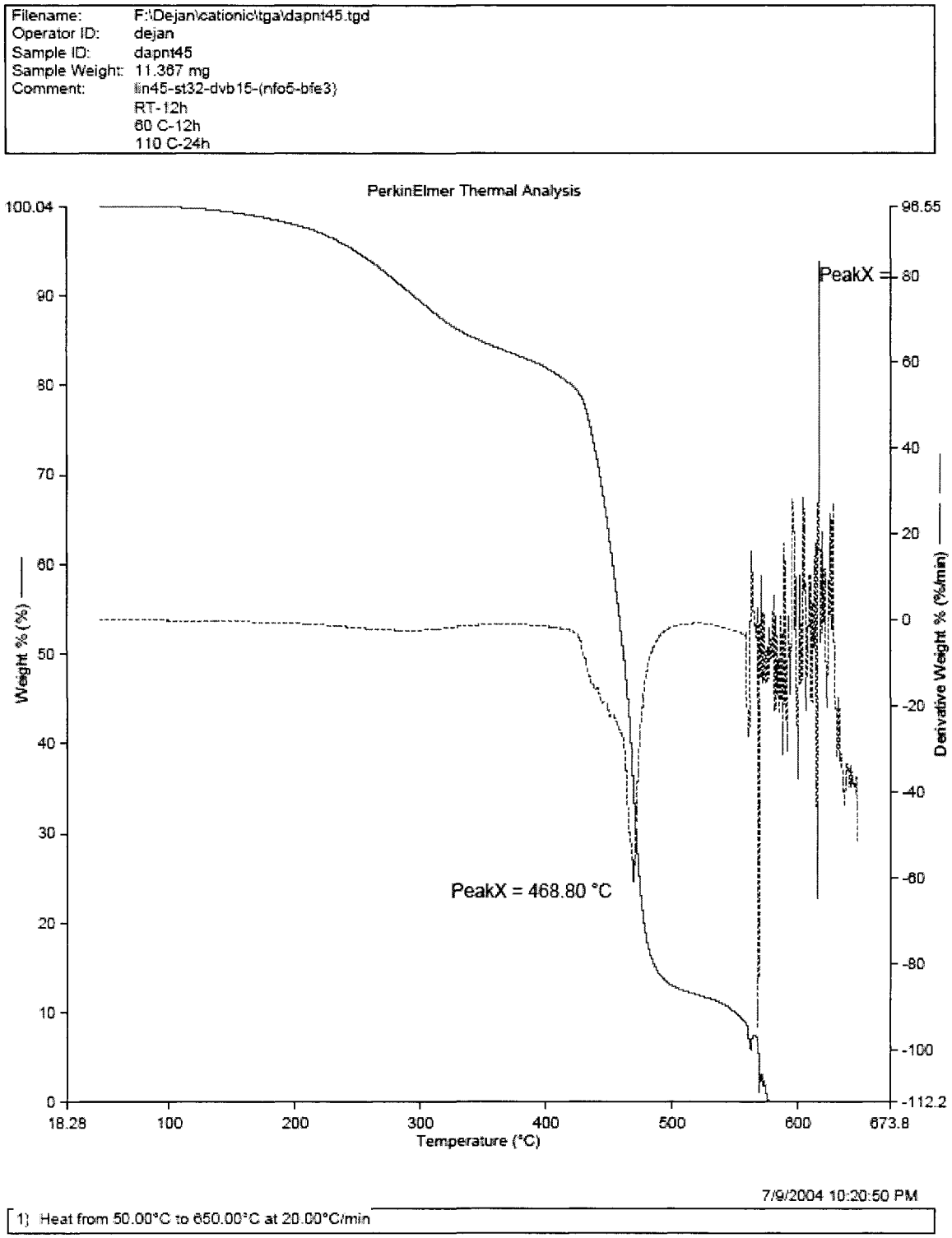

TGA thermogram of copolymer PNT45-ST32-DVB15-(NFO5-BFE3) in air.

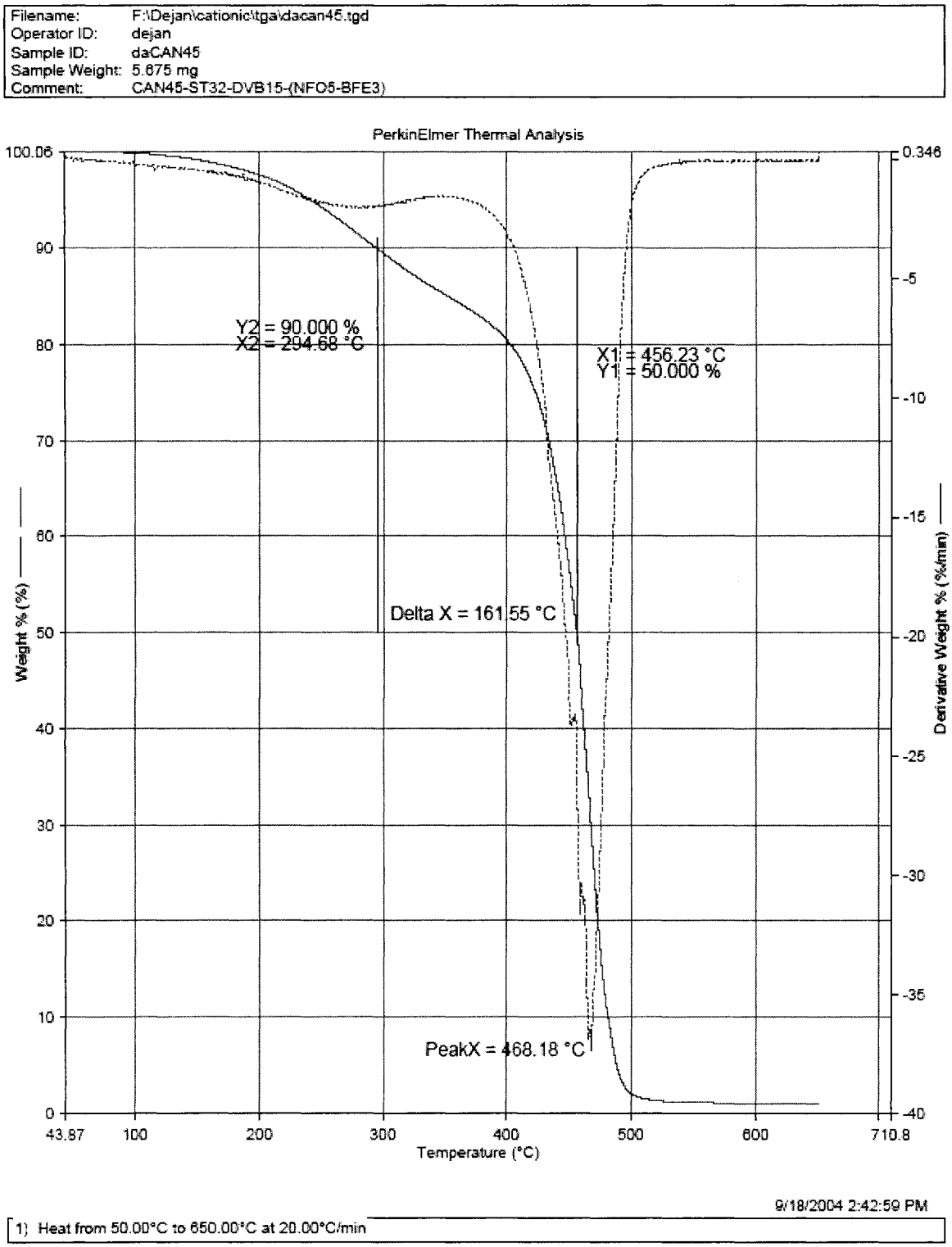

TGA thermogram of copolymer CAN45-ST32-DVB15-(NFO5-BFE3) in air.

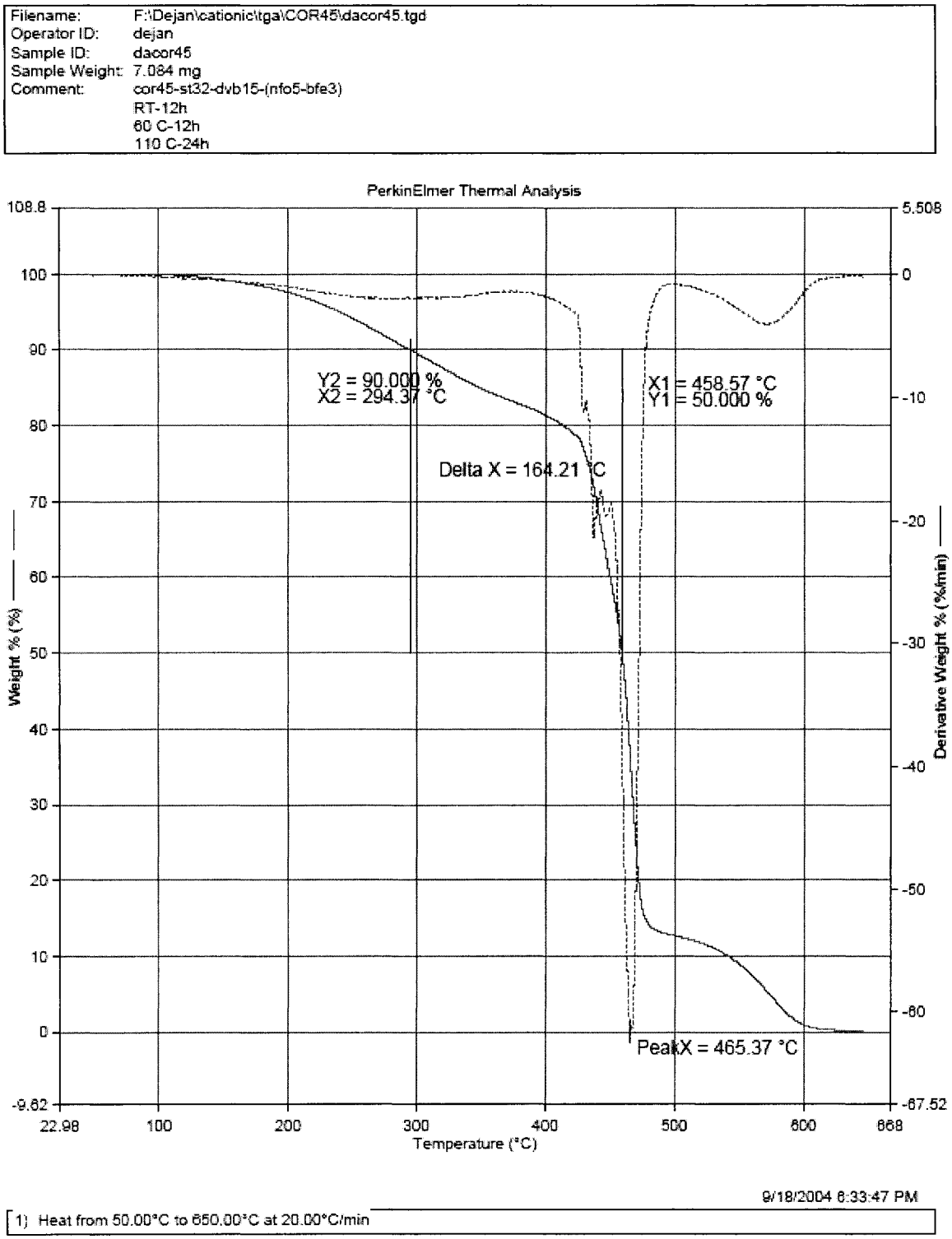

TGA thermogram of copolymer COR45-ST32-DVB15-(NFO5-BFE3) in air.

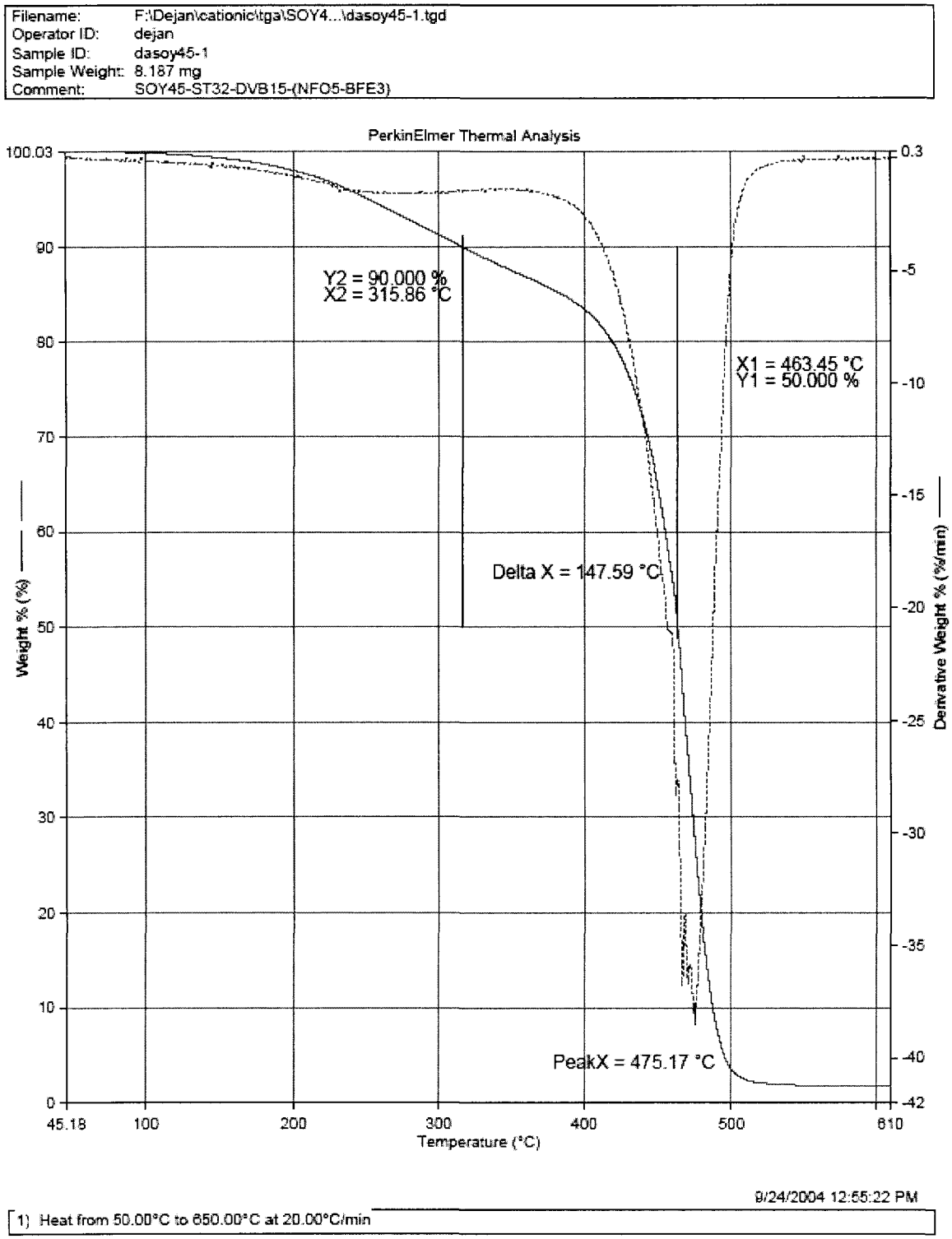

TGA thermogram of copolymer SOY45-ST32-DVB15-(NFO5-BFE3) in air.

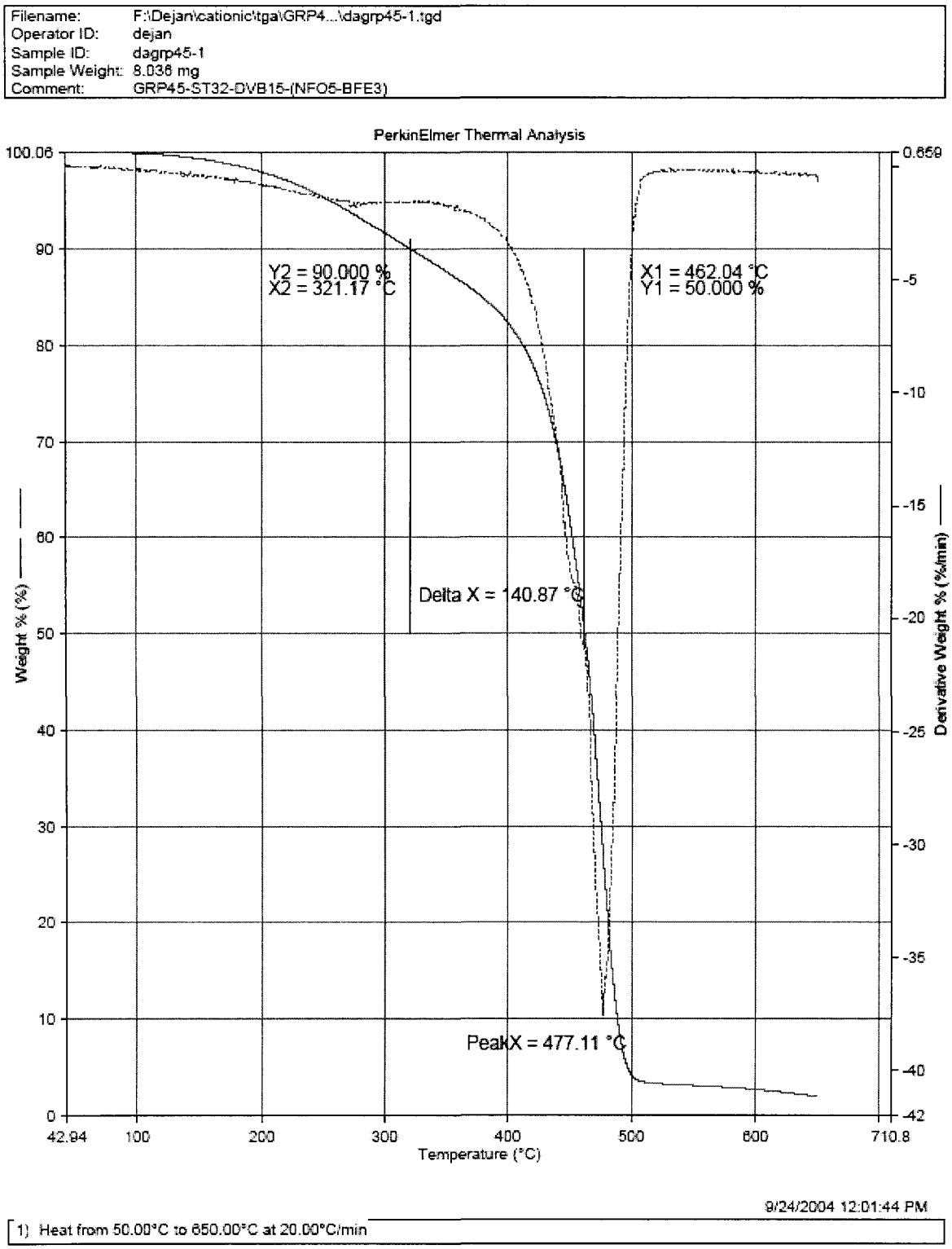

TGA thermogram of copolymer GRP45-ST32-DVB15-(NFO5-BFE3) in air.

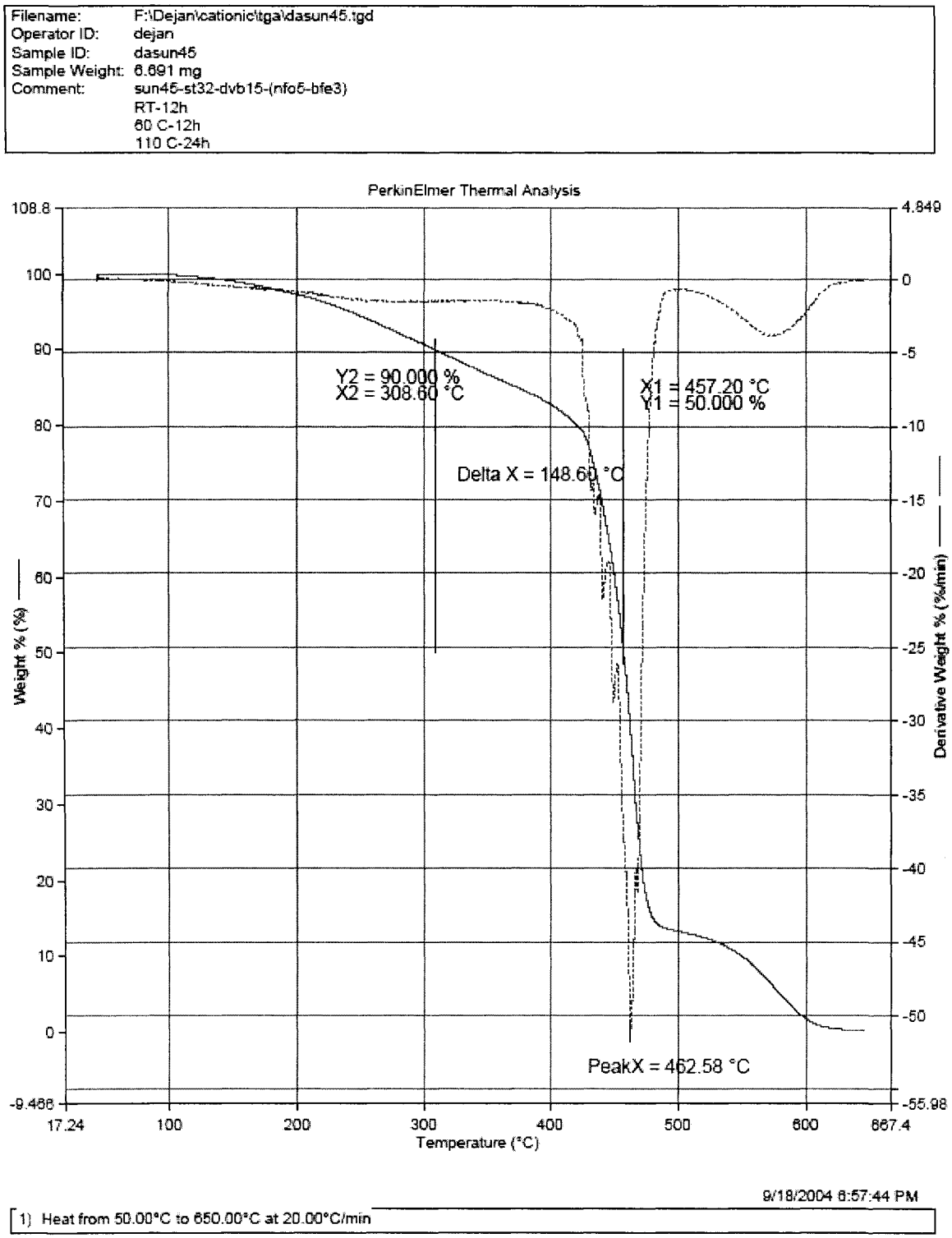

TGA thermogram of copolymer SUN45-ST32-DVB15-(NFO5-BFE3) in air.

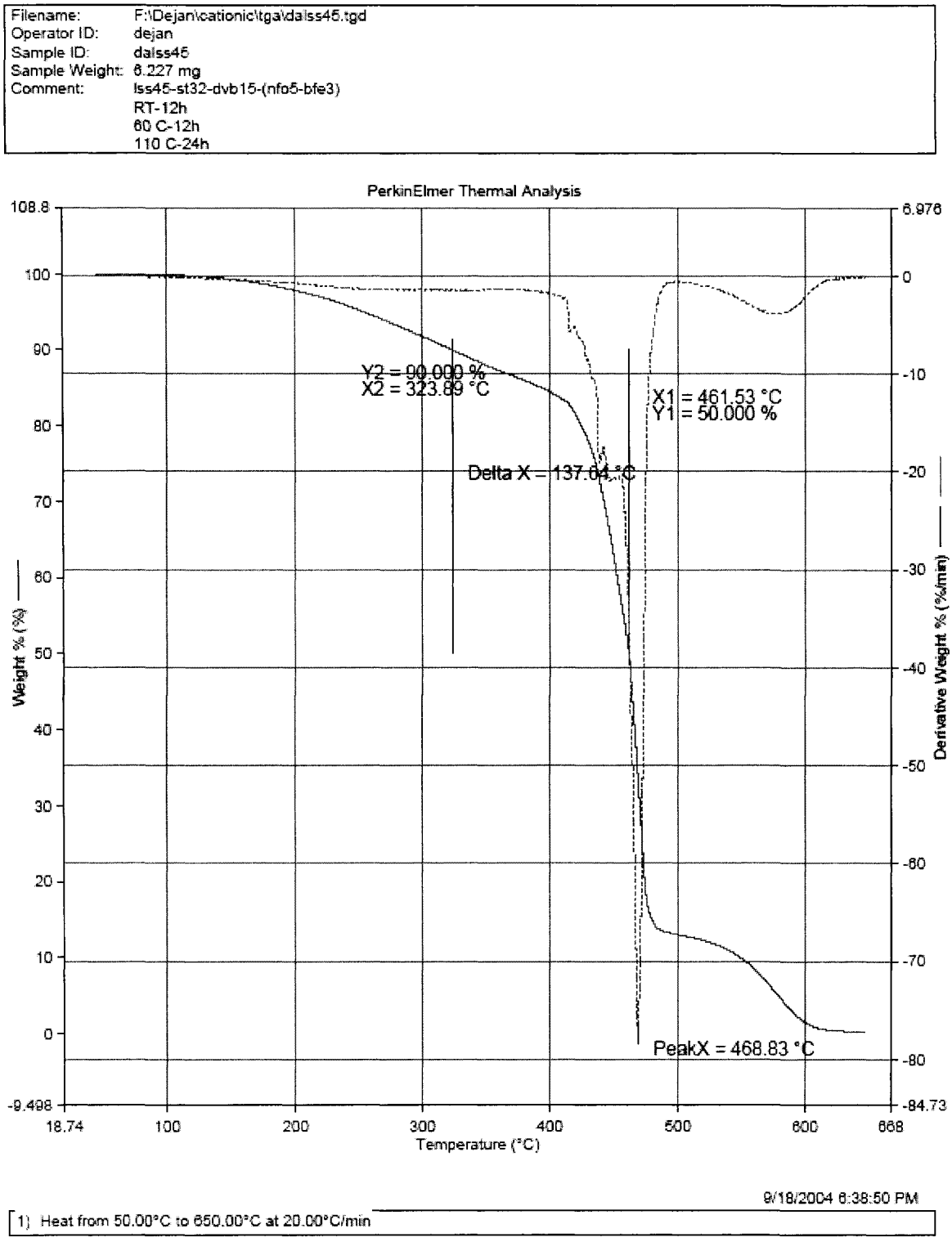

TGA thermogram of copolymer LSS45-ST32-DVB15-(NFO5-BFE3) in air.

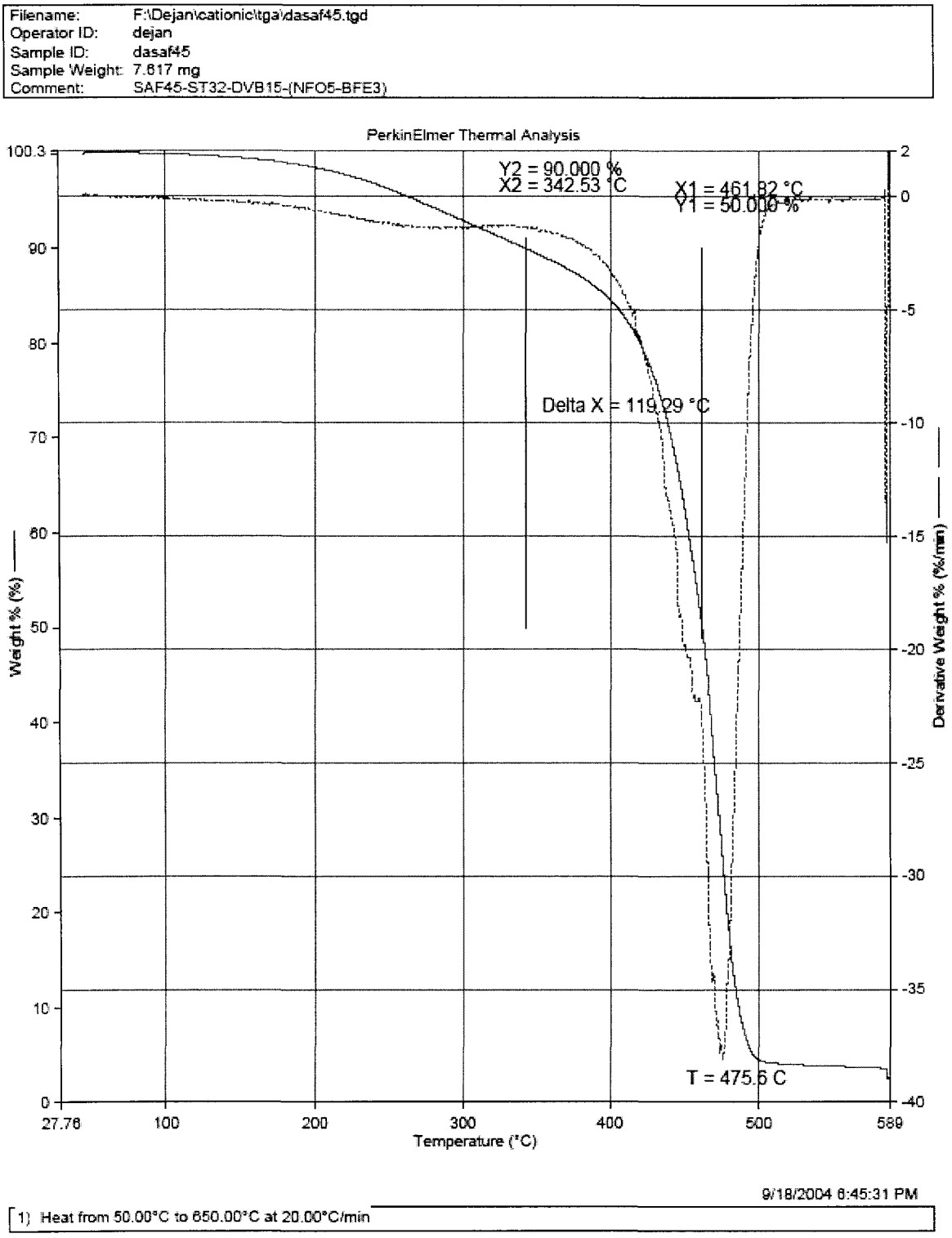

TGA thermogram of copolymer SAF45-ST32-DVB15-(NFO5-BFE3) in air.

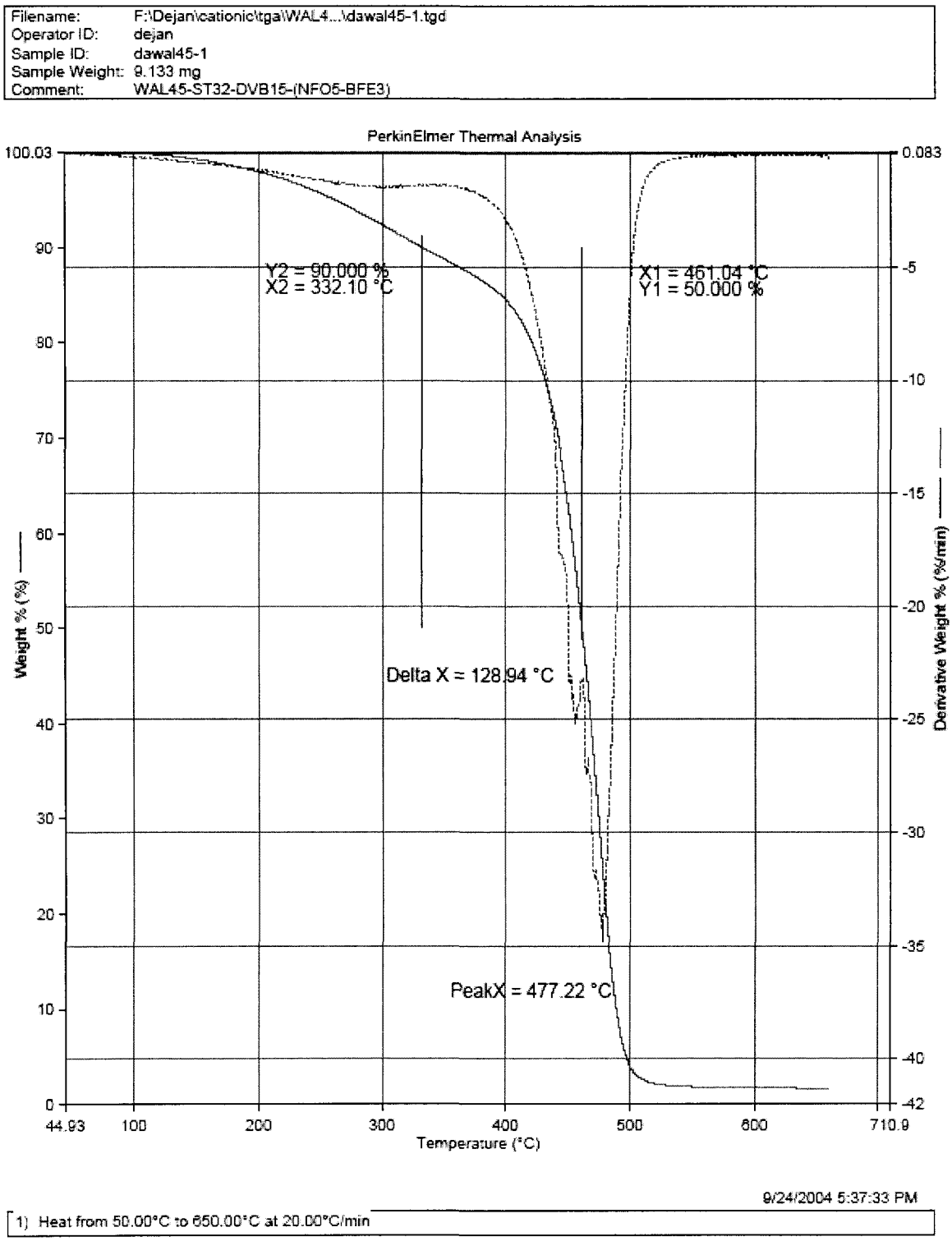

TGA thermogram of copolymer WNT45-ST32-DVB15-(NFO5-BFE3) in air.

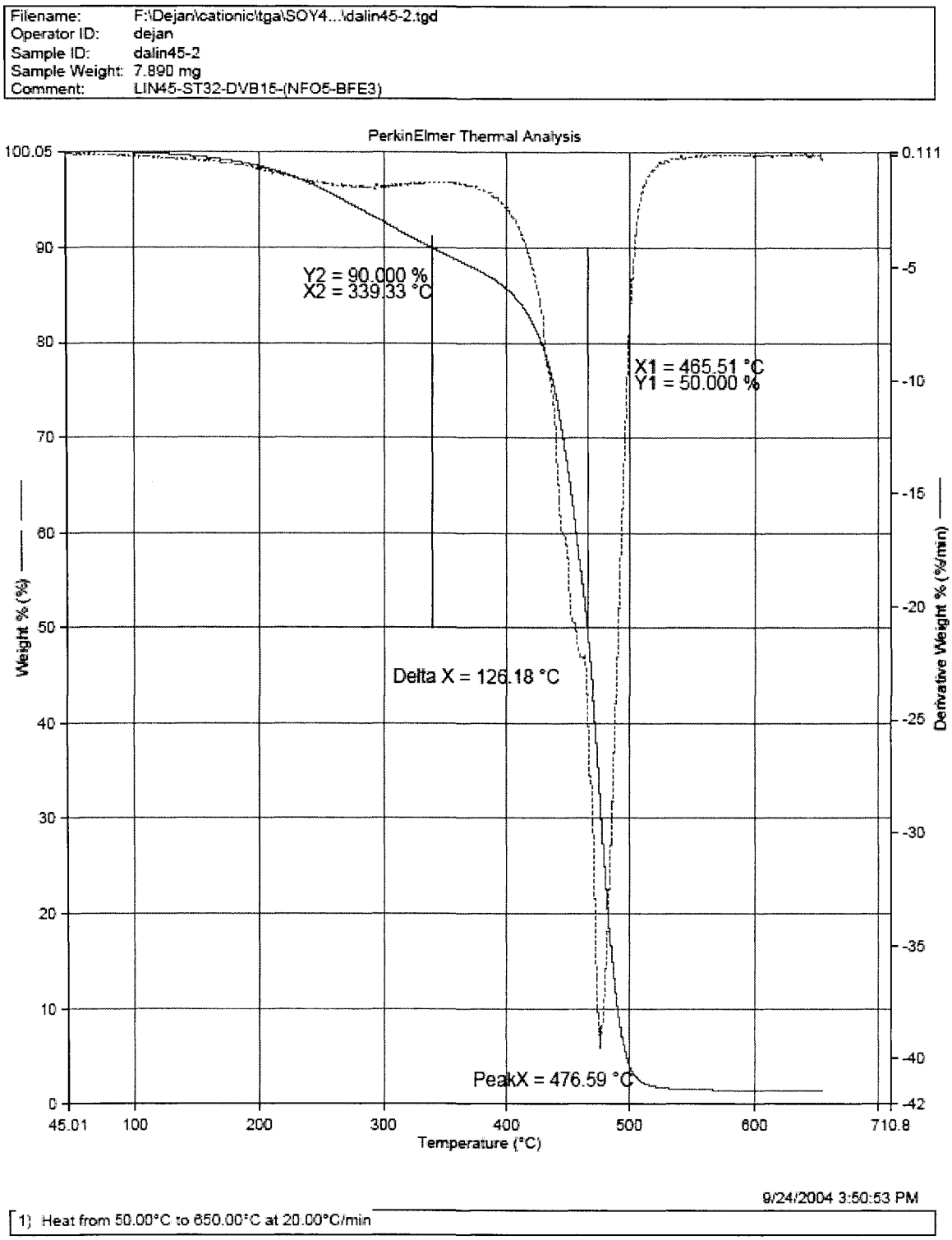

TGA thermogram of copolymer LIN45-ST32-DVB15-(NFO5-BFE3) in air.

APPENDIX C. SUPPLEMENTAL DATA FOR CHAPTER 5

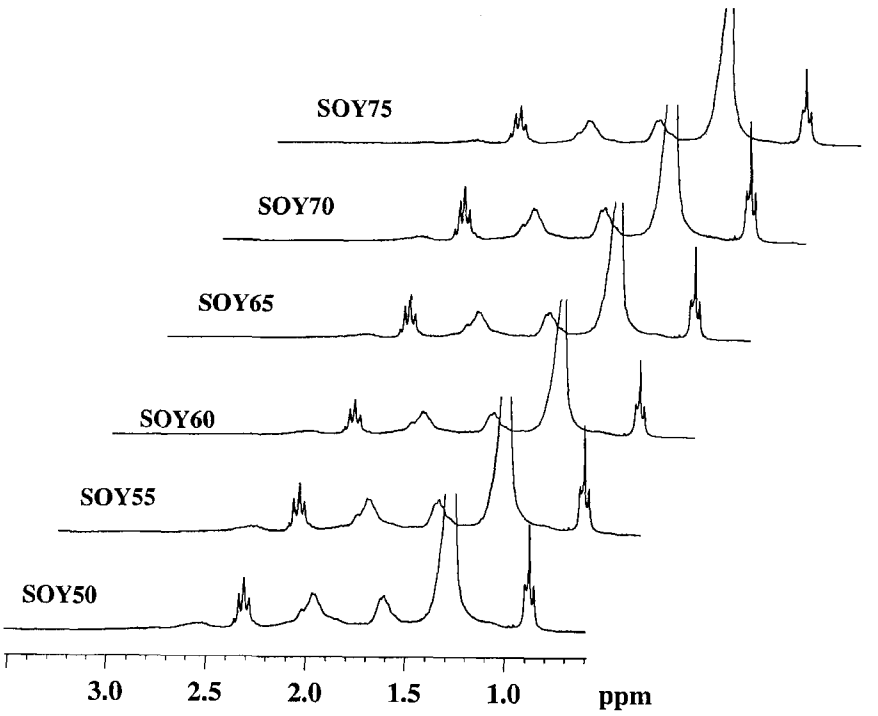

^{1}H NMR spectra of (SOY-DCP)92-(SOY5-BFE3) extracts in $CHCl_3$.

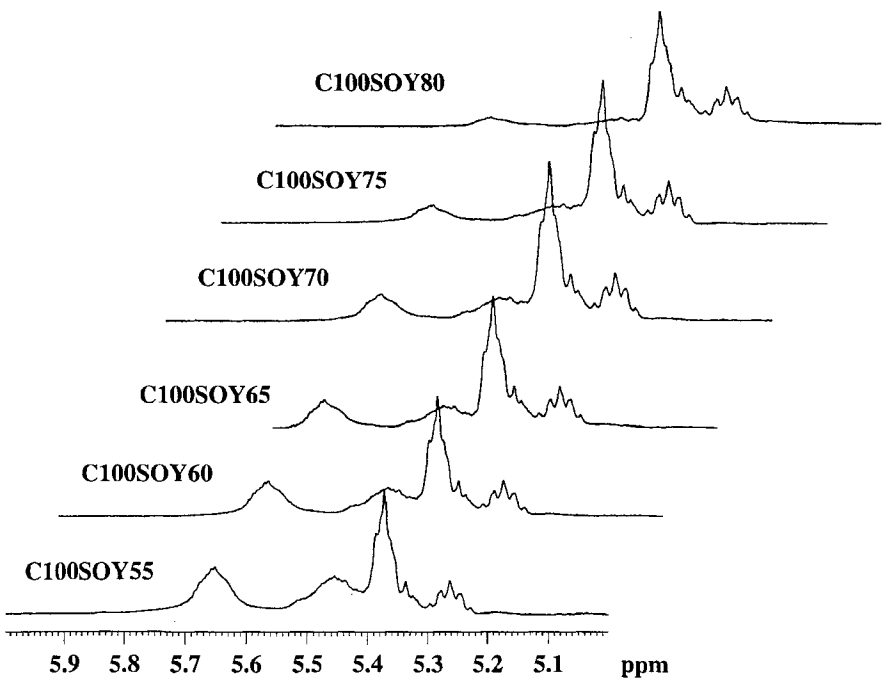

^{1}H NMR spectra of (C_{100}SOY-DCP)92-(C_{100}SOY5-BFE3) extracts in $CHCl_3$.

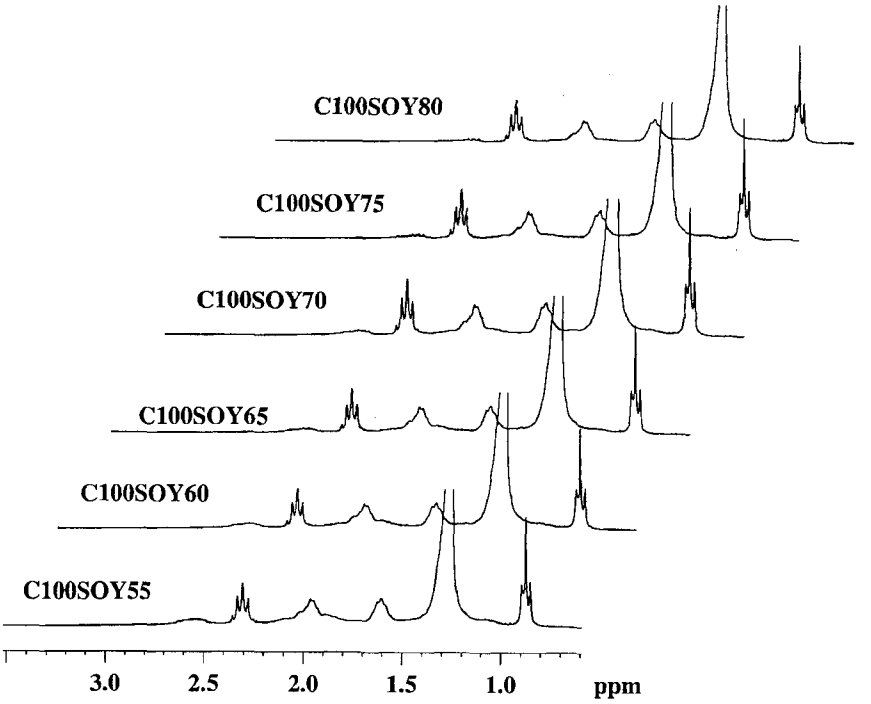

^{1}H NMR spectra of (C_{100}SOY-DCP)92-(C_{100}SOY5-BFE3) extracts in $CHCl_3$.

APPENDIX D. SUPPLEMENTAL DATA FOR CHAPTER 6

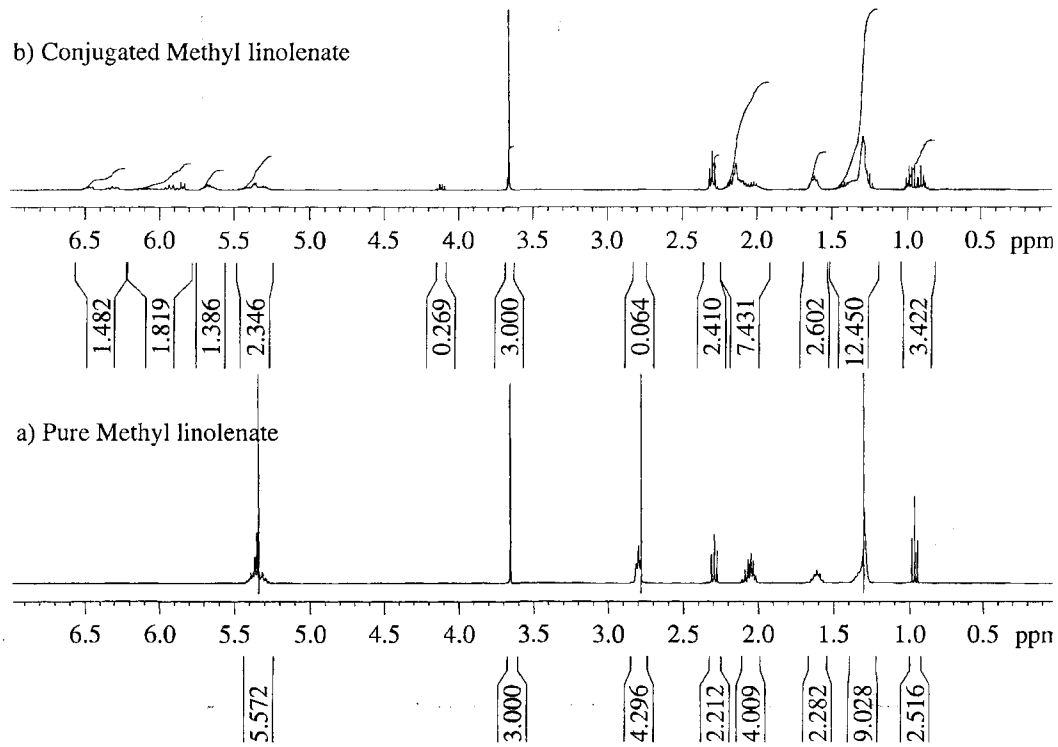

^{1}H NMR spectra of the methyl esters of a) regular and b) conjugated linolenic acids.